Beneath the surface

Boon, Lennard Ivo

2023

DOI (link to publisher)
10.5463/thesis.229

document version
Publisher's PDF, also known as Version of record

BENEATH THE SURFACE

Functional brain imaging in Parkinson's disease

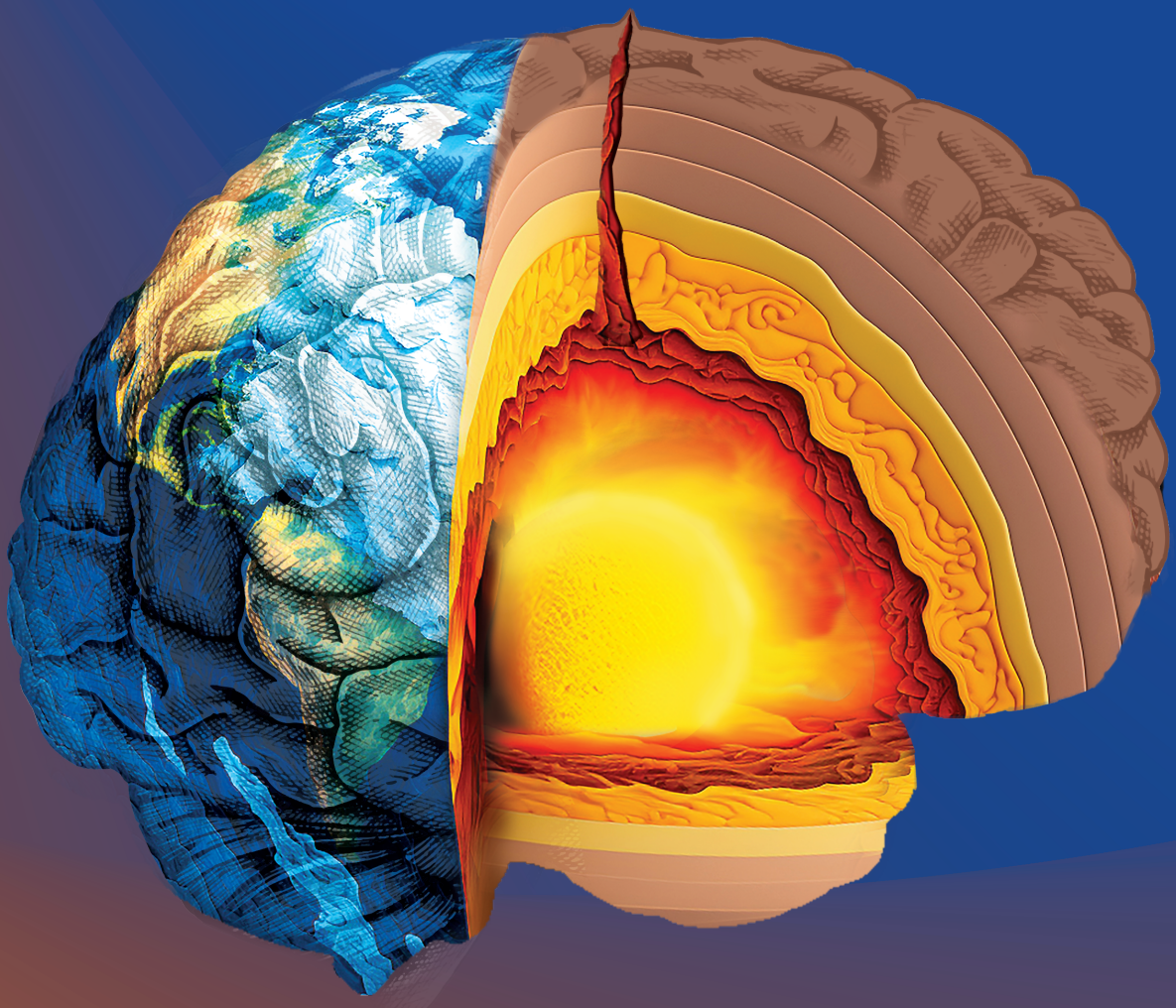

Lennard Ivo Boon

BENEATH THE SURFACE

Functional brain imaging in Parkinson's disease

Lennard Ivo Boon

ISBN: 978-94-6483-364-5
Cover design and lay-out: Publiss | www.publiss.nl
Print: Ridderprint | www.ridderprint.nl

The printing of this thesis was financially supported by the doctoral school of VUmc, stichting Alkemade-Keuls, Benelux Neuromodulation Society (BNS), and the Nederlandse Vereniging voor Klinische Neurofysiologie (NVKNF).

VRIJE UNIVERSITEIT

Beneath the surface

Functional brain imaging in Parkinson's disease

ACADEMISCH PROEFSCHRIFT

ter verkrijging van de graad Doctor
aan de Vrije Universiteit Amsterdam,
op gezag van de rector magnificus
prof.dr. J.J.G. Geurts,
in het openbaar te verdedigen
ten overstaan van de promotiecommissie van de faculteit der Geneeskunde
op dinsdag 31 oktober 2023 om 13.45 uur
in een bijeenkomst van de universiteit,
De Boelelaan 1105

door

Lennard Ivo Boon

geboren te Castricum

promotoren:	prof.dr. H.W. Berendse prof.dr. C.J. Stam
copromotoren:	dr.ir. A. Hillebrand dr. A.F. van Rootselaar
promotiecommissie:	prof.dr. Y.D. van der Werf dr. R.C.G. Helmich prof.dr. Y.A.L. Pijnenburg prof.dr. B.A. Schmand prof.dr. Y. Temel dr. B.C.M. van Wijk

Content

1

CHAPTER 1

General introduction,
aim and outline of the thesis

Parkinson's disease (PD) is a neurodegenerative brain disorder affecting more than seven million people worldwide.[1] Over the last decades, we have seen a rapid increase in the prevalence of PD, due to the ageing of the population in combination with factors we do not yet fully understand.[2] PD is best known for the motor symptoms that clinically characterize the disease and these are a prerequisite for the clinical diagnosis: bradykinesia, muscle rigidity, resting tremor, and postural instability.[3] However, PD is not solely a movement disorder. Most patients also suffer from a wide variety of non-motor symptoms such as olfactory dysfunction, autonomic dysfunction, apathy, anxiety, depression, sleep disturbances, psychotic symptoms, fatigue and cognitive decline.[4,5]

An important neuropathological feature of PD is the degeneration of nigrostriatal dopaminergic neurons in the midbrain. These neurons demonstrate a deposition of Lewy bodies of which alpha synuclein is one of the main constituents.[6] The pathological process in PD is not limited to the midbrain: years before the PD motor symptoms become overt, the olfactory system and lower brainstem are already affected.[7] Furthermore, early in the disease, neurotransmitter systems, other than the dopaminergic system, are also affected by the degenerative process, such as the cholinergic, noradrenergic, and serotonergic systems. With progression of the disease, the pathological changes spread in a predictable caudal to rostral pattern to the midbrain (containing the dopaminergic neurons), and hence via the limbic system towards cortical brain regions.[6] PD is therefore a multisystem neurodegenerative disorder, in which the timing of specific symptoms is consistent with the involvement of specific brain areas.

Cognitive decline in PD

The prevalence of cognitive decline and dementia in PD is high. Mild cognitive impairment (MCI), i.e. one or more cognitive domains affected without interference with normal daily life, is already present at the time of diagnosis in 10-20% of patients.[8] Eventually, after 20 years of follow-up, PD dementia will have developed in up to 80% of surviving PD patients.[9] In the advanced stages of the disease, cognitive decline and PD dementia contribute significantly (and more than motor symptoms) to an impaired quality of life, impose a heavy burden on caregivers, and lead to high societal costs.[10] The mechanisms are far from being elucidated and effective treatment options are lacking. To date, treatment with cholinesterase inhibitors is the only approved symptomatic treatment for early-stage PD dementia, although the effect is only limited.[11]

PD patients generally exhibit cognitive decline in the executive, attentional and visuospatial domains.[12] There is a heterogeneity in cognitive profiles that seems to be caused by differences in pathophysiological mechanisms. Dysfunction in posteriorly located cognitive functions, for instance in the visuospatial domain, may be caused by spreading of Lewy body pathology to cortical brain areas in combination with non-dopaminergic degeneration, such as cholinergic and noradrenergic deficits.[13,14] Frontostriatal dopaminergic deficits are associated not only with motor dysfunction, but

also with executive dysfunction,[15] in addition to a range of other non-motor symptoms such as apathy, anxiety and depression.[16]

Executive dysfunction and apathy (Box 1) are two highly prevalent non-motor symptoms in PD that often co-exist.[17,18] Studying these symptoms is not only relevant for improvements in their clinical management, but may also teach us about interactions between cortical and subcortical brain regions and the mediating role of interventions, such as dopaminergic medication or deep brain stimulation, that target subcortical brain regions.

Despite major advances in our understanding of the neuropathological and neurochemical changes in PD over the last decades, our knowledge of the functional brain mechanisms that lead to clinical symptoms, in particular non-motor symptoms such as cognitive decline, is far from complete. A better understanding of the mechanisms involved in these symptoms is a prerequisite for the development of better symptomatic treatments, the prediction of the course of the disease, and monitoring of the effects of future disease-modifying drugs.

Box 1 Executive dysfunction and apathy

Executive function is the most commonly affected cognitive domain in PD (in 93% of patients, independent of disease stage). It represents a broad set of cognitive skills involving attentional control, cognitive inhibition, inhibitory control, working memory and cognitive flexibility.[58] Executive function is demanded in many situations in daily life, from planning a trip (initiation, working memory, organizing), to saying "no" to a chocolate cake that is offered when one is on a diet (self-monitoring, inhibitory control).

Apathy is defined as a primary loss of motivation, diminished goal-directed behavior and decreased emotional involvement. It is a common clinical feature following strategic lesions in the prefrontal cortex (PFC) or basal ganglia and of brain disorders involving the basal ganglia.[59-61] The PFC-basal ganglia system circuits are linked to a diverse range of limbic, cognitive and motor control functions.[62,63] Clinically, apathy may manifest in the context of three conditions: emotional-affective dysfunction (depression), cognitive dysfunction, or a deficit in auto-activation (inability to self-activate thoughts or behavior).[64]

Apathy in PD is at least partly caused by dopaminergic deficits, as it may fluctuate with the dopaminergic state of patients.[65,66] PD-related apathy can have both an emotional-affective or (executive) cognitive component.[67]

Functional brain imaging techniques

Functional brain imaging techniques allow us to study the activity of the PD brain in relation to its clinical symptoms in a non-invasive way. Proper (cognitive) functioning relies on the coordination and integration of neuronal activity within and between distinct brain regions,[19,20] which the brain accomplishes by synchronizing oscillatory brain activity.[21] In this thesis, we measured brain activity in a resting-state, task-free condition, in which the brain is remarkably active.[22] Characteristics of resting-state brain activity are associated with cognitive function both in healthy subjects[23] and in patients with neurological diseases.[24] An explanation of the two functional brain imaging techniques used in this thesis, magnetoencephalography (MEG) and functional MRI (fMRI), can be found in Box 2 and an explanation of the measures of brain activity and connectivity in Box 3.

Box 2 Functional brain imaging techniques

Electroencephalography (EEG) measures bioelectric brain activity that is caused by groups of active neurons. It is recorded by (typically 20) electrodes attached to the scalp. It is available in many hospitals, which makes the translation of research findings into clinical practice relatively easy.

Magnetoencephalography (MEG) measures fluctuations in the magnetic field close to the scalp. These magnetic fluctuations are induced by changes in the electric fields caused by groups of active neurons. The resulting magnetic fields are very weak. Therefore, to measure the brain's magnetic fields, very sensitive sensors, so-called superconducting quantum interference devices (SQUIDS), have to be used. To reduce the influence of (fluctuations in) background magnetic fields (i.e. noise), measurements are carried out inside a magnetically shielded room. Like EEG, MEG has an excellent temporal resolution. Unlike EEG, the MEG signal does not require a reference electrode. In addition, it is hardly disturbed by the underlying tissues such as the skull or scalp. Furthermore, it is more sensitive to signals from deeper structures, such as subcortical brain areas. Therefore, MEG offers a better spatial resolution and can be used to map sensor data back to the brain locations where the signal originates from, for example by using so-called 'beamforming', which is a spatial filtering technique.

Functional MRI (fMRI) is based on the so-called Blood Oxygenation Level Dependent (BOLD) response. As neural activity in brain regions increases, these regions consume more oxygen and attract more blood. The BOLD contrast depends on changes in levels of deoxyhemoglobin, which acts a paramagnetic contrast agent and is an indirect measure of neural activity.[68] Although fMRI offers excellent spatial resolution, allowing deep brain structures to be studied with millimeter precision, its temporal resolution is rather limited, in the order of seconds, due to the sluggishness of the hemodynamic response.

Box 3 Measures of brain activity and connectivity

Power spectrum

At a local scale, neurons are connected with each other via synapses. The activity of large groups of interconnected excitatory and inhibitory neurons can synchronize into an oscillating unit. The amplitude of oscillatory activity in different frequency bands can be measured by applying power spectral analysis to the recorded signals. An often-applied method is the Fast Fourier Transformation (FFT). This can be used to decompose the measured EEG or MEG signal into local oscillatory activity and its power within separate frequency bands. The following frequency bands were used in this thesis: delta (0.5-4 Hz), theta (4-8 Hz), alpha (8-13 Hz), beta (13-30 Hz) and gamma (30-48 Hz). In addition, we determined the peak frequency, i.e. the frequency at which the spectral power is highest, within the 4-13 Hz frequency range.

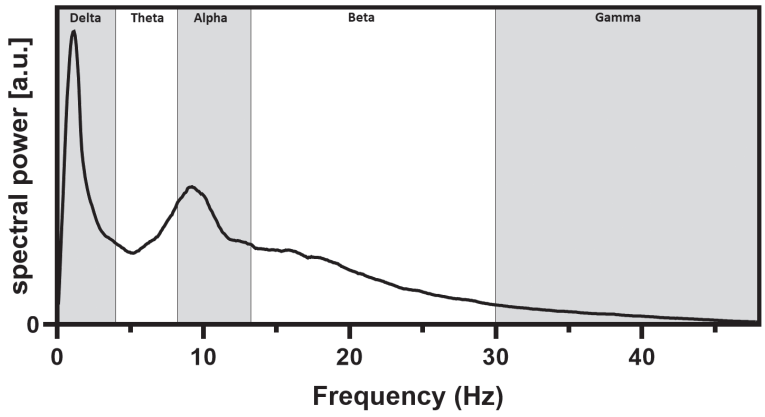

Figure 1 Power spectrum between 0.5 and 48 Hz, with a peak frequency around 10 Hz

Functional connectivity

At a larger scale, groups of thousands of neurons form functional modules, or local circuits. The communication between these populations in spatially separated brain regions as well as the integration of their activity is vital for normal brain functioning. The functional coupling between two brain regions can be estimated by computing the statistical relationship between the time-series of activity generated by the two brain regions.

In the MEG studies in this thesis, we calculated functional connectivity using the corrected amplitude envelope correlation (AEC-c). First, the so-called amplitude envelopes were computed for the time-series that had been filtered in a specific frequency band (delta to gamma; Figure 2). Using a symmetric orthogonalisation procedure (meaning time-series X is regressed out from time-series Y and vice versa), we accounted for the effects of volume conduction/field spread. Next, the correlation between pairs of amplitude envelopes was calculated.

Box 3 Measures of brain activity and connectivity *Second part*

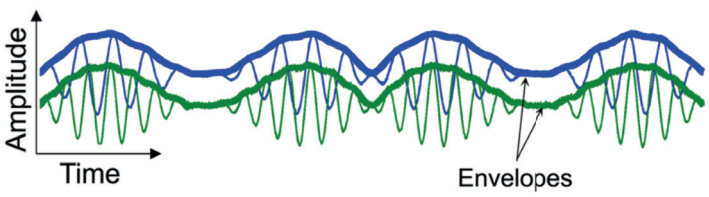

Figure 2 Amplitude envelope correlation

In fMRI research, several consistent networks of interacting brain regions can be identified during the (task-free) resting-state of the brain by applying an independent component analysis (ICA), which maximizes the statistical independence of the estimated components.[69,70] Based on the ICA, brain regions were clustered into 30 components, which we visually appointed to seven literature-based resting-state networks (see Figure 3). Functional connectivity, calculated using Pearson correlations, within and between these resting-state networks was used as measure of brain function.

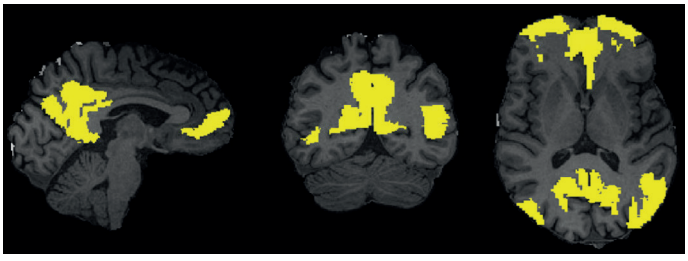

Figure 3 In yellow the brain regions involved in the default mode network (DMN), one of the dominant resting-state networks. The DMN is a network that becomes overt during "wakeful rest" and classically involves the medial prefrontal cortex, posterior cingulate cortex and the inferior parietal lobule.

Dynamic functional connectivity (derived from fMRI data) represents a measure of the fluctuations in functional connectivity over time. In our fMRI project, we implemented this measure by calculating the standard deviation of the functional connectivity over multiple consecutive time windows.

Directed functional connectivity (derived from MEG data) represents the balance between incoming and outgoing information in a brain region. In the MEG study described in Chapter 4 this was estimated using the directed Phase Transfer Entropy (dPTE). PTE is based on the principle that a source signal must have a causal influence (flow of information) if knowledge of the past of both signals improves the ability to predict the target's future, compared to the situation of only knowing the target's past.[71]

Current EEG, MEG and fMRI findings and cognitive changes in PD

Previous neurophysiological (EEG and MEG) research has revealed that already at the earliest stages of PD, slowing of cortical oscillatory brain activity is present.[25,26] This slowing continues as the disease progresses from a later-stage non-demented situation up to PD dementia and is associated with cognitive dysfunction.[27-30] Studies of functional connectivity in PD have shown an initial increase, and a subsequent decrease over time in relation to clinical disease progression, especially cognitive decline.[31-34] In fMRI studies, the association between clinical symptoms of PD and measures of functional connectivity

is rather complex. Both decreases and increases in functional connectivity have been reported in relation to cognitive decline,[35,36] even within the same cross-sectional study.[37] Quite possibly, functional connectivity may decrease as a result of the underlying disease process, whilst compensatory mechanisms inherent to the brain, pathological processes[38] or the effects of dopaminergic medication[39] may lead to an increase in functional connectivity. Although the results of the aforementioned studies suggest that changes in the different measures of brain activity and connectivity (spectral power, functional connectivity) may reflect relevant pathophysiological mechanisms underlying PD symptoms, including cognitive decline, several questions remained unanswered.

Knowledge gaps

Previous studies using EEG and MEG in PD focused on cortical brain regions, as until recently these techniques were more sensitive to cortical brain activity. Yet, the mechanisms that lead to the previously observed widespread cortical neurophysiological changes may find their origin in subcortical brain regions. Furthermore, dysfunction of subcortical brain regions is related to the occurrence of several non-motor symptoms.[40,41] Thanks to technical advances in beamforming, we can now project MEG-signals onto subcortical brain regions, allowing for a reliable measurement of the functional properties of these areas.[42-47] As nigrostriatal changes are early-stage manifestations of PD, we expected to find functional changes in subcortical brain regions at the earliest clinical disease stages, or even to precede the onset of changes in cortical brain activity. Should the latter be the case, this would not only improve our understanding of the cascade of changes in brain activity and connectivity in PD, but also provide us with an earlier biomarker of disease activity. In addition, if subcortical changes are present in addition to cortical changes, it would be of interest to know whether subcortical changes are leading or lagging the cortical changes and how this relates to a decline in clinical measures of disease progression.

Second, many previous findings were based on cross-sectional data. Although it is possible to reconstruct a time-line of functional changes using multiple cross-sectional data points, this carries the risk of introducing bias in the analysis (e.g. differences in group characteristics between study cohorts or differences in outcome measures due to site-specific differences in measuring techniques). Therefore, the conclusions that can be drawn from this type of study are generally less reliable than those derived from longitudinal studies. The previous MEG studies in this PD cohort had a follow-up duration of approximately four years and demonstrated that cortical slowing and loss of functional connectivity were correlated with cognitive decline and motor dysfunction.[28,31] However, it was not clear whether the observed trends in neurophysiological changes would be maintained with further disease progression. This issue could be addressed by adding data obtained at a third time point to the analysis. Moreover, the heterogeneous baseline disease duration of the patients in the PD cohort allowed an analysis using a so-called *multiple longitudinal design*. Adding a third time point would lead to an individual follow-

up duration of seven years, and at the same time would enable us to obtain a better view of the changes in brain activity and connectivity over the whole range of disease durations of about 20 years.

Third, in a previous fMRI analysis, a global decrease in functional connectivity was found, which correlated with worsening cognitive function.[35] In addition, it was shown that domain-specific cognitive dysfunction correlated with differences in interactions between cortical resting-state networks.[37,48] However, it remained to be established how interactions between cortical and subcortical resting-state networks would relate to domain-specific cognitive decline.

Fourth, an emerging topic in PD research is the influence of (symptomatic) treatment on brain activity and connectivity in relation to changes in clinical measures of motor and non-motor function, not only to better understand its mechanism, but also to map its effects. Deep brain stimulation (DBS) of the subthalamic nucleus (STN) is an effective surgical intervention for motor symptoms in PD,[49,50] but can induce negative cognitive and psychiatric side effects in up to 25% of patients, among which apathy is the most prevalent.[51] These side-effects can partly be explained by the fact that multiple functional systems (emotional-affective, cognitive, motor) converge in the subthalamic nucleus.[52,53] Each DBS electrode generally has four stimulation (also: contact) points and electrodes are generally implanted bilaterally.[54] Clinical improvement and side effects differ from one contact point to another, but the cause of these effects is only partly understood. At present, it may take months to identify the optimal DBS settings via trial and error, as stimulation-related non-motor effects may take long to develop, in contrast to the effects on motor function that can appear rather quickly upon changes in stimulation settings. DBS can induce changes in brain activity and connectivity on a minute scale, which probably extend beyond the motor system.[55-57] It was an open question whether these 'acute changes' in brain activity could reflect non-motor side effects that take longer to develop. If a relation between the location of the stimulated contact point and brain activity/connectivity was found, then this could aid in the process of selection of the optimal contact point. In addition, it would improve our knowledge on the structural and functional brain networks involved in PD symptoms as well as in the side effects of STN-DBS.

Research questions

The main objectives of this thesis were to gain more insight into the functional brain mechanisms related to motor and non-motor symptoms in PD, as well as its progression over the course of the disease, both from a cortical and a subcortical perspective. In addition, we wanted to determine the neurophysiological effects of DBS on the PD brain in relation to clinical parameters of motor and non-motor functioning. We studied whether MEG can be used to measure DBS effects on brain activity and functional connectivity, in order to answer the question if MEG could aid in the process of selecting

the optimal contact point. Furthermore, studying the neurophysiological and clinical effects of manipulation of a subcortical brain structure such as the STN would add to our knowledge of the pathophysiology of PD and, hence, might provide a stepping-stone towards new treatments.

We addressed the following main research questions:

1. Which EEG biomarkers of PD progression have been reported in the literature?
2. What are the insights derived from previous MEG studies in PD and which knowledge gaps can we identify?
3. What is the longitudinal relationship between the development of changes in brain activity and connectivity in cortical vs subcortical brain regions, and what is their relationship with clinical measures of disease progression?
4. Are subcortical changes leading or lagging the cortical changes and how does this relate to a decline in clinical measures of disease progression?
5. How do altered functional interactions between resting-state brain networks, including subcortical brain regions, relate to domain-specific cognitive decline, and how do they develop over the course of the disease?
6. Does DBS in PD patients induce changes in brain activity and connectivity (measured using MEG) and what is the relationship of these changes with motor improvement and non-motor side effects?
7. Does a change in stimulation location in PD patients treated with DBS produce acute changes in brain activity and connectivity that can be detected with MEG?

Patients, methods and outline of the thesis

The studies described in this thesis were performed in two study cohorts of PD patients. The first cohort consisted of a total of 61 non-demented PD patients and 21 healthy controls who were longitudinally followed for seven years. These subjects underwent repeated motor and cognitive assessments, as well as MEG recordings, at baseline and at two follow-up visits scheduled four and seven years after the baseline visit. MEG recordings performed at the third time point were performed on a different recording system than recordings at the first two time points. fMRI recordings were performed during the second and third study visit.

The second cohort consisted of a group of 29 PD patients treated with STN-DBS. The patients underwent pre-operative as well as post-operative clinical assessments (motor, psychiatric, cognitive; the same for both study visits) six months after surgery. A minimum of six months after surgery, MEG recordings were performed in ten conditions: stimulation ON using the regular DBS settings of the patient, stimulation OFF, and during stimulation at each of the eight (four on each side) individual contact points. Figure 4 provides an overview of the conditions in which data were obtained from the second cohort.

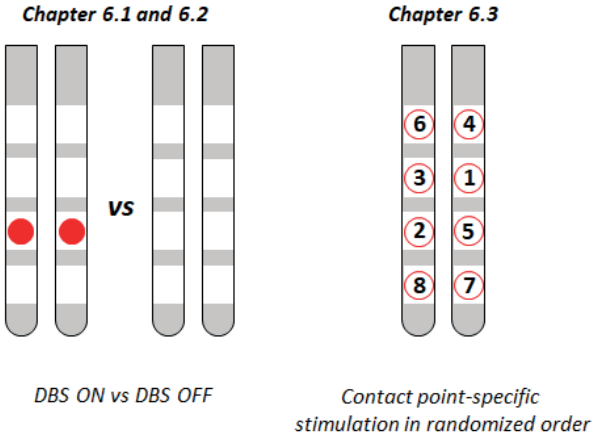

Figure 4 Overview of the conditions in which data were obtained from the second study cohort

In **chapter 2.1** we performed a systematic review on EEG findings in PD, in which we identified the reported biomarkers of clinical PD symptoms. In **chapter 2.2** we systematically reviewed the MEG literature on PD to obtain an overview of the neurophysiological characteristics of PD (in relation to clinical symptoms, disease progression, and treatment effects).

In **chapter 3.1** we determined the feasibility to longitudinally analyze MEG data that had been recorded using two different MEG systems in eight healthy controls, using both spectral and functional connectivity metrics. Next, in **chapter 3.2** we analyzed the MEG data of 61 PD patients obtained using two different recording systems over a follow-up period of seven years. Including 61 non-demented PD patients with variable disease durations and using a multiple longitudinal analysis allowed us to obtain a view of the changes in brain activity and connectivity over a disease duration of approximately 20 years. Using this approach, we aimed to determine whether neurophysiological changes involving subcortical brain regions would precede the changes in cortical brain regions. In addition to studying the changes in both cortical and subcortical brain activity over time, we analyzed their association with clinical measures of disease severity.

In **chapters 4 and 5** we focused specifically on cognitive decline and the role of functional connectivity changes in subcortical brain regions. In **chapter 4** we describe an MEG study in which we applied a novel functional connectivity measure to assess directed functional connectivity, i.e. the direction/balance of information flow. We performed these analyses in 34 late-stage PD patients and 12 healthy controls with a specific focus on the role of subcortical brain regions in cognitive decline. In **chapter 5** we report on a study using fMRI recordings obtained from 50 PD patients at the second, and 31 patients at the third study visit. We aimed to longitudinally assess functional interactions between cortical

and subcortical resting-state brain networks, in relation to domain-specific cognitive functioning. We also included a new measure of time-varying fluctuations in functional connectivity, so-called dynamic functional connectivity.

In the second part of the thesis we focused on the final two research questions. First, we studied the effects of DBS on brain activity and connectivity in PD patients recorded using MEG, including the relationship with clinical (side) effects. Secondly, we addressed the question whether we would be able to detect neurophysiological effects of changes in DBS stimulation location using MEG. **Chapter 6.1** is a description of a study in which we analyzed which DBS stimulation-related changes in functional connectivity were correlated with optimal clinical effect on motor symptoms in eighteen PD patients. In **chapter 6.2** we report on a study to assess whether apathy, which is highly prevalent after DBS, could be an effect of the stimulation itself. We analyzed this in 26 PD patients by correlating the stimulation location (structural) and the changes in functional connectivity of three pre-selected brain regions, known to be associated with apathy, with changes in apathy scores after DBS. Lastly, in **chapter 6.3** we describe a study in which we explored whether switching the active stimulation site to another contact point would lead to measurable changes in brain activity and connectivity. We analyzed this by (1) observing the effects within a single subject, and (2) by correlating the position of the active contact points with spectral power and functional connectivity measures at a group level.

In **chapter 7** we summarize and discuss the results presented in the preceding chapters, and provide suggestions for future research.

References

1. Global, regional, and national burden of neurological disorders, 1990-2016: a systematic analysis for the Global Burden of Disease Study 2016. Lancet Neurol. 2019;18(5):459-80.
2. Dorsey ER, Sherer T, Okun MS, et al. The Emerging Evidence of the Parkinson Pandemic. J Parkinsons Dis. 2018;8(s1):S3-s8.
3. Postuma RB, Berg D, Stern M, et al. MDS clinical diagnostic criteria for Parkinson's disease. Mov Disord. 2015;30(12):1591-601.
4. Chaudhuri KR, Healy DG, Schapira AH. Non-motor symptoms of Parkinson's disease: diagnosis and management. Lancet Neurol. 2006;5(3):235-45.
5. Weintraub D, Aarsland D, Chaudhuri KR, et al. The neuropsychiatry of Parkinson's disease: advances and challenges. Lancet Neurol. 2022;21(1):89-102.
6. Braak H, Del Tredici K, Rüb U, et al. Staging of brain pathology related to sporadic Parkinson's disease. Neurobiol Aging. 2003;24(2):197-211.
7. Doty RL, Deems DA, Stellar S. Olfactory dysfunction in parkinsonism: a general deficit unrelated to neurologic signs, disease stage, or disease duration. Neurology. 1988;38(8):1237-44.
8. Svenningsson P, Westman E, Ballard C, et al. Cognitive impairment in patients with Parkinson's disease: diagnosis, biomarkers, and treatment. Lancet Neurol. 2012;11(8):697-707.
9. Aarsland D, Kurz MW. The epidemiology of dementia associated with Parkinson's disease. Brain Pathol (Zurich, Switzerland). 2010;20(3):633-9.
10. Aarsland D, Larsen JP, Karlsen K, et al. Mental symptoms in Parkinson's disease are important contributors to caregiver distress. Int J Geriatr Psychiatry. 1999;14(10):866-74.
11. Maidment I, Fox C, Boustani M. Cholinesterase inhibitors for Parkinson's disease dementia. Cochrane Database Syst Rev. 2006(1):Cd004747.
12. Locascio JJ, Corkin S, Growdon JH. Relation between clinical characteristics of Parkinson's disease and cognitive decline. J Clin Exp Neuropsychol. 2003;25(1):94-109.
13. Bohnen NI, Kaufer DI, Hendrickson R, et al. Cognitive correlates of cortical cholinergic denervation in Parkinson's disease and parkinsonian dementia. J Neurol. 2006;253(2):242-7.
14. Bohnen NI, Albin RL. The cholinergic system and Parkinson disease. Behav Brain Res. 2011;221(2):564-73.
15. Kehagia AA, Barker RA, Robbins TW. Neuropsychological and clinical heterogeneity of cognitive impairment and dementia in patients with Parkinson's disease. Lancet Neurol. 2010;9(12):1200-13.
16. Chaudhuri KR, Schapira AH. Non-motor symptoms of Parkinson's disease: dopaminergic pathophysiology and treatment. Lancet Neurol. 2009;8(5):464-74.
17. Czernecki V, Pillon B, Houeto JL, et al. Motivation, reward, and Parkinson's disease: influence of dopatherapy. Neuropsychologia. 2002;40(13):2257-67.
18. Meyer A, Zimmermann R, Gschwandtner U, et al. Apathy in Parkinson's disease is related to executive function, gender and age but not to depression. Front Aging Neurosci. 2014;6:350.
19. Bullmore E, Sporns O. The economy of brain network organization. Nat Rev Neurosci. 2012;13(5):336-49.
20. Schnitzler A, Gross J. Normal and pathological oscillatory communication in the brain. Nat Rev Neurosci. 2005;6(4):285-96.
21. Fries P. A mechanism for cognitive dynamics: neuronal communication through neuronal coherence. Trends Cogn Sci. 2005;9(10):474-80.
22. Damoiseaux JS, Rombouts SA, Barkhof F, et al. Consistent resting-state networks across healthy subjects. Proc Natl Acad Sci U S A. 2006;103(37):13848-53.
23. van den Heuvel MP, Stam CJ, Kahn RS, et al. Efficiency of functional brain networks and intellectual performance. J Neurosci. 2009;29(23):7619-24.

24. Fox MD, Snyder AZ, Vincent JL, et al. The human brain is intrinsically organized into dynamic, anticorrelated functional networks. Proc Natl Acad Sci U S A. 2005;102(27):9673-8.
25. Stoffers D, Bosboom JL, Deijen JB, et al. Slowing of oscillatory brain activity is a stable characteristic of Parkinson's disease without dementia. Brain. 2007;130(Pt 7):1847-60.
26. De Micco R, Agosta F, Basaia S, et al. Functional Connectomics and Disease Progression in Drug-Naïve Parkinson's Disease Patients. Mov Disord. 2021;36(7):1603-16.
27. Neufeld MY, Blumen S, Aitkin I, et al. EEG frequency analysis in demented and nondemented parkinsonian patients. Dementia. 1994;5(1):23-8.
28. Olde Dubbelink KT, Stoffers D, Deijen JB, et al. Cognitive decline in Parkinson's disease is associated with slowing of resting-state brain activity: a longitudinal study. Neurobiol Aging. 2013;34(2):408-18.
29. Klassen BT, Hentz JG, Shill HA, et al. Quantitative EEG as a predictive biomarker for Parkinson disease dementia. Neurology. 2011;77(2):118-24.
30. Caviness JN, Hentz JG, Belden CM, et al. Longitudinal EEG changes correlate with cognitive measure deterioration in Parkinson's disease. J Parkinsons Dis. 2015;5(1):117-24.
31. Olde Dubbelink KT, Stoffers D, Deijen JB, et al. Resting-state functional connectivity as a marker of disease progression in Parkinson's disease: A longitudinal MEG study. Neuroimage Clin. 2013;2:612-9.
32. Geraedts VJ, Marinus J, Gouw AA, et al. Quantitative EEG reflects non-dopaminergic disease severity in Parkinson's disease. Clin Neurophysiol. 2018;129(8):1748-55.
33. Stoffers D, Bosboom JL, Deijen JB, et al. Increased cortico-cortical functional connectivity in early-stage Parkinson's disease: an MEG study. Neuroimage. 2008;41(2):212-22.
34. Yassine S, Gschwandtner U, Auffret M, et al. Functional Brain Dysconnectivity in Parkinson's Disease: A 5-Year Longitudinal Study. Mov Disord. 2022;37(7):1444-53.
35. Olde Dubbelink KT, Schoonheim MM, Deijen JB, et al. Functional connectivity and cognitive decline over 3 years in Parkinson disease. Neurology. 2014;83(22):2046-53.
36. Tessitore A, Esposito F, Vitale C, et al. Default-mode network connectivity in cognitively unimpaired patients with Parkinson disease. Neurology. 2012;79(23):2226-32.
37. Baggio HC, Segura B, Sala-Llonch R, et al. Cognitive impairment and resting-state network connectivity in Parkinson's disease. Hum Brain Mapp. 2015;36(1):199-212.
38. de Haan W, Mott K, van Straaten EC, et al. Activity dependent degeneration explains hub vulnerability in Alzheimer's disease. PLoS Comput Biol. 2012;8(8):e1002582.
39. Esposito F, Tessitore A, Giordano A, et al. Rhythm-specific modulation of the sensorimotor network in drug-naive patients with Parkinson's disease by levodopa. Brain. 2013;136(Pt 3):710-25.
40. Prell T. Structural and Functional Brain Patterns of Non-Motor Syndromes in Parkinson's Disease. Front Neurol. 2018;9:138.
41. Cools R. Dopaminergic modulation of cognitive function-implications for L-DOPA treatment in Parkinson's disease. Neurosci Biobehav Rev. 2006;30(1):1-23.
42. Pizzo F, Roehri N, Medina Villalon S, et al. Deep brain activities can be detected with magnetoencephalography. Nat Commun. 2019;10(1):971.
43. Hillebrand A, Barnes GR. Beamformer analysis of MEG data. Int Rev Neurobiol. 2005;68:149-71.
44. Hillebrand A, Barnes GR, Bosboom JL, et al. Frequency-dependent functional connectivity within resting-state networks: an atlas-based MEG beamformer solution. Neuroimage. 2012;59(4):3909-21.
45. Hillebrand A, Singh KD, Holliday IE, et al. A new approach to neuroimaging with magnetoencephalography. Hum Brain Mapp. 2005;25(2):199-211.
46. Boon LI, Hillebrand A, Dubbelink KTO, et al. Changes in resting-state directed connectivity in cortico-subcortical networks correlate with cognitive function in Parkinson's disease. Clin Neurophysiol. 2017;128(7):1319-26.

47. Hillebrand A, Nissen I, Ris-Hilgersom I, et al. Detecting epileptiform activity from deeper brain regions in spatially filtered MEG data. Clin Neurophysiol. 2016;127(8):2766-9.
48. Baggio HC, Sala-Llonch R, Segura B, et al. Functional brain networks and cognitive deficits in Parkinson's disease. Hum Brain Mapp. 2014;35(9):4620-34.
49. Benabid AL, Koudsie A, Benazzouz A, et al. Deep brain stimulation of the corpus luysi (subthalamic nucleus) and other targets in Parkinson's disease. Extension to new indications such as dystonia and epilepsy. J Neurol. 2001;248 Suppl 3:Iii37-47.
50. Deuschl G, Schade-Brittinger C, Krack P, et al. A randomized trial of deep-brain stimulation for Parkinson's disease. N Engl J Med. 2006;355(9):896-908.
51. McIntyre CC, Hahn PJ. Network perspectives on the mechanisms of deep brain stimulation. Neurobiol Dis. 2010;38(3):329-37.
52. Bevan MD, Clarke NP, Bolam JP. Synaptic integration of functionally diverse pallidal information in the entopeduncular nucleus and subthalamic nucleus in the rat. J Neurosci. 1997;17(1):308-24.
53. Kolomiets BP, Deniau JM, Mailly P, et al. Segregation and convergence of information flow through the cortico-subthalamic pathways. J Neurosci. 2001;21(15):5764-72.
54. Odekerken VJ, van Laar T, Staal MJ, et al. Subthalamic nucleus versus globus pallidus bilateral deep brain stimulation for advanced Parkinson's disease (NSTAPS study): a randomised controlled trial. Lancet Neurol. 2013;12(1):37-44.
55. Abbasi O, Hirschmann J, Storzer L, et al. Unilateral deep brain stimulation suppresses alpha and beta oscillations in sensorimotor cortices. Neuroimage. 2018;174:201-7.
56. Hirschmann J, Ozkurt TE, Butz M, et al. Distinct oscillatory STN-cortical loops revealed by simultaneous MEG and local field potential recordings in patients with Parkinson's disease. Neuroimage. 2011;55(3):1159-68.
57. Cao CY, Zeng K, Li DY, et al. Modulations on cortical oscillations by subthalamic deep brain stimulation in patients with Parkinson disease: A MEG study. Neurosci Lett. 2017;636:95-100.
58. Diamond A. Executive Functions. Annu Rev Psychol. 2013;64(1):135-68.
59. Bhatia KP, Marsden CD. The behavioural and motor consequences of focal lesions of the basal ganglia in man. Brain. 1994;117 (Pt 4):859-76.
60. Engelborghs S, Marien P, Pickut BA, et al. Loss of psychic self-activation after paramedian bithalamic infarction. Stroke. 2000;31(7):1762-5.
61. Ghika-Schmid F, Bogousslavsky J. The acute behavioral syndrome of anterior thalamic infarction: a prospective study of 12 cases. Ann Neurol. 2000;48(2):220-7.
62. Chudasama Y, Robbins TW. Functions of frontostriatal systems in cognition: comparative neuropsychopharmacological studies in rats, monkeys and humans. Biol Psychol. 2006;73(1):19-38.
63. Pennartz CM, Berke JD, Graybiel AM, et al. Corticostriatal Interactions during Learning, Memory Processing, and Decision Making. J Neurosci. 2009;29(41):12831-8.
64. Levy R, Dubois B. Apathy and the Functional Anatomy of the Prefrontal Cortex–Basal Ganglia Circuits. Cerebral Cortex. 2005;16(7):916-28.
65. Czernecki V, Pillon B, Houeto JL, et al. Motivation, reward, and Parkinson's disease: influence of dopatherapy. Neuropsychologia. 2002;40(13):2257-67.
66. Czernecki V, Schupbach M, Yaici S, et al. Apathy following subthalamic stimulation in Parkinson disease: a dopamine responsive symptom. Mov Disord. 2008;23(7):964-9.
67. Pagonabarraga J, Kulisevsky J, Strafella AP, et al. Apathy in Parkinson's disease: clinical features, neural substrates, diagnosis, and treatment. Lancet Neurol. 2015;14(5):518-31.
68. Pauling L, Coryell CD. The Magnetic Properties and Structure of Hemoglobin, Oxyhemoglobin and Carbonmonoxyhemoglobin. Proc Natl Acad Sci U S A. 1936;22(4):210-6.
69. Damoiseaux JS, Rombouts SA, Barkhof F, et al. Consistent resting-state networks across healthy subjects. Proc Natl Acad Sci U S A. 2006;103(37):13848-53.

70. Hyvärinen A. Independent component analysis: recent advances. Philos Trans A Math Phys Eng Sci. 2013;371(1984):20110534.
71. Hillebrand A, Tewarie P, Van Dellen E, et al. Direction of information flow in large-scale resting-state networks is frequency-dependent. Proc Natl Acad Sci U S A. 2016;113(14):3867-72.

CHAPTER 2.1

Clinical correlates of quantitative EEG in Parkinson's disease: a systematic review

Victor J Geraedts, Lennard I Boon, Johan Marinus, Alida A Gouw, Jacobus J van Hilten, Cornelis J Stam, Martijn R Tannemaat, Maria Fiorella Contarino

Neurology 2018:871-883
DOI: 10.1212/WNL.0000000000006473

Abstract

Objective To assess the relevance of quantitative electroencephalography (qEEG) measures as outcomes of disease severity and progression in PD.

Methods Main databases were systematically searched (January 2018) for studies of sufficient methodological quality that examined correlations between clinical symptoms of idiopathic PD and cortical (surface) qEEG metrics.

Results Thirty-six out of 605 identified studied were included. Results were classified into four domains: cognition (23 studies), motor function (13 studies), responsiveness to interventions (7 studies), and other (10 studies). In cross-sectional studies, EEG slowing correlated with global cognitive impairment and with diffuse deterioration in other domains. In longitudinal studies, decreased dominant frequency and increased θ power, reflecting EEG slowing, were biomarkers of cognitive deterioration at an individual level. Results on motor dysfunction and treatment yielded contrasting findings. Studies on functional connectivity at an individual level, longitudinal studies on other domains or on connectivity measures, were lacking.

Conclusions qEEG parameters reflecting EEG slowing, particularly decreased dominant frequency and increased θ power, correlate with cognitive impairment and predict future cognitive deterioration. QEEG could provide reliable and widely available biomarkers for non-motor disease severity and progression in PD, potentially promoting early diagnosis of non-motor symptoms and an objective monitoring of progression. More studies are needed to clarify the role of functional connectivity and network analyses.

Introduction

Parkinson's disease (PD) is a complex multisystem neurodegenerative disease characterized by motor features and non-motor symptoms[1] such as cognitive impairment, neuropsychiatric disturbances and sleep abnormalities.[2] Non-motor symptoms can present early in the disease course, worsen with advancing disease, and largely do not improve on dopaminergic treatment, suggesting that they may more accurately reflect severity and progression of the underlying disease.[3] To date, there are no reliable objective biomarkers for disease progression in PD.

By definition, a biomarker is objectively measured and evaluated as an indicator of normal biological processes, pathophysiological processes, or pharmacologic response to a therapeutic intervention.[4] Quantitative biomarkers may identify systems at-risk before overt expression of the disorder. Ideally, biomarkers are cheap, unsusceptible to bias, widely available and non-invasive. Electroencephalography (EEG) combines these aspects[5] and provides insight into cortical dysfunction by measuring brain activity directly.[6] Quantitative analyses of brain rhythms measured by EEG (qEEG) provide not only spectral information of cortical rhythms, but also additional data on regional or whole-brain synchronization ("connectivity") of brain activity. Connectivity-derived graph-theory matrices quantify the efficiency of such functional networks (Figure 1).[7] If detectable, early signs of cortical dysfunction may serve as prognostic markers of future clinical deterioration, thereby reducing diagnostic delay and improving patient management.

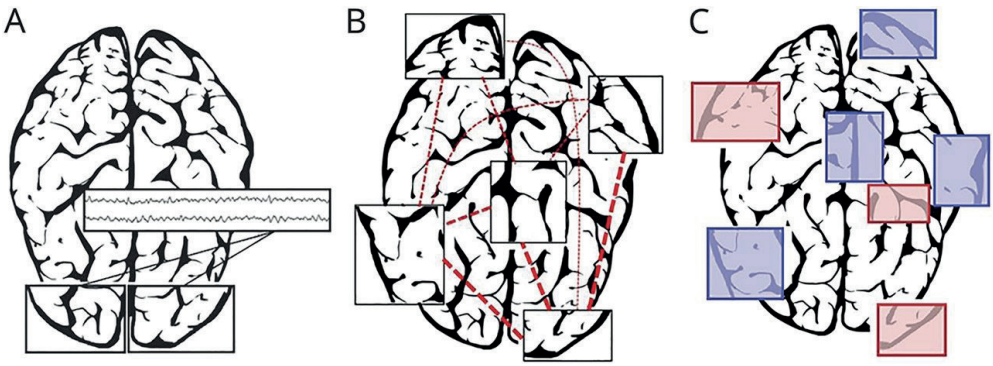

Figure 1 Principles of quantitative EEG analyses (A) *Spectral analyses:* an estimation of the amount of oscillations at given frequencies via a Fast Fourier Transformation (FFT), generally expressed as either power per frequency-band (i.e. δ 0.5–4.0 Hz, θ 4.0–8.0 Hz, α 8.0–13.0 Hz, β 13.0–30.0 Hz), or as a dominant frequency (i.e. FFT peak). (B) *Connectivity analyses:* an assessment of the strength of functional connections between individual electrodes / brain regions (red dashed lines) throughout the brain to quantify brain synchronization. Connectivity-strength can be low (i.e. thin dashed line) compared to high connectivity (e.g. occipital regions (thicker lines)). Functional connectivity is typically assessed within separate frequency-bands. (C) *Network analyses:* whole-brain networks derived from connectivity analyses are reflected in a coherent 'graph' which accounts for hierarchy and can therefore identify which brain regions are most important, i.e. 'hub-nodes' (red), or less important, i.e. 'non-hub-nodes' (blue).

Previous studies explored correlations of qEEG features with domains such as motor impairment[8,9] or cognition[10-12] in PD patients. However, there is a wide variety in EEG acquisition-methodology, processing and analysis, and patient population. Moreover, most studies focus primarily on reporting results rather than emphasizing methodological quality and reproducibility. The relationship between qEEG and its clinical correlates remains unclear; there is no complete overview of associations between cortical EEG rhythms and clinical symptoms of PD. In this systematic review, we aim to present a comprehensive overview of studies of sufficient methodological quality on clinical correlates of resting-state qEEG in PD. Particularly, we evaluate the relevance of this method to characterize brain function and connectivity as reliable and easy utilizable outcomes of PD severity and progression.

Methods

In this systematic review we adhered to the Preferred Reporting Items for Systematic Reviews and Meta-Analyses (PRISMA) guidelines (http://www.prisma-statement.org/) (checklist available from Dryad (Appendix 1)).

Data sources and search

PubMed, Embase, Web of Science, COCHRANE Library, Emcare, Academic Search Premier and Sciencedirect were systematically searched for potentially relevant studies up to January 2, 2018 (date of search), using appropriate keywords (data available from Dryad (Appendix 2)).

Study selection

Eligibility was initially assessed by screening titles and abstracts, based on the following inclusion criteria: (1) data available on cohorts with idiopathic PD of at least 10 patients; (2) original research; (3) quantitative cortical (surface) EEG measures analyzed; (4) article in English or German; (5) qEEG data on correlations with clinical symptoms. A clinical correlate was defined as a correlation with an important clinical symptom, therapy or disease-specific characteristic relevant to PD. Two exclusion criteria were used: (1) no resting state EEG; (2) analysis focusing exclusively on local field potentials (LFP). Task-based methodology was excluded because it is difficult to standardize, often semi-quantitative and thereby subject to observer-bias. LFPs recordings measure activity from subcortical structures rather than cortical. The use of implantable electrodes makes them invasive and thereby less attractive as a biomarker.

Data extraction and risk of bias assessment

Screening of titles and abstracts was performed by two independent reviewers (VJG and LIB). Data extraction was performed using piloted forms (forms available from

Dryad (Appendix 3)). Inclusion for full-text screening was decided after discussion of discrepancies and re-reading of the pertinent sections until mutual agreement was reached. Cohen's kappa for interrater agreement was calculated.

Results were categorized in the following domains: cognition, motor function, responsiveness to interventions, and 'other'. For purposes of clarity, terms like 'Background Rhythm Frequency', 'peak frequency', 'mean frequency' and 'median frequency' have been designated as 'dominant frequency' in this review.

Risk of bias was assessed using the Checklist for Case Series developed by the Joanna Briggs Institute (JBI),[13] extended with an item addressing clear reporting of EEG acquisition conditions allowing for reproducibility (data available from Dryad (Appendix 4)). The quality threshold for inclusion was set at six or more 'yes' responses in total, provided that at least one 'yes' response was obtained for items 1-3, at least two 'yes' responses for items 4-8, and a 'yes' for the item on EEG acquisition.

Results

Search results and study characteristics

The initial search yielded 605 studies; 123 of these studies were examined in detail, after which 36 remained for final inclusion (Figure 2). Interrater agreement κ was 0.713. Reasons for exclusion were: no resting-state EEG (n=26); no correlation of EEG measures to clinical symptoms of PD (n=21); insufficient methodological quality (n=15); no separate measures of cortical activity (e.g. only coupling with EMG) (n=10); no separate idiopathic PD cohorts of more than 10 patients (n=7); no original research (n=4); and LFP-focused analysis (n=4).

The selected studies are detailed in table 1. Nine studies were classified as medium quality studies (JBI=6), 21 as high quality (JBI 7-8) and six as very high quality (JBI 9-10). Seventeen articles were case-control studies, 13 case-series, and six longitudinal follow-up (FU) studies (table 1).

Results were categorized into 'cognition' (n=23), 'motor function' (n=13), 'responsiveness to interventions' (n=7), and 'other' (not otherwise specified) (n=10). The studied qEEG measures are defined in table 2.

Table 1 Selected studies

Reference	Region, Country	Study type	N (PD)	Psycho-active drugs	Age (years)	Classic band power definitions	EEG in ON or OFF	Quality	Comments
Cozac et al.[33]	Basel, Switzerland	FU	37		67		?	**	High-density EEG (256 electrodes)
Cozac et al.[43]	"	CC	54	?	68		?	**	High-density EEG (214 electrodes)
Eichelberger et al.[29]	"	CS	57	?	67	No	?	**	High-density EEG (256 electrodes)
Hatz et al.[40]	"	CS	40	?	68		ON	**	High-density EEG (256 electrodes)
Filipovic et al.[39]	Belgrade, Yugoslavia	CS	24		50	No	OFF	**	
Pozzi et al.[25]	Buenos Aires, Argentina	CC	47		65		ON	**	
Fonseca et al.[23]	Campinas, Brazil	CC	32		67	No	ON	**	
Fonseca et al.[42]	"	CC	32		68	No	ON	*	
Babiloni et al.[34]	Cassino, Italy	CC	13	?	72		ON	*	
Mostile et al.[19]	Catania, Italy	CC	34	?	66		Both	*	L-dopa naïve patients
Bonanni et al.[10]	Chieti, Italy	FU	35		70		ON	**	
Arnaldi et al.[32]	Genoa, Italy	FU	54	?	69	?	?	**	
He et al.[21]	Guangzhou, China	CC	135	Yes	60		?	**	
He et al.[37]	"	CC	52	Yes	46		ON	**	Early-onset PD patients
Helkala et al.[16]	Kuopio, Finland	CC	18	Yes	68	No	?	**	
Soikkeli et al.[26]	"	CC	36	Yes	72	No	?	*	
Gagnon et al.[41]	Montreal, Canada	CC	15		64		Both	***	Low-density EEG (2 electrodes)
Latreille et al.[12]	"	FU	68	?	65		OFF	**	Low-density EEG (12 electrodes)
Moisello et al.[9]	New York, USA	CC	15	?	61		ON	*	High-density EEG (256 electrodes)
Jech et al.[8]	Prague, Czech Republic	CS	12	?	57	No	Both	*	
Hassan et al.[28]	Rennes, France	CS	124	?	66		ON	**	High-density EEG (128 electrodes)
Melgari et al.[35]	Rome, Italy	CS	24		73		Both	**	
Stanzione et al.[20]	"	CC	19		64	No	OFF	**	

Reference	Region, Country	Study type	N (PD)	Psycho-active drugs	Age (years)	Classic band power definitions	EEG in ON or OFF	Quality	Comments
George et al.[38]	San Diego, USA	CC	16	?	63	?	Both	**	
Swann et al.[48]	"	CC	15	?	63		Both	**	Low-density EEG (2 electrodes)
Caviness et al.[14]	Scottsdale, USA	CS	66		76		ON	**	
Caviness et al.[11]	"	FU	71		74		ON	***	
Caviness et al.[22]	"	CS	134		76		ON	***	
Klassen et al.[31]	"	FU	106		76		ON	***	
Utianski et al.[30]	"	CS	88		76		ON	*	
Neufeld et al.[24]	Tel-Aviv, Israel	CS	20		72	No	OFF	*	
Guner et al.[15]	Tepecik, Turkey	CC	45		67		ON	**	
Kamei et al.[17]	Tokyo, Japan	CS	32	?	70	No	?	**	
Morita et al.[36]	"	CS	106	?	68	No	?	***	
Morita et al.[18]	"	CS	100		68	No	?	***	
Tanaka et al.[27]	Zürich, Switzerland	CC	29		66	No	ON	*	

*CC: Case Control, CS: Case series, FU: follow-up; HC: healthy controls; *: JBI=6; **: JBI=7-8; ***: JBI=9-10*
Classic band power ranges was defined as: δ: ± 0.5-4 Hz, θ: 4-8 Hz, α 8-13 Hz, β: 13- ±30 Hz

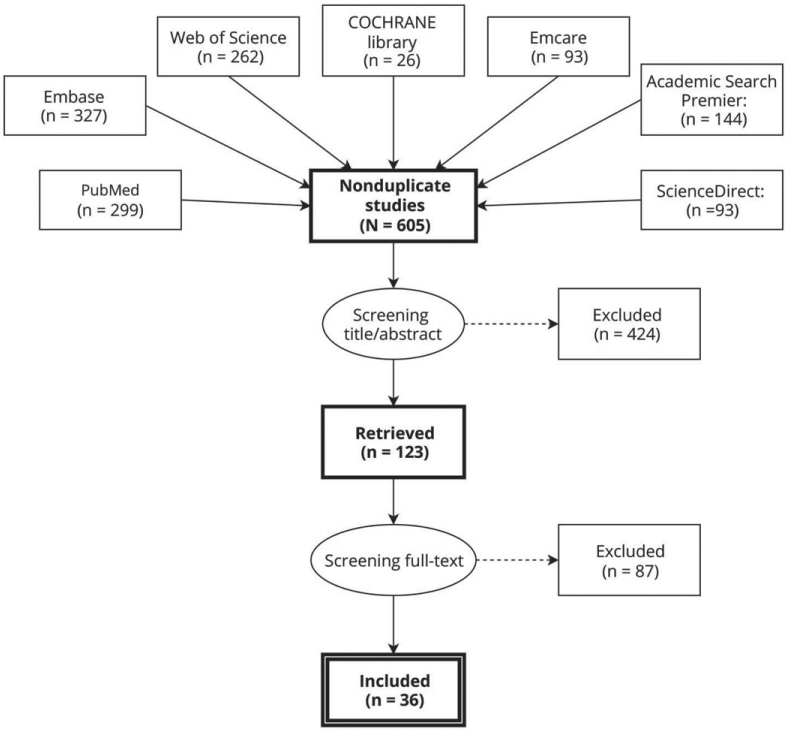

Figure 2 PRISMA flow diagram of selected studies

Cognition

Nineteen cross-sectional studies investigated cognitive function. Increased EEG slowing correlated with severity of cognitive impairment, defined as lower scores on global cognitive tests or tests evaluating separate cognitive domains,[11, 12, 14-21] or with the patients cognitive state (either cognitively normal (NCOG), Mild Cognitive Impairment (MCI) or PD Dementia (PDD)) (Figure 3, Supplementary Table 1)).[14,21-28] Five studies (four different cohorts) described a spectral ratio of fast-over-slow EEG power correlating positively with cognition,[12,15,17,18,29] although in one study the results depended on the cognitive test within the same domain (i.e. either Clock Drawing Test or Block Design Test for visuospatial abilities).[29] Four out of five studies found that a higher dominant frequency correlated positively with cognition.[12,14,20,26] A fifth study reported that five out of seven cognitive tests correlated positively with dominant frequency, while the other two tests showed no correlation.[16] EEG slowing reflected by specific frequency bands, i.e. either increased δ (± 0.5–4 Hz) or θ (4–8 Hz) power, or decreased α (8–13 Hz) or β (13– ±30 Hz) power, showed a trend towards reflecting cognitive dysfunction, although these results were inconsistent. Especially in the β range results were inconclusive, with three studies reporting a positive correlation between a higher absolute and relative β power and a better cognitive function,[14,16,26] contrasted by six studies that found no correlation.[12,20-24]

Table 2 Definition of qEEG metrics

Spectral analyses	*Band power*		Reflects the amount of oscillations within a given frequency band, typically assessed with a Fast Fourier Transformation (FFT). Power can be absolute, or relative (as a fraction of total power).
	Dominant frequency		The frequency with the most oscillations (dominant peak in the FFT spectrum), typically between 4 and 13 Hz.
Connectivity	*Index of lateralization (IL)*		Reflects EEG asymmetry by calculating power-differences between homologous pairs of EEG-electrodes.
	Phase Lag Index (PLI)		Assesses differences in relative phase distribution around 0 phase difference between brain regions.
	Phase Locking Value (PLV)		Absolute value of phase differences between brain regions.
	Coherence		The level of consistency between brain regions for relative amplitude and phase.
Network	*Edge-Wise Connectivity Index (EWCI)*		$EWCI = \sum_i^n \mathrm{Wi\ x\ 100}$, in which N is the number of edges in the subnetwork and W_i is the weight of edge i in the network. Defines the sum of weights of the (significant) subnetwork.
	Weighted Network (WN)	*γ*	Normalized weighted clustering coefficient (all weights divided by the maximum weight): functional connectivity between neighboring nodes.
		λ	Normalized characteristic path length (all weights divided by the maximum weight): average weight of shortest paths between any two nodes within the network.
		K_w	Weighted degree divergence: reflects the broadness of weighted degree distribution.
		Modularity	Ratio of inter-group connections over total number of edges.
	Minimum Spanning Tree	*Betweenness Centrality*	Number of paths between all other nodes in the MST crossing the node of interest, divided by the total number of paths in the MST.
		Diameter	Longest distance between any two nodes in the MST network.
		Eccentricity	Maximum distance between a node and any other node in the MST.
		Leaf fraction	Ratio between number of leaf nodes (only one edge) divided by the total number of nodes within the MST.
		Tree hierarchy	T_h = leaf number / (2m B_{max}), in which m is the number of edges and B_{max} is the highest betweenness centrality of any node in the tree. Defines hierarchy of the MST organization (optimal topology.
		Degree	Number of edges for each node divided by maximum number of possible edges.

One study (n=88, JBI=6)) compared connectivity and graph theory metrics, i.e. Phase-Lag-Index (PLI), Weighted Network (WN) and Minimum Spanning Trees (MST), with cognitive status (PDD vs. PD-NCOG).[30] Reduced synchronization and network integration, particularly in the α1 band (8–10 Hz), were observed in cognitively impaired patients, although whether the sign of the correlation was positive or negative depended on the type of measure studied. This well-defined cohort was used in four other studies reviewed here.[11,14,22,31] A different large study (n=124, JBI=7) investigated Phase-Locking-Value (PLV) and Edge-Wise Connectivity Index (EWCI).[28] Lower α1 and α2 (network) edge-wise connectivity correlated with lower cognitive state, whilst global-level PLV-derived

network-metrics were not correlated. EWCI correlated positively with outcomes of cognitive tests. More basic connectivity measures such as signal asymmetry did not correlate with global cognitive tests.[19]

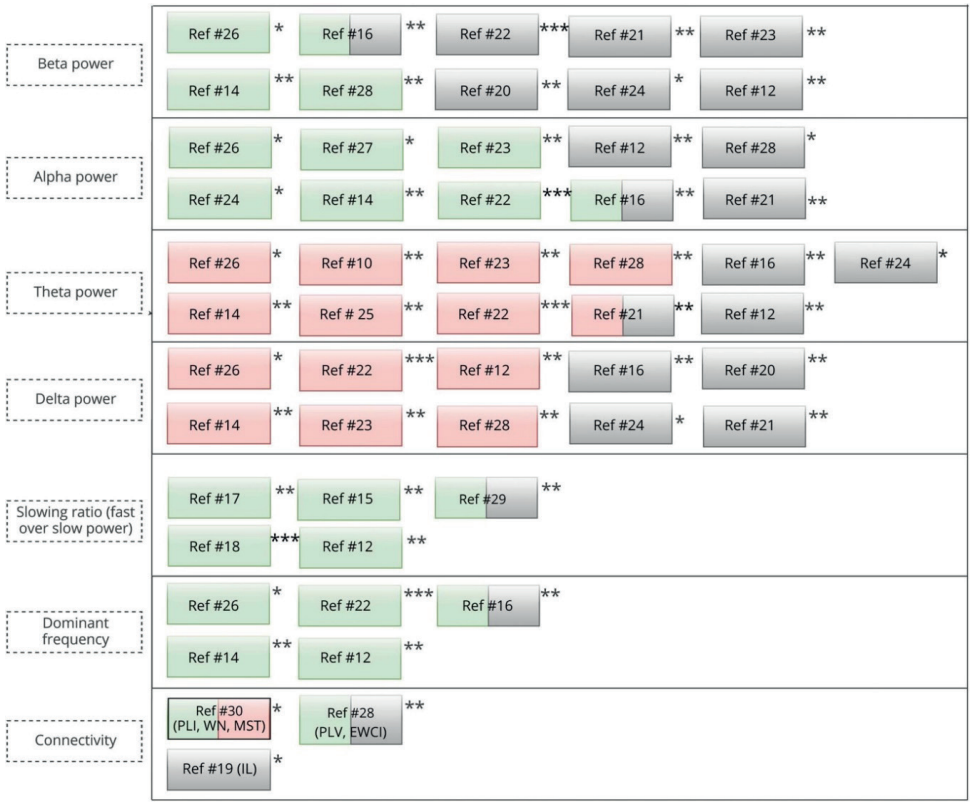

Figure 3 Correlation of qEEG measures with cognition
Green indicates that the measure is positively correlated with cognition, red indicates that the measure is negatively correlated with cognition, grey indicates no correlation. Dual-shaded boxes indicate that the sign of the correlation varied per test and/or variable. One asterisk indicates 'medium quality' (JBI); two indicates 'high quality' and three indicates 'very high quality'.
EWCI: Edge-Wise Connectivity Index, IL: Index of Lateralization, MST: Medium Spanning Tree, PLI: Phase Lag Index, PLV: Phase Locking Value, wMNE: weighted Minimum Norm Estimation, WN: Weighted Network

Longitudinal cognitive assessment

Five studies investigated qEEG measures as predictors of cognitive functioning (Figure 4, Supplementary Table 2)). Four studies investigated the predictive effect of a baseline qEEG measure[12,31-33] and one study correlated longitudinal changes in EEG rhythms to change in cognition over time.[11]

In three studies, dominant frequency at baseline correlated with cognitive deterioration.[11,12,31] Likewise, higher θ power at baseline predicted cognitive deterioration

in three studies.[11,31,33] A machine-learning algorithm, applying a random forest classifier, identified θ power as the most important classifying feature, although no corresponding model accuracy was reported.[33] A survival analysis showed that dominant frequency was predictive of cognitive worsening with an accuracy of 92% (sensitivity 84%, specificity 80%).[32] One study examined spectral powers and dominant frequency, but did not report the predictive value of these measures.[10]

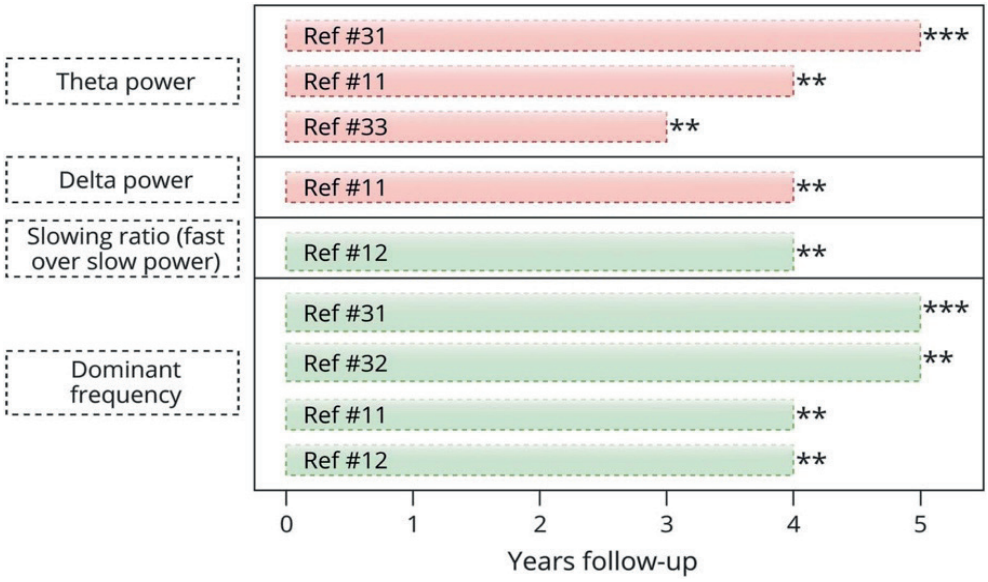

Figure 4 Correlation of qEEG measures with cognition in longitudinal follow-up studies
Green indicates that the measure is positively correlated with cognition, red indicates that the measure is negatively correlated with cognitive performance. Grey indicates no correlation. One asterisk indicates 'medium quality' (JBI); two indicates 'high quality' and three indicates 'very high quality'. The length of the bars reflects the length of the follow-up duration. All studies investigated the predictive value of baseline EEG measures, with the exception of Caviness et al.[11] which investigated the effect of change in spectral measures over time on longitudinal change in cognitive function.

Motor function

Thirteen cross-sectional studies investigated a relation between motor function and qEEG (Figure 5, Supplementary Table 3)). Across studies, no consistent pattern of relations emerged between qEEG variables and measures of the motor domain. Four studies found no significant correlations between spectral powers and MDS-UPDRS III subscores or HY stage.[15,20,24,34] Levodopa-induced increases of α and β power correlated with decreased MDS-UPDRS III subscores in one study.[35] Global dominant frequency correlated negatively with the rigidity subscore in one small study (n=12, JBI=6).[8] A ratio of fast-over-slow EEG power correlated negatively to HY stage in two studies using identical participants (mean HY stage 2.7).[18,36] HY stage further correlated positively with α2 amplitude (n=32, JBI=7), [23] β power (n=52, JBI=8)[37] or θ power (n=135, JBI=7),[21] the latter

only at three electrode positions (T5, F4 and O1). β band coherence correlated positively with MDS-UPDRS III scores in one study (n=16, JBI=7),[38] which was not supported by another study including early-onset PD patients (n=52, JBI=8)[37] β band power asymmetry correlated positively with HY stage, whilst θ band asymmetry correlated negatively. EEG asymmetry was not correlated to MDS-UPDRS III composite scores (n=34, JBI=6) in any frequency band, although motor asymmetry was not examined.[19]

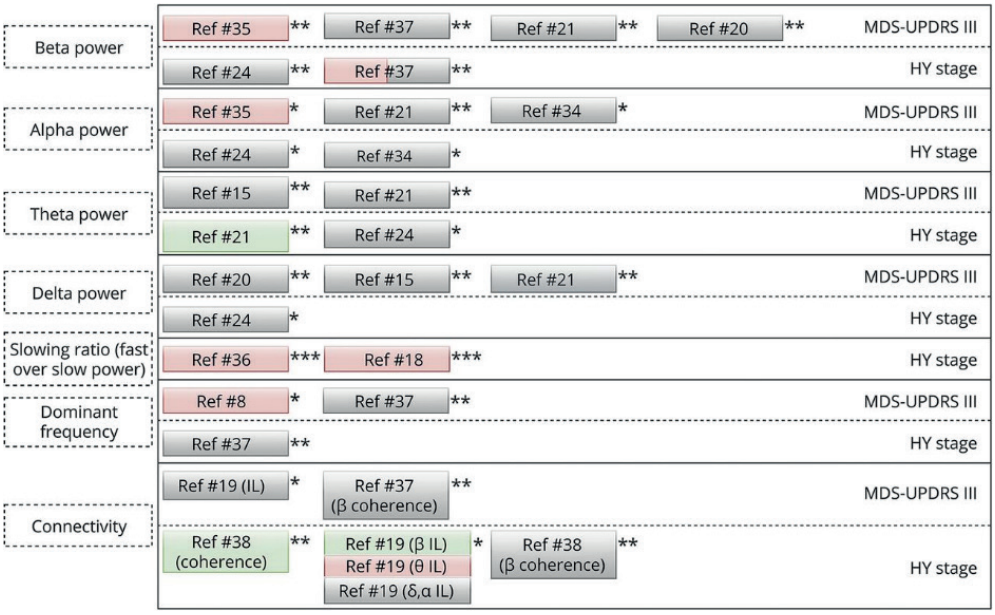

Figure 5 Correlation of quantitative EEG measures with motor functioning
Green indicates that the measure is positively correlated with motor impairment; red indicates that the measure is negatively correlated with motor impairment; gray indicates no correlation. Dual-shaded boxes indicate that the sign of the correlation varied per test and/or variable. One asterisk indicates medium quality (Joanna Briggs Institute); 2 indicates high quality; 3 indicates very high quality. HY = Hoehn & Yahr; IL = index of lateralization; MDS-UPDRS III = Movement Disorders Society–Unified Parkinson's Disease Rating Scale III.

Responsiveness of qEEG measures to interventions

Five studies investigated responsiveness of qEEG measures to both L-dopa and dopamine agonists (Figure 6, Supplementary Table 4)). Two studies found no effect of long-term oral dopaminergic treatment on spectral measures.[18,20] In contrast, α and β power increased within 60 minutes of L-dopa administration in one study (n=24, JBI=8),[35] and the L-dopa short-duration response correlated positively with α band power asymmetry.[19] L-dopa administration reduced β and γ band coherence, which was increased in PD patients compared to healthy controls in the same study.[38]

Two studies evaluated the responsiveness of qEEG measures to Deep Brain Stimulation (DBS). Switching DBS 'ON' increased dominant frequency amplitude in one study (n=12,

JBI=6), although the level of frequency changes depended on the EEG derivation.[8] DBS 'ON' increased frontal and parietal β power in another study (n=15, JBI=8). In both studies, DBS-related artifacts were observed.

Overall, no consistent pattern of responsiveness of qEEG variables was found for oral- or DBS treatment.

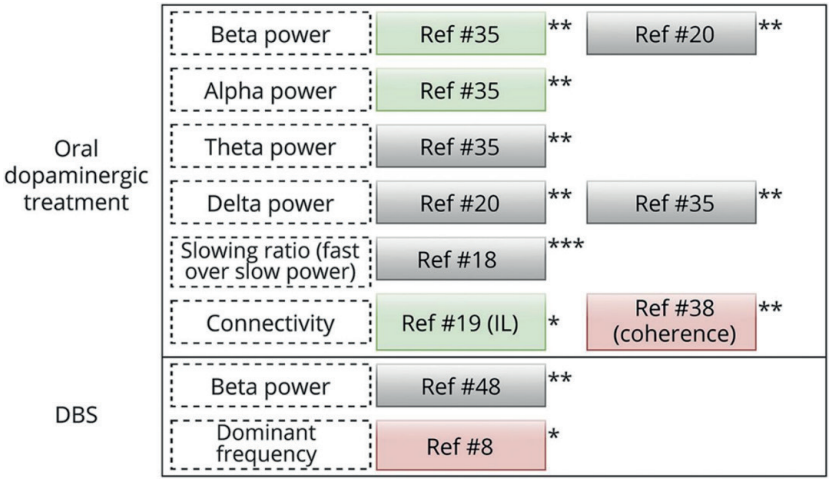

Figure 6 Correlation of qEEG measures with treatment
Green indicates that the measure is positively correlated with treatment administration; red indicates that the measure is negatively correlated with treatment; gray indicates no correlation. One asterisk indicates medium quality (JBI); 2 indicates high quality; and 3 indicates very high quality. DBS = deep brain stimulation; IL = index of lateralization.

Other clinical measures

Ten studies investigated a variety of other clinical measures (Supplementary Table 5). Longer disease duration correlated with higher β power in one study (n=15, JBI=6),[9] while in three larger studies of higher quality no significant relation emerged.[18,21,37] Depressed PD patients demonstrated lower α1 (7.5–10 Hz) power than non-depressed patients in one study (n=24, JBI=7),[39] whereas the Hamilton Rating Scale for Depression did not correlate with EEG asymmetry in another study (n=34, JBI=6).[19] Higher apathy scores correlated with higher δ power, but not with other spectral measures in one study. Apathy scores correlated negatively with α2 PLI and α2 WN metrics. PLI classified mild vs. low apathy groups (median-split) with an accuracy of 82.5% (sensitivity 70% and specificity 90%).[40] A high-quality (JBI=10) study showed that PD patients with REM sleep behavior disorder (RBD) had a higher (wakefulness) θ power and lower dominant frequency compared to PD patients without RBD.[41] No correlation of coherence with quality of life (as assessed with the QoL-AD) was found in one study (n=32, JBI=6).[42] Olfactory function did not correlate with resting-state qEEG in one study (n=20, JBI=7).[43]

Discussion

The present systematic review included 36 studies examining relations between resting-state qEEG measures and clinical features of PD. The cognitive domain was studied most extensively. Both global and domain-specific cognitive impairments correlated with EEG slowing, i.e. lower α and β power and higher δ and θ power. PD patients with dementia had markedly slower EEGs than patients with a normal cognitive function. QEEG values of MCI patients were ranged between those of PD-NCOG and PDD, likely reflecting the transitional nature of MCI.[14,22,23,31] It should be noticed that these correlations partly depended on the used measurement instrument, as demonstrated by discrepant results obtained when using MoCA or MMSE scores in the same study.[21] It remains unclear which EEG metric best reflects oscillatory slowing and shows the strongest correlation with cognition. Spectral ratios showed consistent significant correlations with cognition across all pertaining studies, whereas other spectral measures, such as the power in individual spectral bands, showed minor inconsistencies between studies. Although relative power reflects a ratio of a certain spectrum band to total band power, a spectral ratio such as (α + β) / (δ + θ) encompasses a larger range of the EEG spectrogram than individual spectral bands and is therefore more informative and may provide a better reflection of EEG slowing. When using individual band powers, assessing both absolute- and relative band powers seems appropriate, according to the aim of the analysis, to facilitate direct comparison between individuals or to more accurately identify the actual changes that occurred within a specific frequency band. However, activity above 20 Hz is frequently affected by tonic scalp and neck muscle activity. The individual β and γ band ranges may reflect EMG activity rather than cortical oscillations.[44] Consideration of possible EMG artifacts is therefore required when interpreting spectral power above 20 Hz.[44]

Presence or severity of cognitive impairment correlated with desynchronization in the α bands and reduced network integration,[28,30] but the sign and strength of the correlation depended strongly on the type of connectivity variable analyzed. Based on the findings of this review, there is still insufficient evidence for the use of measures of connectivity as a biomarker of cognitive function. Careful consideration of the methodology is required when interpreting results on connectivity or network metrics, as exemplified by significant results for edge-wise level network measures (uncorrected for volume conduction) which were not observed on global-level (unweighted) network metrics in the same study.[28]

Ideally, qEEG measures would provide prognostic biomarkers of future clinical deterioration. Five studies reported longitudinal data on cognition and qEEG.[11,12,31-33] A slower dominant frequency was shown to be particularly predictive of future cognitive deterioration, both at group level and at an individual level.[11,12,31,32] These findings have also been replicated using MEG.[45] However, although several studies reported 'biomarkers' of cognitive deterioration, only two studies reported biomarkers at an individual level: both θ power[33] and dominant frequency could predict cognitive decline for individual patients.[32] Both measures can be calculated relatively easily in a clinical setting. Whether the utility

of dominant frequency and θ power as a biomarker for cognitive decline is similar for every stage of cognitive decline is unknown. We recommend that these variables are interpreted as indicators of potential cognitive decline that warrant further investigation, rather than definitive proof of a transition to a different cognitive state.

Findings on correlations of qEEG and motor dysfunction were inconclusive. Overall, EEG variables did not significantly correlate with the MDS-UPDRS III total score; the only two studies that reported significant correlations had methodological limitations associated with the small sample size[8] or confounding drug-induced spectral changes.[35] Whether spectral differences between ON-medication and OFF-medication state are induced by medication directly or due to improved motor function currently remains unknown. Correlations with HY motor stage were either non-significant, or showed an association between cortical slowing and increased global dysfunction, suggesting that disease progression may have been the underlying cause of both. The correlation of motor function and connectivity depended on the type of connectivity measures, exemplified by a positive correlation with HY stage and β power asymmetry, a negative correlation with θ power asymmetry and a non-significant correlation with δ and α power asymmetry.[19] Compared to the cognitive domain which involves interactions between large sections of the cortex, motor function is less well reflected by cortical regions other than the motor cortex. Although basal ganglia activity may influence cortical rhythms, resting state qEEG likely has insufficient spatial resolution to pick up focal oscillatory alterations related to motor dysfunction. Task-based registrations, e.g. evaluating μ rhythm, may be more sensitive to reflect motor activity.[46] Techniques with a higher spatial resolution such as MEG or LFPs recording may be more useful, but are less applicable as clinical tools since they are not widely available or invasive.

The effect of treatment on qEEG measures remains equally unclear. Four studies investigated ON-OFF transition, but comparability is limited by differences in design, patient population and qEEG measures. Again, results on connectivity were highly dependent on the type of connectivity measures. This is not surprising, given that the characteristics of connectivity measures are highly variable and may be subject to volume conduction (e.g. synchronization likelihood, PLV, coherence), non-linearity (coherence), and distinction of direct or indirect relations (coherence, PLV, PLI). Phase-based measures, such as PLI, are robust against volume conduction and thereby less sensitive to spurious interactions, and are therefore recommended. Additionally, PLI does not depend on signal-amplitudes although small phase-differences may be missed with increasing noise.[47] Subsequent network metrics that are robust against the effect of network density may be useful, such as MST metrics. Careful consideration of the individual advantages and disadvantages of different connectivity measures is advised.[47]

Both studies on DBS were limited by DBS-related artifacts and require further verification. Especially in these studies, volume conduction may account for the spreading of β power over the frontoparietal EEG electrodes.[48] Moreover, MEG studies showed that DBS

induces artifacts within the β band range.[49] Other clinical characteristics, including disease duration and depression, were studied in a limited number of studies with inconsistent findings. Whereas the correlation between spectral measures and cognitive function emerged as robust, this was not the case for other disease- or clinically-related features.

Limitations of available studies

Several potential confounders across studies may have influenced the results, such as variability in the age range of patients. Since the effect of aging on EEG slowing is well-known, this should be consistently taken into account in the analysis. Various studies did not report whether patients took psychoactive medication, whereas others mentioned that these drugs were withdrawn 48 hours prior to registration.[21,37] In two studies, however, the use of psychoactive medication was allowed,[16,26] which might have influenced the results.[50] As it may not always be safe or ethical to withdraw psychoactive medication, we recommend that studies account for the use of these drugs during their analyses.

Another confounder could be the different definitions of spectral variables used. Three studies on cognition defined dominant frequency as Background Rhythm Frequency (BRF). However, two other studies (investigating the same cohort) defined BRF as the dominant peak in the FFT average at electrodes P3, P4 and Oz by means of visual inspection.[11,31] Another study defined BRF as the dominant α peak at positions O1 and O2.[12] While visual inspection limits reproducibility, the FFT peak may lie outside the α-range in case of severe EEG slowing and may inaccurately reflect the true 'dominant' frequency. Comparability between studies may thus be improved by a uniform definition of 'dominant frequency', e.g. the FFT peak within the range of 4–13 Hz, at similar electrode positions (e.g. O1 and O2 to capture the dominant α peak). Likewise, different cutoff values for frequency bands were used in various studies: 20 studies used classic band power definitions (i.e. δ: ± 0.5-4 Hz, θ: 4-8 Hz, α 8-13 Hz, β: 13- ±30 Hz), whilst 14 studies used non-consecutive band power definitions (e.g. δ: ± 1.17-3.91 Hz, θ: 4.30-7.81 Hz, α 8.20-12.89 Hz, β: 13.28-30.08 Hz).[17,18,36] Two studies did not describe band power definitions.[8,32] Although the differences are small, consecutive band power definitions warrants that all spectral information is included, but may lead to overflowing of one frequency band into another.[31] However, using a pre-defined interval may result in loss of potentially interesting data, e.g. when the Fast Fourier Transformation (FFT) peak lies in the out-filtered range. Consecutive band power definitions warrant that the crucial FFT peak is analyzed, which is required for correct interpretation of the EEG spectrogram. To this end, we find the use of an average FFT both more practical and accurate with respect to other methods.

MEG-studies demonstrated oversynchronization in early-stage PD patients (relative to controls) which reversed with disease progression, indicating a non-linear correlation of connectivity to clinical symptoms.[51,52] Although this pattern has not been studied with EEG, these results implicate that the disease stage of the source population needs to be considered when assessing connectivity.[52]

Another issue concerned the definition of the outcomes, for example the classification of PD-MCI. This classification varied over time,[53] which resulted in the Movement Disorders Society delineating diagnostic criteria for PD-MCI in 2012.[54] The variable definitions of MCI used in seven studies may account for discrepancies in results.

Several studies investigated qEEG metrics at electrode-level rather than focal areas of several electrodes.[9,21,35,37,48] Adjacent electrodes are influenced by common sources or volume conduction and are therefore dependent on the type of reference used. We speculate that the use of global EEG measures may be more informative of widespread cortical involvement (α-synucleiopathy), rather than focal EEG measures.[55] Moreover, the use of single references, such as the central electrode or the mastoid, may be influenced by brain activity and therefore affect the difference in electric potential between electrodes. Whereas spectral analyses are less dependent on the choice of reference, the choice of reference influences both the strength and directionality of functional connectivity.[47] Although the choice of reference may have little clinical consequences, the scientific (pathophysiological) background of these correlations may be limited. Re-referencing towards a source derivation can aid in correctly interpreting localization of findings.[47]

The use of different setups, e.g. polysomnographic registration with two electrodes versus high-density acquisition, may not be directly comparable. The choice of setup depends both on the clinical correlation of interest and on the type of EEG analysis. In case of spectral analyses, we recommend a standard 21-electrode setup to allow sufficient spatial resolution whilst maintaining proper source localization. This setup is also readily utilizable in a clinical setting. For connectivity and network analyses, higher density setups may improve accuracy in identifying brain networks, but careful consideration of source reconstruction is required.[47]

Strengths and limitations of this review

Strengths of our systematic review include the use of the PRISMA guideline, the application of a systematic search strategy and the use of a validated risk of bias assessment tool. When interpreting the findings of this review, it should be considered that differences between studies in (non-standard) methods of EEG acquisition and/or the use of psychoactive medication may have influenced the results. In addition, our review excluded studies with task-based registrations to improve comparability between studies; however, previous literature suggests that centralization and network integration may be task-dependent.[56]

Applicability to clinical practice and knowledge gaps

QEEG is widely available, relatively inexpensive, and easily reproducible. As depression and RBD may manifest early in the course of PD,[2] the few observations supporting associations between qEEG variables and both RBD[41] and depression[19,39] suggests that oscillatory changes may also be present early in the disease course. Moreover, since

RBD may be a risk factor for cognitive impairment in patients with PD,[57] the EEG slowing observed in PD patients with RBD[41] may be an early indicator of cognitive deterioration. The observation that EEG slowing precedes the development of PDD in the absence of clinically manifest dementia supports the notion that qEEG alterations may have predictive value early in the disease course. One study reported that patients with PDD who received rivastigmine to improve cognitive performance showed increases in α power. However, improvements in cognition were not significantly correlated with qEEG changes.[58] This study did not meet our inclusion criteria and was excluded from this review. Whether the pattern of qEEG slowing related to cognitive impairment is reversible, either with medication or cognitive training, remains unknown.

Spectral analyses may be applied as biomarkers of future (cognitive) deterioration and be utilized to complement current evaluation strategies. Desynchronization patterns reflecting altered connectivity may be more domain-specific but have been sparsely studied. Moreover, interpretation of either desynchronization or oversynchronization may be more difficult than evaluation of spectral changes in widespread clinical practice. There is currently limited evidence for utilizing qEEG to reflect non-cognitive domains or to apply connectivity measures as biomarkers. Moreover, the pattern of correlation is highly dependent on the type of connectivity measure; careful consideration of the nature of the connectivity measure is required for correct interpretation.[47] Future research should focus on studying functional connectivity and network measures to further explore biomarker specificity, and assess the utility scope of advanced EEG analyses. The accuracy of qEEG in reflecting progression of non-cognitive symptoms over time remains unresolved and should be further studied. Solid large prospective studies with sufficient follow-up and longitudinal assessments of other non-cognitive domains, which are currently lacking, should be performed. Big data analysis, i.e. artificial neural networks, machine learning, and deep learning, may further play a role in identifying specific prognostic biomarkers of clinical symptoms. Given the variability in design and analysis in the described studies, standardization in both acquisition and reporting may improve comparison between studies.[59] In order to ensure reliable data analysis, careful selection of epochs free of artifacts or automatic artifact detection is crucial.

The use of qEEG as a biomarker in PD likely reflects cortical α-synucleiopathy. Other biomarkers may reflect different aspects of PD pathology, such as cardiac scintigraphy reflecting α-synucleiopathy in the peripheral nervous system. The use of complementary biomarkers may identify different systems-at-risk and may be studied in parallel.

The observed qEEG changes may not be specific for PD patients, although qEEG differentiates between other neurodegenerative diseases such as Alzheimer's Disease and dementia with Lewy Bodies with high accuracy.[60] However, a comparison of qEEG changes between these pathologies was not considered to be a clinical symptom related to PD and therefore beyond the scope of this review.

Conclusion

The correlation between qEEG and cognitive impairment is well established: a lower dominant frequency or increased θ power is correlated with cognition and is predictive of future cognitive deterioration also at the individual level.

At present, there is insufficient evidence to support the use of qEEG metrics to examine other domains or treatment effects in PD patients. Functional connectivity and network analyses may have potential utility as novel specific biomarkers, but further studies are needed to investigate their clinical applicability.

Altogether the results of this review suggest that qEEG provide inexpensive, reliable, and widely available measures that could serve as biomarkers for non-motor disease severity in patients with PD. The availability of objective biomarkers of disease severity and progression in PD could directly contribute to patient management, potentially providing the opportunity of an early diagnosis of non-motor symptoms, a more reliable prognosis, and an objective monitoring of progression, both in the context of clinical practice and clinical trials.

References

1. Barone P, Antonini A, Colosimo C, et al. The PRIAMO study: A multicenter assessment of nonmotor symptoms and their impact on quality of life in Parkinson's disease. Mov Disord. 2009;24(11):1641-9.
2. Chaudhuri KR, Healy DG, Schapira AH, et al. Non-motor symptoms of Parkinson's disease: diagnosis and management. Lancet Neurol. 2006;5(3):235-45.
3. van der Heeden JF, Marinus J, Martinez-Martin P, et al. Importance of nondopaminergic features in evaluating disease severity of Parkinson disease. Neurology. 2014;82(5):412-8.
4. Biomarkers and surrogate endpoints: preferred definitions and conceptual framework. Clin Pharmacol Ther. 2001;69(3):89-95.
5. Mikolajewska E, Mikolajewski D. Non-invasive EEG-based brain-computer interfaces in patients with disorders of consciousness. Mil Med Research. 2014;1:14.
6. Stam CJ. Nonlinear Brain Dynamics. New York: Nova Science; 2006.
7. Stam CJ, Tewarie P, Van Dellen E, et al. The trees and the forest: Characterization of complex brain networks with minimum spanning trees. Int J Psychophysiol. 2014;92(3):129-38.
8. Jech R, Ruzicka E, Urgosik D, et al. Deep brain stimulation of the subthalamic nucleus affects resting EEG and visual evoked potentials in Parkinson's disease. Clin Neurophysiol. 2006;117(5):1017-28.
9. Moisello C, Blanco D, Lin J, et al. Practice changes beta power at rest and its modulation during movement in healthy subjects but not in patients with Parkinson's disease. Brain Behav. 2015;5(10):e00374.
10. Bonanni L, Thomas A, Tiraboschi P, et al. EEG comparisons in early Alzheimer's disease, dementia with Lewy bodies and Parkinson's disease with dementia patients with a 2-year follow-up. Brain : a J Neurol. 2008;131(Pt 3):690-705.
11. Caviness JN, Hentz JG, Belden CM, et al. Longitudinal EEG changes correlate with cognitive measure deterioration in Parkinson's disease. J Parkinsons Dis. 2015;5(1):117-24.
12. Latreille V, Carrier J, Gaudet-Fex B, et al. Electroencephalographic prodromal markers of dementia across conscious states in Parkinson's disease. Brain. 2016;139(Pt 4):1189-99.
13. Critical Appraisal Checklist for Case Series 2016 [Available from: http://joannabriggs.org/research/critical-appraisal-tools.html.
14. Caviness JN, Hentz JG, Evidente VG, et al. Both early and late cognitive dysfunction affects the electroencephalogram in Parkinson's disease. Parkinsonism Relat Disord. 2007;13(6):348-54.
15. Guner D, Tiftikcioglu BI, Tuncay N, et al. Contribution of Quantitative EEG to the Diagnosis of Early Cognitive Impairment in Patients With Idiopathic Parkinson's Disease. Clin EEG Neurosci. 2017;**48**:348–354
16. Helkala E-L, Laulumaa V, Soikkeli R, et al. Slow-wave activity in the spectral analysis of the electroencephalogram is associated with cortical dysfunctions in patients with Alzheimer's disease. Behav Neurosci. 1991;105(3):409-15.
17. Kamei S, Morita A, Serizawa K, et al. Quantitative EEG analysis of executive dysfunction in Parkinson disease. J Clin Neurophysiol. 2010;27(3):193-7.
18. Morita A, Kamei S, Mizutani T. Relationship between slowing of the EEG and cognitive impairment in Parkinson disease. J Clin Neurophysiol. 2011;28(4):384-7.
19. Mostile G, Nicoletti A, Dibilio V, et al. Electroencephalographic lateralization, clinical correlates and pharmacological response in untreated Parkinson's disease. Parkinsonism Relat Disord. 2015;21(8):948-53.
20. Stanzione P, Marciani MG, Maschio M, et al. Quantitative EEG changes in non-demented Parkinson's disease patients before and during L-dopa therapy. European J Neurol. 1996;3(4):354-62.

21. He X, Zhang Y, Chen J, et al. Changes in theta activities in the left posterior temporal region, left occipital region and right frontal region related to mild cognitive impairment in Parkinson's disease patients. Int J Neurosci 2017;127:66-72.
22. Caviness JN, Utianski RL, Hentz JG, et al. Differential spectral quantitative electroencephalography patterns between control and Parkinson's disease cohorts. European J Neurol. 2016;23(2):387-92.
23. Fonseca LC, Tedrus GM, Letro GH, et al. Dementia, mild cognitive impairment and quantitative EEG in patients with Parkinson's disease. Clin EEG Neurosci. 2009;40(3):168-72.
24. Neufeld MY, Blumen S, Aitkin I, et al. EEG frequency analysis in demented and nondemented parkinsonian patients. Dementia (Basel, Switzerland). 1994;5(1):23-8.
25. Pozzi D, Petracchi M, Sabe L, et al. Quantified electroencephalographic changes in Parkinson's disease with and without dementia. European J Neurol. 1994;1(2):147-52.
26. Soikkeli R, Partanen J, Soininen H, et al. Slowing of EEG in Parkinson's disease. Electroencephalogr Clin Neurophysiol. 1991;79(3):159-65.
27. Tanaka H, Koenig T, Pascual-Marqui RD, et al. Event-related potential and EEG measures in Parkinson's disease without and with dementia. Dement Geriatr Cogn Dis. 2000;11(1):39-45.
28. Hassan M, Chaton L, Benquet P, et al. Functional connectivity disruptions correlate with cognitive phenotypes in Parkinson's disease. Neuroimage Clin. 2017;14:591-601.
29. Eichelberger D, Calabrese P, Meyer A, et al. Correlation of Visuospatial Ability and EEG Slowing in Patients with Parkinson's Disease. Parkinsons Dis. 2017;2017:3659784.
30. Utianski RL, Caviness JN, van Straaten ECW, et al. Graph theory network function in parkinson's disease assessed with electroencephalography. Clin Neurophysiol. 2016;127(5):2228-36.
31. Klassen BT, Hentz JG, Shill HA, et al. Quantitative EEG as a predictive biomarker for Parkinson disease dementia. Neurology. 2011;77(2):118-24.
32. Arnaldi D, De CF, Fama F, et al. Prediction of cognitive worsening in de novo Parkinson's disease: Clinical use of biomarkers. Mov Disord. 2017;32(12):1738-47.
33. Cozac VV, Chaturvedi M, Hatz F, et al. Increase of EEG Spectral Theta Power Indicates Higher Risk of the Development of Severe Cognitive Decline in Parkinson's Disease after 3 Years. Front Aging Neurosci. 2016;8:284.
34. Babiloni C, De Pandis MF, Vecchio F, et al. Cortical sources of resting state electroencephalographic rhythms in Parkinson's disease related dementia and Alzheimer's disease. Clin Neurophysiol. 2011;122(12):2355-64.
35. Melgari JM, Curcio G, Mastrolilli F, et al. Alpha and beta EEG power reflects L-dopa acute administration in parkinsonian patients. Front Aging Neurosci. 2014;6:302.
36. Morita A, Kamei S, Serizawa K, et al. The relationship between slowing EEGs and the progression of Parkinson's disease. J Clin Neurophysiol. 2009;26(6):426-9.
37. He X, Zhang Y, Chen J, et al. The patterns of EEG changes in early-onset Parkinson's disease patients. Int J Neurosci. 2017;127(11):1028-35.
38. George JS, Strunk J, Mak-McCully R, et al. Dopaminergic therapy in Parkinson's disease decreases cortical beta band coherence in the resting state and increases cortical beta band power during executive control. Neuroimage Clin. 2013;3:261-70.
39. Filipovic SR, Covickovic-Sternic N, Stojanovic-Svetel M, et al. Depression in Parkinson's disease: an EEG frequency analysis study. Parkinsonism Relat Disord. 1998;4(4):171-8.
40. Hatz F, Meyer A, Zimmermann R, et al. Apathy in Patients with Parkinson's Disease Correlates with Alteration of Left Fronto-Polar Electroencephalographic Connectivity. Front Aging Neurosci. 2017;9:262.
41. Gagnon JF, Fantini ML, Bedard MA, et al. Association between waking EEG slowing and REM sleep behavior disorder in PD without dementia. Neurology. 2004;62(3):401-6.
42. Fonseca LC, Tedrus GM, Rezende AL, et al. Coherence of brain electrical activity: a quality of life indicator in Alzheimer's disease? Arq Neuropsiquiatr. 2015;73(5):396-401.

43. Cozac VV, Auschra B, Chaturvedi M, et al. Among Early Appearing Non-Motor Signs of Parkinson's Disease, Alteration of Olfaction but Not Electroencephalographic Spectrum Correlates with Motor Function. Front Neurol. 2017;8:545.
44. Whitham EM, Lewis T, Pope KJ, et al. Thinking activates EMG in scalp electrical recordings. Clin Neurophysiol. 2008;119(5):1166-75.
45. Olde Dubbelink KT, Hillebrand A, Twisk JW, et al. Predicting dementia in Parkinson disease by combining neurophysiologic and cognitive markers. Neurology. 2014;82(3):263-70.
46. Kumar S, Riddoch MJ, Humphreys G. Mu rhythm desynchronization reveals motoric influences of hand action on object recognition. Front Hum Neurosci. 2013;7:66.
47. van Diessen E, Numan T, van Dellen E, et al. Opportunities and methodological challenges in EEG and MEG resting state functional brain network research. Clin Neurophysiol. 2015;126(8):1468-81.
48. Swann N, Poizner H, Houser M, et al. Deep brain stimulation of the subthalamic nucleus alters the cortical profile of response inhibition in the beta frequency band: a scalp EEG study in Parkinson's disease. J Neurosci. 2011;31(15):5721-9.
49. Cao CY, Zeng K, Li DY, et al. Modulations on cortical oscillations by subthalamic deep brain stimulation in patients with Parkinson disease: An MEG study. Neurosci Lett. 2017;636:95-100.
50. Galderisi S, Sannita WG. Pharmaco-EEG: A history of progress and a missed opportunity. Clin EEG Neurosci. 2006;37(2):61-5.
51. Stoffers D, Bosboom JL, Deijen JB, et al. Increased cortico-cortical functional connectivity in early-stage Parkinson's disease: an MEG study. Neuroimage. 2008;41(2):212-22.
52. Olde Dubbelink KT, Stoffers D, Deijen JB, et al. Resting-state functional connectivity as a marker of disease progression in Parkinson's disease: A longitudinal MEG study. NeuroImage Clin. 2013;2:612-9.
53. Petersen RC, Caracciolo B, Brayne C, et al. Mild cognitive impairment: a concept in evolution. Journal of intern med. 2014;275(3):214-28.
54. Litvan I, Goldman JG, Troster AI, et al. Diagnostic criteria for mild cognitive impairment in Parkinson's disease: Movement Disorder Society Task Force guidelines. Mov Disord. 2012;27(3):349-56.
55. Geraedts VJ, Marinus J, Gouw AA, et al. Quantitative EEG reflects non-dopaminergic disease severity in Parkinson's disease. Clin Neurophysiol. 2018;129(8):1748-55.
56. Fraga Gonzalez G, Van der Molen MJW, Zaric G, et al. Graph analysis of EEG resting state functional networks in dyslexic readers. Clin Neurophysiol. 2016;127(9):3165-75.
57. Gagnon JF, Vendette M, Postuma RB, et al. Mild cognitive impairment in rapid eye movement sleep behavior disorder and Parkinson's disease. Ann Neurol. 2009;66(1):39-47.
58. Fogelson N, Kogan E, Korczyn AD, et al. Effects of rivastigmine on the quantitative EEG in demented Parkinsonian patients. Acta Neurol Scand. 2003;107(4):252-5.
59. Keil A, Debener S, Gratton G, et al. Committee report: publication guidelines and recommendations for studies using electroencephalography and magnetoencephalography. Psychophysiology. 2014;51(1):1-21.
60. Dauwan M, van der Zande JJ, van Dellen E, et al. Random forest to differentiate dementia with Lewy bodies from Alzheimer's disease. Alzheimers Dement. 2016;4:99

Supplementary materials

We here provide Supplementary Tables 1-5. For appendix 1-4 we refer the reader to *doi.org/10.5061/dryad.29254rn.*

Supplementary Table 1 Correlation of qEEG and cognition

Reference	qEEG variable described	Main conclusions
Global cognition		
Bonanni et al.[10]	Rel. SP, dom. freq., CSA	**Fast θ**: PDD-F>PDD-NF
Caviness et al.[14]	Rel. SP, dom. freq.	**Dom. freq.**: PDD<PD-MCI<PD-NCOG. **δ**: PDD>PD-NCOG, PDD>PD-MCI. **θ**: PD-MCI>PD-NCOG. **α**:PDD<PD-NCOG. **β1** and **β2**: PDD<PD-NCOG, PD-MCI<PD-NCOG + corr.: MMSE with **BRF** and **α power**. Trails B score with **frontal δ and θ power**. CDT and JLO scores with **parietal δ power** - corr.: MMSE and **δ power**. No correlation: Stroop with **SP**.
Caviness et al.[22]	Dom. freq., Rel. SP	**Dom. freq.**: PDD<PD-PD-MCI<PD-NCOG. **δ**: PD-NCOG<PD-MCI<PDD. **θ**: PD-MCI>PD-NCOG, **α**: PD-NCOG>PD-MCI>PD-MCI
Eichelberger et al.[29]	Ratio (α / θ)	Lower **ratio** when incorrectly drawn CDT, lower **par. occ. ratio** with worse ROCF No corr.: **ratio** with block design test, digit span
Fonseca et al.[23]	Abs. and rel. SP	**Post. rel. δ**: PD-MCI<PDD, PD-NCOG<PDD. **Post. abs. δ**: PD-NCOG<PDD, PD-MCI<PDD. **Post. rel. θ**: PD-NCOG<PD-MCI, PD-NCOG<PDD. **Post. rel. α**: PD-NCOG>PDD
Guner et al.[15]	Ratio α/β over δ/θ power, abs. SP	+ corr.: **ratio** with MMSE. Extensive neuropsychological tests correlated weakly and diffusely with **ratio**
Hassan et al.[28]	Rel. SP, PLV, wMNE, EWCI	+ corr.: cognitive state and **δ, θ power, edge-wise level PLV-derived α1 and α2**. **EWCI** and cognitive score **-** corr.: cognitive state and **β power** No corr.: **α1 and α2 power** and cognitive state. **Global level PLV-derived P_L, C_c, Str, E_G**
He et al.[21]	Rel. SP	**Left post. temp., left occ.,** and **left front. θ**: PD-NCOG<PD-MCI - corr.: **θ F4** and **T5** with MOCA (particularly visuospatial function and attention). No corr.: **SP** with MMSE
Helkala et al.[16]	Abs. spect. amp., dom. freq.	+ corr: **α amp**. With WAIS VIQ and PIQ, visual and praxic functions and list learning. **β amp.** With WAIS VIQ and PIQ and list learning. **Dom. freq.** with WAIS VIQ, visual functions, speech understanding, list learning and category fluency
Kamei et al.[17]	Ratio (α + β) / (δ + θ)	+ corr.: **ratio** with BADS
Latreille et al.[12]	Abs. SP, ratio (δ +θ) / (α + β), dom. freq.	**δ, ratio**: PD-NCOG<PDD. **Dom. freq.:** PDD<PD-NCOG. No corr.: **qEEG** with extensive neuropsychological tests
Morita et al.[18]	Ratio (α + β) / (δ + θ)	+ corr.: **ratio** with MMSE
Mostile et al.[19]	IL	No corr.: **IL** with MMSE or FAB
Neufeld et al.[24]	Rel. SP	**α**: PD-NCOG>PDD
Pozzi et al.[25]	Abs. SP	**θ**: PD-NCOG<PDD
Soikkeli et al.[26]	Abs. and rel. SP, dom. freq.	**Abs.** and **rel. δ, rel. θ**: PD-NCOG<PDD. **Abs.** and **rel. α** and **β, dom. freq.:** PD-NCOG>PDD
Stanzione et al.[20]	Rel. SP, dom. freq.	No corr.: **δ** and **β1** with WCST

Reference	qEEG variable described	Main conclusions
Tanaka et al.[27]	Abs. SP	+ corr.: **total power** and **α** with intellectual status
Utianski et al.[30]	Phase-lag-index (PLI), weighted network (WN), minimum spanning tree (MST)	**α1 PLI**: PD-NCOG>PDD, **α1 WN (γ, λ, κ_w)**: PD-NCOG>PDD, **α1 WN (mod.)**: PD-NCOG<PDD, **α2 WN (mod.)**: PD-NCOG<PDD, **δ MST (BC)** PD-NCOG<PDD, **α1 MST (BC, leaf)**: PD-NCOG<PDD; **MST (diam., ecc.)**: PD-NCOG<PDD, **α2 MST (diam.)**: PD-NCOG<PDD. **δ** and **θ PLI**: PD-NCOG<PD-MCI, **α1 WN (γ, κ_w)**: PD-NCOG>PD-MCI), **α1 MST (leaf)**: PD-NCOG>PD-MCI. + corr.: **α1 PLI, α1 WN (γ, $\kappa_{w)}$, α2 WN (κ_w), δ MST (diam., ecc.)** with MMSE. **α1** and **α2 WN (γ), δ** and **α1 WN (κ_w)** and **θ** and **α1 MST (leaf)** with MOCA - corr.: **θ WN (γ), α1** and **α2 WN (mod.), δ MST (BC), α2 MST (diam., ecc.)** with MMSE. **δ** and **α1 WN (mod.)** and **θ** and **α1 MST (ecc.)** with MOCA

Supplementary Table 2 Longitudinal assessments

Reference	qEEG variable described	Main conclusions
Global cognition		
Arnaldi et al.[32]	Dom. freq.	**Dom. freq.:** 82% acc. In predicting cognitive outcome
Caviness et al.[11]	Change in dom. freq., change in Rel. SP (FU ±4 years)	**δ:** PD-incident dementia > PD-NCOG + corr.: change in **dom. freq**.with AVLT-LTM, Stroop - corr.: change in **δ** with MMSE, AVLT-LTM, Stroop, COWA, Trails B and CDT. Change in **θ** with Stroop. Change in **α** with Stroop. Change in **β** with AVLT-LTM
Cozac et al.[33]	GRMP	- corr.: **GRMP θ** with change-index overall cognition (3 years FU)
Klassen et al.[31]	Dom. freq., rel. SP	- corr.: **dom. freq**.with conversion to PDD (5 years FU) + corr.: **Θ** with conversion to PDD (5 years FU)
Latreille et al.[12]	Abs. SP, ratio (δ +θ) / (α + β), BRF	**Temp. ratio and BRF**: predict development PDD (4 years FU)

Supplementary Table 3 Motor function

Reference	qEEG variable described	Main conclusions
Motor function		
Babiloni et al.[34]	Rel. SP	No corr.: **α1** and MDS-UPDRS III or HY stage
Fonseca et al.[23]	Abs. and rel. SP	+ corr.: **post., frontotemp. and global α2** with HY stage
George et al.[38]	SP, coherence	+ corr.: **coherence** and MDS-UPDRS III
Guner et al.[15]	Ratio α/β over δ/θ power, abs. SP	No corr.: **δ and θ** and MDS-UPDRS III
He et al[21]	Rel. SP	+ corr.: **θ (T5, F4, O1)** with HY stage No corr.: **SP** and MDS-UPDRS III
He et al.[37]	Dom. freq., rel. SP	- corr.: **β with HY** no corr.: **rel. SP, β coherence, dom. freq**. with HY or MDS-UPDRS III
Jech et al.[8]	Dom. freq.	- corr.: **dom. freq.** and MDS-UPDRS III-rigidity
Melgari et al.[35]	Abs. SP	- corr.: post-L-dopa increase in **α (C4)** with rest tremor arms. Post-L-dopa increase in **β (C3, C4, P4)** with rigidity of arms and bradykinesia, **β (P3)** with rigidity of arms
Morita et al.[36]	Ratio (α + β) / (δ + θ)	- corr.: **ratio** with HY stage
Morita et al.[18]	Ratio (α + β) / (δ + θ)	- corr.: **ratio** with HY stage
Mostile et al.[19]	IL	+ corr.: **β IL (F3, F4)** with HY stage - corr.: **θ IL (F7, F8)** with HY stage No corr.: **IL** with MDS-UPDRS III
Neufeld et al.[24]	Rel. SP	No corr.: **SP** with HY stage
Stanzione et al.[20]	Rel. SP, dom. freq.	No corr.: **δ and β1** with MDS-UPDRS III or HY stage

Supplementary Table 4 Treatment

Reference	qEEG variable described	Main conclusions
George et al.[38]	SP, coherence	- corr.: **coherence** with L-dopa
Jech et al.[8]	Dom. freq	- corr.: **power of dom. freq.** with DBS
Morita et al.[18]	Ratio (α + β) / (δ + θ)	No corr.: **ratio** with L-dopa or DA
Melgari et al.[35]	Abs. SP	No corr.: **δ and θ** with L-dopa responsiveness + corr.: **α (C3, C4, T5, P3, P4, Pz)** with L-dopa, **β power (C4, P3, P4, Pz)** with L-dopa
Mostile et al.[19]	IL	+ corr.: **IL (O1, O2)** with L-dopa SDR
Stanzione et al.[20]	Rel. SP, dom. freq., inter-hemispheric asymm.	No corr.: **δ and dom. freq.** with L-dopa
Swann et al.[48]	Abs. SP	+ corr.: **β (Fz, F1, F2; P5, P7, CP5; P6, P8, CP6)** with DBS-ON

Supplementary Table 5 Other

Reference	qEEG variable described	Main conclusions
Cozac et al.[43]	Ratio (α / θ)	No corr.: **ratio** with olfactory function
Filipovic et al.[39]	Abs. and rel. SP	**Rel. α1:** depressed<non-depressed
Fonseca et al.[42]	Inter-hemispheric coherences	No corr.: **inter-hemispheric coherences** and QoL
Gagnon et al.[41]	Abs. and rel. SP, dom. freq.	**Abs.** and **rel. θ (front., temp., par., occ.), abs. δ (front., par., occ.):** PD-RBD>PD-NRBD, **dom. freq.:** PD-RBD<PD-NRBD
Hatz et al.[40]	WN, PLI, rel SP.	+ corr: **Right. Front. δ.** No corr.: **other rel. SP** with AES. - corr.: apathy with **α2 PLI** , **α2 WN λ, γ, Kw. α2-msPLI** classifies median-split AES with sens. 70%, spec. 90%, AUC 82.5%
He et al.[21]	Rel. SP	No corr.: **SP** with disease duration
He et al.[37]	Dom. freq., rel. SP	+ corr.: **dom. freq**. with disease duration No corr.: **rel. SP**, **β coherence** with disease duration
Moisello et al.[9]	SP	+ corr.: **β** with disease duration
Morita et al.[18]	Ratio (α + β) / (δ + θ)	No corr.: **ratio** with disease duration
Mostile et al.[19]	IL	No corr.: **IL** with HPRSD

AVLT-LTM: Auditory Verbal Learning Test – Long Term Memory; BADS: Behavioral Assessment of the Dysexecutive Syndrome; CDT: Clock Drawing Test; COWA: Controlled Word Association; CSA: compressed spectral array; DA: dopamine agonists; DBS: Deep Brain Stimulation; EWCI: Edge-Wise Connectivity Index; FAB: Frontal Assessment Battery; FU: follow-up; GRMP: Global Relative Median Power; HPRSD: Hamilton Psychiatric Rating Scale for Depression; HY stage: Hoehn and Yahr Stage; IL: Index of Lateralization; JLO: Judgement of Line Orientation; MST: Minimum Spanning Tree (mod.: modularity; BC: betweenness centrality; diam.: diameter; leaf: leaf number; ecc.: eccentricity); MDS-UPDRS III: Movement Disorders Society – Unified Parkinson's Disease Rating Scale III; MMSE: Minimal Mental State Examination; MOCA: Montreal Cognitive Assessment; (N)RBD: (non) REM Sleep Behavior Disorder; PDD: PD Dementia; PDD-F: PDD with fluctuating cognition; PDD-NF: PDD without fluctuating cognition; PD-MCI: PD Mild Cognitive Impairment; PD-NCOG: cognitively normal PD patients; PIQ: Performance IQ; PLI: Phase-Lag-Index; PLV: Phase-Locking Value; QoL-AD: Quality of Life – Alzheimer's Disease scale; SDR: short duration response; SP: spectral powers; TMT: Trail Making Test; VIQ: Verbal IQ; WAIS: Wechsler Adult Intelligence Scale; WCST: Wisconsin Card Sorting Test; wMNE: weighted Minimum Norm Estimator WN: Weighted Network

2.1

CHAPTER 2.2

A systematic review of MEG-based studies in Parkinson's disease: The motor system and beyond

Lennard I Boon, Victor J Geraedts, Arjan Hillebrand, Martijn R Tannemaat, Maria Fiorella Contarino, Cornelis J Stam, Henk W Berendse

Human Brain Mapping 2019:2827-2848
DOI: 10.1002/hbm.24562

Abstract

Parkinson's disease (PD) is accompanied by functional changes throughout the brain, including changes in the electromagnetic activity recorded with magnetoencephalography (MEG). An integrated overview of these changes, its relationship with clinical symptoms, and the influence of treatment is currently missing. Therefore, we systematically reviewed the MEG studies that have examined oscillatory activity and functional connectivity in the PD-affected brain. The available papers could be separated into motor network-focused and whole-brain focused studies. Motor network studies revealed PD-related changes in beta band (13-30 Hz) neurophysiological activity within and between several of its components, although it remains elusive to what extent these changes underlie clinical motor symptoms. In whole-brain studies PD-related oscillatory slowing and decrease in functional connectivity correlated with cognitive decline and less strongly with other markers of disease progression. Both approaches offer a different perspective on PD-specific disease mechanisms and could therefore complement each other. Combining the merits of both approaches will improve the setup and interpretation of future studies, which is essential for a better understanding of the disease process itself and the pathophysiological mechanisms underlying specific PD symptoms, as well as for the potential to use MEG in clinical care.

Introduction

Parkinson's disease (PD) is the second most common neurodegenerative disease after Alzheimer's disease, with a global disease burden of more than five million people.[1] The neuropathological hallmark of PD is the deposition of Lewy bodies, of which alpha synuclein is the main constituent. Nigrostriatal dopaminergic neurons are notoriously affected, and loss of these neurons leads to prominent motor features that can be treated symptomatically using levodopa suppletion and, in later disease stages, deep brain stimulation (DBS). In early disease stages, the alpha synuclein depositions mainly affect the brainstem and the surviving neurons of the nigrostriatal dopamine system, and extend to widespread cortical brain regions in later disease stages.[2] PD is therefore increasingly recognised as a whole-brain disease with functional disturbances at both subcortical and cortical levels, and is characterized clinically by both motor and non-motor symptoms.

The past two decades have seen rapid developments in functional imaging techniques aimed at the detection, characterization and localisation of brain activity. These techniques have yielded important insights into the neuronal mechanisms that may underlie PD and its broad range of clinical symptoms. One such technique is magnetoencephalography (MEG), which non-invasively records the weak magnetic fields that are induced by electrical activity in the cerebral cortex[3,4] and subcortical structures.[5-7] MEG's high temporal resolution can be used to study neuronal activity as well as functional interactions between distinct brain regions in great detail.[8]

Using MEG, PD-related neurophysiological characteristics have been studied both within the motor system and for the brain as a whole. MEG analyses aimed at motor networks are spatially restricted to the motor cortex and are usually performed in source-space. They can be combined with neurophysiological signals of different origin, such as muscle activity recorded using electromyography (EMG)[9,10] or local field potentials (LFPs) from the subthalamic nucleus (STN) recorded during DBS).[11,12] The study of whole-brain networks using MEG generally involves resting state recordings. Roughly three different approaches have been used in the analysis of whole-brain networks: the analysis of oscillatory brain dynamics using measures of band-limited power or peak frequency, investigation of functional (or directed/effective[13]) connectivity (FC) between brain areas, and assessment of the topological organization of brain networks.

MEG studies increasingly use source reconstruction techniques, such as beamforming, to project the extracranially recorded (sensor-level) signals to source-space. In sensor-level analysis, several factors that may lead to erroneous estimates of functional connectivity should be considered. Multiple sensors pick up the signal from a single source because of volume conduction (the transmission of electromagnetic fields from a primary current source through biological tissue) and field spread (multiple sensors picking up activity of a common source). In addition, the same sensor picks up signals of multiple sources due

to signal mixing. Moreover, the neuronal generators are generally not located directly underneath the sensor with the maximum power (particularly for axial gradiometers). The source-level approach can resolve some of these ambiguities and enables interpretation of the functional results in an anatomical context.[14-18]

So far, review articles tend to treat motor network-focused studies[19,20] and whole-brain studies[21] separately. Although some efforts have been made to relate findings from motor networks to non-motor symptoms,[22] it is unknown to what extent findings from motor networks and whole-brain networks can be compared and if so, which similarities and discrepancies are present. A full understanding of the neurophysiological changes associated with PD is a stepping-stone towards the development of biomarkers and novel therapies that are urgently needed. Therefore, we set out to systematically review the MEG literature on PD not only to provide an overview of the neurophysiological characteristics of PD, their relationship with clinical symptoms, the effect of disease progression, and the influence of treatment on these characteristics, but also to explore how the results of motor network studies and whole-brain approaches can be integrated.

Methods

We performed this systematic review of the MEG literature in PD in accordance with the Preferred Reporting Items for Systematic Reviews and Meta-Analyses (PRISMA) guidelines.[23] We carried out web-based searches using medical databases: PubMed, Embase, Web of Science, Emcare, Academic Search Premier, and ScienceDirect. We used combinations of the key-words Magnetoencephalography (MEG) and Parkinson's disease. The full search strategies can be found in Supplement A. References up to October 15th 2018 (date of latest search) were used for further study. Two researchers (LIB and VJG) independently screened all articles on title and abstract using the following inclusion criteria: original research article, published in English or Dutch, including a separate cohort of a minimum of five PD patients, and quantification of at least one MEG-parameter.

Although the underlying sources of MEG and EEG are the same, these techniques measure different components of the generated electromagnetic fields (resulting in different sensitivity profiles).[24] In addition, MEG is more suitable for source-space analysis than EEG,[8] as it typically uses a higher number of sensors and is less affected by the details of the volume conductor. Even though neurophysiological information obtained using both techniques might be complimentary, a direct comparison would be challenging. We have therefore chosen to limit this review to MEG studies in PD (see Gereadts et al. (2018) for a recent review of quantitative electroencephalography (EEG) studies in PD).[25] Studies in which data analysis was confined to evoked fields were excluded, but studies aimed at induced/event-related MEG activity were included. Induced/event-related activity differs from evoked fields by not being phase-locked to a certain stimulus.[26] Cohen's kappa for inter-rater agreement was calculated during this selection process. In case of disagreement, relevant sections were re-read until agreement was reached.

Next, both reviewers evaluated the full-text of all included articles using the Joanna Briggs Institute (JBI) checklist for case series, extended with an item addressing clear reporting of MEG data acquisition and analysis (see Supplement B). Articles had to score a minimum of 5 points (indicating a sufficient quality study) to be included in this review, of which at least one point was scored on the first 3 items, at least two points on item 4-8, and one point on item 11. In this descriptive review, we chose to include a much-cited paper[9] that did not fulfil the latter (item 11) more stringent criteria on conducting and reporting the MEG research. Nonetheless, the importance of clear reporting of MEG data acquisition and analysis procedures is obvious [27]. We subdivided the included papers into two main groups according to the brain network the analysis was focused on: motor network-focused, in which we treated the tremor network as a sub-category, and whole-brain network focused. Since a series of articles on the neurophysiological basis of neuronal entrainment in PD,[28-31] as well as four other articles[32-35] tended to stand alone from the rest of this review, these will not be discussed in the results section, but the main findings are provided in Table 1.

Table 1 Profiles of the motor-network studies included in this review

Authors	Year	Center	N=	Type of PD cohort	Disease duration/ stage §	JBI	Neuro-physiological measures º
Abbasi et al.	2018	Heinrich-Heine University, Düsseldorf, Germany	17	All DBS	4-19 years	8	Spectral analysis
Airaksinen et al.	2015	Helsinki University, Finland	19	All DBS	12 (5) years	6	Coherence: CMC
Hall et al.	2014	Aston University, Birmingham, UK	9	Early, DRT- naive	Unknown	6	Spectral analysis
Heinrichs-Graham et al.	2014a	University of Nebraska, USA	15		1-9 years	7	Spectral analysis FC: PLV
Heinrichs-Graham et al.	2014b	University of Nebraska, USA	13		1-9 years	6	ERD, PMBR power
Heinrichs-Graham et al.	2017	University of Nebraska, USA	23		0-16 years (mean 6.5)	6	ERD, PMBR power
Hirschmann et al.	2011	Heinrich-Heine University Düsseldorf, Germany	8	All DBS	11-26 years	6	Coherence: cortex-STN
Hirschmann et al.	2013a	Heinrich-Heine University Düsseldorf, Germany	11	All DBS	7.7 (3.4) years	6	-Spectral analysis -CMC and cortico-cortical coherence
Hirschmann et al.	2013b	Heinrich-Heine University Düsseldorf, Germany	10	All DBS	15.5 (5.2) years	6	Cortex-STN coherence and CMC
Jha et al.	2017	UCL London, UK	7	All DBS	9-25 years	7	Coherence: Cortex-PPN
Krause et al.	2013	Heinrich-Heine University Düsseldorf, Germany	10	Early	1.9 (0.5) years	8	CMC
Litvak et al.	2011	UCL London, UK	17	All DBS	8-17 years	6	Coherence: Cortex-STN (incl. directed coherence)
Litvak et al.	2012	UCL London, UK	13	All DBS	8-17 years	7	-Spectral analysis -Coherence: Cortex-STN -Granger causality
Luoma et al.	2018	Helsinki University Hospital, Finland	16	All DBS	11.9 (5.0) years	7	-Spectral analysis -CMC
Mäkelä et al.	1993	Helsinki University, Finland	5		1.5-6.3 years	6	Spectral analysis
Meissner et al.	2018	Heinrich-Heine University, Düsseldorf, Germany	20		5.5 (3) years	5	ERD, ERS and PMBR power

Source-/ sensor-space	Main findings
Source	Unilateral DBS (both 130 Hz and 340 Hz) leads to a lowering of alpha and beta power over both sensorimotor cortices. Recordings took place the day after surgery with eyes closed. No correlation with motor improvement was found.
Sensor	STN-DBS modified the CMC with large inter individual variability, correlation with motor improvement was inconsistent.
Source	Contralateral M1 showed greater resting-state beta power than ipsilateral M1 in PD. Zolpidem normalized the ratio between left and right. Normalization correlated positively with improvement in UPDRS-III scores. M1 beta power differences during different phases of movement (a.o. PMBR), normalized after zolpidem.
Source	PD (DRT OFF) vs controls: -Power: significantly lower beta band power in bilateral motor regions. After DRT, this largely normalizes. -FC: increased synchronicity between motor cortices, partially normalized by DRT.
Source	Controls: alpha and beta band desynchronization prior to and during movement. PD patients: significantly lower response amplitudes. Trend towards lower amplitude PMBR
Source	Response amplitudes were affected more severely in PD patients suffering from right-dominant disease
Source	Cortical sources coherent with oscillations STN in PD DBS patients: -Alpha band: ipsilateral temporal regions -Beta band: ipsilateral sensorimotor and adjacent premotor cortex
Both	Tremor-associated increase in STN-M1 coherence correlated positively with tremor severity. Beta band power in cortical motor regions lower during tremor. CMC was unaffected by DRT.
Source	Beta band motor cortex-STN coherence reduced by DRT, but no change upon movement contralateral limb. Alpha and beta band CMC reduced during repetitive movement compared to static contraction forearm, not affected by DRT. STN-cortical and beta band CMC negatively correlated with akinesia/rigidity during dopamine OFF state.
Source	Alpha band coherence between the PPN and posterior brain stem and cingulum. Beta band coherence between PPN and medial frontal wall, SMA and primary motor cortex
Source	tACS of the motor cortex at beta frequency (20 Hz), but not at 10 Hz, attenuated beta band CMC during isometric contraction and reduced performance (amplitude variability) of a finger tapping task in PD, but not in controls.
Source	Cortical sources coherent with oscillations STN in PD DBS patients: -Alpha band: ipsilateral temporo-parietal regions. -Beta band: ipsilateral anterior parietal and frontal cortex. -STN activity predominantly led by cortical activity in both frequency bands. -No changes upon DRT
Source	Gamma-band coherence between STN and M1, with the STN mostly driving the cortex. Upon movement of the hand, gamma band STN-M1 event-related coherence increased. DRT increased gamma band coherence between the STN and M1, which correlated with the degree of improvement in bradykinesia-rigidity.
Sensor	-Lowering of alpha and beta band power during DBS ON, only during resting state when the eyes were open. During eyes-closed or a motor task: no significant difference between ON and OFF stimulation. -Maximum CMC over sensorimotor area contralateral to extended hand.
Sensor	Beta band power in cortical motor regions lower during tremor.
Source	PD patients performed worse than controls on motor task (motor sequence acquisition). During random presentation of the task no differences in beta band power. After learning a sequence: less training-related beta power suppression in motor cortex in PD versus HC. In addition, less training related theta activity in cortical motor regions, paralleling susceptibility to inference.

Authors	Year	Center	N=	Type of PD cohort	Disease duration/ stage §	JBI	Neuro-physiological measures º
Oswal et al.	2013	University of Oxford, UK	17	All DBS	8-17 years	7	Coherence: STN-cortex
Oswal et al.	2016	University of Oxford, UK	15	All DBS	6-22 years	6	Coherence: STN-cortex; Granger causality variant
Pollok et al.	2009	Heinrich-Heine University Düsseldorf, Germany	10		10.9 (2.4) years Range: 4-30 years	6	CMC and cortico-cortical coherence
Pollok et al.	2012	Heinrich-Heine University Düsseldorf, Germnany	20	Early PD, of which 10 patients DRT naive	HY stage (all): I-II DRT naïve: 0.4-2.5 years Treated group: 1-3.5 years	8	-Spectral analysis -Coherence: cortico-cortical
Pollok et al.	2013	Heinrich-Heine University Düsseldorf, Germany	7		11.9 (0.6)years	6	Cortico-cortical coherence
Salenius et al.	2002	Helsinki University, Finland	8		HY stage: I-III	6	-Spectral analysis -CMC
Te Woerd et al.	2014	Radboud University Medical Centre Nijmegen, The Netherlands	12		1-12 years (mean 6)	6	ERD, ERS, PMBR power
Te Woerd et al.	2015	Radboud University Medical Centre Nijmegen, The Netherlands	15		7 (4) years	6	ERD, ERS, PMBR power
Te Woerd et al.	2017	Radboud University Medical Centre Nijmegen, The Netherlands	14		8 (5) years	6	ERD, ERS, PMBR power
Te Woerd et al.	2018	Radboud University Medical Centre Nijmegen, The Netherlands	12		7 (5) years	6	ERD, ERS, PMBR power
Timmermann et al.	2003	Heinrich-Heine University Düsseldorf, Germany	6		1-21 years (mean 7)	6	CMC and cortico-cortical coherence
van Wijk et al.	2016	UCL London, UK	33	Subset of patients previously described by [12, 63, 64]	12 (5-25) years	8	Coherence: STN-cortex
Vardy et al.	2011	VUmc, Amsterdam, The Netherlands	11		5.1 (3.3) years HY stage 1.5-III	7	Spectral analysis
Volkmann et al.	1996	New York University Medical Center, USA	7		7.8 (2.5) years HY stage I-III	6	Coherence: CMC

§ Mean (Standard deviation) or Range (..-..)
º Neurophysiological measures relevant for this review; explanation of the measures can be found in Table 3
N, number of PD subjects studied; PD, Parkinson's disease; JBI, Joanna Briggs Institute (score); DBS, Deep Brain Stimulation; STN, subthalamic nucleus; CMC, cortico-muscular coherence; FC, functional connectivity; HY stage, Hoehn & Yahr stage; DRT, dopamine replacement therapy; UPDRS, Unified Parkinson's disease Rating Scale; PLV, phase locking value; ERD, Event-Related Desynchronization; PMBR, Post-Movement Beta Rebound; PPN,

Source-/ sensor-space	Main findings
Source	Alpha band coherence between temporal cortical areas and the STN reduced following movement onset: degree of suppression in is significantly greater ON DRT than OFF DRT.
Source	DBS relatively selectively suppressed lower beta band synchronization of activity between STN and mesial premotor regions, including SMA. Motor cortical regions 'driving' STN in beta band, with different delays for lower and higher beta band.
Source	Oscillatory network associated with tremor comprising: contralateral S1/M1, SMA, PMC, thalamus, S2, PPC and ipsilateral cerebellum oscillating at 8-10 Hz. M1/S1 CMC at double the tremor frequency, CMC decreased following DRT. When controls imitated a tremor, oscillatory network comparable to PD-tremor network when observed in DRT OFF.
Source	In early PD: -Increased resting-state S1/M1 beta band power -CMC did not differ between PD and controls.
Source	During rest in DRT ON (but not during DRT OFF): positive correlation between disease duration and SMA–M1 coherence. During isometric contraction in DRT OFF (but not during DRT ON): inverse correlation between UPDRS III and SMA–M1 coherence.
Source	Trend towards lower beta band power in motor cortex PD patients. Beta and gamma band CMCs during steady-state contraction of the forearm significantly lower in PD than in controls
Source	Pre-stimulus beta band power: patients showed a lower proportion of beta band ERD in the sensorimotor cortex *preceding* the reaction stimuli, while the proportion of beta band ERD *following* the event was larger, hence there was a change in timing of the ERD: a shift from predictive to more reactive modulation of beta band oscillations.
Source	Rhythmic auditory stimulation regime: entrainment of slow oscillations and increases in modulation depth of beta oscillatory activity, in PD and controls. Due to increased beta ERS post-movement, that improves the predictive movement related beta suppression, reflecting a predictive mode of cue utilization.
Source	PD patients have demonstrated comparable auditory entrainment as controls. Therefore: Deficient entrainment in PD patients concerns the motor circuits only.
Sensor	PD patients showed reduced motor entrainment compared to controls during tasks containing rhythmic stimuli, even in situations encouraging entrainment. This is also reflected by beta oscillatory power changes, both regarding phase and modulation depth.
Source	Tremor-related oscillatory network, consisting of a cerebello-diencephalic-cortical loop and cortical motor (M1, SMA/CMA, PM) and sensory (SII, PPC) areas contralateral to the tremor hand.
Source	Beta band power and phase-amplitude coupling within the STN correlated positively with severity of motor impairment (lower beta). Coherence between STN and motor cortex dominant in the high-beta range.
Source	Cortical motor slowing during rest in correlation with cognitive UPDRS scores, whereas slowing during movement correlated best with the motor UPDRS scores.
Source	Tremor network contralateral to the 3-6 Hz Parkinson resting tremor, involving the diencephalic level (assumed to be the thalamus), lateral PMC, S1 and M1

pedunculopontine nucleus; tACS, transcranial alternating current stimulation; SMA, supplementary motor area; S1/M1; primary sensorymotor cortex; PPC, posterior parietal cortex; PMC, premotor cortex; ERS, Event-Related Synchronization

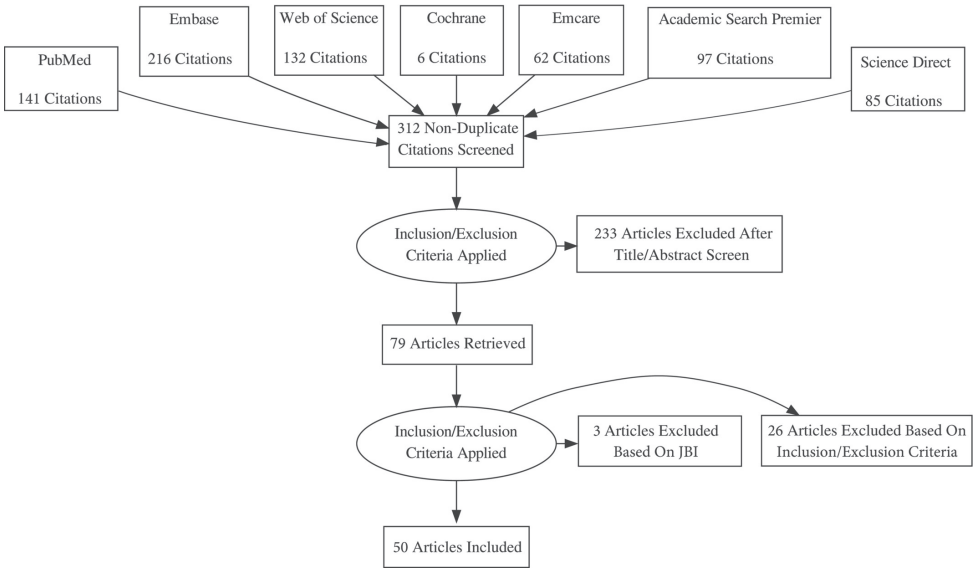

Figure 1 Flowchart for inclusion of studies

Results

Search results and study characteristics

Fig. 1 shows the selection procedure with corresponding numbers of publications. 312 papers matched the search terms and were included for title and abstract screening, leading to 79 articles meeting the pre-specified in- and exclusion-criteria (Kappa = 0.832). These articles were selected for full-text analysis, risk of bias assessment was performed, and data extraction took place. Three articles were excluded based on the JBI checklist (see Supplement C) and 26 articles were excluded based on the inclusion/exclusion criteria. Eventually, 50 papers were included for review. Frequency bands were defined as follows: delta (0.5-4 Hz), theta (4-8 Hz), alpha1 (8-10 Hz), alpha2 (10-13 Hz), beta (13-30 Hz) and gamma (30-48 Hz). In several motor-network focused studies, the beta band has been divided into low and high-beta. The upper limit of the low-beta band is 20 Hz,[11,36] 21 Hz,[37] 22 Hz,[38] or 25 Hz.[39] An explanation of the neurophysiological measures described in the reviewed articles is presented in Table 3.

Table 3 Definitions of the neurophysiological measures described in the review

Category	Measure	Interpretation
Oscillatory behaviour	Band power	Average spectral power in a particular frequency band.
	Mean frequency	
	Peak frequency	Dominant frequency in the power spectrum, within a given frequency range (e.g. 6-15 Hz in;[77] 4-13 Hz).[72]
Complexity	Lempel-Ziv Complexity	Related to the number of distinct patterns and the rate of their occurrence along a given sequence. A high value indicates a high variation of the binary signal.[123]
Functional connectivity	Coherence	The degree of similarity of frequency components of two time series. Field spread and volume conduction, as well as power, influence the estimate. High values indicate strong functional connectivity.[124]
	Phase lag index	Instantaneous phases of two time series are compared at each time point and the asymmetry of the distribution of the phase differences between these time series is quantified. A high value indicates that there is a consistent non-zero (modulus π) phase relation between the two time series, indicative of functional coupling.[125] Relatively insensitive to the effects of field spread and volume conduction.
	Phase locking value	Reflects the consistency of the phase covariance between two signals in a frequency range over time (phase-locking). Field spread/volume conduction affect the estimate.[82]
	Synchronization likelihood	The strength of synchronization between two time series based on state-space embedding. High values indicate strong functional connectivity, but field spread/volume conduction affects the estimate.[78]
Directed functional connectivity	Directed Phase Transfer Entropy	Based on the Wiener-Granger Causality principle, namely that a source signal has a causal influence on a target signal if knowing the past of both signals improves the ability to predict the target's future compared with knowing only the target's past: dPTE was implemented as a ratio between 'incoming' and 'outgoing' information flow.[126]
	Granger causality	Quantifies whether the past of one time series contains information that helps to predict the future of another signal. Does not capture non-linear effects and requires construction of a model of the data.[127]
	Partial directed coherence	Based on the notion of Granger causality. Frequency-domain approach to describe the (direction of) relationships between time series. Decomposes the relationships into "feedforward" and "feedback" aspects.[128]

Motor network-focused research

A summary of the data extraction and risk of bias assessment of the motor network-focused articles can be found in Table 1 and a schematic overview to place the main findings in an anatomical context are provided in Figure 2. Unless stated otherwise, motor network-focused studies in this review have been performed in source-space.

Early disease stages

Larger sensorimotor cortical (S1/M1) beta band power has been reported both in early-stage PD patients on dopamine replacement therapy (DRT) and in medication naïve patients as compared to controls, recorded during the resting state.[40] In this study, during isometric contraction of the contralateral forearm, beta band power was suppressed in controls, but not in PD patients. Only during isometric contraction, contralateral beta band power correlated with Unified Parkinson's Disease Rating Scale (UPDRS)-III scores in PD patients.[40] Hall and coworkers found larger resting-state beta band power in the motor cortex contralateral to the most affected hemibody in DRT-naïve patients. The benzodiazepine zolpidem, known for its modulating effects on PD motor symptoms, normalized the ratio in resting-state beta band power between the 'affected' and 'non-affected' motor cortex and this correlated positively with improvement in UPDRS-III scores.[41] Cortico-muscular coherence (CMC) has been studied by correlating M1 activity with EMG signals recorded in the forearm. CMC was not different between PD patients and controls during steady-state contraction of the forearm.[40]

Later disease stages

Studies in later-stage PD patients found that beta band power in cortical motor regions was lower during the resting state compared to controls (both OFF and ON DRT).[42,43] Vardy and colleagues demonstrated that slowing of event-related beta band oscillations in the motor cortex correlated positively with UPDRS-III scores when recorded during a motor task and with cognitive UPDRS components when recorded during the resting state.[43] DRT significantly increased cortical motor beta band power, thus having a normalizing effect.[42] In contrast, STN-DBS lowered alpha and low-beta band power in the sensorimotor cortex in two studies (both a sensor-space and a source-space study) during eyes-open, resting-state.[38,44] However, no correlation with motor improvement has been observed. In addition, during a motor task, as well as during eyes-closed, no differences between ON and OFF stimulation were found.

Even in the absence of stimulation, MEG data are contaminated by high-amplitude, low frequency artefacts mainly originating from the influence of cardiovascular pulsations and breathing on the percutaneous extension wire (before implantation of a stimulator),[45] and the stimulator itself.[46] Upon stimulation, electromagnetic artefacts generated by the stimulator, such as jump artefacts and ringing artefacts obscure neuronal activity (see[46] for a detailed description of DBS-artefacts). However, MEG recordings are still technically feasible as DBS artefacts can be minimized using spatial filters,[47-49] beamforming techniques,[46,50] or independent component analyses in combination with mutual information.[51] For a recent review on the effect of DBS on multiple diseases, studied using MEG, see Harmsen and colleagues.[52]

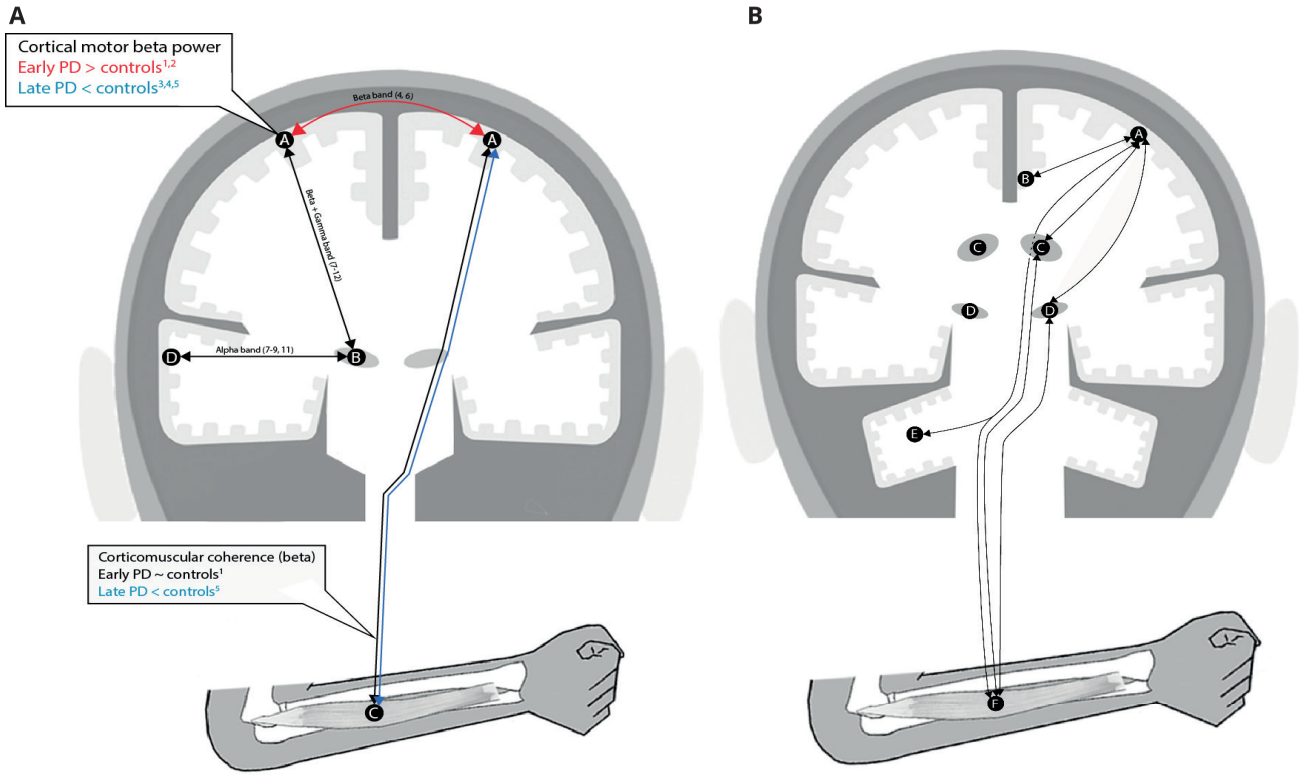

Figure 2 Overview of main findings in motor network-focused research
(A) schematic representation of a coronal view of the brain, combined with the forearm muscle extensor digitorum communis. All displayed findings involve undirected functional connectivity, depicted using lines with double arrow heads. *A* = Motor cortex; *B* = Subthalamic nucleus; *C* = Forearm muscle; *D* = Temporal cortex
Red and *blue* represent higher respectively lower values found in PD patients compared with controls; *Black* lines represent no significant difference between PD patients and controls, or no comparison with a control group. References: 1=[4]; 2=[41]; 3=[43]; 4=[42]; 5=[59]; 6=[58]; 7=[11]; 8=[60]; 9=[12]; 10=[63]; 11=[37]; 12=[36];

(B) Overview of main findings in tremor network-focused research
A schematic representation of a coronal view of the brain, combined with the forearm muscle extensor digitorum communis.
All displayed findings involve coherence at tremor frequency and its (sub)harmonics.
A = Sensorimotor and premotor cortex; B = Cingulate motor area; C = Thalamus; D = Subthalamic Nucleus; E = Cerebellum; F = Forearm muscle. Not depicted in this figure: Posterior parietal cortex. References: [9,10,67,68]

When studying induced MEG activity, prior to movement onset, in healthy individuals a desynchronization in cortical motor oscillations (beta band) occurs, that disappears during the actual execution of the movement: Event-related desynchronization (ERD). This is followed by a post-movement beta band rebound: Event-related synchronization (ERS).[53,54] In PD patients OFF DRT, ERD and ERS response amplitudes are reportedly lower compared to controls,[55] mainly for right-dominant diseased patients,[56] but ON DRT these differences could not be substantiated.[57]

One study demonstrated higher resting-state beta band coherence between bilateral primary cortical motor regions in PD patients compared to controls, which normalized after DRT administration.[42] In akinesia-dominant PD patients, coherence between the ipsilateral supplementary motor area (SMA) and M1 correlated with disease duration, not with UPDRS III scores, during rest (only ON DRT). During isometric contraction of the forearm, coherence between SMA and M1 was inversely correlated with UPDRS III scores (only OFF DRT).[58]

Forearm CMCs in the beta and gamma band were demonstrated to be significantly lower in PD patients than in controls when recorded during steady-state contraction[59] and this correlated with higher akinesia and rigidity sub-scores.[60] This difference normalized after DRT in one study,[59] but not in another.[60] It was speculated by Hirschmann and colleagues that this differential response to DRT was caused by the fact that tremor-dominant PD patients were not excluded from the study from Salenius and colleagues,[59,60] as CMC increases might be a characteristic of tremor alleviation.[61] Transcranial alternating current stimulation (tACS) of the motor cortex at beta frequency (20 Hz), but not at 10 Hz, further attenuated both the beta band CMC during isometric contraction and reduced performance (amplitude variability) on a finger tapping task in PD patients, but not in controls.[62] In a sensor-space study on the effect of DBS on motor CMC, results varied and the correlation with improvement in motor function inconsistent.[39]

By combining LFP recordings with MEG recordings in STN-DBS patients, a frequency-dependent coherence has been demonstrated between signals from the STN and the ipsilateral S1/M1 cortex in the beta and gamma band during the resting state.[11,12,36,37,60,63] Beta coherence was most dominant in the high beta band,[36] which was mainly located in the mesial premotor regions.[11,12,37] Resting-state M1-STN beta band coherence was inversely correlated[60] or not correlated with bradykinesia/rigidity UPDRS-III scores (DRT ON and OFF).[12] DRT increased beta band coherence between the STN and a small region in the prefrontal cortex in one study,[12] but in other studies DRT suppressed[60] or did not modulate[36] beta band coherence between the motor cortex and the STN. In one study, stimulation of the STN suppressed resting-state high-beta band coupling of the STN with mesial cortical motor regions, yet the degree of suppression did not correlate with motor improvement.[37]

Resting-state alpha band coherence has been observed between the STN and ipsilateral temporal cortex.[11,12,37,60] The alpha band coherence was not influenced by arm movements in one study,[60] but decreased upon movement in another study (in DRT ON more than in DRT OFF).[64] DRT and DBS did not influence the resting-state alpha band coupling.[11,12,37] The former authors suggested that the identified alpha band network may reflect non-motor functioning, for example auditory processing involving the (8-10 Hz) tau rhythm in the auditory cortex,[65] or attentional processes.[11,12,22]

Tremor network-focused research

Tremor most likely involves neuronal mechanisms different from those underlying bradykinesia and rigidity, as the latter symptoms worsen at the same rate as gait and balance impairments, whereas tremor does not.[66] MEG studies aimed at revealing PD-related tremor networks have identified a number of brain regions with oscillatory activity that is coherent with forearm EMG signals at tremor frequency. First, a motor network contralateral to the 3-6 Hz Parkinson resting tremor has been identified involving the diencephalic level (likely corresponding to the thalamus), the lateral premotor cortex, S1 and M1.[10] Thereafter, cortico-cortical coherence analysis with contralateral M1 as a seed region (i.e. in which signals from the selected brain region are used to calculate correlations with the rest of the brain) revealed harmonic involvement (at single and double frequency) of the ipsilateral cerebellum, contralateral cingulate motor area (CMA) and contralateral posterior parietal cortex (PPC).[9,67] Over the years, several interesting additional observations have been made: i) using MEG in combination with LFP recordings in DBS-patients, a muscular-STN-M1 coupling was found during tremor.[68] ii) when controls were asked to imitate a tremor, an oscillatory network could be identified that is comparable to the PD-tremor network observed in the dopamine-OFF state.[67] iii) beta band power in cortical motor regions was lower during simultaneous measurement of an intermittent tremor.[68,69]

Table 2 Profiles of the whole-brain studies included in this review

Authors	Year	Center	N=	Type of PD cohort	Disease duration/ stage §	JBI	Neuro-physiological measures º
Airaksinen et al.	2012	Helsinki University, Finland	11	All DBS	7-19 years	6	Spectral analysis
Anninos et al.	2016	Democritus University of Thrace, Alexandropouli, Greece	10	All male	Unknown	7	Spectral analysis
Boesveldt et al.	2009	VUmc, Amsterdam, The Netherlands	20		HY stage I-III	8	-Spectral analysis -FC: SL
Boon et al.	2017	VUmc, Amsterdam, The Netherlands	34	6 PDD	HY stage II-III 11.9 (3.8) years	7	FC: dPTE
Bosboom et al.†	2006	VUmc, Amsterdam, The Netherlands	26	13 PD, 13 PDD	PD: 9.69 (4.5) years, HY stage 2.5 PDD: 11.2 (4.0) years, HY stage 2.9	7	Spectral analysis
Bosboom et al.	2009a	VUmc, Amsterdam, The Netherlands	8	All PDD	12.8 (2.6) years HY stage II-IV	7	Spectral analysis
Bosboom et al.†	2009b	VUmc, Amsterdam, The Netherlands	26	Cohort previously described by [73]	Previously described	7	FC: SL
Cao et al.	2015	Shanghai Jiatong University, China	32	16 PD, 16 PD-DBS	PD: 2-30 years PD-DBS 4-13 years	8	Spectral analysis
Cao et al.	2017	Shanghai Jiatong University, China	27	13 DBS	PD: 11.3 (1.3) years PD-DBS: 9.4 (1.3) years	7	Spectral analysis
Gomez et al.	2011	University of Valladolid, Spain	18	Early	<2 years	7	Complexity of oscillations
Olde Dubbelink et al.	2013a	VUmc, Amsterdam, The Netherlands	49	Longitudinal, 3 PDD (last time point)	Baseline: 5.4 (3.5) years	6	Spectral analysis
Olde Dubbelink et al.‡	2013b	VUmc, Amsterdam, The Netherlands	43	Longitudinal 4 PDD (last time point)	Baseline: 5.2 (3.6) years	6	-Spectral analysis -FC: PLI
Olde Dubbelink et al.‡	2014a	VUmc, Amsterdam, The Netherlands	43	Cohort previously described by [81]	Previously described	6	-Graph analysis -Minimum spanning tree (MST)

Source/ sensor space	Main findings
Sensor	STN-DBS modulated alpha (occipital) and beta band (central sulcus) power. Lowering of the latter correlated positively with relief of rigidity.
Sensor	TMS over the five main cortical brain regions led to non-significant increases in PD-related abnormally low peak frequency.
Sensor	Upon odor stimulation task: -PD-related decrease in alpha power. -Controls: decrease in local beta band SL. PD: decrease in intrahemispheric alpha2 band SL.
Source	Lower resting-state beta band directed connectivity (dPTE) in posterior brain regions in PD. Lower posterior dPTE values correlated with poor global cognitive performance.
Sensor	PD: slowing of resting-state brain activity involving theta, beta and gamma bands. PDD: further slowing of resting-state brain activity, additionally involving delta and alpha bands, as well as a lower reactivity to eye-opening.
Sensor	Rivastigmine administration to PDD patients: shift spectrum towards higher frequencies: increase in parieto-occipital and temporal alpha power and a diffuse increase in beta power, together with a decrease in fronto-central and parieto-occipital delta power.
Sensor	PDD vs. PD: -Lower fronto-temporal SL in alpha band and lower intertemporal SL in delta, theta and alpha1 band. -Higher left sided parieto-occipital SL in alpha2 and beta band.
Sensor	PD vs controls: general occipitotemporal slowing. PD-DBS first week after STN-DBS placement: No band power differences upon stimulation. Long-term STN-DBS: average cortical frequency increased upon stimulation. Relative 9-13 Hz power over left hemisphere correlated positively with UPDR-III scores in DBS-ON state.
Sensor	PD vs. controls: increase in absolute power between 8 and 30 Hz. Upon STN stimulation: Frontal/parietal increase in lower gamma band power (34–38 Hz) and higher gamma band power (55–65 Hz). Improvement of motor symptoms correlated with alpha and beta band power suppression over right temporal area.
Sensor	PD patients have lower complexity values in MEG signals than controls: statistical group differences for all (10) major cortical regions.
Sensor	PD patients vs. controls: -Slowing dominant peak frequency -Global increase in low frequency and decrease in high frequency relative spectral power over time. -Degree of slowing associated with clinical measures of disease progression, in particular cognitive decline.
Source	PD patients vs. controls: -Baseline: Lower delta and higher alpha1 FC in temporal regions -Longitudinal follow-up (4 years): decrease alpha1 and alpha2 band FC -Motor and cognitive dysfunction correlated positively to the latter.
Source	Early-stage PD: Lower local integration delta band, preserved global efficiency. Longitudinal analysis: More random brain topology. Local integration (multiple frequency bands) and global efficiency (alpha2) affected. Worsening global cognition associated with more random topology in the theta band, motor dysfunction was associated with lower alpha2 global efficiency. MST analysis: a progressive decentralization of the network configuration, in correlation with deteriorating motor function and cognitive performance

Authors	Year	Center	N=	Type of PD cohort	Disease duration/ stage §	JBI	Neuro-physiological measures º
Olde Dubbelink et al.	2014b	VUmc, Amsterdam, The Netherlands	63	Longitudinal 19 PDD (last time point)	Baseline: PD: 60.9 (6.5) PDD: 66.0 (5.2)	7	Spectral analysis
Ponsen et al.†	2012	VUmc, Amsterdam, The Netherlands	26	Cohort previously described by [73]	Previously described	6	Spectral analysis FC: PLI
Stoffers et al.¶	2007	VUmc, Amsterdam, The Netherlands	70		HY stage I-III 5.5 (3.7) years	7	Spectral analysis
Stoffers et al.¶	2008a	VUmc, Amsterdam, The Netherlands	70	Cohort previously described by [70]	Previously described	6	Spectral analysis FC: SL
Stoffers et al.	2008b	VUmc, Amsterdam, The Netherlands	37		HY stage I-III 8.0 (2.7) years	7	Spectral analysis FC: SL
Suntrup et al.	2013	University of Münster, Germany	20	10 dysfagia and 10 non-dysfagia PD patients	-Dysfagic PD: 5.3 (6.7) -Non-dysfagic PD: 8.2 (4.4)	7	Event (swallowing)-related power
Wiesman et al.	2016	University of Nebraska, USA	16		1-9 years HY stage 1.5-III	6	Spectral analysis Coherence: CMC

§ Mean (Standard deviation) or Range (..-..)
º Neurophysiological measures relevant for this review; explanation of the measures can be found in Table 3
N, number of PD subjects studied; PD, Parkinson's disease; JBI, Joanna Briggs Institute (score); DBS, Deep Brain Stimulation; STN, subthalamic nucleus; TMS, transcranial magnetic stimulation; FC, functional connectivity; HY stage, Hoehn & Yahr stage; SL, synchronization likelihood; dPTE, directed phase transfer entropy; PDD, Parkinson's disease dementia; DRT, dopamine replacement therapy; PLV, phase locking value; ERD, PLI, phase lag index; MST, Minimum spanning tree

†, ‡, ¶; Articles that have studied the same patient cohort

Whole-brain focused research

A summary of the data extraction and risk of bias assessment of the whole-brain focused articles can be found in Table 2 and a schematic overview of the main findings is provided in Figure 3. Unless stated otherwise, the whole-brain focused studies have been performed in sensor-space.

Spectral power

The mean frequency of cortical oscillations in PD patients decreases over the course of the disease. In a study involving PD patients at the earliest (drug-naïve) disease stage, oscillatory slowing was already present, most pronounced over the posterior brain regions.[70] When more advanced PD patients were studied, oscillatory slowing was hardly influenced by DRT.[71] Longitudinal analysis of PD patients revealed increases in

Source/ sensor space	Main findings
Source	Addition of neurophysiological markers to neuropsychological tests substantially improved prediction of the risk of conversion to PDD. Lower beta power was associated with the greatest risk of developing dementia.
Source	PDD vs. PD: -Lower alpha and beta band power in occipito-parieto-temporal and frontal regions. -Lower FC in delta and alpha bands in respectively the fronto-temporal and occipito-parieto-temporal areas. -FC between pairs of regions generally weaker in delta and alpha band, stronger in theta band.
Sensor	Widespread slowing of resting-state brain activity in de novo, untreated PD patients.
Sensor	Drug-naive PD patients vs controls: Overall increase in alpha1 SL Moderately advanced PD: increased theta, alpha1, alpha2 and beta SL, particularly with regard to local SL. Total cohort: disease duration positively associated with alpha2 and beta SL, and severity of motor disease with theta and beta SL measures.
Sensor	Elevated levels of cortico-cortical FC are increased even further by an acute DRT challenge, in parallel with motor improvement. Increases involved local FC (4–30 Hz) and intra- and interhemispheric FC (13–30 Hz).
Source	A strong decrease in overall task-related cortical activation was found in all PD patients, most prominent in dysfagic patients. In non-dysfagic patients a compensatory activation towards lateral motor, premotor and parietal cortices seems to take placed upon swallowing, whereas the supplementary motor area was markedly reduced in activity.
Source	During a memory task, a significant reduction in alpha FC between left inferior frontal cortices and left supramarginal/superior temporal cortices in PD compared to controls.

band power of the 'slower' frequencies (theta and alpha1 band), whereas band power of the 'faster' frequencies (beta and gamma) decreased. The spectral slowing correlated with clinical progression of motor symptoms as well as global cognitive decline.[72] In a cross-sectional analysis involving Parkinson's disease dementia (PDD) patients, spectral power had progressed towards diffuse slowing, independent of motor and cognitive scores.[73,74] The spectral slowing in PDD patients could at least partly be reversed by treatment with the cholinesterase inhibitor rivastigmine.[75] MEG-derived spectral markers may help in predicting conversion to PDD: lower beta band power at baseline was the strongest predictor for conversion to PDD over a period of seven years, followed by peak frequency and theta power. Moreover, the combination of impaired fronto-executive task performance and low beta band power strongly increased the risk of conversion to PDD in this source-space study (hazard ratio of 27.3 for both risk factors versus none).[76]

Stimulation of the STN can have widespread effects on oscillatory brain activity in multiple frequency bands. Whole-brain average cortical frequency has been shown to increase upon stimulation of the STN.[48] In sensors overlying the central sulcus, power in the beta band and of the mu rhythm decreased non-significantly, but the lowering in mu rhythm power (9-13 Hz in this study) correlated positively with relief of rigidity.[77] In another study, suppression of 9-13 Hz power (band width in line with Airaksinen and colleagues)[77] in posterior cortical brain regions and 8-30 Hz power in right temporal regions correlated positively with DBS-related global motor improvement.[48,49] In frontal and parietal regions, an increase in gamma band power has been reported following DBS, which in frontal regions correlated negatively with the improvement of total motor function.[49]

Functional connectivity

In sensor-space studies, local FC can be estimated by averaging FC values for all possible pairs of sensors within a given region of interest (ROI), whereas between-ROI FC can be estimated by averaging FC for all possible pairs of sensors between ROIs. In a sensor-space study, recently diagnosed (drug-naïve) PD patients showed an overall higher local and between-ROI alpha1 FC compared to controls (measured using synchronization likelihood (SL;[71,78] an FC measure that captures both linear and non-linear interactions). When moderately-advanced PD patients were compared with controls, higher local functional connectivity (SL in one study and the phase lag index (PLI; less sensitive to volume conduction) in another) was found in PD patients, involving the theta, alpha1, alpha2 and beta band.[71,79] Motor symptom severity and disease duration were positively associated with higher local and between-ROI SL-values.[80] Furthermore, in one study DRT further increased between-ROI beta band FC, as well as local FC in the range of 4-30 Hz in association with clinical motor improvement (especially over centroparietal brain regions).[71] These findings are in contradiction with the findings of Cao and colleagues, who found the higher alpha PLI in PD patients to normalize upon DRT administration, in correlation with UPDRS-III improvement.[79] This discrepancy could perhaps be explained by a differential response to DRT observed by Stoffers and coworkers: in the majority of patients, already elevated levels of resting-state local FC (4-30Hz) further increased, but in patients with a strong improvement in motor function local beta band FC decreased.[71] It was speculated that the differential response to DRT points at differences in the susceptibility to the development of response fluctuations and/or dyskinesias.

Longitudinal follow-up of PD patients using the PLI in source-space (the average PLI from a ROI with all other ROIs) revealed a higher baseline alpha1 PLI in cortical temporal regions in PD compared to controls. With disease progression however, the initial changes in alpha1 PLI reversed, and an additional global decrease in alpha2 PLI appeared. These longitudinal changes correlated positively with worsening motor and global cognitive function. Interestingly, changes in alpha1 and alpha2 PLI in lower temporal regions, but not in the beta band, correlated with motor impairment.[81] Additional connectivity measures that have been used in source-space analysis to demonstrate cross-sectional differences

between PD patients and controls include the phase locking value (PLV; comparable to PLI but sensitive to volume conduction/field spread)[82] and directed Phase Transfer Entropy (dPTE), a measure of directed connectivity.[83] The PLV study demonstrated that during a working memory task, PD patients had significantly lower alpha band (9-16 Hz) PLV within the left-hemispheric fronto-temporal circuitry compared to controls, which correlated negatively with verbal working memory performance.[84] The dPTE has been used to reveal lower beta band directed connectivity from posterior cortical brain regions towards frontal and subcortical brain regions in PD versus controls. In this study, lower directed connectivity from posterior cortical regions with the rest of the brain correlated with poor global cognitive performance in PD patients.[5]

Comparison of a cohort of PDD patients with non-demented PD patients using two different processing pipelines led to conflicting outcomes that could at least partly be explained by differences in methodology:[74,85] in the first study, analysis was based on (ten) clusters of extracranial sensors and SL was used as FC measure. Compared to PD, PDD was characterized by lower fronto-temporal SL in lower frequency bands (delta, theta and alpha1), and higher left-sided parieto-occipital SL in the higher frequency bands (alpha2 and beta).[85] In the second (source-level) analysis, FC was calculated using PLI. In the PDD group, PLI between pairs of regions was generally lower for the delta, alpha and beta band, and higher in the theta band. In the gamma band, differences went both ways.[74]

Topological organization

Olde Dubbelink and colleagues (2014a) characterized the topological organization of PD brain networks in source-space using graph analysis techniques. In early-stage PD patients, lower local integration with preserved global efficiency of the whole-brain network has been observed in the delta band. A longitudinal analysis demonstrated a tendency towards a more random brain topology, in which both local integration (multiple frequency bands) and global efficiency (alpha2 band) were affected. Worsening global cognition was associated with more random topology in the theta band, and motor dysfunction was associated with lower alpha2 global efficiency. In contrast to the more conventional application of graph analysis techniques, minimum spanning tree (MST) analysis is free of threshold and normalization biases. MST analysis revealed a progressive decentralization of the network configuration, starting in the early-stage, untreated patients, which correlated with deteriorating motor function and cognitive performance.[86]

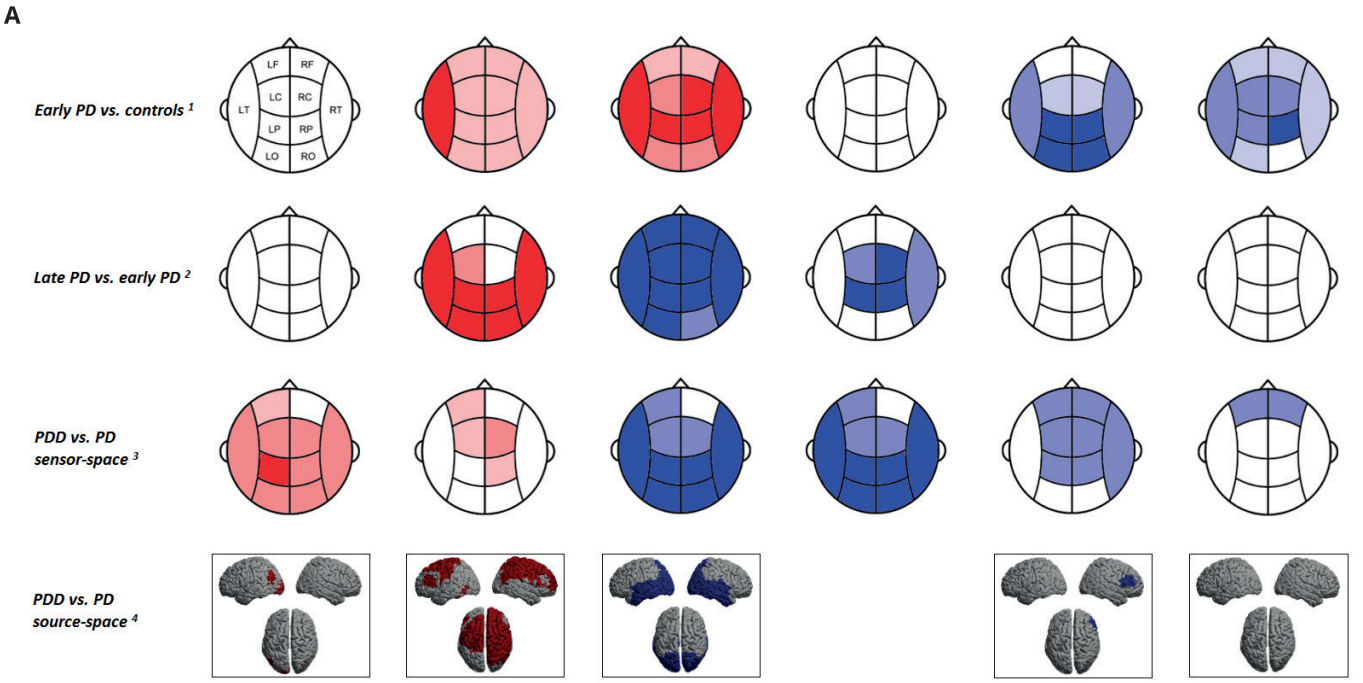

Figure 3 Overview of main findings in whole brain network-focused research: Band power
(A) Band power Schematic representation of observed statistical differences in relative band power between groups. Both sensor-space and source-space analyses are included in the figure. In case of sensor-space analysis, the brain region underlying the relevant sensor was colored. In case of source-space analysis results for each region of interest (ROI) are displayed as a color-coded map on a parcellated template brain viewed from, in clockwise order, the left, right, and top. An area is colored red when the mean power early PD > controls, late PD > early PD, and PDD > PD and blue when the difference was in the opposite direction. The three color codes of magnitudes (from light to dark) illustrate the effect size of the observed difference. Areas that did not show statistically significant differences are represented in white/grey. In the study by [74] the alpha1 and alpha2 band were combined. Figure adapted from 1=[70]; 2=[72]; 3=[73]; 4=[74]

(B) Schematic representation of observed statistical differences. In case of a sensor-space analysis differences are depicted for local (colored regions) and interregional (arrows) functional connectivity (FC; synchronization likelihood and phase lag index) between groups. In case of a source-space analysis differences in FC from one region of interest (ROI) to the rest of the brain (using phase lag index) are displayed as a color-coded map on a parcellated template brain viewed from, in clockwise order, the left, right, and top. An area is colored red when the FC of early PD > controls, moderately advanced PD > controls, and PDD > PD and blue when the difference was in the opposite direction. Areas that did not show statistically significant differences are represented in white/grey. In the study by Ponsen et al.[74] the alpha1 and alpha2 band were combined. Figure adapted from 4=[74]; 5=[80]; 6=[81]; 7=[79]; 8=[85]

PD, Parkinson's disease without dementia; PDD, Parkinson's disease related dementia; L or R, cortical area on the left (L) or right (R) side of the head; C, central; F, frontal; O, occipital; P, parietal; T, temporal.

B
Delta
Theta
Alpha1
Alpha2
Beta
Gamma
LF
RF
LC
RC
LT
RT
LP
RP
LO
RO
Early PD vs. controls sensor-space [5]
Early PD vs. controls source-space [6]
Moderately advanced PD vs. controls [7]
PDD vs. PD sensor-space [8]
PDD vs. PD source-space [9]

Discussion

In this review of the MEG literature on PD, we provide an overview of the neurophysiological characteristics of PD, their relationship with clinical motor and non-motor symptoms, the effect of disease progression, and the influence of treatment on these characteristics. The design of the studies included in this review is very diverse, regarding both the MEG-recordings itself (e.g. task-based versus resting-state, eyes-closed versus eyes-open, MEG signals alone or in relation to other measures, such as LFPs from the STN) and data analysis (e.g. source-space versus sensor-space, different FC measures). Despite these challenging differences in data analytical approaches, we were able to extract several robust findings.

Motor-network focused studies have uncovered a tremor network involving the motor cortex. In addition, these studies support the notion that, in contrast with the pathophysiology of bradykinesia and rigidity, not only basal-ganglia-cortical motor circuits but also cerebello-thalamo-cortical circuits are important for PD-related tremor (for further reading see Helmich et al. (2018)).[87] Another robust finding is the presence of functional loops between the STN and the temporal lobe (alpha band) and the STN and the sensorimotor cortex (beta and gamma band), although the clinical relevance and the effect of DRT on these loops remain to be established. Furthermore, as illustrated in Figures 2 and 3, the neurophysiological characteristics of the PD brain may vary over the course of the disease. For motor network-focused studies this could be exemplified by increased cortical motor beta band power early in the disease and decreased cortical motor beta band power later in the disease. Whole-brain studies showed a gradual slowing of the power spectrum and an initial increase in functional connectivity, which decreased over time in relation to disease progression, especially cognitive decline. Posterior cortical dysfunction seems to play a crucial role here.[5,70,76] Treatments such as DRT and rivastigmine generally normalized disrupted neurophysiological characteristics in both research fields, although many discrepancies exist, for example the increase in cortical motor beta power upon DRT,[42] versus the decrease observed upon DBS,[38,44] or the differential effect of DRT on whole-brain functional connectivity.[71,79] Potential explanations for these discrepancies include methodological differences and differences in the underlying neurophysiological characteristics between PD patients (Fig. 2 and 3).

When comparing the MEG findings discussed in this review with the EEG studies recently reviewed by Geraedts and colleagues,[25] there is a prominent agreement on the link between spectral slowing and cognitive decline. Lower peak frequency and higher delta/theta power were the best predictors for future conversion to PDD in longitudinal EEG studies[88-91] and in an MEG study a lower beta band power was the best predictor.[76] The effect of DRT on whole-brain power was inconclusive for both EEG[92] and MEG studies,[71] as well as the relationship between EEG/MEG-findings and UPDRS-III scores. Although EEG-based longitudinal functional connectivity studies are missing, a few cross-sectional studies hint at lower functional connectivity and network disruptions in cognitively disturbed PD patients[93,94], in accordance with the results of MEG studies.[74,81,86]

The results section of this review reflects the clear distinction between motor network-focused MEG research and whole-brain MEG research. Although this distinction often leaves little room for direct comparisons, both fields do share common grounds and we will further explore these in the next two sections.

Motor network-focused research from a whole-brain point of view

Beta band hypersynchrony within the STN and the basal ganglia-thalamo-cortical, cortico-cortical and cerebro-muscular loops is a well-established electrophysiological phenomenon in PD, not only in the MEG field.[59,80,95-97] It has been suggested that the changes in beta band power/connectivity in PD might be a causal mechanism underlying the motor symptoms bradykinesia and rigidity, also considering the indirect evidence that treatment (either DRT or high-frequency DBS) alleviates symptoms and at the same time causes a normalization of local band power and interregional coupling of beta activity.[42,96,98,99] However, there is no clear evidence that beta band synchronization directly accounts for the motor deficits in PD. Neurophysiological changes in motor network studies did not correlate with UPDRS-III scores when recorded during the resting state.[12,38,40,43,58] Furthermore, several unexpected negative correlations were observed when late-stage PD patients were recorded during isometric contraction or a motor task of the forearm in the DRT-OFF state.[58,60] It has therefore been speculated that excessive beta band power and/or connectivity may not represent a pathological disinhibition with an anti-kinetic effect, but could rather be interpreted as a compensatory mechanism that becomes redundant when DRT is administered.[58,60] Hyperconnectivity has also been demonstrated in whole-brain (both source-space and sensor-space) studies in the early stages of PD, most pronounced in the alpha1 band.[80,81] The interpretation of hyperconnectivity in early disease stages is not trivial and the discussion on this matter takes place in a broader context than that of PD only.[100,101] Both pathological disinhibition and compensatory mechanisms may lead to higher FC values, but only a compensatory mechanism would be a purposeful reaction to a pathological process. However, it is unlikely that the latter mechanism is the sole explanation, since the majority of the studies in the present review did not show a positive correlation between higher FC and better clinical performance.[12,40,43,58,80]

The functional subdivision between low and high-beta frequencies might be of value in unraveling the relationship between interregional coupling of beta activity and clinical functioning. Whereas dopaminergic treatment mainly affected low-beta spectral power in the STN, STN-cortical coherence was strongest in the high-beta band frequencies and was not modulated by levodopa.[12,36] Perhaps more complex functional interactions, such as cross-frequency coupling,[102] could play a role in the pathophysiology of PD motor symptoms. Cross-frequency coupling was previously found within the STN[36] and within the motor cortex[103] (but see also [104]) but not between these two structures.

Alternatively, negative correlations such as between M1-STN beta band synchrony and UPDRS-III scores could merely reflect normal physiology, in which case one would expect healthy individuals to show stronger M1-STN coherence than PD patients.[60] Obviously, it is not possible to perform invasive recordings of brain activity in controls to confirm this, but a case study in an obsessive-compulsive disorder patient, treated with STN-DBS, confirmed the presence of a high STN-motor cortical connectivity in the beta band.[105] Furthermore, advances in source reconstruction techniques, such as beamforming, increasingly allow the study of subcortical regions by means of MEG.[5-7] At this point, however, additional methodological and experimental studies are necessary to evaluate the ability of beamformer techniques to reliably distinguish between individual subcortical brain regions.

Another important consideration is that the local neurophysiological processes observed in the motor network take place in a brain that is both structurally[2] and functionally[72,81] affected by PD on a whole-brain scale. The interpretation of correlations between neurophysiological changes and motor symptoms is further complicated when studying the effect of DRT, since DRT can have varying effects on cortico-cortical functional connectivity, dependent on disease stage and/or degree of UPDRS motor response to DRT.[80]

Thus, neurophysiological changes on a whole-brain scale may have directly or indirectly influenced findings in motor network-focused MEG studies. Whole-brain studies have demonstrated that neurophysiological changes associated with PD motor symptoms are not restricted to the 'classical' motor network, which may have influenced findings *directly*: the slowing of beta band oscillations in the motor cortex observed in motor network-focused studies in relatively advanced-stage patients[42,59] may in fact be part of the more general process of cortical oscillatory slowing.[70,72] Along the same line, the higher beta band functional connectivity between cortical motor regions[42] should be considered against the background of global increases in beta band cortico-cortical FC that have been observed both using EEG and MEG in moderately advanced PD patients, and which correlated with both bradykinesia sub scores and disease duration.[80,98] In contrast, in early disease stages larger beta band power has been observed in cortical motor regions in both PD patients and animal models of PD,[40,41,106-108] yet this has not been mirrored by the results of whole-brain studies.[70,72]

Variability in ongoing brain activity contributes to the way the brain responds to certain sensory stimuli and therefore might *indirectly* influence differences in event-related/induced motor responses between controls and PD patients.[109] Furthermore, whole-brain band power changes are known to confound estimates of coherence between two neurophysiological signals and can thereby influence findings in motor network MEG studies.[14] In studies that estimated motor CMC, beta band power in cortical motor regions (and possibly also global beta band power) also differed between PD patients and controls and could therefore have impacted the CMC findings.[58,59] In addition, the occipital dominant alpha band rhythm, mainly present when the eyes are closed, may dilute differences observed in the motor network studies.[44]

The interpretation of cortico-subcortical interactions in DBS patients is hampered by the fact that these patients are generally in an advanced stage of disease and therefore have often received high doses of DRT for several years. Chronic DRT is known to influence cortical oscillations via neuronal plasticity.[108] Furthermore, a longitudinal evaluation of the effect of STN-DBS on beta band oscillations within the STN, coherence with cortical regions, and cortical oscillations along the disease course has not been performed yet. Therefore, when studying cortico-subcortical coherence, the effects of the underlying disease, chronic use of medication and DBS itself on whole-brain cortical oscillations should be taken into account.

Whole-brain research: towards a more focused approach

In whole-brain MEG studies in PD, global oscillatory slowing, widespread changes in the strength of functional connectivity within and between brain areas, and a disruption of functional brain network organization have been observed. The consistent relationship between these findings and cognitive decline, motor dysfunction and disease duration support the notion that these whole-brain neurophysiological changes may represent a general marker of the disease processes underlying PD,[70,72,73,86] a conclusion that is further supported by the results of EEG studies.[110-112] However, the mechanisms that lead to these widespread neurophysiological changes remain unknown, as well as the way in which these neurophysiological changes induce the clinical symptoms of PD, particularly the non-motor symptoms.

There is increasing evidence to suggest that cortical neurophysiological changes in PD find their origin in subcortical brain regions. In early-stage PD, involvement of brainstem dopaminergic, noradrenergic and serotonergic projection systems may be important factors that contribute to cortical oscillatory slowing.[73,113] In later disease stages – including PD dementia – local cortical Lewy body and tau pathology, local pathology in thalamo-cortical circuits,[114,115] and degeneration of the cholinergic nucleus of Meynert[75,116] may contribute to cortical neurophysiological changes in PD.

Observations that highlight the importance of cortico-subcortical interactions in PD include the influence of STN-DBS on whole-brain oscillations,[48,49,77] the possible influence of STN-DBS on a multitude of non-motor symptoms[117] and the presence of an STN-temporal network in the alpha band that shows PD-related functional changes and is influenced by movement.[11,12,46,64,76] Future whole-brain studies could build on these observations by including estimation of cortico-subcortical interactions using source reconstruction techniques, and correlate findings to both motor and non-motor symptoms.

The neurophysiological changes observed in whole-brain resting-state studies correlated with both motor and non-motor symptoms of PD,[72,73,80,81,86] hence the interpretation of these changes might be more ambiguous than the observations in task-related conditions. On the other hand, whole-brain resting-state neurophysiological changes

might be a more accurate marker of the underlying disease process. A reliable (non-invasive) in vivo marker of the disease process can be used to predict the disease course in individual patients and to monitor the effects of modulatory techniques such as DBS or future disease-modifying drugs.

The approach of focusing on average FC from a ROI with all other regions in a whole-brain analysis might be too diffuse to pick up changes restricted to certain sub systems. When trying to bridge the gap between the underlying disease and specific PD-related symptoms – referred to as pathophysiology in this context – a more focused approach would be preferable. A seed-based analysis could be used to confirm hypotheses that have arisen based on whole-brain research. In addition, particular symptoms such as cognitive dysfunction in specific domains may be correlated to changes in (dynamic) connectivity between specific subnetworks.[118,119] A more focused approach can provide important additional information on the pathophysiology of specific disease-related symptoms, which may prove useful for the development of symptomatic treatments, e.g. targeting key brain regions or subnetworks using TMS or DBS. These exciting therapeutic possibilities are already being tested in PD patients.[120,121]

Clinical utility of MEG in PD

Of the robust findings we have presented in this review, up to now only MEG-derived spectral markers (markers of spectral slowing) as predictors for conversion to PDD have potential for routine clinical use.[76] As these in-vivo biomarkers of disease progression can also be derived from cheaper and more widely available EEG recordings,[25] the need to include MEG in standard clinical care is currently low. However, with MEG patients would benefit from a more comfortable and faster recording technique. In addition, when the higher spatial resolution of MEG over EEG is exploited, application of MEG in routine clinical care could become more rational (see Hillebrand et al.[122] for further reading on the clinical application of MEG). Future studies are required to establish whether measures of functional connectivity or brain network structure, which could be determined more reliably using MEG, can surpass spectral slowing as an in-vivo biomarker of cognitive decline or disease progression in a broader sense.

The optimization of stimulation settings after DBS-placement could also benefit from MEG-recordings, both for non-motor and motor effects. Potentially, beta band power in the sensorimotor cortex could serve as a biomarker for optimal motor effects, although the link between cortical beta oscillations and motor function is not clear yet.[38,44] Alternatively, a more dispersed cortical fingerprint could serve as a biomarker for optimal clinical (both motor and non-motor) effects.

Conclusion

Macro-scale neurophysiological changes in the PD brain have classically been studied from two different perspectives. Some research groups have studied PD-related changes in the brain as a whole, while others have explored relationships between more localized brain activity and motor symptoms, thereby focusing on pathophysiological mechanisms. However, the two research fields are certainly not mutually exclusive and the knowledge gained from both approaches may even be complementary: motor network function is influenced by whole-brain changes in neuronal activity related to the ongoing disease processes, whereas whole-brain analysis may not fully capture local pathophysiological mechanisms underlying specific symptoms. Up to now, results of MEG studies have been very diverse and the application of MEG in standard clinical care is limited. Future studies that combine the merits of both approaches could increase reproducibility and interpretation of results, which will undoubtedly lead to valuable insights into the neuronal mechanisms underlying PD as well as into the pathophysiology of the broad range of clinical symptoms that characterize this disease.

Acknowledgements

The authors thank J. Schoones MSc, Medical Library, Universiteit Leiden Medical Centre, for his help on the literature search. Theauthors thank T. Lehmann BSc and S. Sharifi MD MSc for their input on the figures.

References

1. Olanow CW, Stern MB, Sethi K. The scientific and clinical basis for the treatment of Parkinson disease (2009). Neurology. 2009;72(21 Suppl 4):S1-136.
2. Braak H, Del Tredici K, Rüb U, et al. Staging of brain pathology related to sporadic Parkinson's disease. Neurobiol Aging. 2003;24(2):197-211.
3. Cohen D. Magnetoencephalography: detection of the brain's electrical activity with a superconducting magnetometer. Science (New York, NY). 1972;175(4022):664-6.
4. Cohen D. Magnetoencephalography: evidence of magnetic fields produced by alpha-rhythm currents. Science (New York, NY). 1968;161(3843):784-6.
5. Boon LI, Hillebrand A, Dubbelink KTO, et al. Changes in resting-state directed connectivity in cortico-subcortical networks correlate with cognitive function in Parkinson's disease. Clin Neurophysiol. 2017;128(7):1319-26.
6. Hillebrand A, Nissen I, Ris-Hilgersom I, et al. Detecting epileptiform activity from deeper brain regions in spatially filtered MEG data. Clin Neurophysiol. 2016;127(8):2766-9.
7. Jha A, Litvak V, Taulu S, et al. Functional Connectivity of the Pedunculopontine Nucleus and Surrounding Region in Parkinson's Disease. Cereb Cortex. 2017;27(1):54-67.
8. Baillet S. Magnetoencephalography for brain electrophysiology and imaging. Nat Neurosci. 2017;20(3):327-39.
9. Timmermann L, Gross J, Dirks M, et al. The cerebral oscillatory network of parkinsonian resting tremor. Brain. 2003;126(Pt 1):199-212.
10. Volkmann J, Joliot M, Mogilner A, et al. Central motor loop oscillations in parkinsonian resting tremor revealed by magnetoencephalography. Neurology. 1996;46(5):1359-70.
11. Hirschmann J, Ozkurt TE, Butz M, et al. Distinct oscillatory STN-cortical loops revealed by simultaneous MEG and local field potential recordings in patients with Parkinson's disease. Neuroimage. 2011;55(3):1159-68.
12. Litvak V, Jha A, Eusebio A, et al. Resting oscillatory cortico-subthalamic connectivity in patients with Parkinson's disease. Brain. 2011;134(Pt 2):359-74.
13. Friston KJ. Functional and effective connectivity: a review. Brain Connect. 2011;1(1):13-36.
14. Schoffelen JM, Gross J. Source connectivity analysis with MEG and EEG. Hum Brain Mapp. 2009;30(6):1857-65.
15. Hillebrand A, Singh KD, Holliday IE, et al. A new approach to neuroimaging with magnetoencephalography. Hum Brain Mapp. 2005;25(2):199-211.
16. Hillebrand A, Barnes GR, Bosboom JL, et al. Frequency-dependent functional connectivity within resting-state networks: an atlas-based MEG beamformer solution. Neuroimage. 2012;59(4):3909-21.
17. Brookes MJ, Stevenson CM, Barnes GR, et al. Beamformer reconstruction of correlated sources using a modified source model. Neuroimage. 2007;34(4):1454-65.
18. Baillet S, Mosher JC, Leahy RM. Electromagnetic brain mapping. IEEE Signal processing magazine. 2001;18(6):14-30.
19. Magrinelli F, Picelli A, Tocco P, et al. Pathophysiology of motor dysfunction in Parkinson's disease as the rationale for drug treatment and rehabilitation. Parkinsons Dis. 2016;2016.
20. Burciu RG, Vaillancourt DE. Imaging of Motor Cortex Physiology in Parkinson's Disease. Mov Disord. 2018.
21. Cozac VV, Gschwandtner U, Hatz F, et al. Quantitative EEG and Cognitive Decline in Parkinson's Disease. Parkinsons Dis. 2016;2016.
22. Oswal A, Brown P, Litvak V. Synchronized neural oscillations and the pathophysiology of Parkinson's disease. Curr Opin Neurol. 2013;26(6):662-70.
23. Liberati A, Altman DG, Tetzlaff J, et al. The PRISMA statement for reporting systematic reviews

and meta-analyses of studies that evaluate health care interventions: explanation and elaboration. PLoS medicine. 2009;6(7):e1000100.

24. Goldenholz DM, Ahlfors SP, Hamalainen MS, et al. Mapping the signal-to-noise-ratios of cortical sources in magnetoencephalography and electroencephalography. Hum Brain Mapp. 2009;30(4):1077-86.
25. Geraedts VJ, Boon LI, Marinus J, et al. Clinical correlates of quantitative EEG in Parkinson disease: A systematic review. Neurology. 2018.
26. David O, Kilner JM, Friston KJ. Mechanisms of evoked and induced responses in MEG/EEG. Neuroimage. 2006;31(4):1580-91.
27. Gross J, Baillet S, Barnes GR, et al. Good practice for conducting and reporting MEG research. Neuroimage. 2013;65:349-63.
28. Te Woerd ES, Oostenveld R, De Lange FP, et al. A shift from prospective to reactive modulation of beta-band oscillations in Parkinson's disease. Neuroimage. 2014;100:507-19.
29. Te Woerd ES, Oostenveld R, Bloem BR, et al. Effects of rhythmic stimulus presentation on oscillatory brain activity: the physiology of cueing in Parkinson's disease. Neuroimage Clin. 2015;9:300-9.
30. Te Woerd ES, Oostenveld R, De Lange FP, et al. Impaired auditory-to-motor entrainment in Parkinson's disease. J Neurophysiol. 2017:jn.
31. Te Woerd ES, Oostenveld R, de Lange FP, et al. Entrainment for attentional selection in Parkinson's disease. Cortex 2018;99:166-78.
32. Anninos P, Adamopoulos A, Kotini A, et al. Combined MEG and pT-TMS study in Parkinson's disease. J Integr Neurosci. 2016;15(2):145-62.
33. Gomez C, Olde Dubbelink KT, Stam CJ, et al. Complexity analysis of resting-state MEG activity in early-stage Parkinson's disease patients. Ann Biomed Eng. 2011;39(12):2935-44.
34. Suntrup S, Teismann I, Bejer J, et al. Evidence for adaptive cortical changes in swallowing in Parkinson's disease. Brain. 2013;136(Pt 3):726-38.
35. Boesveldt S, Stam CJ, Knol DL, et al. Advanced time-series analysis of MEG data as a method to explore olfactory function in healthy controls and Parkinson's disease patients. Hum Brain Mapp. 2009;30(9):3020-30.
36. van Wijk BC, Beudel M, Jha A, et al. Subthalamic nucleus phase-amplitude coupling correlates with motor impairment in Parkinson's disease. Clin Neurophysiol. 2016;127(4):2010-9.
37. Oswal A, Beudel M, Zrinzo L, et al. Deep brain stimulation modulates synchrony within spatially and spectrally distinct resting state networks in Parkinson's disease. Brain. 2016;139(Pt 5):1482-96.
38. Abbasi O, Hirschmann J, Storzer L, et al. Unilateral deep brain stimulation suppresses alpha and beta oscillations in sensorimotor cortices. Neuroimage. 2018;174:201-7.
39. Airaksinen K, Makela JP, Nurminen J, et al. Cortico-muscular coherence in advanced Parkinson's disease with deep brain stimulation. Clin Neurophysiol. 2015;126(4):748-55.
40. Pollok B, Krause V, Martsch W, et al. Motor-cortical oscillations in early stages of Parkinson's disease. J Physiol. 2012;590(13):3203-12.
41. Hall SD, Prokic EJ, McAllister CJ, et al. GABA-mediated changes in inter-hemispheric beta frequency activity in early-stage Parkinson's disease. Neuroscience. 2014;281:68-76.
42. Heinrichs-Graham E, Kurz MJ, Becker KM, et al. Hypersynchrony despite pathologically reduced beta oscillations in patients with Parkinson's disease: a pharmaco-magnetoencephalography study. J Neurophysiol. 2014;112(7):1739-47.
43. Vardy AN, van Wegen EE, Kwakkel G, et al. Slowing of M1 activity in Parkinson's disease during rest and movement--an MEG study. Clin Neurophysiol. 2011;122(4):789-95.
44. Luoma J, Pekkonen E, Airaksinen K, et al. Spontaneous sensorimotor cortical activity is suppressed by deep brain stimulation in patients with advanced Parkinson's disease. Neurosci Lett. 2018;683:48-53.

45. Litvak V, Eusebio A, Jha A, et al. Optimized beamforming for simultaneous MEG and intracranial local field potential recordings in deep brain stimulation patients. Neuroimage. 2010;50(4):1578-88.
46. Oswal A, Jha A, Neal S, et al. Analysis of simultaneous MEG and intracranial LFP recordings during Deep Brain Stimulation: a protocol and experimental validation. J Neurosci Methods. 2016;261:29-46.
47. Airaksinen K, Makela JP, Taulu S, et al. Effects of DBS on auditory and somatosensory processing in Parkinson's disease. Hum Brain Mapp. 2011;32(7):1091-9.
48. Cao C, Li D, Jiang T, et al. Resting state cortical oscillations of patients with Parkinson disease and with and without subthalamic deep brain stimulation: a magnetoencephalography study. J Clin Neurophysiol. 2015;32(2):109-18.
49. Cao CY, Zeng K, Li DY, et al. Modulations on cortical oscillations by subthalamic deep brain stimulation in patients with Parkinson disease: A MEG study. Neurosci Lett. 2017;636:95-100.
50. Mohseni HR, Kringelbach ML, Probert Smith P, et al. Application of a null-beamformer to source localisation in MEG data of deep brain stimulation. Conference proceedings: Annual International Conference of the IEEE Engineering in Medicine and Biology Society IEEE Engineering in Medicine and Biology Society Annual Conference. 2010;2010:4120-3.
51. Abbasi O, Hirschmann J, Schmitz G, et al. Rejecting deep brain stimulation artefacts from MEG data using ICA and mutual information. J Neurosci Methods. 2016;268:131-41.
52. Harmsen IE, Rowland NC, Wennberg RA, et al. Characterizing the effects of deep brain stimulation with magnetoencephalography: A review. Brain stimul. 2018;11(3):481-91.
53. Jurkiewicz MT, Gaetz WC, Bostan AC, et al. Post-movement beta rebound is generated in motor cortex: evidence from neuromagnetic recordings. Neuroimage. 2006;32(3):1281-9.
54. Gaetz W, Macdonald M, Cheyne D, et al. Neuromagnetic imaging of movement-related cortical oscillations in children and adults: age predicts post-movement beta rebound. Neuroimage. 2010;51(2):792-807.
55. Heinrichs-Graham E, Wilson TW, Santamaria PM, et al. Neuromagnetic evidence of abnormal movement-related beta desynchronization in Parkinson's disease. Cereb Cortex. 2014;24(10):2669-78.
56. Heinrichs-Graham E, Santamaria PM, Gendelman HE, et al. The cortical signature of symptom laterality in Parkinson's disease. Neuroimage Clin. 2017;14:433-40.
57. Meissner SN, Krause V, Sudmeyer M, et al. The significance of brain oscillations in motor sequence learning: Insights from Parkinson's disease. Neuroimage Clin. 2018;20:448-57.
58. Pollok B, Kamp D, Butz M, et al. Increased SMA-M1 coherence in Parkinson's disease - Pathophysiology or compensation? Exp Neurol. 2013;247:178-81.
59. Salenius S, Avikainen S, Kaakkola S, et al. Defective cortical drive to muscle in Parkinson's disease and its improvement with levodopa. Brain. 2002;125(Pt 3):491-500.
60. Hirschmann J, Ozkurt TE, Butz M, et al. Differential modulation of STN-cortical and cortico-muscular coherence by movement and levodopa in Parkinson's disease. Neuroimage. 2013;68:203-13.
61. Park H, Kim JS, Paek SH, et al. Cortico-muscular coherence increases with tremor improvement after deep brain stimulation in Parkinson's disease. Neuroreport. 2009;20(16):1444-9.
62. Krause V, Wach C, Sudmeyer M, et al. Cortico-muscular coupling and motor performance are modulated by 20 Hz transcranial alternating current stimulation (tACS) in Parkinson's disease. Front Hum Neurosci. 2013;7:928.
63. Litvak V, Eusebio A, Jha A, et al. Movement-related changes in local and long-range synchronization in Parkinson's disease revealed by simultaneous magnetoencephalography and intracranial recordings. J Neurosci. 2012;32(31):10541-53.
64. Oswal A, Brown P, Litvak V. Movement related dynamics of subthalmo-cortical alpha connectivity in Parkinson's disease. Neuroimage. 2013;70:132-42.
65. Weisz N, Hartmann T, Müller N, et al. Alpha rhythms in audition: cognitive and clinical

perspectives. Front Psychol. 2011;2.

66. Louis ED, Tang MX, Cote L, et al. Progression of parkinsonian signs in Parkinson disease. Arch Neurol. 1999;56(3):334-7.
67. Pollok B, Makhloufi H, Butz M, et al. Levodopa affects functional brain networks in Parkinsonian resting tremor. Mov Disord. 2009;24(1):91-8.
68. Hirschmann J, Hartmann CJ, Butz M, et al. A direct relationship between oscillatory subthalamic nucleus-cortex coupling and rest tremor in Parkinson's disease. Brain. 2013;136(Pt 12):3659-70.
69. Makela JP, Hari P, Karhu J, et al. Suppression of magnetic mu rhythm during parkinsonian tremor. Brain Res. 1993;617(2):189-93.
70. Stoffers D, Bosboom JL, Deijen JB, et al. Slowing of oscillatory brain activity is a stable characteristic of Parkinson's disease without dementia. Brain. 2007;130(Pt 7):1847-60.
71. Stoffers D, Bosboom JL, Wolters EC, et al. Dopaminergic modulation of cortico-cortical functional connectivity in Parkinson's disease: an MEG study. Exp Neurol. 2008;213(1):191-5.
72. Olde Dubbelink KT, Stoffers D, Deijen JB, et al. Cognitive decline in Parkinson's disease is associated with slowing of resting-state brain activity: a longitudinal study. Neurobiol Aging. 2013;34(2):408-18.
73. Bosboom JL, Stoffers D, Stam CJ, et al. Resting state oscillatory brain dynamics in Parkinson's disease: an MEG study. Clin Neurophysiol. 2006;117(11):2521-31.
74. Ponsen MM, Stam CJ, Bosboom JL, et al. A three dimensional anatomical view of oscillatory resting-state activity and functional connectivity in Parkinson's disease related dementia: An MEG study using atlas-based beamforming. Neuroimage Clin. 2012;2:95-102.
75. Bosboom JL, Stoffers D, Stam CJ, et al. Cholinergic modulation of MEG resting-state oscillatory activity in Parkinson's disease related dementia. Clin Neurophysiol. 2009;120(5):910-5.
76. Olde Dubbelink KT, Hillebrand A, Twisk JW, et al. Predicting dementia in Parkinson disease by combining neurophysiologic and cognitive markers. Neurology. 2014;82(3):263-70.
77. Airaksinen K, Butorina A, Pekkonen E, et al. Somatomotor mu rhythm amplitude correlates with rigidity during deep brain stimulation in Parkinsonian patients. Clin Neurophysiol. 2012;123(10):2010-7.
78. Stam C, Van Dijk B. Synchronization likelihood: an unbiased measure of generalized synchronization in multivariate data sets. Physica D: Nonlinear Phenomena. 2002;163(3):236-51.
79. Cao C, Li D, Zeng K, et al. Levodopa Reduces the Phase lag Index of Parkinson's Disease Patients: A Magnetoencephalographic Study. Clin EEG Neurosci. 2018:1550059418781693.
80. Stoffers D, Bosboom JL, Deijen JB, et al. Increased cortico-cortical functional connectivity in early-stage Parkinson's disease: an MEG study. Neuroimage. 2008;41(2):212-22.
81. Olde Dubbelink KT, Stoffers D, Deijen JB, et al. Resting-state functional connectivity as a marker of disease progression in Parkinson's disease: A longitudinal MEG study. Neuroimage Clin. 2013;2:612-9.
82. Lachaux JP, Rodriguez E, Martinerie J, et al. Measuring phase synchrony in brain signals. Hum Brain Mapp. 1999;8(4):194-208.
83. Lobier M, Siebenhuhner F, Palva S, et al. Phase transfer entropy: a novel phase-based measure for directed connectivity in networks coupled by oscillatory interactions. Neuroimage. 2014;85 Pt 2:853-72.
84. Wiesman AI, Heinrichs-Graham E, McDermott TJ, et al. Quiet connections: Reduced fronto-temporal connectivity in nondemented Parkinson's Disease during working memory encoding. Hum Brain Mapp. 2016;37(9):3224-35.
85. Bosboom JL, Stoffers D, Wolters EC, et al. MEG resting state functional connectivity in Parkinson's disease related dementia. J Neural Transm (Vienna). 2009;116(2):193-202.
86. Olde Dubbelink KT, Hillebrand A, Stoffers D, et al. Disrupted brain network topology in Parkinson's disease: a longitudinal magnetoencephalography study. Brain. 2014;137(Pt 1):197-207.

87. Helmich RC. The cerebral basis of Parkinsonian tremor: A network perspective. Mov Disord. 2018;33(2):219-31.
88. Caviness JN, Hentz JG, Belden CM, et al. Longitudinal EEG changes correlate with cognitive measure deterioration in Parkinson's disease. J Parkinsons Dis. 2015;5(1):117-24.
89. Latreille V, Carrier J, Gaudet-Fex B, et al. Electroencephalographic prodromal markers of dementia across conscious states in Parkinson's disease. Brain. 2016;139(Pt 4):1189-99.
90. Klassen BT, Hentz JG, Shill HA, et al. Quantitative EEG as a predictive biomarker for Parkinson disease dementia. Neurology. 2011;77(2):118-24.
91. Cozac VV, Chaturvedi M, Hatz F, et al. Increase of EEG Spectral Theta Power Indicates Higher Risk of the Development of Severe Cognitive Decline in Parkinson's Disease after 3 Years. Front Aging Neurosci. 2016;8:284.
92. Mostile G, Nicoletti A, Dibilio V, et al. Electroencephalographic lateralization, clinical correlates and pharmacological response in untreated Parkinson's disease. Parkinsonism Relat Disord. 2015;21(8):948-53.
93. Hassan M, Chaton L, Benquet P, et al. Functional connectivity disruptions correlate with cognitive phenotypes in Parkinson's disease. Neuroimage Clin. 2017;14:591-601.
94. Utianski RL, Caviness JN, van Straaten EC, et al. Graph theory network function in Parkinson's disease assessed with electroencephalography. Clin Neurophysiol. 2016;127(5):2228-36.
95. Brown P. Oscillatory nature of human basal ganglia activity: relationship to the pathophysiology of Parkinson's disease. Mov Disord. 2003;18(4):357-63.
96. Hammond C, Bergman H, Brown P. Pathological synchronization in Parkinson's disease: networks, models and treatments. Trends Neurosci. 2007;30(7):357-64.
97. Kühn AA, Kupsch A, Schneider GH, et al. Reduction in subthalamic 8–35 Hz oscillatory activity correlates with clinical improvement in Parkinson's disease. Eur J Neurosci. 2006;23(7):1956-60.
98. Silberstein P, Pogosyan A, Kühn AA, et al. Cortico-cortical coupling in Parkinson's disease and its modulation by therapy. Brain. 2005;128(6):1277-91.
99. Levy R, Ashby P, Hutchison WD, et al. Dependence of subthalamic nucleus oscillations on movement and dopamine in Parkinson's disease. Brain. 2002;125(6):1196-209.
100. de Haan W, Mott K, van Straaten EC, et al. Activity dependent degeneration explains hub vulnerability in Alzheimer's disease. PLoS Comput Biol. 2012;8(8):e1002582.
101. Hillary FG, Grafman JH. Injured Brains and Adaptive Networks: The Benefits and Costs of Hyperconnectivity. Trends Cogn Sci. 2017;21(5):385-401.
102. Tewarie P, Hillebrand A, van Dijk BW, et al. Integrating cross-frequency and within band functional networks in resting-state MEG: A multi-layer network approach. Neuroimage. 2016;142:324-36.
103. de Hemptinne C, Ryapolova-Webb ES, Air EL, et al. Exaggerated phase-amplitude coupling in the primary motor cortex in Parkinson disease. Proc Natl Acad Sci U S A. 2013;110(12):4780-5.
104. Cole SR, van der Meij R, Peterson EJ, et al. Nonsinusoidal Beta Oscillations Reflect Cortical Pathophysiology in Parkinson's Disease. J Neurosci. 2017;37(18):4830-40.
105. Wojtecki L, Hirschmann J, Elben S, et al. Oscillatory coupling of the subthalamic nucleus in obsessive compulsive disorder. Brain. 2017;140(9):e56.
106. Javor-Duray BN, Vinck M, van der Roest M, et al. Early-onset cortico-cortical synchronization in the hemiparkinsonian rat model. J Neurophysiol. 2015;113(3):925-36.
107. Brazhnik E, Cruz AV, Avila I, et al. State-dependent spike and local field synchronization between motor cortex and substantia nigra in hemiparkinsonian rats. J Neurosci. 2012;32(23):7869-80.
108. Degos B, Deniau J-M, Chavez M, et al. Chronic but not acute dopaminergic transmission interruption promotes a progressive increase in cortical beta frequency synchronization: relationships to vigilance state and akinesia. Cereb cortex. 2008;19(7):1616-30.
109. Sadaghiani S, Hesselmann G, Friston KJ, et al. The relation of ongoing brain activity, evoked

neural responses, and cognition. Front Syst Neurosci. 2010;4:20.

110. He X, Zhang Y, Chen J, et al. Changes in theta activities in the left posterior temporal region, left occipital region and right frontal region related to mild cognitive impairment in Parkinson's disease patients. Int J Neurosci. 2017;127(1):66-72.
111. Fonseca L, Tedrus G, Letro G, et al. Dementia, mild cognitive impairment and quantitative EEG in patients with Parkinson's disease. Clin EEG Neurosci. 2009;40(3):168-72.
112. Morita A, Kamei S, Serizawa K, et al. The relationship between slowing EEGs and the progression of Parkinson's disease. J Clin Neurophysiol. 2009;26(6):426-9.
113. Bosboom J, Stoffers D, Wolters EC. Cognitive dysfunction and dementia in Parkinson's disease. Journal of neural transmission. 2004;111(10-11):1303-15.
114. Freunberger R, Werkle-Bergner M, Griesmayr B, et al. Brain oscillatory correlates of working memory constraints. Brain research. 2011;1375:93-102.
115. Steriade M, Gloor P, Llinas RR, et al. Basic mechanisms of cerebral rhythmic activities. Electroencephalogr Clin Neurophysiol. 1990;76(6):481-508.
116. Hepp DH, Foncke EM, Berendse HW, et al. Damaged fiber tracts of the nucleus basalis of Meynert in Parkinson's disease patients with visual hallucinations. Sci Rep. 2017;7(1):10112.
117. Castrioto A, Lhommée E, Moro E, et al. Mood and behavioural effects of subthalamic stimulation in Parkinson's disease. Lancet Neurol. 2014;13(3):287-305.
118. Park H-J, Friston K, Pae C, et al. Dynamic effective connectivity in resting state fMRI. NeuroImage. 2017.
119. Kucyi A, Hove MJ, Esterman M, et al. Dynamic brain network correlates of spontaneous fluctuations in attention. Cereb Cortex. 2016;27(3):1831-40.
120. Freund H-J, Kuhn J, Lenartz D, et al. Cognitive functions in a patient with Parkinson-dementia syndrome undergoing deep brain stimulation. Arch Neurol. 2009;66(6):781-5.
121. Manenti R, Brambilla M, Benussi A, et al. Mild cognitive impairment in Parkinson's disease is improved by transcranial direct current stimulation combined with physical therapy. Mov Disord. 2016;31(5):715-24.
122. Hillebrand A, Gaetz W, Furlong PL, et al. Practical guidelines for clinical magnetoencephalography - Another step towards best practice. Clin Neurophysiol. 2018;129(8):1709-11.
123. Lempel A, Ziv J. On the complexity of finite sequences. IEEE Transactions on information theory. 1976;22(1):75-81.
124. White LB, Boashash B. Cross spectral analysis of nonstationary processes. IEEE Transactions on Information Theory. 1990;36(4):830-5.
125. Stam CJ, Nolte G, Daffertshofer A. Phase lag index: assessment of functional connectivity from multi channel EEG and MEG with diminished bias from common sources. Hum Brain Mapp. 2007;28(11):1178-93.
126. Hillebrand A, Tewarie P, Van Dellen E, et al. Direction of information flow in large-scale resting-state networks is frequency-dependent. Proc Natl Acad Sci U S A. 2016;113(14):3867-72.
127. Granger CW. Investigating causal relations by econometric models and cross-spectral methods. Econometrica 1969:424-38.
128. Baccala LA, Sameshima K. Partial directed coherence: a new concept in neural structure determination. Biol Cybern. 2001;84(6):463-74.

Supplementary materials

Supplement A: Web-based searches

PubMed

((“Parkinson Disease”[Mesh] OR “Parkinson Disease, Secondary”[Mesh:NoExp] OR “Parkinsonian Disorders”[Mesh:noexp] OR “parkinsonian”[tw] OR parkinsonian*[tw] OR “parkinsonism”[tw] OR parkinsonism*[tw] OR “parkinson disease”[tw] OR “parkinson’s disease”[tw] OR “parkinsons disease”[tw] OR “Paralysis Agitans”[tw] OR parkinson*[tw]) AND (“Magnetoencephalography”[Mesh] OR “magnetoencephalography”[tw] OR magnetoencephalogr*[tw] OR “magneto-encephalography”[tw] OR magneto-encephalogr*[tw] OR “MEG”[tw]))

Embase

((exp “Parkinson Disease”/ OR “Parkinsonism”/ OR “parkinsonian”.mp OR parkinsonian*.mp OR “parkinsonism”.mp OR parkinsonism*.mp OR “parkinson disease”.mp OR “parkinson’s disease”.mp OR “parkinsons disease”.mp OR “Paralysis Agitans”.mp OR parkinson*.mp) AND (“Magnetoencephalography”/ OR “magnetoencephalography”.mp OR magnetoencephalogr*.mp OR “magneto-encephalography”.mp OR magneto-encephalogr*.mp OR “MEG”.mp)) NOT conference review.pt

Web of Science

(TS=(“Parkinson Disease” OR “Parkinsonism” OR “parkinsonian” OR parkinsonian* OR “parkinsonism” OR parkinsonism* OR “parkinson disease” OR “parkinson’s disease” OR “parkinsons disease” OR “Paralysis Agitans” OR parkinson*) AND TI=(“Magnetoencephalography” OR “magnetoencephalography” OR magnetoencephalogr* OR “magneto-encephalography” OR “magneto-encephalogr*” OR “MEG”)) OR (TI=(“Parkinson Disease” OR “Parkinsonism” OR “parkinsonian” OR parkinsonian* OR “parkinsonism” OR parkinsonism* OR “parkinson disease” OR “parkinson’s disease” OR “parkinsons disease” OR “Paralysis Agitans” OR parkinson*) AND TS=(“Magnetoencephalography” OR “magnetoencephalography” OR magnetoencephalogr* OR “magneto-encephalography” OR “magneto-encephalogr*” OR “MEG”))

Cochrane

((“Parkinson Disease” OR “Parkinsonism” OR “parkinsonian” OR parkinsonian* OR “parkinsonism” OR parkinsonism* OR “parkinson disease” OR “parkinson’s disease” OR “parkinsons disease” OR “Paralysis Agitans” OR parkinson*) AND (“Magnetoencephalography” OR “magnetoencephalography” OR magnetoencephalogr* OR “magneto-encephalography” OR “magneto-encephalogr*” OR “MEG”))

Emcare

((exp "Parkinson Disease"/ OR "Parkinsonism"/ OR "parkinsonian".mp OR parkinsonian*.mp OR "parkinsonism".mp OR parkinsonism*.mp OR "parkinson disease".mp OR "parkinson's disease".mp OR "parkinsons disease".mp OR "Paralysis Agitans".mp OR parkinson*.mp) AND ("Magnetoencephalography"/ OR "magnetoencephalography".mp OR magnetoencephalogr*.mp OR "magneto-encephalography".mp OR magneto-encephalogr*.mp OR "MEG".mp)) NOT conference review.pt

Academic Search Premier

(("Parkinson Disease" OR "Parkinsonism" OR "parkinsonian" OR parkinsonian* OR "parkinsonism" OR parkinsonism* OR "parkinson disease" OR "parkinson's disease" OR "parkinsons disease" OR "Paralysis Agitans" OR parkinson*) AND ("Magnetoencephalography" OR "magnetoencephalography" OR magnetoencephalogr* OR "magneto-encephalography" OR "magneto-encephalogr*" OR "MEG"))

ScienceDirect

TITLE-ABSTR-KEY(("Parkinson Disease" OR "Parkinsonism" OR "parkinsonian" OR parkinsonian* OR "parkinsonism" OR parkinsonism* OR "parkinson disease" OR "parkinson's disease" OR "parkinsons disease" OR "Paralysis Agitans" OR parkinson*) AND ("Magnetoencephalography" OR "magnetoencephalography" OR magnetoencephalogr* OR "magneto-encephalography" OR "magneto-encephalogr*" OR "MEG"))

Supplement B

JBI Critical Appraisal Checklist for Case Series

Reviewer.....
Date.....
Author.....
Year..... Record number.....

		Yes	No	Unclear	Not Applicable
1.	Were there clear criteria for inclusion in the case series?	☐	☐	☐	☐
2.	Was the condition measured in a standard, reliable way for all participants included in the case series?	☐	☐	☐	☐
3.	Were valid methods for identification of the condition for all participants included in the case series?	☐	☐	☐	☐
4.	Did the case series have consecutive inclusion of participants?	☐	☐	☐	☐
5.	Did the case series have complete inclusion of participants?	☐	☐	☐	☐
6.	Was there clear reporting of the demographics of the participants in the study?	☐	☐	☐	☐
7.	Was there clear reporting of clinical information of the participants?	☐	☐	☐	☐
8.	Were the outcomes or follow up results of cases clearly reported?	☐	☐	☐	☐
9.	Was there clear reporting of the presenting site(s)/ clinic(s) demographic information?	☐	☐	☐	☐
10.	Was statistical analysis appropriate?	☐	☐	☐	☐
11.	Was there clear reporting of MEG data acquisition and analysis?*	☐	☐	☐	☐

Overall appraisal: Include Exclude Seek further info

Minimum requirements: 1x 'yes' question 1-3, 2x 'yes' question 4-8, 1x 'yes' question 11.
Comments (Including reason for exclusion)

** Minimum requirements: details MEG acquisition (system and sensor type, sampling frequency, position participant, description task/resting state), amount of data gathered (length and number of data segments), in case of source reconstruction: details on the atlas or grid/resolution used*

Supplement C

Author (year)	Title	Reason exclusion	JBI scores
Anninos et al. (2000)	*Nonlinear analysis of brain activity in magnetic influenced Parkinson patients*	-No quantification of an MEG outcome parameter -No statistics performed -No reproducible MEG acquisition (item 11) -Total JBI score too low, too low score for items 4-8	Total: 3 Item 1-3: 1 Item 4-8: 1 Item 9-10: 1 Item 11: 0
Park et al. (2009)	*Cortico-muscular coherence increases with tremor improvement after deep brain stimulation in Parkinson's disease*	-No reproducible MEG acquisition (item 11) -Total JBI too low	Total: 4 Item 1-3: 1 Item 4-8: 2 Item 9-10: 1 Item 11: 0
Bock et al. (2013)	*Validity of subthalamic-cortical coherency observed in patients with Parkinson's disease*	-Main goal of article was validation of method: Total -Total JBI score too low, too low score for items 4-8.	Total: 3 Item 1-3: 1 Item 4-8: 1 Item 9-10: 0 Item 11: 1

3

CHAPTER 3.1

Longitudinal consistency of source-space spectral power and functional connectivity using different magnetoencephalography recording systems

Lennard I Boon, Prejaas Tewarie, Henk W Berendse, Cornelis J Stam, Arjan Hillebrand

Scientific Reports 2021:16336
DOI: 10.1038/s41598-021-95363-2

Abstract

Background Longitudinal analyses of magnetoencephalography (MEG) data are essential for a full understanding of the pathophysiology of brain diseases and the development of brain activity over time. However, time-dependent factors, such as the recording environment and the type of MEG recording system may affect such longitudinal analyses. We hypothesized that, using source-space analysis, hardware and software differences between two recordings systems may be overcome, with the aim of finding consistent neurophysiological results.

Methods We studied eight healthy subjects who underwent three consecutive MEG recordings over 7 years, using two different MEG recordings systems; a 151-channel VSM-CTF system for the first two time points and a 306-channel Elekta Vectorview system for the third time point. We assessed the within (longitudinal) and between-subject (cross-sectional) consistency of power spectra and functional connectivity matrices.

Results Consistency of within-subject spectral power and functional connectivity matrices was good and was not significantly different when using different MEG recording systems as compared to using the same system. Importantly, we confirmed that within-subject consistency values were higher than between-subject values.

Conclusions We demonstrated consistent neurophysiological findings in healthy subjects over a time span of seven years, despite using data recorded on different MEG systems and different implementations of the analysis pipeline.

Introduction

Magnetoencephalography (MEG) allows for measurement of fluctuating magnetic fields induced by neuronal currents. It provides information about normal and pathological brain activity with excellent temporal and good spatial resolution.[1,2] Communication between distributed brain regions is assumed to be reflected in the statistical relationships between the regions' time series of activity, referred to as functional connectivity.[3] Disruption of resting-state functional interactions between brain regions is considered to be a final common pathway in many brain disorders.[4,5]

Longitudinal MEG studies are essential for a full understanding of disease-specific pathophysiological mechanisms and the development of (changes in) functional brain networks over time, but can be complicated by changes in site-specific factors, such as environmental noise and the MEG recording system itself. In our center, a VSM-CTF system was replaced by an Elekta Vectorview system, resulting in changes in both hardware and software, including a different number of sensors (151 third-order axial gradiometers versus 306 magnetometers/planar gradiometers, respectively), and a different beamformer implementation. Although this has hardly been studied, the type of MEG sensor that is used affects the MEG signals that are recorded: For a given number of measurement channels, axial magnetometers provided more information than vector magnetometers.[6] In addition, it has been shown [7] that radial gradiometers i) have a better signal-to-noise ratio than radial magnetometers, ii) have slower signal-strength decay with increasing depth than planar gradiometers, and iii) of the third order are less sensitive to head-motion and vibrational noise than those of the first order.

Since replacement of a recording system is a common and reoccurring event at many centers, we considered it important to evaluate the consistency of longitudinal MEG data obtained in a group of healthy volunteers using different MEG recording systems. We longitudinally analyzed data from eight healthy volunteers who all underwent a resting-state MEG recording at three time points as controls in a longitudinal cohort study: baseline (BL); follow-up 4 years after baseline (FU1); follow-up 7 years after baseline (FU2). BL and FU1 were recorded using a VSM-CTF MEG system, FU2 using an Elekta Vectorview system.

We applied an often-used atlas-based beamforming approach[8-11] to project MEG signals into source space, allowing for interpretation in an anatomical context[12,13] and comparison across recording sessions and systems. We assessed consistency of within-subject spectral power and functional connectivity over time and across different MEG systems and compared this with between-subject findings. We hypothesized that the within-subject consistency between different MEG systems would be i) comparable to the within-subject consistency of data recorded using the same MEG system; ii) higher than the between-subject consistency.

Materials and methods

Participants

Data from healthy participants were recorded in the context of a longitudinal case-control follow-up study in Parkinson's disease[14-18] over a period of 7 years (the first follow-up visit being ~4 years after inclusion). The healthy participants did not suffer from neurological or psychiatric diseases and did not use any drugs or medication. From an initial group of 20 healthy participants, 10 had undergone an MEG recording at all three time points. Two subjects were excluded from further analysis due to an excess of head movement during the baseline MEG recordings. Hence, data from 8 healthy participants aged 45-72 years (55 ± 5.92) were used. The study was approved by the Medical Ethics Committee of Amsterdam UMC, location VU University Medical Center (Amsterdam, The Netherlands), and all participants gave written informed consent before participation. All methods were carried out in accordance with relevant guidelines and regulations.

Data acquisition

BL and FU1 MEG data were acquired using a 151-channel whole-head MEG system with axial gradiometers (CTF systems Inc., Vancouver, Canada) in an eyes-closed resting-state condition for five minutes while subjects were seated inside a magnetically shielded room. A recording passband of 0.25-200 Hz, and sample rates of 312.5 (BL) and 625 Hz (FU1) were used, and a 3rd order software gradient was applied.[19] At the beginning and end of each recording the head position relative to the coordinate system of the helmet was assessed by leading small currents through three head position indicator (HPI) coils attached to the left and right pre-auricular points and the nasion.

FU2 MEG data were recorded using a 306-channel Vectorview system with 102 magnetometers and 204 planar gradiometers (Elekta Neuromag, Oy, Helsinki, Finland) in an eyes-closed resting-state condition for five minutes in a supine position. An online anti-aliasing (410 Hz) and high-pass filter (0.1 Hz) were used and the sample rate was 1250 Hz. The head position relative to the MEG sensors was recorded continuously using the signals from four HPI coils. The coil positions were digitized before each recording, as well as the outline of the patient's scalp (~500 points), using a 3D digitizer (Fastrak, Polhemus, Colchester, VT, USA).

Structural T1-weighted MR imaging was performed at all three time points (BL; 1.0 T, Impact, Siemens, Erlangen, Germany; FU1 and FU2; 3.0 T, GE Signa HDxt, Milwaukee, WI, USA). In preparation of the MR imaging at BL and FU1, vitamin E capsules were placed at the same anatomical landmarks where the three HPI coils had been placed during MEG-registration.

Data pre-processing

A schematic representation of the pre-processing steps can be found in Figure 1A-C.

We used two different pipelines to pre-process the data, each one dedicated to a given hardware. Both FU1 and FU2 MEG-data were downsampled to 312.5 Hz, to obtain the same sample rate as BL. MEG channels that were malfunctioning, for example due to excessive noise, were removed after visual inspection of the data (all by the same observer KTEOD; mean number of excluded channels: BL/FU1 2.4, range 2-7; FU2 6, range 2-11). BL and FU1 data were split into epochs (13.11 seconds, 4096 samples) and epochs containing strong artefacts were discarded (BL mean 2.1 (range 0-4); FU1 mean 4.6 (range 0-13); KTEOD). In addition, the temporal extension of Signal Space Separation (tSSS) in MaxFilter software (Elekta Neuromag Oy, version 2.2.15) was applied to FU2 data to remove artefacts[20,21] with a sliding window of 10 seconds and a subspace correlation-limit of 0.9 (the correlation limit provides a trade-off between removal of noise and preservation of brain signal,[22] where a value of 0.9 was found to be optimal in our specific (urban) environment). Note that tSSS (also) reconstructs the data for the identified malfunctioning channels. Participants' MEG data were co-registered to their structural MRIs, in case of BL/FU1 through identification of the same anatomical landmarks (left and right pre-auricular points and nasion; estimated co-registration error < 6 mm) in both modalities, and in case of FU2 through a surface-matching procedure, with an estimated resulting accuracy of 4 mm.[23] For all three time points, the automated anatomical labelling (AAL) atlas was used to label the voxels in 78 cortical and 12 subcortical regions of interest (ROIs) in a subject's co-registered MRI.[24,25] In order to obtain a single time series for a ROI we used each ROI's centroid as representative for that ROI.[9] A scalar beamformer[12,26] was used to reconstruct beamformer weights for each centroid using broad-band data (0.5-48 Hz; mean 201 seconds (range 131 – 262 seconds) for BL, mean 238 seconds (range 197 – 288 seconds) for FU1, and mean 297 seconds (range 288 – 341 seconds) for FU2), and using Synthetic Aperture Magnetometry[27] for BL and FU1, and Elekta's beamformer implementation (version 2.2.15; Elekta Neuromag Oy), which finds the optimum beamformer orientation through an eigendecomposition,[28] for FU2. The beamformer used lead fields for equivalent current dipoles at the centroid locations, using a multi-sphere[29] or single-sphere head model for BL and FU1 or FU2, respectively. Broad-band data (0.5-48 Hz) were subsequently projected through the normalized[30] beamformer weights in order to project the sensor signals to source space, i.e. broadband (0.5-48 Hz) time-series of neuronal activity were reconstructed for each centroid of the 90 ROIs.

Subsequently, FU2 time-series were downsampled (4x) and split into epochs of 4096 samples (13.11s) as well. All beamformed data was used for further analysis (BL range 10-20 epochs, FU1 15-18 epochs and FU2 19-22 epochs), hence no further epoch-selection took place.

Data analysis

Spectral power and functional connectivity analyses were performed using in-house software (BrainWave, version 0.9.152.12.26; CJS, available from http://home.kpn.nl/stam7883/brainwave.html). For each subject and time point separately, we estimated the overall spectral power (0.5-48 Hz) averaged over all ROIs and epochs, normalized based on the area under the curve. Peak frequency values were determined within the 4-13 Hz frequency range. In addition, for each epoch, we band-pass filtered the data into the alpha (8-13 Hz) and beta (13-30 Hz) band using a Fast Fourier transform to produce a so-called 'brickwall' filter. We subsequently corrected for signal leakage by pairwise orthogonalisation (in both directions),[31] and estimated functional connectivity by amplitude envelope correlation (AEC), separately for each epoch. The AEC computes the correlation between the amplitude of the envelopes of two time series obtained with the Hilbert transform (in our case) or wavelet analysis.[31-33] To adjust for any negative correlations, 1 was added to the raw AEC values and subsequently divided by 2. The AEC was calculated for all possible pairs of ROIs, leading to a 90 x 90 weighted adjacency matrix for each epoch. For each subject, the matrices were then averaged over epochs. A schematic representation of the spectral power and functional connectivity analyses can be found in Figure 1D.

Statistical analysis

First, measures of within- (longitudinal) and between-subject (cross-sectional) consistency in spectral power and functional connectivity were calculated for each individual. Within-subject correlations were assessed between BL-FU1, FU1-FU2, and BL-FU2. Between-subject consistency was calculated by taking the average of the cross-sectional consistency of one subject with the other subjects. The two sample Kolmogorov-Smirnov test was used to estimate differences in the shape of power spectra (as a measure of consistency) within- (longitudinal) and between (cross-sectional) subjects. To study consistency in functional connectivity within- and between subjects, we compared functional connectivity matrices, averaged over all epochs of each individual. We vectorized the average matrix (while excluding the diagonal) and calculated Spearman correlations between these vectors, since the functional connectivity data were not Gaussian distributed.

Second, we tested the hypothesis that no significant differences between within-subject correlations were present across time, and hence that two recordings performed on the same MEG system (BL-FU1) would show comparable results with recordings performed on two different MEG systems (FU1-FU2 and BL-FU2). We also tested the hypothesis that no significant differences in between-subject correlations were present over time, in which a p-value >0.05 suggests there is no difference. As all values conformed to the normality assumption, these correlations were tested using repeated measures ANOVAs.

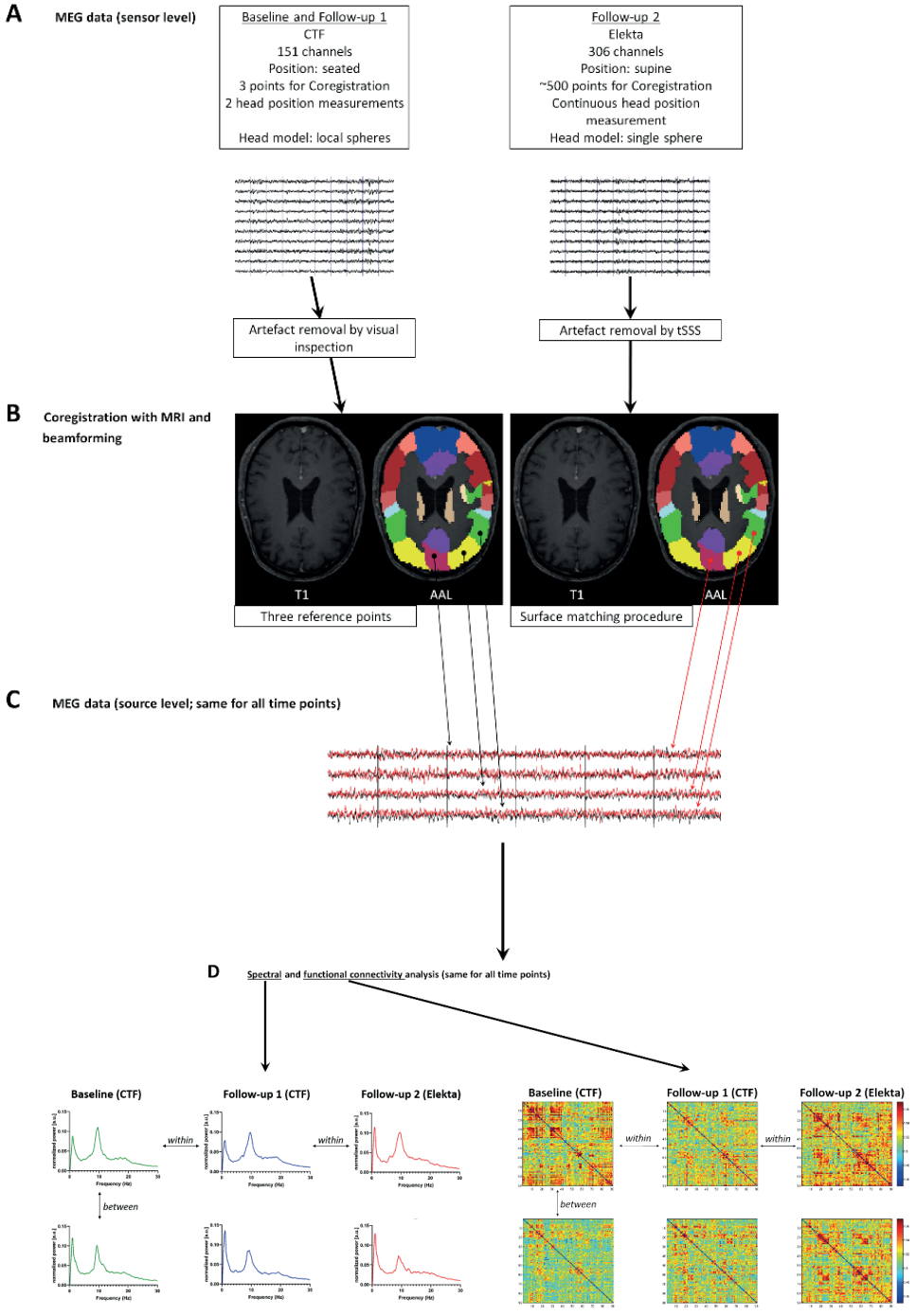

Figure 1 Schematic overview of preprocessing and analysis
Five minutes of eyes-closed, resting-state MEG recordings (A) took place on a VSM-CTF system (baseline (BL; t=0) and follow-up 1 (FU1; t=4 years), and on an Elekta Vectorview system (FU2; t=7 years). (B) Data from all channels were

projected onto an anatomical framework of 90 brain regions (automated anatomical labeling (AAL) atlas), leading to source-space MEG data for all time points (C). (D) Whole-brain spectral analysis, as well as functional connectivity between all pairs of brain regions, was assessed by means of the leakage-corrected amplitude envelope correlate (AEC). Power spectra and connectivity matrices were compared over time *within* patients (horizontal arrows), as well as cross-sectionally *between* patients (vertical arrows).

Third, we tested the hypothesis that within-subject correlations were higher than between-subject correlations. We averaged the within-subject correlations (assessed between BL-FU1, FU1-FU2, and BL-FU2), and compared this with the average between-subject correlations (BL, FU1, and FU2) using two-tailed unpaired t-tests.

Results

Spectral power

Overall normalized spectral power averaged over all subjects is shown in Figures 2A and 2B. Figure 2A demonstrates broadband spectral power (0.5-48 Hz). As can be observed from this figure, the normalized power spectra from the three time points overlapped in the range of 0.5-30 Hz, but the spectra obtained from BL and FU1 (CTF data) showed more gamma power (30-48 Hz) than the power spectrum from FU2 (Elekta data). As the presence of artefacts may have contributed to this difference (for example magnetometers/planar gradiometers of the Elekta Vectorview system (FU2) may be less sensitive to muscle artefacts or these artefacts may be suppressed more optimally by using tSSS compared to the use of synthetic third-order gradiometers in the CTF system (BL, FU1)), we subsequently restricted the spectral analysis to 0.5-30 Hz (Figure 2B).

We estimated the within- and between-subject difference in shape (as a measure of consistency) of the power spectra using the two sample Kolmogorov-Smirnov tests (Figure 2C), in which lower values represent higher consistency. The average within- and between-subject consistency did not differ significantly between time-points (Table 1). Importantly, comparison of power spectra within subjects over time showed significantly higher consistency than power spectra between subjects (cross-sectional; Figure 2C). In addition, the peak frequency did not significantly differ between time points: BL (mean 8.78 SD 0.87), FU1 (mean 8.78 SD 0.92), FU2 (mean 8.91 (SD 0.89), ($F(2, 7) = 0.76$, $p = 0.53$, $\eta p^2 = 0.24$).

Table 1

	Within-subject			Statistics	Between-subject			Statistics
	BL-FU1	FU1-FU2	BL-FU2		BL	FU1	FU2	
Spectral power	0.090 (0.035)	0.107 (0.040)	0.085 (0.030)	$F(2, 7) = 1.151$, $\eta p^2 = 0.277$, $p = 0.378$	0.154 (0.010)	0.164 (0.021)	0.152 (0.022)	$F(2, 21) = 1.031$, $\eta p^2 = 0.001$, $p = 0.374$
Alpha cAEC	0.380 (0.167)	0.407 (0.156)	0.438 (0.095)	$F(2, 7) = 0.405$, $\eta p^2 = 0.021$, $p = 0.684$	0.279 (0.063)	0.211 (0.072)	0.317 (0.068)	$F(2, 21) = 5.028$, $\eta p^2 = 0.046$, $p = 0.016$**
Beta cAEC	0.440 (0.121)	0.453 (0.099)	0.426 (0.098)	$F(2, 7) = 2.26$, $\eta p^2 = 0.430$, $p = 0.185$	0.319 (0.059)	0.338 (0.040)	0.371 (0.051)	$F(2, 21) = 2.132$, $\eta p^2 = 0.011$, $p = 0.144$

Within- and between-subject consistency values, expressed as mean (standard deviation). Note that in case of spectral power, lower Kolmogorov-Smirnov 2 test statistic values represent a higher consistency. In case of the functional connectivity analyses (leakage corrected AEC), higher Spearman's rho values indicate a higher consistency.

BL, baseline; FU1, follow-up 1; FU2, follow-up 2; ηp^2, partial eta squared (effect size); Statistics on correlation values over time was performed using repeated measures ANOVAs

*Consistency values expressed as Kolmogorov-Smirnov 2 test statistic ** Post-hoc paired *t*-tests; BL-FU1 $t(7) = 2.53$, $p = 0.039$; FU1-FU2 $t(7) = 4.04$, $p = 0.005$; BL-FU2 $t(7) = 1.51$, $p = 0.1$

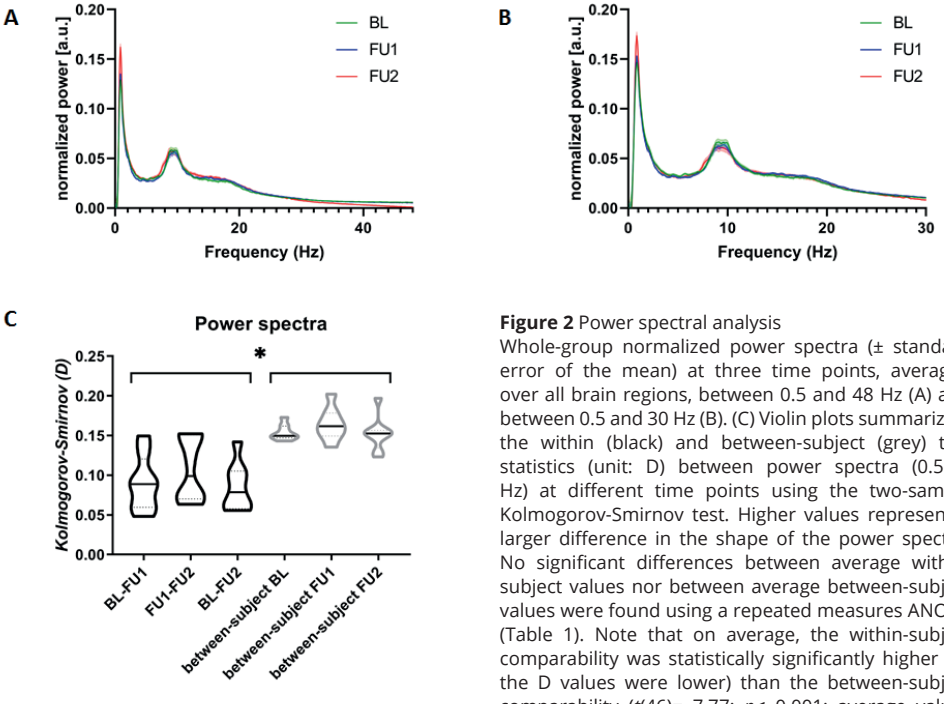

Figure 2 Power spectral analysis

Whole-group normalized power spectra (± standard error of the mean) at three time points, averaged over all brain regions, between 0.5 and 48 Hz (A) and between 0.5 and 30 Hz (B). (C) Violin plots summarizing the within (black) and between-subject (grey) test statistics (unit: D) between power spectra (0.5-30 Hz) at different time points using the two-sample Kolmogorov-Smirnov test. Higher values represent a larger difference in the shape of the power spectra. No significant differences between average within-subject values nor between average between-subject values were found using a repeated measures ANOVA (Table 1). Note that on average, the within-subject comparability was statistically significantly higher (as the D values were lower) than the between-subject comparability ($t(46) = 7.77$; $p < 0.001$; average values also provided in Table 1).

*$p < 0.05$

Functional connectivity

We calculated within- and between-subject correlations between connectivity matrices for the three time points (Figure 3). For both alpha and beta band functional connectivity, the highest within-subject correlations were found in the correlation with FU2 (BL-FU2 for alpha band FC, FU1-FU2 for beta band FC; in which FU2 represented a *different* MEG recording system). For alpha band FC, the within-subject correlation values were highest in the parieto-occipito-temporal cortical brain regions (panel A). For beta band FC, the correlation values were highest for the central and frontal brain regions (panel B). The average within- and between-subject correlations were not significantly different over time (Table 1). Importantly, both in the alpha and beta band, within-subject correlations were significantly higher than between-subject correlations (Figure 3).

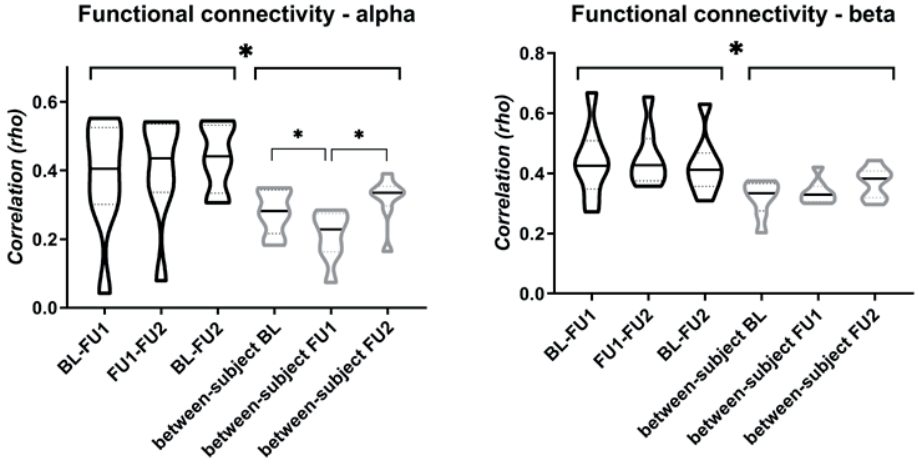

Figure 3 Functional connectivity analysis
Violin plots summarizing within and between-subject correlation values (Spearman's rho) between functional connectivity matrices at different time points. Connectivity matrices consisted of alpha (8-13) and beta (13-30) band amplitude envelope correlation (AEC) values, corrected for signal leakage. No significant differences were found between average within-subject values using repeated measures ANOVAs, but between-subject alpha band functional connectivity values differed between time points BL-FU1 and FU1-FU2 (Table 1). Note that on average, the within-subject correlations were significantly higher than the between-subject correlations (alpha band $t(46)=4.27$, $p= 0.011$; beta band $t(46)=4.12$, $p< 0.001$); average values also provided in Table 1).
*$p< 0.05$

Discussion

In this study we have demonstrated that longitudinal within-subject neurophysiological results in healthy subjects were consistent across MEG systems. We demonstrated this by restricting the normalized power spectral analysis to 0.5-30 Hz and using amplitude-envelope coupling as a measure of functional connectivity. Furthermore, within-subject consistency values were significantly higher than between-subject consistency values, confirming that over time, neurophysiological information of individuals is retained.

We here demonstrate the feasibility of a *longitudinal* MEG analysis using data from the same subjects recorded on different MEG systems over a timespan of seven years. A previous *cross-sectional* study used a median-nerve stimulation paradigm and demonstrated the stability of the location of the N20m response, both in terms of location and latency, within the same subject on three different MEG systems (including a Neuromag Vectorview and CTF-VSM system), although the magnitude of later evoked components was more variable.[34,35] This suggests that cross-sectional pooling of MEG data recorded at different sites may be possible as well. However, other site-specific factors than the MEG system and preprocessing pipeline, such as environmental noise and the site-specific agreement on epoch selection criteria, may complicate such an effort. Future studies should further explore the feasibility of pooling MEG data from different sites (see for example the MRC/EPSRC partnership initiative for MEG in the UK, e.g.).[36]

Although we reported consistency of spectral power and functional connectivity estimates over time, several factors and sources of error could have negatively affected this, most of which were related to hardware differences between the CTF and Elekta systems. i) Different number and type of sensors (151 vs 306; axial vs planar gradiometers; third-order gradiometers versus magnetometers and first-order gradiometers). Although the information content of the raw data was therefore different, we performed our analysis using the same number of (virtual) sensors through the use of the same anatomical atlas for all datasets. ii) The artefact correction method, which was performed manually in case of the CTF system (i.e. rejection of bad data segments) and was done using tSSS in case of the Elekta system (automatic removal of artefacts from the data). This difference may have caused the lower normalized gamma power found at FU2, since tSSS may have removed (e.g. muscle) artefacts from the data more successfully than a visual analysis. In the visual analysis on BL and FU1 data, only data segments with clear artefacts were removed, and less obvious (muscle) artefacts may therefore have been left in the remaining data. Importantly, after excluding the gamma band from the spectral analysis, the power spectra were similar over time/systems. However, the influence of tSSS on gamma activity may not have been the sole explanation for this difference: tSSS may also affect alpha and high-beta relative power, as demonstrated in Supplementary Figure 2. Another factor of influence may be a different sensitivity of magnetometers/planar gradiometers of the Elekta Vectorview system (FU2) to muscle artefacts. In addition, the use of a sliding window (of 10 seconds) may introduce artificial discontinuities in the data, although we did not encounter these. iii) Measurement of head position during the recording (at two time points vs continuous; where the first could lead to an underestimation of actual head movement during recordings). iv) Co-registration accuracy (three fiducials for co-registration vs surface-matching; the first method being more prone to errors).[37] This may have affected both the spectral analysis and the functional connectivity assessment,[38] although the influence of differences in the co-registration approach was probably limited, as the spatial resolution of the beamforming approach was already reduced through the use of (the centroids of atlas-based) regions-of-interest. v) Differences in the head model (local spheres vs single sphere) used for the computation of the lead fields. vi) The implementation of the scalar

beamformer differed between the CTF and Elekta systems. vii) The CTF recordings (BL and FU1) were performed in seated position, whereas the Elekta recordings were performed in supine position. Although not systematically tested, participants may have shown more movement during recordings in the seated position, for example due to subsiding as the recording progresses. On the other hand, participants recorded in the supine position may be more prone to drowsiness. However, this was probably not an issue in our study, as drowsiness is related to a slowing of the dominant background rhythm which we did not find (peak frequency and spectra were consistent over time/systems, despite the fact that we did not select data on the absence of drowsiness). Importantly, in spite of the differences in hardware and the processing pipeline there was no difference in within-subject consistency between BL-FU1 and FU1-FU2. This would seem to indicate robustness of the estimation of spectral power and functional connectivity across recording systems by performing the analyses in source-space.

The present study has some limitations. Firstly, the data collection in this study was not designed with the idea to answer the question whether data recorded on two different MEG system would show comparable results. To better answer this question, the data collection should have included a cross-sectional comparison between two different MEG systems (instead of only a longitudinal comparison between systems). However, as we assume that the adult healthy controls in our analysis have stable brain activity over time (we did not observe a trend over time, nor did another study;[39] moreover in the presence of any significant aging effects our analyses would not have shown neurophysiological results to be stable over time), we believe that we were able to answer this question successfully.

Secondly, we used a leakage-corrected metric of functional connectivity that has previously been demonstrated to be a metric with a good within-subject reproducibility in the alpha band[40] and to be stable during healthy ageing.[39] As one of the aims of this study was to study its consistency over time (and systems), we did not perform an exhaustive test of available connectivity measures, such as metrics for phase-based coupling,[41] generalized synchronization,[42] or information based metrics.[43] However, both our within- and between-subject alpha band functional connectivity reproducibility values did not reach the levels as reported by Colclough and colleagues (average within-subject correlation ~0.55 and average between-subject correlation ~0.45).[40] A possible explanation for the lower within-subject consistency found in our study might be the longer duration between recordings (several years versus several hours).

Thirdly, in contrast to earlier work from our group,[14,16,44,45] no epoch selection took place before our analysis. Epoch selection is generally performed to prevent the inclusion of data segments during which the subject was drowsy and/or which contained artefacts. However, as a previous study demonstrated that high between-session repeatability can be reached by using large amounts of MEG data (> ~100 seconds),[46] we chose not to perform epoch selection here. As a result, we obtained rather high within-subject

reproducibility both regarding spectral power and functional connectivity. Intuitively, without epoch selection, MEG data may contain drowsiness in the recordings, which may affect spectral power. We do however think this effect was limited in this analysis as i) the reproducibility values of the spectral data were rather good, ii) the peak frequencies hardly changed between unselected (all) and selected data (n=5 epochs; based on a previous epoch selection)[14,17]: BL *all data* mean 8.78 Hz, *selected data* mean 8.75 Hz. FU1 *all data* mean 8.78 Hz, *selected data* mean 8.92 Hz FU2 *all data* mean 8.91, *selected data* mean 8.92 Hz.

Fourthly, the number of subjects in this study was small. This may have lowered the power to find statistical differences between consistency values over time points (within the same scanner type versus between different scanner types). We are well aware that the absence of statistically significant differences does not mean that our neurophysiological results were the same over time points.[47] However, the observation that the power spectra (0.5-30 Hz) visually aligned, both at the group level and at the individual level (Supplementary Figure 1), suggests stability.

Fifthly, a disadvantage of the AAL atlas is that some central, frontal and temporal regions span a relatively large surface. Consequently, the centroid (most central voxel) may be relatively distant from the voxel that is most representative for the activity of that brain region. However, in a previous study from our group, we compared the centroid-voxel and peak-voxel approaches (maximum power) and there were no major differences between the two methods for the neurophysiological measures that were assessed.[9] Also, we think we can draw meaningful conclusions on the spatial distribution of the correlations in our analysis, as high FC correlations values were present in central, frontal (beta band FC) and temporal (alpha band FC) brain regions. Interestingly, the highest correlation values are reflected by the posterior cortical alpha rhythm (alpha band FC) and mu rhythm (beta band FC; Figure 4), which is possibly related to higher signal-to-noise ratio's in these brain regions. Another reason not to use an atlas with a much denser parcellation scheme is the fact that the number of brain regions of the AAL atlas roughly matches the number of (data-driven) parcels that can be obtained in beamformed resting-state MEG data,[48] indicating that, on average, the resolution of the AAL atlas matches that of beamformed resting-state data. We do however think that optimization of the parcellation approach warrants a separate study, in which existing atlases with different parcellation densities and adaptive parcellation strategies are compared.[48]

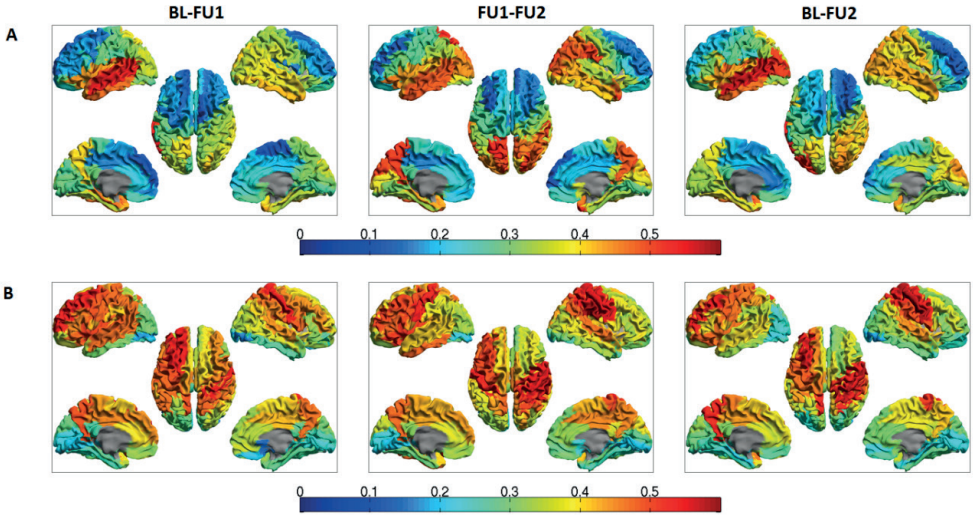

Figure 4 Functional connectivity analysis; region of interest-specific display
Distribution of within-subject functional connectivity correlation values displayed on a parcellated template brain viewed from, in clockwise order, the left, right, left midline, and right midline. For alpha band functional connectivity, the correlation values were highest in the parieto-occipito-temporal cortical brain regions (panel A). For beta band functional connectivity, the correlation values were highest for the central and frontal brain regions (panel B). The subcortical regions had an intermediate level of correlation, both for the alpha and beta band functional connectivity (not shown).

Lastly, we draw the conclusion that the estimation of spectral power and functional connectivity is robust across recording systems, but this conclusion applies to the specific analysis pipeline that we used. This includes the fact that we had to exclude the gamma band to increase consistency between systems. Future work is necessary to demonstrate that other functional connectivity measures and source reconstruction approaches[49] offer the same consistency over time and recording systems.

In conclusion, in this longitudinal study using two different MEG systems, we demonstrated that source-space power spectral as well as functional connectivity results showed high within-subject reproducibility and remained stable over time in a group of healthy participants, despite differences in analysis pipelines and relatively long follow-up periods. Therefore, the use of the leakage-corrected AEC in source-space may allow future longitudinal analyses of the healthy and diseased brain using data recorded from different MEG systems.

Acknowledgements

We thank Kim T.E. Olde Dubbelink (KTEOD) for identifying the study subjects and obtaining MEG data, as well as for her help on preprocessing the MEG data.

Funding

This project was supported by Stichting Parkinson NL.

References

1. Schnitzler A, Gross J. Normal and pathological oscillatory communication in the brain. Nat Rev Neurosci. 2005;6(4):285-96.
2. Baillet S. Magnetoencephalography for brain electrophysiology and imaging. Nat Neurosci. 2017;20(3):327-39.
3. Friston KJ. Functional and effective connectivity: a review. Brain Connect. 2011;1(1):13-36.
4. Vidal M, Cusick ME, Barabasi AL. Interactome networks and human disease. Cell. 2011;144(6):986-98.
5. Stam CJ. Modern network science of neurological disorders. Nat Rev Neurosci. 2014;15(10):683-95.
6. Hughett P, Miyauchi S. A Comparison of Vector and Radial Magnetometer Arrays for Whole-Head Magnetoencephalography. Aine CJ, Stroink G, Wood CC, Okada Y, Swithenby SJ (eds) Biomag 96 Springer, New York, NY 2000.
7. Vrba J, Robinson SE. Signal processing in magnetoencephalography. Methods (San Diego, Calif). 2001;25(2):249-71.
8. Hillebrand A, Barnes GR, Bosboom JL, et al. Frequency-dependent functional connectivity within resting-state networks: an atlas-based MEG beamformer solution. Neuroimage. 2012;59(4):3909-21.
9. Hillebrand A, Tewarie P, Van Dellen E, et al. Direction of information flow in large-scale resting-state networks is frequency-dependent. Proc Natl Acad Sci U S A. 2016;113(14):3867-72.
10. Hunt BAE, Tewarie PK, Mougin OE, et al. Relationships between cortical myeloarchitecture and electrophysiological networks. Proc Natl Acad Sci U S A. 2016;113(47):13510-5.
11. Sorrentino P, Rucco R, Jacini F, et al. Brain functional networks become more connected as amyotrophic lateral sclerosis progresses: a source level magnetoencephalographic study. Neuroimage Clin. 2018;20:564-71.
12. Hillebrand A, Barnes GR. Beamformer analysis of MEG data. Int Rev Neurobiol. 2005;68:149-71.
13. Baillet S, Mosher JC, Leahy RM. Electromagnetic brain mapping. IEEE Signal processing magazine. 2001;18(6):14-30.
14. Boon LI, Hillebrand A, Dubbelink KTO, et al. Changes in resting-state directed connectivity in cortico-subcortical networks correlate with cognitive function in Parkinson's disease. Clin Neurophysiol. 2017;128(7):1319-26.
15. Olde Dubbelink KT, Hillebrand A, Stoffers D, et al. Disrupted brain network topology in Parkinson's disease: a longitudinal magnetoencephalography study. Brain. 2014;137(Pt 1):197-207.
16. Olde Dubbelink KT, Schoonheim MM, Deijen JB, et al. Functional connectivity and cognitive decline over 3 years in Parkinson disease. Neurology. 2014;83(22):2046-53.
17. Olde Dubbelink KT, Stoffers D, Deijen JB, et al. Cognitive decline in Parkinson's disease is associated with slowing of resting-state brain activity: a longitudinal study. Neurobiol Aging. 2013;34(2):408-18.
18. Stoffers D, Bosboom JL, Deijen JB, et al. Slowing of oscillatory brain activity is a stable characteristic of Parkinson's disease without dementia. Brain. 2007;130(Pt 7):1847-60.
19. Vrba J, Anderson G, Betts K, et al. 151-Channel whole-cortex MEG system for seated or supine positions. Recent advances in biomagnetism. 1999:93-6.
20. Taulu S, Hari R. Removal of magnetoencephalographic artifacts with temporal signal-space separation: demonstration with single-trial auditory-evoked responses. Hum Brain Mapp. 2009;30(5):1524-34.
21. Taulu S, Simola J. Spatiotemporal signal space separation method for rejecting nearby interference in MEG measurements. Phys Med Biol. 2006;51(7):1759-68.
22. Medvedovsky M, Taulu S, Bikmullina R, et al. Fine tuning the correlation limit of spatio-temporal signal space separation for magnetoencephalography. J Neurosci Methods. 2009;177(1):203-11.

23. Whalen C, Maclin EL, Fabiani M, et al. Validation of a method for coregistering scalp recording locations with 3D structural MR images. Hum Brain Mapp. 2008;29(11):1288-301.
24. Gong G, He Y, Concha L, et al. Mapping anatomical connectivity patterns of human cerebral cortex using in vivo diffusion tensor imaging tractography. Cereb Cortex. 2009;19(3):524-36.
25. Tzourio-Mazoyer N, Landeau B, Papathanassiou D, et al. Automated anatomical labeling of activations in SPM using a macroscopic anatomical parcellation of the MNI MRI single-subject brain. Neuroimage. 2002;15(1):273-89.
26. Hillebrand A, Singh KD, Holliday IE, et al. A new approach to neuroimaging with magnetoencephalography. Hum Brain Mapp. 2005;25(2):199-211.
27. Vrba J, Robinson S. SQUID sensor array configurations for magnetoencephalography applications. Supercond Sci Technol. 2002;15(9):R51.
28. Sekihara K, Nagarajan SS, Poeppel D, et al. Asymptotic SNR of scalar and vector minimum-variance beamformers for neuromagnetic source reconstruction. IEEE Trans Biomed Eng. 2004;51(10):1726-34.
29. Huang MX, Mosher JC, Leahy RM. A sensor-weighted overlapping-sphere head model and exhaustive head model comparison for MEG. Phys Med Biol. 1999;44(2):423-40.
30. Cheyne D, Bostan AC, Gaetz W, et al. Event-related beamforming: a robust method for presurgical functional mapping using MEG. Clin Neurophysiol. 2007;118(8):1691-704.
31. Hipp JF, Hawellek DJ, Corbetta M, et al. Large-scale cortical correlation structure of spontaneous oscillatory activity. Nat Neurosci. 2012;15(6):884-90.
32. Brookes MJ, Woolrich MW, Barnes GR. Measuring functional connectivity in MEG: a multivariate approach insensitive to linear source leakage. Neuroimage. 2012;63(2):910-20.
33. Bruns A, Eckhorn R, Jokeit H, et al. Amplitude envelope correlation detects coupling among incoherent brain signals. Neuroreport. 2000;11(7):1509-14.
34. Ou W, Golland P, Hamalainen M. Sources of variability in MEG. Medical image computing and computer-assisted intervention : MICCAI International Conference on Medical Image Computing and Computer-Assisted Intervention. 2007;10(Pt 2):751-9.
35. Weisend MP, Hanlon FM, Montaño R, et al. Paving the way for cross-site pooling of magnetoencephalography (MEG) data. International Congress Series. 2007;1300:615-8.
36. Hunt BAE, Liddle EB, Gascoyne LE, et al. Attenuated Post-Movement Beta Rebound Associated With Schizotypal Features in Healthy People. Schizophr Bull. 2018;45(4):883-91.
37. Adjamian P, Barnes GR, Hillebrand A, et al. Co-registration of magnetoencephalography with magnetic resonance imaging using bite-bar-based fiducials and surface-matching. Clin Neurophysiol. 2004;115(3):691-8.
38. Chella F, Marzetti L, Stenroos M, et al. The impact of improved MEG-MRI co-registration on MEG connectivity analysis. Neuroimage. 2019;197:354-67.
39. Coquelet N, Mary A, Peigneux P, et al. The electrophysiological connectome is maintained in healthy elders: a power envelope correlation MEG study. Sci Rep. 2017;7(1):13984.
40. Colclough GL, Woolrich MW, Tewarie PK, et al. How reliable are MEG resting-state connectivity metrics? Neuroimage. 2016;138:284-93.
41. Siegel M, Donner TH, Engel AK. Spectral fingerprints of large-scale neuronal interactions. Nat Rev Neurosci. 2012;13(2):121-34.
42. Hunt BR, Ott E, Yorke JA. Differentiable generalized synchronization of chaos. Phys Rev E. 1997;55(4):4029.
43. Shannon C. A mathematical theory of communication. Bell Syst Tech. 1948;27.
44. Olde Dubbelink KT, Hillebrand A, Twisk JW, et al. Predicting dementia in Parkinson disease by combining neurophysiologic and cognitive markers. Neurology. 2014;82(3):263-70.
45. Olde Dubbelink KT, Stoffers D, Deijen JB, et al. Resting-state functional connectivity as a marker of disease progression in Parkinson's disease: A longitudinal MEG study. Neuroimage Clin. 2013;2:612-9.

46. Liuzzi L, Gascoyne LE, Tewarie PK, et al. Optimising experimental design for MEG resting state functional connectivity measurement. Neuroimage. 2017;155:565-76.
47. Drummond GB, Vowler SL. Not different is not the same as the same: how can we tell? J Physiol. 2012;590(21):5257-60.
48. Farahibozorg SR, Henson RN, Hauk O. Adaptive cortical parcellations for source reconstructed EEG/MEG connectomes. Neuroimage. 2018;169:23-45.
49. Hincapie AS, Kujala J, Mattout J, et al. The impact of MEG source reconstruction method on source-space connectivity estimation: A comparison between minimum-norm solution and beamforming. Neuroimage. 2017;156:29-42.

Supplementary materials

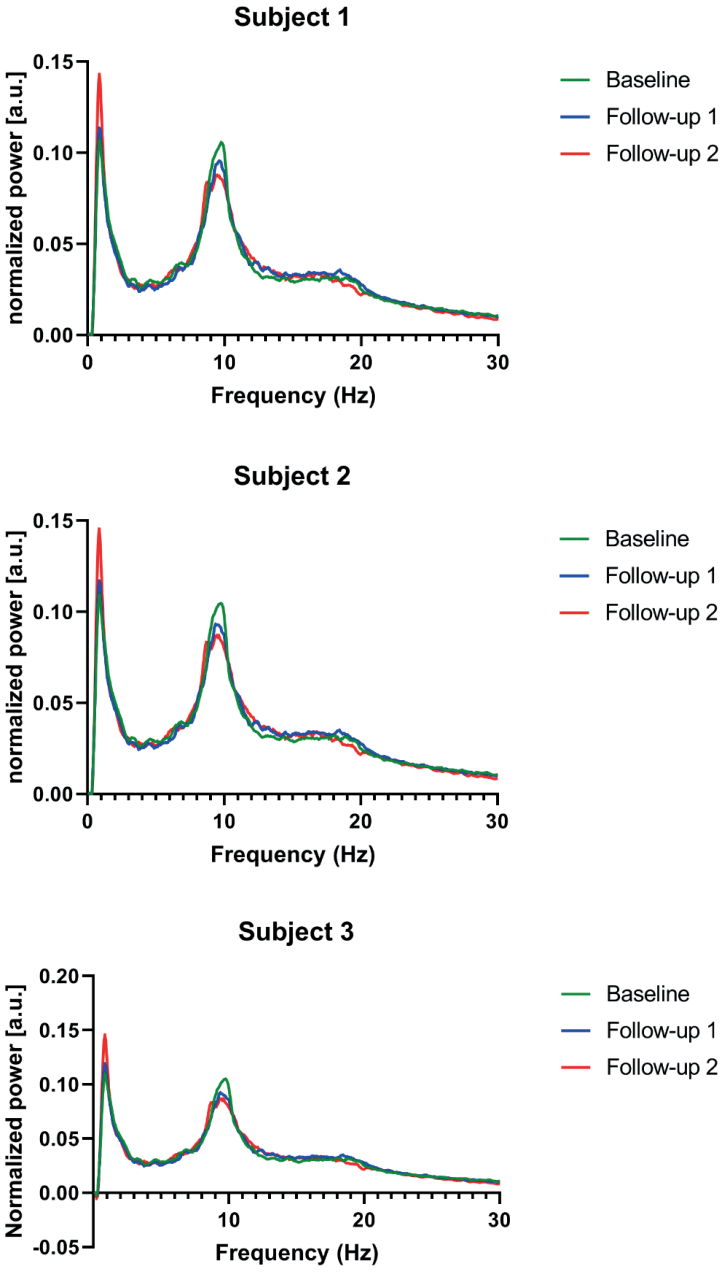

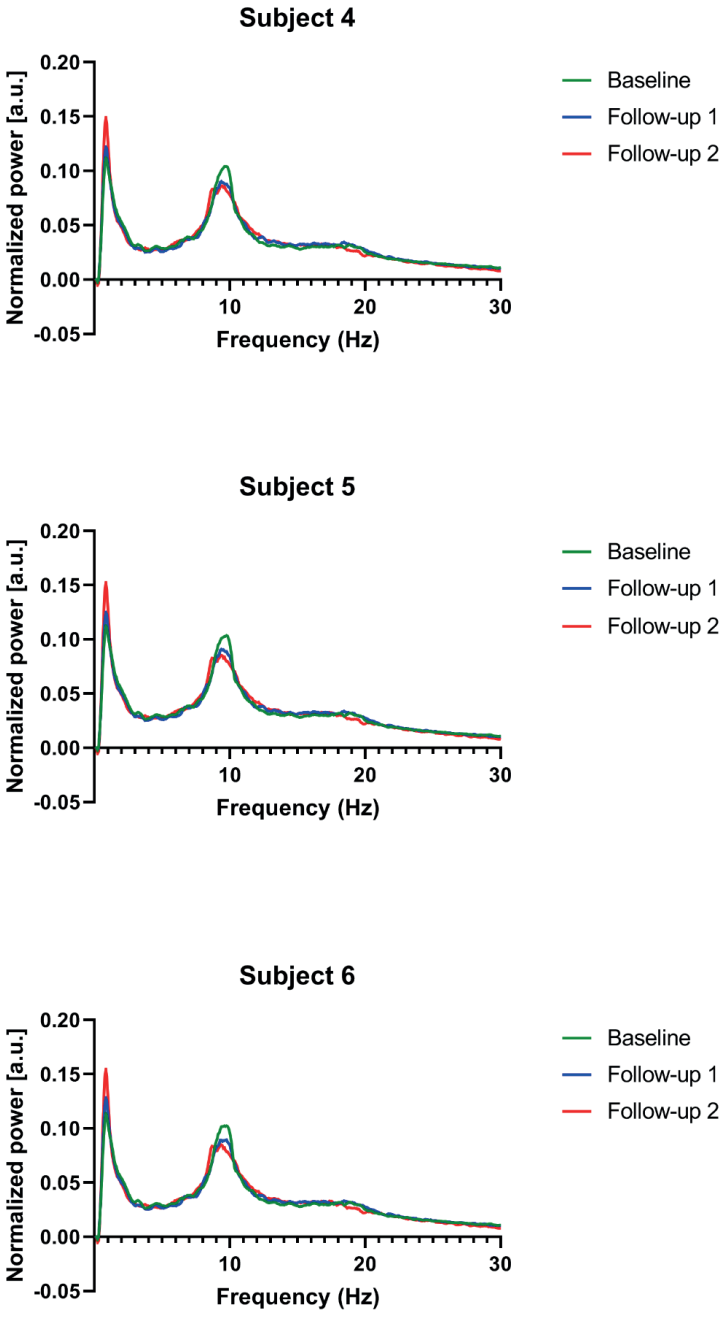
Subject 4
Normalized power [a.u.]
0.20
0.15
0.10
0.05
0.00
-0.05
10
20
30
Frequency (Hz)
Baseline
Follow-up 1
Follow-up 2
Subject 5
Normalized power [a.u.]
0.20
0.15
0.10
0.05
0.00
-0.05
10
20
30
Frequency (Hz)
Baseline
Follow-up 1
Follow-up 2
Subject 6
Normalized power [a.u.]
0.20
0.15
0.10
0.05
0.00
-0.05
10
20
30
Frequency (Hz)
Baseline
Follow-up 1
Follow-up 2

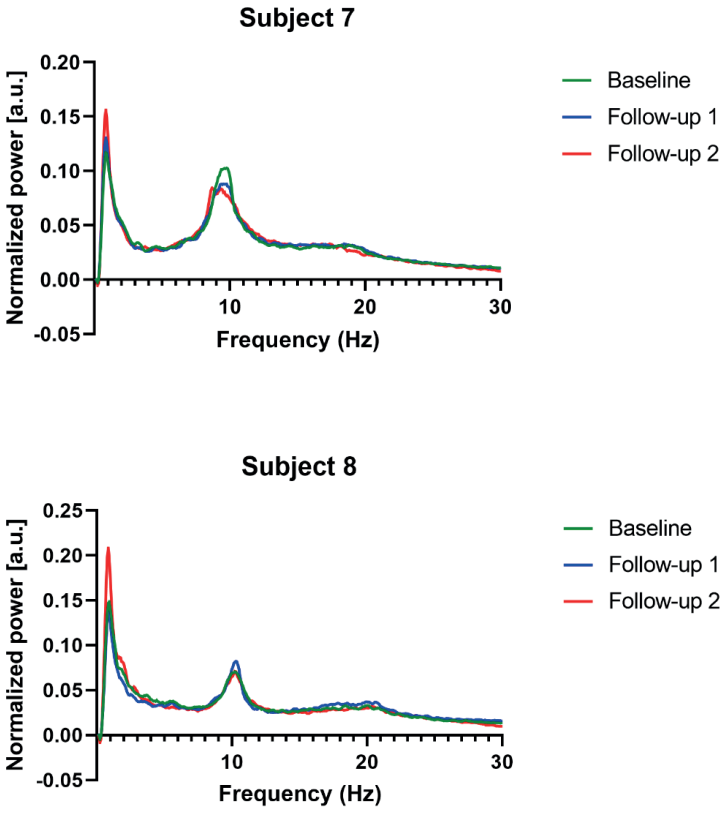

Supplementary Figure 1 Individual power spectra
Individual normalized power spectra for all subjects (all data) at three time points, averaged over all brain regions. As can be seen in this figure, in general, spectral results of the three time points visually aligned well.

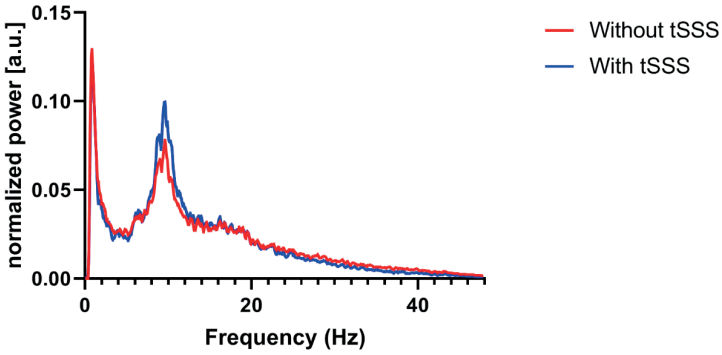

Supplementary Figure 2
Power spectra for averaged over all brain regions for subject 1 (FU2; 5 highest-quality epochs), both with and without tSSS. As can be substantiated from the figure, normalized power differences can be seen both in the alpha, high-beta and gamma band.

CHAPTER 3.2

Cortical and subcortical changes in MEG activity reflect Parkinson's progression over a period of 7 years

Lennard I Boon, Arjan Hillebrand, Menno M Schoonheim, Jos W Twisk, Cornelis J Stam, Henk W Berendse

Brain topography 2023 566-580
DOI: 10.1007/s10548-023-00965

Abstract

Background In this study of early functional changes in Parkinson's disease (PD), we aimed to provide a comprehensive assessment of the development of changes in both cortical and subcortical neurophysiological brain activity, including their association with clinical measures of disease severity.

Methods Repeated resting-state MEG recordings and clinical assessments were obtained in the context of a unique longitudinal cohort study over a seven-year period using a multiple longitudinal design. We used linear mixed models to analyze the relationship between neurophysiological (spectral power and functional connectivity) and clinical data.

Results At baseline, early-stage (drug-naïve) PD patients demonstrated spectral slowing compared to healthy controls in both subcortical and cortical brain regions, most outspoken in the latter. Over time, spectral slowing progressed in strong association with clinical measures of disease progression (cognitive and motor). Functional connectivity hardly changed over time and was therefore not further analyzed.

Conclusions Our results suggest that spectral measures are promising candidates in the search for non-invasive markers of both early-stage PD and of the ongoing disease process.

Introduction

Parkinson's disease is a progressive neurodegenerative disease characterized by classical motor symptoms as well as a wide range of non-motor symptoms, among which cognitive decline.[1] The pathological hallmark of Parkinson's disease is the deposition of alpha synuclein in the brain, which initially mainly affects the brainstem, including the neurons of the nigrostriatal dopamine system, and extends to widespread cortical brain regions in later disease stages.[2] This pathology affects the brain function, although its mechanism is as yet unknown.

Magnetoencephalography (MEG) can be used to measure brain activity with high temporal and good spatial resolution.[3,4] Changes in neurophysiological measures of cortical brain activity such as spectral slowing and loss of interactions between brain regions, i.e. functional connectivity, are well-established phenomena in Parkinson's disease.[5-10] These changes correlate with clinical measures of disease progression[11-14] and can have predictive value for cognitive deterioration, such as the conversion to Parkinson's disease dementia.[15-17] Hence, neurophysiological patterns hold promise as biomarkers of the degenerative process in Parkinson's disease, for instance for prognosis or the assessment of treatment effects of future disease-modifying therapies.

Already at the earliest Parkinson's disease stages, slowing of oscillatory brain activity and functional connectome changes have been demonstrated.[7,18] As nigrostriatal changes lie at the heart of early-stage Parkinson's disease (i.e. motor) symptoms, one would expect functional changes in subcortical brain regions as well. Previous neurophysiological studies have focused on cortical brain regions, with the exception of local field potentials recorded from the subthalamic nucleus in deep brain stimulation-treated patients. In recent years, increasing evidence suggests the feasibility to project MEG-signals onto other subcortical brain regions,[19-24] which allows for a reliable measurement of functional properties of these subcortical brain areas.

Previous longitudinal studies in Parkinson's disease using EEG or MEG had a follow-up duration of approximately four years[11,12,14,25] or were performed in moderately advanced Parkinson's disease patients (average disease duration of 8.5 years at baseline in that study).[25] Hence, the full picture of the neurophysiological changes that occur throughout the course of Parkinson's disease is currently lacking. Ideally, one would follow a cohort of Parkinson's disease patients from disease onset up to a disease duration of 15-20 years. In our study we have met this aim by using a so-called 'multiple longitudinal design' in which we included patients with different baseline disease durations (ranging from early-stage, drug-naive patients to patients with a disease duration of 13 years) in combination with a seven year follow-up duration. We recently demonstrated the feasibility of combining data recorded longitudinally on two different MEG systems in healthy controls, by analyzing the MEG data in source-space and excluding the gamma band.[26] This allowed us to combine the MEG data recorded in a Parkinson's disease

cohort over a period of seven years using two different recording systems (CTF at BL and FU1; Elekta Vectorview at FU2).

In the present study, we assessed MEG-based measures of spectral power and functional connectivity (the corrected amplitude envelope correlation (AEC-c)) at three time points in a cohort of 61 Parkinson's disease patients and 16 healthy controls. We hypothesized to find neurophysiological changes in subcortical brain regions in de novo Parkinson's disease, and expected these to be more prominent than the changes in cortical brain regions. In addition, we expected longitudinal neurophysiological changes in subcortical brain regions to be associated most strongly with Parkinson's disease-related motor impairments and neurophysiological changes in (mainly posterior) cortical brain regions to be associated most strongly with cognitive decline.[15,23,27]

Materials and methods

Participants

At baseline, 70 non-demented patients with idiopathic Parkinson's disease (disease duration 0-13 years, including 18 early-stage drug-naïve (de novo) patients) and 21 healthy controls (age-matched to the de novo patients) were consecutively approached and included in this multiple longitudinal study at Amsterdam UMC from April 2003 to March 2006.[7,11,12,15,23,28] The inclusion and exclusion criteria have previously been described in.[7] Patients underwent motor and cognitive assessments, as well as MEG and MRI recordings at three time points (BL and two follow-up visits scheduled approximately 4 and 7 years later). Only data of the BL study visit were used in case of the HCs, part of the follow-up data has previously been used [26]. Figure 1 shows the number of participants at each time point, as well as the number of participants included in the final analysis (and the reason for exclusion). 61 patients (including 17 de novo patients) and 16 HCs were analyzed at BL, 39 patients at follow-up 1 (FU1), and 35 patients at follow-up 2 (FU2).

All participants gave written informed consent to the research protocol, which was approved by the medical ethical committee of Amsterdam UMC, location VU University Medical Center (Amsterdam, The Netherlands). Ethics review conformed to the Helsinki declaration. All recordings/assessments were carried out in accordance with relevant guidelines and regulations. Reporting of this study meets the STROBE guidelines.[29]

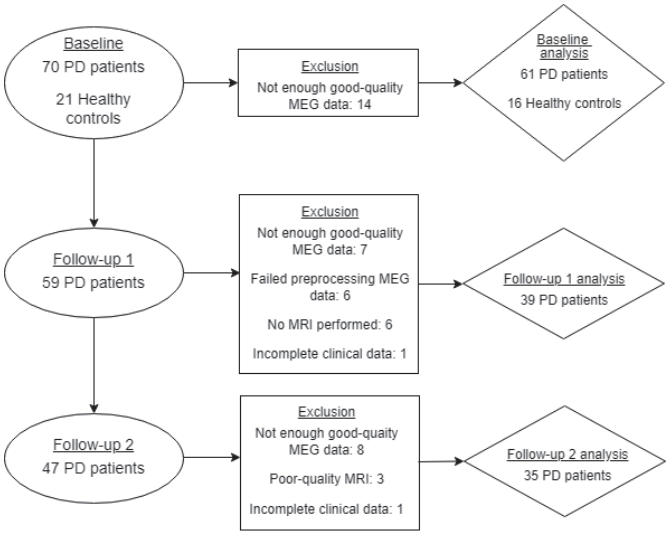

Figure 1 Flowchart of patient inclusion
PD, Parkinson's disease; MEG, magnetoencephalography

Participants characteristics

Disease duration was calculated on the basis of the patients' estimation of the onset of the classical Parkinson's disease motor symptoms. Educational level was determined on the basis of the International Standard Classification of Education (ISCED).[30] Unified Parkinson's Disease Rating Scale motor ratings (UPDRS-III)[31] were obtained in the 'ON' medication state by a trained physician (with the exception of 17 de novo Parkinson's disease patients at baseline who were not on dopaminergic medication yet). For each patient, the Hoehn and Yahr stage was determined.[32] The total dose of dopamine replacement therapy was converted to a so-called levodopa equivalent daily dose (LEDD) as described previously.[11] Levodopa was always used in combination with a peripheral decarboxylase inhibitor. Two patients were using rivastigmine at the time of FU1 and one patient at the time of FU2. Global cognitive function was assessed using the Cambridge Cognitive Examination (CAMCOG) scale.[33] Conversion to PD dementia was assessed using the clinical criteria recommended by the Movement Disorders Society Task Force.[34]

Data acquisition

During all recordings, patients were on their usual dose of dopaminergic medication (note that the 17 de novo cases did not use dopaminergic medication at BL). BL and FU1 MEG data were acquired using a 151-channel whole-head MEG system (CTF systems Inc., Vancouver, Canada) in an eyes-closed resting-state condition for five minutes while participants were seated inside a magnetically shielded room. Sample rates of 312.5 (BL) and 625 Hz (FU1) were used during recordings. At the beginning and end of each

recording the head position relative to the coordinate system of the helmet was assessed by leading small currents through three head position indicator (HPI) coils attached to the left and right pre-auricular points and the nasion. For more details on the recordings, see previous publications from our group.[11,26]

FU2 MEG data were recorded using a 306-channel Vectorview system (Elekta Neuromag, Oy, Helsinki, Finland) in an eyes-closed resting-state condition for five minutes in a supine position, with a sample rate of 1250 Hz. The head position relative to the MEG sensors was recorded continuously using the signals of four HPI coils. The coil positions were digitized before each recording, as well as the outline of the patient's scalp (~500 points), using a 3D digitizer (Fastrak, Polhemus, Colchester, VT, USA).

Structural T1-weighted MR imaging was performed at all three time points (BL; 1.0 T, Impact, Siemens, Erlangen, Germany; FU1 and FU2; 3.0 T, GE Signa HDxt, Milwaukee, WI, USA). In preparation for the MR imaging at BL and FU1, vitamin E capsules were placed at the same anatomical landmarks where the three HPI coils had been placed during MEG-registration.

Data preprocessing

Standard implementations of the analysis pipeline were used for both MEG systems as described below. FU1 MEG data were downsampled to 312.5 Hz to obtain the same sample rate as at BL. MEG channels that were malfunctioning, for example due to excessive noise, were identified based on visual inspection and not included in the further analysis (all by the same observer KTEOD; mean number of excluded channels: BL/FU1 2.4, range 2-7; FU2 6.7, range 2-11). BL and FU1 data were split into epochs (13.11 s, 4096 samples) and epochs containing artefacts were discarded (BL mean 2.5, range 0-11; FU1 mean 2.8, range 0-12). In addition, the temporal extension of Signal Space Separation (tSSS) in MaxFilter software (Elekta Neuromag Oy, version 2.2.15) was applied to FU2 data to remove artefacts,[35,36] using a sliding window of 10 s and a subspace correlation-limit of 0.9.

Participants' MEG data were co-registered to their structural MRIs using in-house software, in case of BL/FU1 through identification of the same anatomical landmarks (left and right pre-auricular points and nasion; estimated co-registration error < 6 mm) in both modalities, and in case of FU2 through a surface-matching procedure, with an estimated resulting accuracy of 4 mm.[37] For all three time points, the automated anatomical labelling (AAL) atlas was used to label the voxels in 78 cortical and 12 subcortical regions of interest (ROIs) in the subjects' co-registered MRI using SPM.[38,39] In order to reconstruct a single time-series of neuronal activity for a ROI [21] we used each ROI's centroid as representative for that ROI.[40] A scalar beamformer was used to reconstruct beamformer weights for each centroid using broadband data (0.5-48 Hz)[20,22] (Synthetic Aperture Magnetometry (SAM))[41] for BL and FU1, and Elekta's beamformer implementation, a scalar beamformer comparable to SAM (version 2.2.15; Elekta Neuromag Oy) for FU2).

Mean length of broadband data was 231 s (range 157 – 432 s) for BL, 252 s (range 130 – 328 s) for FU1, and 313 s (range 296 – 495 s) for FU2. Broadband data were subsequently projected through the normalized[42] beamformer weights for each centroid of the 90 ROIs. For further details on the projection of MEG data to source-space, see our previous publication on the healthy controls of this cohort.[26]

Subsequently, FU2 time-series were downsampled (4x, in order to obtain the same sample rate as at BL) and split into epochs of 4096 samples (13.11 s) as well. Ten artefact and drowsiness-free epochs were selected per subject at each time point by visual analysis (KTEOD/LIB). For frequency band specific analyses, epochs were filtered in five canonical frequency bands (delta (0.5-4 Hz), theta (4-8 Hz), alpha1 (8-10 Hz), alpha2 (10-13 Hz, as the distinction between alpha1 and alpha2 oscillations may have functional significance),[43] and beta (13-30 Hz). We excluded the gamma band, as we previously demonstrated in healthy subjects that gamma power values were not stable between the two different MEG systems, possibly due to a difference in the handling of artefacts.[26]

Data analysis

Spectral and functional connectivity analyses were performed using in-house software (BrainWave, version 0.9.152.12.26; CJS, available from http://home.kpn.nl/stam7883/brainwave.html). We created group-averaged power spectra (0.5-30 Hz) for each time point separately, normalized the spectra using the area under the curve (Figure 2A), and determined the peak frequency within the 4-13 Hz frequency range. Furthermore, for each ROI, we estimated frequency band specific relative power and functional connectivity with the rest of the brain.

We estimated functional connectivity using the AEC-c, an implementation of the AEC[44,45] corrected for volume conduction/field spread, using a symmetric orthogonalisation procedure[44,46] applied to each epoch: To adjust for any negative correlations, 1 was added to the raw AEC values and subsequently divided by 2, leading to values between 0 and 1, and with 0.5 indicating absence of functional connectivity. The AEC-c was calculated for all possible pairs of ROIs, leading to a 90*90 adjacency matrix. AEC-c values were subsequently averaged per ROI. This resulted in a single AEC-c value per ROI (per frequency band), reflecting the mean functional connectivity of that region with the rest of the brain.

Next, both relative power values and functional connectivity values were averaged for i) all cortical brain regions (regions 1-78; ii) all subcortical brain regions (regions 79-90, see Supplementary Table 1 for definitions and order of the regions). Results of 10 epochs were averaged per patient.

Statistical analysis

Patient characteristics

The baseline composition of the study cohort was statistically tested as follows: Age, disease duration, UPDRS-III score, LEDD total dose, and CAMCOG were tested using independent sample *t*-tests. Sex and HY score were tested using Chi-square tests and ISCED using Fisher's exact test. The cohorts studied at BL, FU1 and FU2 showed differences due to drop-out of patients. Hence, our analysis can be considered as a missing data analysis. The group composition over time was therefore not statistically tested.

Spectral power and functional connectivity: Baseline comparison

First, we analyzed spectral power and functional connectivity averaged over i) all cortical brain regions and ii) all subcortical brain regions, separately for HCs, de novo patients and treated (more advanced) patients. Next, we performed linear mixed models separately for the cortical and subcortical brain regions, with a grouping variable (HCs, de novo and late PD patients; represented by dummy variables) and the covariates age, gender and ISCED (dichotomized at 3). In order to explore whether neurophysiological characteristics of subcortical brain regions differed more from HCs than those of cortical brain regions, we created linear mixed models with the neurophysiological measure as dependent variable, the grouping variable (control or de novo PD patient), location variable (cortical or subcortical), the interaction between the group and location variables, as well as the covariates age, gender and ISCED (dichotomized).

Spectral power and functional connectivity: Longitudinal changes

We used linear mixed models to evaluate the longitudinal changes in spectral power and functional connectivity in Parkinson's disease patients. Linear mixed-models can account for the dependency of the observations within the patient and the fact that not all patients had undergone a (complete) study visit at all three time points. In the linear mixed models the time variable (BL, FU1, FU2) was treated as a categorical variable and represented by dummy variables. Age at baseline, disease duration at baseline, gender, ISCED (dichotomized), and LEDD were included in the model as covariates. MEG-machine was not included as covariate here, as it was redundant because of the inclusion of the time variable.

Relative spectral power (per frequency band; delta to beta band), peak frequency, and functional connectivity (per frequency band; functional connectivity of one brain region with the rest of the brain) were each averaged over cortical and subcortical brain regions separately and were used as dependent variables.

Relationship between spectral power measures and clinical measures of disease progression

We analyzed the relationship between the longitudinal courses of the spectral measures and global measures of cognitive (CAMCOG) and motor (UPDRS-III) function using linear mixed models. CAMCOG and UPDRS-III were treated as dependent variables, spectral measures (delta to beta relative power and peak frequency) as independent variables. Age at baseline, disease duration at baseline, gender, ISCED (dichotomized; only included in case of analyses involving CAMCOG), recording system (CTF versus Elekta), and LEDD were included in the model as covariates. Neurophysiological measures of i) cortical brain regions and ii) subcortical brain regions were used as independent variables in separate analyses. Due to collinearity of the neurophysiological measures, it was not possible to combine them in a single linear mixed model.

Statistical analyses were performed using the IBM SPSS Statistics 26 software package (IBM Corporation, New York , USA). A significance level of 0.05/6 was applied in the baseline comparisons and the analyses on longitudinal changes (Bonferroni correction separately for each frequency band). In the other analyses, a significance level of 0.05 was applied. In the linear mixed models, a random intercept was used. Supplementary Figure 1 gives an overview of the statistical tests performed in this study.

Results

Patient characteristics

Participant characteristics and details on statistics are summarized in Table 1. The HCs were age-matched to the de novo PD patients, the later-stage (treated) patients were significantly older. All 17 de novo patients were included in the longitudinal analysis, of which 9 completed all three study visits. HCs had significantly better CAMCOG scores than both Parkinson's disease groups (Table 1A). At FU1, three patients fulfilled the criteria for Parkinson's disease dementia and at FU2 six patients fulfilled these criteria. The composition of the cohorts studied at BL, FU1 and FU2 are demonstrated in Table 1B.

Table 1 Participant characteristics

A

	HC (n=16)	De novo PD (n=17)	Treated PD patients (n=44)	Statistics HC-De novo PD	Statistics HC-Treated PD
Sex (M/F)	10/6	12/5	21/23	$X^2(31)= 0.243$; $p= .622$	$X^2(31)= 1.02$; $p= .387$
Age baseline (years)	58.9 (6.6)	60.6 (7.9)	64.1 (0.9)	t(31)= 0.670 ; $p= .510$	**t(58)= 2.80 ; *p*= .006**
Disease duration baseline (years)	n/a	0.94 (0.42)	7.1 (3.0)	n/a	n/a
ISCED (1/2/3/4/5/6)	0/5/3/0/8/0	0/5/4/0/8/0	1/20/10/4/9/0	Fisher's exact test: $p= 1.00$	Fisher's exact test: $p= 0.226$
UPDRS-III	n/a	13.2 (6.3)	13.4 (5.2)	n/a	n/a
LEDD total dose	n/a	n/a	524 (394)	n/a	n/a
HY stage (0/1/1.5/2.0/2.5/3/4/5)	n/a	0/8/1/7/1/0/0/0	0/6/1/25/12/0/0/0	n/a	n/a
CAMCOG	99.1 (3.6)	95.8 (5.1)	94.6 (5.0)	**t(31)= 2.09 ; *p*= .045**	**t(58)= 3.30 ; *p*= .002**

B

	PD BL (n=61)	FU1 (n=39)	FU2 (n=35)
Sex (M/F)	33/28	25/14	19/16
Age baseline (years)	63.2 (6.8)	61.6 (6.6)	62.1 (6.0)
Disease duration baseline (years)	5.35 (3.8)	4.66 (3.7)	4.92 (3.7)
ISCED (1/2/3/4/5/6)	1/25/14/4/17/0	1/12/12/1/12/1	1/12/10/2/10/0
UPDRS-III	13.4 (5.5)	27.3 (8.7)	32.9 (9.7)
LEDD total dose	382 (409)	746 (435)	1128 (520)
HY stage (0/1/1.5/2.0/2.5/3/4/5)	0/14/2/32/13/0/0/0	1/0/0/12/20/6/0/0	0/0/0/13/10/10/1/1
CAMCOG	94.9 (5.0)	92.8 (8.6)	89.9 (14.0)
Parkinson's disease dementia	0	3	6

A) Cross-sectional analysis B) Longitudinal analysis in PD patients. Numbers are expressed as mean (standard deviation)
PD, Parkinson's disease; M, male; F, female; ISCED, International Standard Classification of Education; n/a, not applicable; UPDRS-III, motor part of Unified Parkinson's Disease Rating Scale; LEDD, levodopa equivalent daily dose; HY stage (Hoehn and Yahr stage); CAMCOG, Cambridge Cognitive examination; n/a, not applicable; BL, baseline; FU1, follow-up 1; FU2, follow-up

Spectral power

Figure 2A shows a global normalized power spectrum, group-averaged per time point, in which de novo and treated Parkinson's disease patients were combined. At BL, the peak frequency was significantly lower in the Parkinson's disease group (Figure 2B). The peak frequency also significantly decreased further over time in the Parkinson's disease group (Figure 2C).

Looking at spectral power, the baseline analysis (Figure 2B) demonstrates significantly higher relative theta band power in both Parkinson's disease groups compared with healthy controls, both for cortical and subcortical brain regions. Relative alpha2 power and peak frequency were significantly lower in the Parkinson's disease groups, both for cortical and subcortical brain regions. In addition, only for the cortical brain regions, alpha1 band power was significantly higher (all Parkinson's disease patients) and beta band power significantly lower (treated patients). There were no significant differences between the de novo patients and the treated patients. In addition, using linear mixed models, we found that de novo PD patients deviated from controls stronger for cortical than for subcortical brain regions for alpha1 and beta band power (p= 0.028 and 0.008, respectively).

Over time, the pattern of slowing further developed as we found increases in relative delta and theta power, and decreases in relative alpha2 and beta power. The magnitude of these changes was comparable between cortical and subcortical brain regions (Figure 2C; see Supplementary Table 2 for statistics).

Functional connectivity

There were no significant baseline group differences in the functional connectivity analysis (Supplementary Figure 2A). We also observed no significant longitudinal changes in whole-brain functional connectivity, except for a significant increase in subcortical beta band functional connectivity between FU1 and FU2 (Supplementary Figure 2B). Because of this scarcity of results, functional connectivity was not evaluated further in the next analysis and beyond.

Relationship between neurophysiological parameters and clinical measures of disease progression

We analyzed the longitudinal relationship between the spectral measures (delta to beta band relative power, peak frequency) and scores on the CAMCOG and UPDRS-III, separately for cortical and subcortical brain regions.

Both for cortical and subcortical brain regions, higher relative delta power was significantly associated with worse performance on CAMCOG. In addition, lower relative alpha1, alpha2, and beta power, as well as lower peak frequency, all in cortical and subcortical areas, were associated with worse performance on CAMCOG (Table 2). Conversely, higher (cortical) relative delta power and (cortical and subcortical) theta power were associated with higher scores on the UPDRS-III. In addition, lower relative (cortical) alpha2, lower relative (cortical and subcortical) beta power, and lower peak frequency (cortical and subcortical) were associated with worse motor performance.

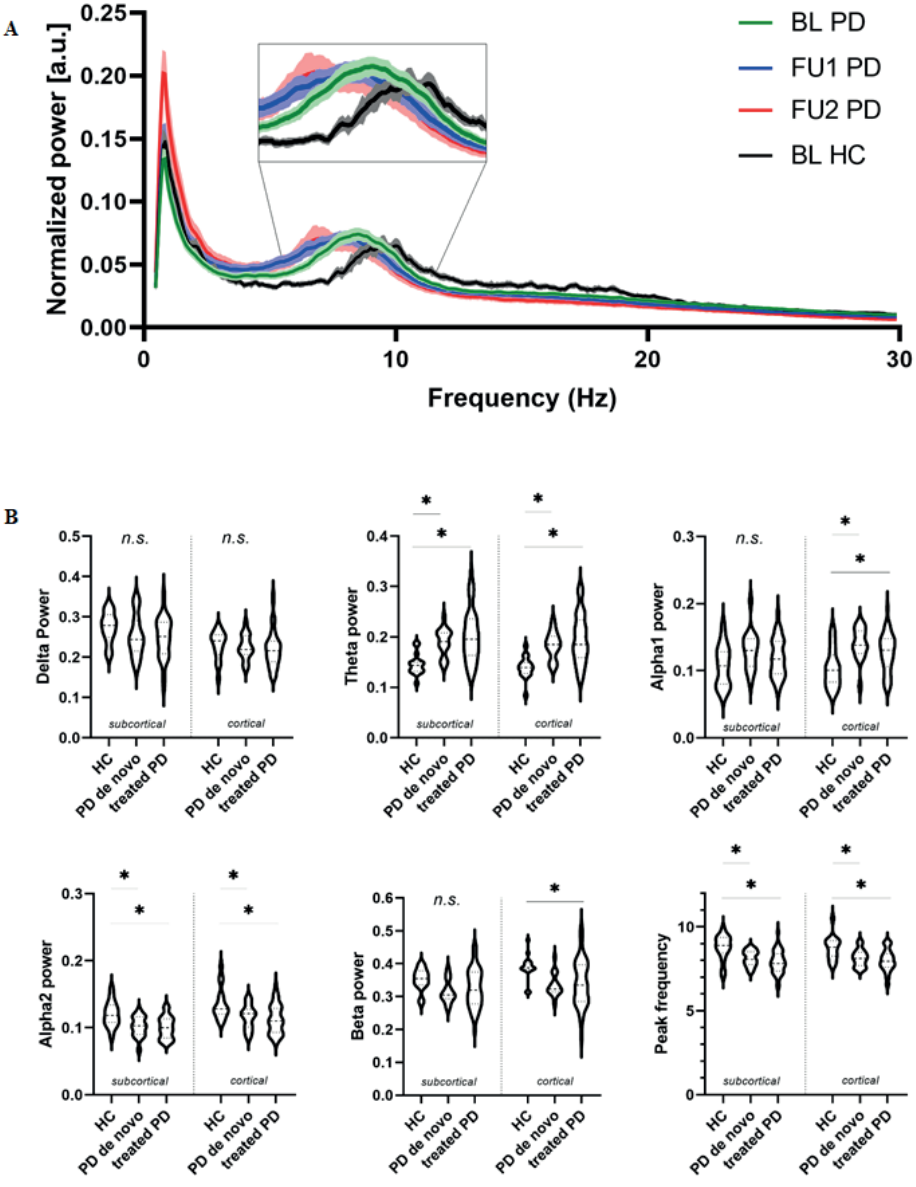
A
Normalized power [a.u.]
0.25
0.20
0.15
0.10
0.05
0.00
0
10
20
30
Frequency (Hz)
BL PD
FU1 PD
FU2 PD
BL HC
B
Delta Power
Theta power
Alpha1 power
Alpha2 power
Beta power
Peak frequency
n.s.
*
subcortical
cortical
HC
PD de novo
treated PD

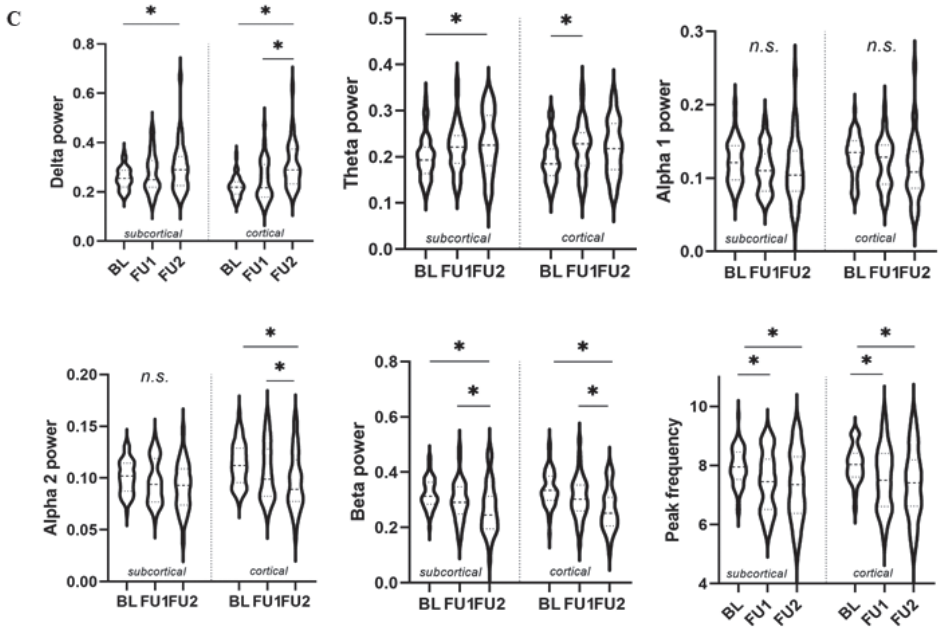

Figure 2 Power spectral analysis
Whole-group normalized power spectra at three time points, including the healthy controls (HC) at baseline (BL). Spectral power between 0.5 and 30 Hz was averaged over all brain regions.
Violin plots summarizing the baseline comparison between three groups; de novo PD patients, later stage treated PD patients and HCs. A significance level of 0.05/6 (Bonferroni correction) was applied.
Violin plots summarizing the longitudinal analysis. Statistical testing was performed using linear mixed models. A significance level of 0.05/6 (Bonferroni correction) was applied.
n.s., non-significant; HC, healthy control; FU1, follow-up 1; FU2, follow-up 2

Table 2 Longitudinal associations between spectral measures and clinical measures of disease severity

CAMCOG	Subcortical brain regions			Cortical brain regions		
	Estimated regression coefficient	**95% CI**	***p* value**	**Estimated regression coefficient**	**95% CI**	***p* value**
Relative power						
Delta	**-75.1**	**-92.1 to -58.1**	**< .001**	**-79.0**	**-96.9 to -61.0**	**< .001**
Theta	-11.7	-43.3 to 19.8	.463	-21.2	-54.0 to 11.5	.201
Alpha1	**115.3**	**71.9 to 158.8**	**< .001**	**112.5**	**68.9 to 156.1**	**< .001**
Alpha2	**201.4**	**123.1 to 279.7**	**< .001**	**166.0**	**102.6 to 299.5**	**< .001**
Beta	**52.4**	**30.9 to 74.0**	**< .001**	**51.2**	**28.9 to 73.5**	**< .001**
Peak frequency	**4.2**	**2.6 to 5.8**	**< .001**	**4.5**	**2.9 to 6.1**	**< .001**

UPDRS-III	Subcortical brain regions			Cortical brain regions		
	Estimated regression coefficient	**95% CI**	***p* value**	**Estimated regression coefficient**	**95% CI**	***p* value**
Relative power						
Delta	24.8	-2.1 to 51.6	.072	**33.3**	**6.7 to 59.9**	**.015**
Theta	**40.1**	**5.9 to 74.2**	**.022**	**48.6**	**13.6 to 83.7**	**.007**
Alpha1	-48.9	-100.6 to 2.6	.062	-38.3	-90.4 to 13.7	.147
Alpha2	-77.9	-175.9 to 20.0	.117	**-79.9**	**-154.1 to -5.6**	**.036**
Beta	**-27.9**	**-53.8 to -2.1**	**.035**	**-37.3**	**-62.8 to -11.7**	**.005**
Peak frequency	**-2.8**	**-4.7 to -0.70**	**.008**	**-2.7**	**-4.6 to -0.80**	**.006**

CAMCOG, Cambridge Cognitive examination; UPDRS-III, motor part of Unified Parkinson's Disease Rating Scale; 95% CI, 95% confidence interval

Next, for the spectral measures that demonstrated a significant association with a clinical measure, we displayed the cortical topographic distribution of (only) the significant associations as a post-hoc analysis. We restricted these figures to the cortical brain regions for visualization purposes, but we did calculate the individual associations of the subcortical brain regions (Supplementary Table 3). Figure 3 illustrates the longitudinal relations of relative beta band power and peak frequency with clinical measures of disease severity. The relationship between lower beta band power and worse cognitive performance was strongest for frontal cortical brain regions, whereas the relationship between lower beta band power and worse motor function was strongest (most negative) for the temporal-occipital brain regions. Interestingly, the relationship was weakest for the sensorimotor regions. For peak frequency, the strongest associations with clinical measures of disease severity were found for the temporal, parietal and occipital brain regions, both for the relationship with cognitive and motor performance. The remaining topographic distributions (delta-alpha2) can be found in Supplementary Figure 3. Higher delta power in parieto-temporal regions was most strongly associated with cognitive and motor impairment (in the latter case also the occipital brain regions), higher frontal theta power with motor dysfunction, lower frontal alpha1 and alpha2 power with cognitive dysfunction, and lower parieto-temporal-occipital alpha2 power with motor impairment.

In Supplementary Table 3 we show the associations of individual subcortical brain regions with clinical measures of disease severity. The most outspoken pattern was the fact that activity in the hippocampus had the weakest association with CAMCOG and UPDRS-III for the frequency bands between delta and alpha2, but the strongest association with CAMCOG and UPDRS-III in the beta band. The results on peak frequency did not show a clear pattern.

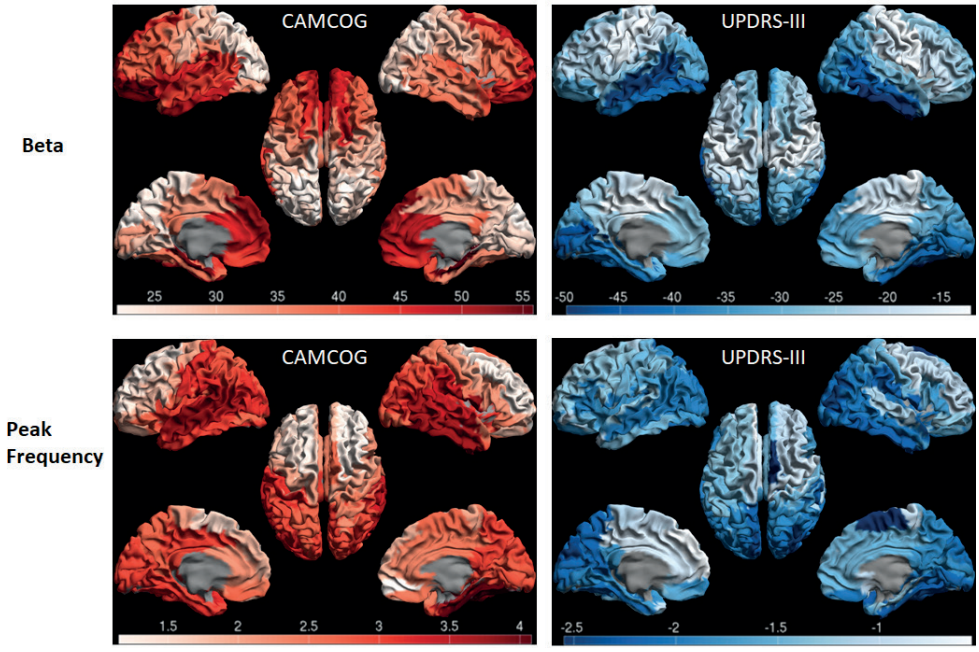

Figure 3 Topographic distribution of clinical associations
Distribution of longitudinal associations between relative beta band power and CAMCOG, relative beta band power and UPDRS-III, peak frequency and CAMCOG, peak frequency and UPDRS-III.
Associations only concern cortical brain regions and are expressed as the estimated regression coefficient and displayed as a color-coded map on a parcellated template brain viewed from, in clockwise order, the left, top, right, right-midline and left-midline.
All individual associations were statistically significant, except for a number of associations concerning the beta band (threshold around an estimated regression coefficient of -20). As we treated this analysis as a post-hoc analysis, we did not correct for multiple comparisons. The distribution of the remaining frequency bands that had significant associations with clinical measures of disease progression can be found in Supplementary Figure 3

Discussion

In this longitudinal MEG study, we used a multiple longitudinal design to be able to analyze the changes in brain activity in Parkinson's disease patients from disease onset up to a disease duration of 15-20 years. In the earliest Parkinson's disease stages, we found activity changes in both cortical and subcortical brain regions, but, surprisingly, the changes in subcortical regions were less prominent than the changes in the cortical regions. Furthermore, in our longitudinal analyses we observed a progressive spectral slowing of brain activity throughout the course of the disease. This spectral slowing was strongly associated with clinical measures of disease progression (cognition and motor function), most outspoken for the cortical brain regions. We did not observe functional connectivity changes in the baseline analysis and functional connectivity hardly changed over time (only one finding for the beta band).

The general pattern of spectral slowing involved both cortical and subcortical brain regions. Although we expected early functional changes in subcortical brain regions to be more outspoken than cortical changes, the subcortical changes were weaker than the cortical changes in case of alpha1 and beta power. Nonetheless, spectral power values were highly correlated between cortical and subcortical brain regions (Pearson's *r* ranging between 0.913 and 0.965 for different frequency bands, $p < .001$). Besides a physiological explanation for this high correlation, as cortical and subcortical activity are structurally connected, field spread may have played a role, which is not corrected for in case of spectral analyses. Clearly, we do not know whether small subcortical changes may have preceded cortical changes at the premotor disease stage. Also, perhaps some of the subcortical changes were too local to be picked up by our MEG system, as the spatial resolution deeper in the brain is not as good as at the cortical level.[47] In addition, local (subcortical) pathological changes may have more distant (cortical) effects via ascending neurotransmitter systems. Spectral slowing at the cortical level is hypothesized to be a consequence of dopaminergic, noradrenergic, serotonergic and cholinergic dysfunction[48-50] and could also be an effect of local Lewy body and tau pathology in thalamocortical circuits.[51,52] There are no previous EEG/MEG studies in early-stage Parkinson's disease to compare our results with, but fMRI studies have shown functional changes (loss of functional connectivity) within the basal ganglia circuit in early-stage Parkinson's disease[53,54] that were paralleled by whole-brain changes in activity.[55]

We found strong longitudinal associations between spectral measures (spectral slowing) and clinical measures of disease severity. Based on the regression coefficients, we conclude that subcortical spectral measures were associated equally strongly with cognitive performance (CAMCOG) as cortical spectral measures (Table 2). However, unexpectedly, subcortical spectral measures were less strongly associated with motor function (UPDRS-III) than with cognitive performance (CAMCOG). Also, of the individual subcortical brain regions, relative beta band power of the hippocampus was most strongly associated with CAMCOG and UPDRS-III. Moreover, relative beta band power in the sensorimotor cortex was only poorly associated with UPDRS-III scores, compared to the rest of the cortex. The finding that both subcortical (except the hippocampus) spectral measures and beta band power in the sensorimotor cortex were associated poorly with UPDRS-III scores may originate from compensatory mechanisms secondary to motor impairment, as was previously hypothesized.[56,57] Alternatively, the lack of strong associations may result from treatment with dopaminergic medication. The amount of dopaminergic medication (LEDD) is associated with lower relative beta power in the motor cortex (Pearson's *r* left motor cortex, -0.213 $p = 0.015$, right motor cortex, -0.240 $p = 0.005$), but this could be both a disease effect or a treatment effect. Supplementary Figure 4 demonstrates that sensorimotor beta power remains largely intact against a background of generalized slowing of cortical brain activity, especially between BL and FU1, despite worsening motor scores over time. For further considerations regarding the complex interplay between motor function and beta band power/functional connectivity we refer the reader to our review on this topic.[58]

When considering the region-specific post-hoc analyses of the other frequency bands, we found that cognitive decline and motor dysfunction were related to spectral slowing, sometimes in the same brain regions (see for example Figure 3C and 3D), sometimes in different brain regions (see alpha2 in Supplementary Figure 3). As hypothesized, lower peak frequency in posterior cortical brain regions correlated strongest with global cognitive decline (Figure 3C). This may reflect 'posterior cortical dysfunction', a clinical profile that may indicate a higher risk of developing PD dementia.[59]

A correlation of oscillatory slowing with motor dysfunction has only been reported incidentally[60] and has not been found in other studies.[11,13] Possibly, our long follow-up duration allowed us to find the correlations between spectral slowing and motor dysfunction. Motor and cognitive impairment may be associated with spectral slowing via a general underlying mechanism. When we added UPDRS-III performance as a covariate in the linear mixed model for the association between CAMCOG and peak frequency, the association remained present (standardized effect size 2.32, p= .001), but not the other way around (standardized effect size -1.50, p= .128). We therefore conclude that, although motor and cognitive impairment are both related to the same underlying disease process, their pathophysiology does not fully overlap.

We chose not to include functional connectivity in our analyses of longitudinal associations with clinical measures of disease severity. At baseline, we did not observe significant group differences in functional connectivity and over time, only subcortical beta band functional connectivity significantly changed. This was unexpected, as a previous analysis in the same cohort showed longitudinal decreases in alpha1 and alpha2 functional connectivity, although only between baseline and FU1 and with another measure of functional connectivity [12]. In addition, a recent high-density EEG study with a longitudinal design demonstrated a progressive loss of functional connectivity in correlation with global cognitive decline and lateralization of motor symptoms.[14] In the present study, we used AEC-c as a measure of functional connectivity, which is a robust leakage-corrected metric with a good within-subject reproducibility in the alpha band.[61-64] In our healthy control cohort this metric remained stable over time and over MEG systems.[26] However, the AEC-c is an amplitude-based measure that is fundamentally different than the phase-based measures (phase lag index, phase locking value) that were used in other longitudinal studies on PD patients.[12,14] Hence, the measure of AEC-c may not have been sensitive or stable enough to pick up more subtle changes in functional connectivity in our cohort. Furthermore, the addition of a third time point and a different MEG system may have confounded the analysis. The only significant change we observed was an increase in beta band functional connectivity between FU1 and FU2. Since an increase in beta band functional connectivity was also present in our healthy control group, this may be related to the change from one MEG system to the other.[26]

Our results confirm that neurophysiological patterns are good candidates in the search for biomarkers of the degenerative process in Parkinson's disease. Although we did not study the risk of conversion to Parkinson's disease dementia, a previous analysis in this study cohort demonstrated that lower beta band power, especially in the posterior brain regions, was a strong predictor for conversion.[15] Our result in Figure 3A was therefore somewhat surprising, as we found that beta band power of frontal cortical brain regions correlated strongest with global cognitive decline. The identification of a subgroup of Parkinson's disease patients at high risk for dementia may be important for patients and caregivers in the context of advanced care planning, and also for future studies aimed at disease-modifying therapies to slow down cognitive decline. In the latter case, a neurophysiological biomarker may also serve as an objective read-out parameter of treatment success.

A strength of the current analysis is the multiple longitudinal design with a long follow-up duration of seven years, which allowed us to longitudinally cover 15-20 years of the disease course. In addition, the inclusion of a third time point (second follow-up) adds robustness to previously published results on spectral power at the first two time points,[11] as it confirms that the observed trends in spectral slowing are progressive over time. In addition, this is the first MEG study exploring the presence of subcortical neurophysiological changes in the earliest clinical motor stages of Parkinson's disease, as well as the further development of these changes over time. Three potential limitations of our study deserve consideration. First, our baseline cohort decreased from 61 patients at BL to 39 patients at FU1. This is explained by the fact that data of 19 patients could not be used (low quality data, no MRI-scan; see also Figure 1). 23 patients were lost to follow-up 2, possibly due to high disease burden. Given that this group was clinically more severely affected, the dropout of these subjects can only have led to an underestimation of true disease effects. In addition, our linear mixed models account for missing data, so that reliable longitudinal associations could still be established. Second, several subjects could not be included in the follow-up visits because they had poor-quality data or because they were lost to follow-up (see Figure 1 for an overview). The majority of missing data was due to poor-quality MEG or MRI data, which is a random phenomenon. We do not have an overview of the reasons why patients were lost to follow-up, but there may have been a selective dropout of patients with a high (subjective) disease burden. However, this could only have led to an underestimation of the true effects.

Third, although there is increasing evidence that projecting MEG to subcortical sources is feasible, MEG is most sensitive to cortical sources.[47] The sensitivity for subcortical sources can be further improved using new analysis techniques such as 'blind source separation',[19,65] methods that increase the contrast between cortical and subcortical sources,[66] or in-mouth sensors.[67]

In conclusion, already at the earliest disease stages of Parkinson's disease, there are neurophysiological changes in Parkinson's disease patients both at the subcortical and cortical level, most outspoken for the latter. In our analysis using a multiple longitudinal design, spanning 15-20 years of disease duration, we found strong longitudinal associations between spectral slowing of brain activity and clinical measures of disease severity, especially cognition. Our results indicate that spectral power is a promising candidate in the search for a non-invasive marker to monitor the ongoing disease process in Parkinson's disease.

References

1. Chaudhuri KR, Healy DG, Schapira AH. Non-motor symptoms of Parkinson's disease: diagnosis and management. Lancet Neurol. 2006;5(3):235-45.
2. Braak H, Del Tredici K, Rüb U, et al. Staging of brain pathology related to sporadic Parkinson's disease. Neurobiol Aging. 2003;24(2):197-211.
3. Baillet S. Magnetoencephalography for brain electrophysiology and imaging. Nat Neurosci. 2017;20(3):327-39.
4. Litvak V, Florin E, Tamás G, et al. EEG and MEG primers for tracking DBS network effects. Neuroimage. 2021;224:117447.
5. Bosboom JL, Stoffers D, Stam CJ, et al. Resting state oscillatory brain dynamics in Parkinson's disease: an MEG study. Clin Neurophysiol. 2006;117(11):2521-31.
6. Bosboom JL, Stoffers D, Wolters EC, et al. MEG resting state functional connectivity in Parkinson's disease related dementia. J Neural Transm (Vienna). 2009;116(2):193-202.
7. Stoffers D, Bosboom JL, Deijen JB, et al. Slowing of oscillatory brain activity is a stable characteristic of Parkinson's disease without dementia. Brain. 2007;130(Pt 7):1847-60.
8. Hassan M, Chaton L, Benquet P, et al. Functional connectivity disruptions correlate with cognitive phenotypes in Parkinson's disease. Neuroimage Clin. 2017;14:591-601.
9. Caviness JN, Utianski RL, Hentz JG, et al. Differential spectral quantitative electroencephalography patterns between control and Parkinson's disease cohorts. European J Neurol. 2016;23(2):387-92.
10. Caviness JN, Hentz JG, Evidente VG, et al. Both early and late cognitive dysfunction affects the electroencephalogram in Parkinson's disease. Parkinsonism Relat Disord. 2007;13(6):348-54.
11. Olde Dubbelink KT, Stoffers D, Deijen JB, et al. Cognitive decline in Parkinson's disease is associated with slowing of resting-state brain activity: a longitudinal study. Neurobiol Aging. 2013;34(2):408-18.
12. Olde Dubbelink KT, Stoffers D, Deijen JB, et al. Resting-state functional connectivity as a marker of disease progression in Parkinson's disease: A longitudinal MEG study. Neuroimage Clin. 2013;2:612-9.
13. Geraedts VJ, Marinus J, Gouw AA, et al. Quantitative EEG reflects non-dopaminergic disease severity in Parkinson's disease. Clin Neurophysiol. 2018;129(8):1748-55.
14. Yassine S, Gschwandtner U, Auffret M, et al. Functional Brain Dysconnectivity in Parkinson's Disease: A 5-Year Longitudinal Study. Mov Disord. 2022;37(7):1444-53.
15. Olde Dubbelink KT, Hillebrand A, Twisk JW, et al. Predicting dementia in Parkinson disease by combining neurophysiologic and cognitive markers. Neurology. 2014;82(3):263-70.
16. Klassen BT, Hentz JG, Shill HA, et al. Quantitative EEG as a predictive biomarker for Parkinson disease dementia. Neurology. 2011;77(2):118-24.
17. Arnaldi D, De Carli F, Famà F, et al. Prediction of cognitive worsening in de novo Parkinson's disease: Clinical use of biomarkers. Mov Disord. 2017;32(12):1738-47.
18. De Micco R, Agosta F, Basaia S, et al. Functional Connectomics and Disease Progression in Drug-Naïve Parkinson's Disease Patients. Mov Disord. 2021;36(7):1603-16.
19. Pizzo F, Roehri N, Medina Villalon S, et al. Deep brain activities can be detected with magnetoencephalography. Nat Commun. 2019;10(1):971.
20. Hillebrand A, Barnes GR. Beamformer analysis of MEG data. Int Rev Neurobiol. 2005;68:149-71.
21. Hillebrand A, Barnes GR, Bosboom JL, et al. Frequency-dependent functional connectivity within resting-state networks: an atlas-based MEG beamformer solution. Neuroimage. 2012;59(4):3909-21.
22. Hillebrand A, Singh KD, Holliday IE, et al. A new approach to neuroimaging with magnetoencephalography. Hum Brain Mapp. 2005;25(2):199-211.

23. Boon LI, Hillebrand A, Dubbelink KTO, et al. Changes in resting-state directed connectivity in cortico-subcortical networks correlate with cognitive function in Parkinson's disease. Clin Neurophysiol. 2017;128(7):1319-26.
24. Hillebrand A, Nissen I, Ris-Hilgersom I, et al. Detecting epileptiform activity from deeper brain regions in spatially filtered MEG data. Clin Neurophysiol. 2016;127(8):2766-9.
25. Caviness JN, Hentz JG, Belden CM, et al. Longitudinal EEG changes correlate with cognitive measure deterioration in Parkinson's disease. J Parkinsons Dis. 2015;5(1):117-24.
26. Boon LI, Tewarie P, Berendse HW, et al. Longitudinal consistency of source-space spectral power and functional connectivity using different magnetoencephalography recording systems. Sci Rep. 2021;11(1):16336.
27. Scheijbeler EP, Schoonhoven DN, Engels MMA, et al. Generating diagnostic profiles of cognitive decline and dementia using magnetoencephalography. Neurobiol Aging. 2022;111:82-94.
28. Olde Dubbelink KT, Hillebrand A, Stoffers D, et al. Disrupted brain network topology in Parkinson's disease: a longitudinal magnetoencephalography study. Brain. 2014;137(Pt 1):197-207.
29. Vandenbroucke JP, von Elm E, Altman DG, et al. Strengthening the Reporting of Observational Studies in Epidemiology (STROBE): explanation and elaboration. PLoS Med. 2007;4(10):e297.
30. UNESCO. International standard classification of education (ISCED). 1997;available at: http://www.uis.unesco.org/Education/Pages/international-standardclassification-of-education.aspx.
31. Fahn S ER, Committee Members of the UPDRS Develeopment. The unified Parkinson's disease rating scale. Recent developments in Parkinson's disease. . 2nd ed Florham Park, NY: Macmillan Healthcare Information. 1987:p.153-63.
32. Hoehn MM, Yahr MD. Parkinsonism. onset, progression, and mortality. 1967;17(5):427-.
33. Roth M, Tym E, Mountjoy CQ, et al. CAMDEX. A standardised instrument for the diagnosis of mental disorder in the elderly with special reference to the early detection of dementia. Br J Psychiatry. 1986;149:698-709.
34. Dubois B, Burn D, Goetz C, et al. Diagnostic procedures for Parkinson's disease dementia: recommendations from the movement disorder society task force. Mov Disord. 2007;22(16):2314-24.
35. Taulu S, Hari R. Removal of magnetoencephalographic artifacts with temporal signal-space separation: demonstration with single-trial auditory-evoked responses. Hum Brain Mapp. 2009;30(5):1524-34.
36. Taulu S, Simola J. Spatiotemporal signal space separation method for rejecting nearby interference in MEG measurements. Phys Med Biol. 2006;51(7):1759-68.
37. Whalen C, Maclin EL, Fabiani M, et al. Validation of a method for coregistering scalp recording locations with 3D structural MR images. Hum Brain Mapp. 2008;29(11):1288-301.
38. Gong G, He Y, Concha L, et al. Mapping anatomical connectivity patterns of human cerebral cortex using in vivo diffusion tensor imaging tractography. Cereb Cortex. 2009;19(3):524-36.
39. Tzourio-Mazoyer N, Landeau B, Papathanassiou D, et al. Automated anatomical labeling of activations in SPM using a macroscopic anatomical parcellation of the MNI MRI single-subject brain. Neuroimage. 2002;15(1):273-89.
40. Hillebrand A, Tewarie P, Van Dellen E, et al. Direction of information flow in large-scale resting-state networks is frequency-dependent. Proc Natl Acad Sci U S A. 2016;113(14):3867-72.
41. Vrba J, Robinson S. SQUID sensor array configurations for magnetoencephalography applications. Supercond Sci Technol. 2002;15(9):R51.
42. Cheyne D, Bostan AC, Gaetz W, et al. Event-related beamforming: a robust method for presurgical functional mapping using MEG. Clin Neurophysiol. 2007;118(8):1691-704.
43. Klimesch W, Schack B, Sauseng P. The functional significance of theta and upper alpha oscillations. Exp Psychol. 2005;52(2):99-108.
44. Brookes MJ, Woolrich MW, Barnes GR. Measuring functional connectivity in MEG: a multivariate approach insensitive to linear source leakage. Neuroimage. 2012;63(2):910-20.

45. Bruns A, Eckhorn R, Jokeit H, et al. Amplitude envelope correlation detects coupling among incoherent brain signals. Neuroreport. 2000;11(7):1509-14.
46. Hipp JF, Hawellek DJ, Corbetta M, et al. Large-scale cortical correlation structure of spontaneous oscillatory activity. Nat Neurosci. 2012;15(6):884-90.
47. Hillebrand A, Barnes GR. A quantitative assessment of the sensitivity of whole-head MEG to activity in the adult human cortex. Neuroimage. 2002;16(3 Pt 1):638-50.
48. Rea RC, Berlot R, Martin SL, et al. Quantitative EEG and cholinergic basal forebrain atrophy in Parkinson's disease and mild cognitive impairment. Neurobiol Aging. 2021;106:37-44.
49. Détári L, Rasmusson DD, Semba K. The role of basal forebrain neurons in tonic and phasic activation of the cerebral cortex. Prog Neurobiol. 1999;58(3):249-77.
50. Bosboom JL, Stoffers D, Stam CJ, et al. Cholinergic modulation of MEG resting-state oscillatory activity in Parkinson's disease related dementia. Clin Neurophysiol. 2009;120(5):910-5.
51. Freunberger R, Werkle-Bergner M, Griesmayr B, et al. Brain oscillatory correlates of working memory constraints. Brain research. 2011;1375:93-102.
52. Steriade M, Gloor P, Llinas RR, et al. Basic mechanisms of cerebral rhythmic activities. Electroencephalogr Clin Neurophysiol. 1990;76(6):481-508.
53. Rolinski M, Griffanti L, Szewczyk-Krolikowski K, et al. Aberrant functional connectivity within the basal ganglia of patients with Parkinson's disease. Neuroimage Clin. 2015;8:126-32.
54. Szewczyk-Krolikowski K, Menke RA, Rolinski M, et al. Functional connectivity in the basal ganglia network differentiates PD patients from controls. Neurology. 2014;83(3):208-14.
55. Pan P, Zhang Y, Liu Y, et al. Abnormalities of regional brain function in Parkinson's disease: a meta-analysis of resting state functional magnetic resonance imaging studies. Sci Rep. 2017;7(1):40469.
56. Hirschmann J, Ozkurt TE, Butz M, et al. Differential modulation of STN-cortical and cortico-muscular coherence by movement and levodopa in Parkinson's disease. Neuroimage. 2013;68:203-13.
57. Pollok B, Kamp D, Butz M, et al. Increased SMA-M1 coherence in Parkinson's disease - Pathophysiology or compensation? Exp Neurol. 2013;247:178-81.
58. Boon LI, Geraedts VJ, Hillebrand A, et al. A systematic review of MEG-based studies in Parkinson's disease: The motor system and beyond. Hum Brain Mapp. 2019;40(9):2827-48.
59. Kehagia AA, Barker RA, Robbins TW. Cognitive impairment in Parkinson's disease: the dual syndrome hypothesis. Neurodegener Dis. 2013;11(2):79-92.
60. Morita A, Kamei S, Serizawa K, et al. The relationship between slowing EEGs and the progression of Parkinson's disease. J Clin Neurophysiol. 2009;26(6):426-9.
61. Colclough GL, Woolrich MW, Tewarie PK, et al. How reliable are MEG resting-state connectivity metrics? Neuroimage. 2016;138:284-93.
62. Briels CT, Schoonhoven DN, Stam CJ, et al. Reproducibility of EEG functional connectivity in Alzheimer's disease. Alzheimers Res Ther. 2020;12(1):68.
63. Demuru M, Gouw AA, Hillebrand A, et al. Functional and effective whole brain connectivity using magnetoencephalography to identify monozygotic twin pairs. Sci Rep. 2017;7(1):9685.
64. Schoonhoven DN, Briels CT, Hillebrand A, et al. Sensitive and reproducible MEG resting-state metrics of functional connectivity in Alzheimer's disease. Alzheimers Res Ther. 2022;14(1):38.
65. López-Madrona VJ, Medina Villalon S, Badier JM, et al. Magnetoencephalography can reveal deep brain network activities linked to memory processes. Hum Brain Mapp. 2022.
66. Quraan MA, Moses SN, Hung Y, et al. Detection and localization of hippocampal activity using beamformers with MEG: a detailed investigation using simulations and empirical data. Hum Brain Mapp. 2011;32(5):812-27.
67. Tierney TM, Levy A, Barry DN, et al. Mouth magnetoencephalography: A unique perspective on the human hippocampus. Neuroimage. 2021;225:117443.

Supplementary Materials

Supplementary Table 1
AAL atlas, with regions ordered as in Gong et al.[38] Regions in bold were grouped as subcortical brain regions (region 79-90).

	Left hemisphere		Right hemisphere
1	Gyrus rectus	40	Gyrus rectus
2	Olfactory cortex	41	Olfactory cortex
3	Super frontal gyrus, orbital part	42	Super frontal gyrus, orbital part
4	Superior frontal gyrus, medial orbital part	43	Superior frontal gyrus, medial orbital part
5	Middle frontal gyrus, orbital part	44	Middle frontal gyrus, orbital part
6	Inferior frontal gyrus, orbital part	45	Inferior frontal gyrus, orbital part
7	Superior frontal gyrus, dorsolateral part	46	Superior frontal gyrus, dorsolateral part
8	Middle frontal gyrus	47	Middle frontal gyrus
9	Inferior frontal gyrus, opercular part	48	Inferior frontal gyrus, opercular part
10	Inferior frontal gyrus, triangular part	49	Inferior frontal gyrus, triangular part
11	Superior frontal gyrus, medial part	50	Superior frontal gyrus, medial part
12	Supplementary motor area	51	Supplementary motor area
13	Paracentral lobule	52	Paracentral lobule
14	Precentral gyrus	53	Precentral gyrus
15	Rolandic operculum	54	Rolandic operculum
16	Postcentral gyrus	55	Postcentral gyrus
17	Superior parietal gyrus	56	Superior parietal gyrus
18	Inferior parietal gyrus	57	Inferior parietal gyrus
19	Supramarginal gyrus	58	Supramarginal gyrus
20	Angular gyrus	59	Angular gyrus
21	Precuneus	60	Precuneus
22	Superior occipital gyrus	61	Superior occipital gyrus
23	Middle occipital gyrus	62	Middle occipital gyrus
24	Inferior occipital gyrus	63	Inferior occipital gyrus
25	Calcarine fissure and surrounding cortex	64	Calcarine fissure and surrounding cortex
26	Cuneus	65	Cuneus
27	Lingual gyrus	66	Lingual gyrus
28	Fusiform gyrus	67	Fusiform gyrus
29	Heschl gyrus	68	Heschl gyrus
30	Superior temporal gyrus	69	Superior temporal gyrus
31	Middle temporal gyrus	70	Middle temporal gyrus
32	Inferior temporal gyrus	71	Inferior temporal gyrus
33	Temporal pole: superior temporal gyrus	72	Temporal pole: superior temporal gyrus
34	Temporal pole: middle temporal gyrus	73	Temporal pole: middle temporal gyrus

	Left hemisphere		Right hemisphere
35	Parahippocampal gyrus	74	Parahippocampal gyrus
36	Anterior (para)cingulate gyrus	75	Anterior (para)cingulate gyrus
37	Median (para)cingulate gyrus	76	Median (para)cingulate gyrus
38	Posterior cingulate gyrus	77	Posterior cingulate gyrus
39	Insula	78	Insula
79	**Hippocampus**	**80**	**Hippocampus**
81	**Amygdala**	**82**	**Amygdala**
83	**Caudate nucleus**	**84**	**Caudate nucleus**
85	**Putamen**	**86**	**Putamen**
87	**Pallidum**	**88**	**Pallidum**
89	**Thalamus**	**90**	**Thalamus**

Supplementary Figure 1 Overview of the statistical analysis using linear mixed models
The blue dotted line indicates a longitudinal analysis using linear mixed models. The blue dotted box indicates a longitudinal association between a neurophysiological measure (blue) and a clinical measure of disease severity (red, motor function; green, cognitive function).

Supplementary Table 2 Longitudinal changes in spectral measures

	BL-FU1			FU1-FU2			BL-FU2		
	Estimated regression coefficient	**95% CI**	***p* value**	**Estimated regression coefficient**	**95% CI**	***p* value**	**Estimated regression coefficient**	**95% CI**	***p* value**
Subcortical brain regions									
Delta power	0.018	-0.009 to 0.046	.187	0.029	-0.002 to 0.059	.060	**0.047**	**0.010 to 0.083**	**.008**
Theta power	0.019	0.004 to 0.035	.017	0.017	-0.001 to 0.337	.053	**0.035**	**0.016 to 0.058**	**.001**
Alpha1 power	-0.011	-0.020 to -0.001	.041	0.002	-0.010 to 0.014	.687	-0.009	-0.025 to 0.005	.217
Alpha2 power	-0.004	-0.011 to 0.002	.267	-0.007	-0.015 to -0.001	.049	-0.011	-0.020 to -0.003	.013
Beta power	-0.021	-0.044 to 0.001	.059	**-0.040**	**-0.060 to -0.017**	**.001**	**-0.061**	**-0.093 to -0.032**	**< .001**
Peak frequency	**-0.459**	**-0.785 to -0.182**	**.002**	-0.182	-0.398 to -0.038	.259	**-0.640**	**-1.09 to -0.277**	**.001**
Cortical brain regions									
Delta power	0.020	-0.005 to 0.045	.115	**0.065**	**0.038 to 0.092**	**< .001**	**0.085**	**0.052 to 0.119**	**< .001**
Theta power	**0.022**	**0.007 to 0.037**	**.003**	0.000	-0.015 to 0.015	.995	0.022	0.002 to 0.042	0.030
Alpha1 power	-0.009	-0.020 to 0.002	.117	-0.004	-0.016 to 0.008	.525	-0.013	-0.018 to 0.002	0.097
Alpha2 power	-0.008	-0.015 to -0.001	.048	**-0.011**	**-0.019 to -0.003**	**.006**	**-0.019**	**-0.029 to -0.009**	**< .001**
Beta power	-0.025	-0.044 to -0.006	.012	**-0.051**	**-0.071 to -0.031**	**< .001**	**-0.076**	**-0.049 to -0.103**	**< .001**
Peak frequency	**-0.429**	**-0.717 to -0.168**	**.004**	-0.247	-0.555 to -0.062	.116	**-0.676**	**-1.07 to -0.283**	**.001**

Overview of the longitudinal changes, separately for each frequency band and for each group of brain regions (subcortical and cortical). Statistics were performed using linear mixed models. We applied a p-value threshold of 0.05/6 for significance (Bonferroni correction). Significant results are indicated in bold.

A) Baseline: Healthy controls, de novo, and treated PD patients

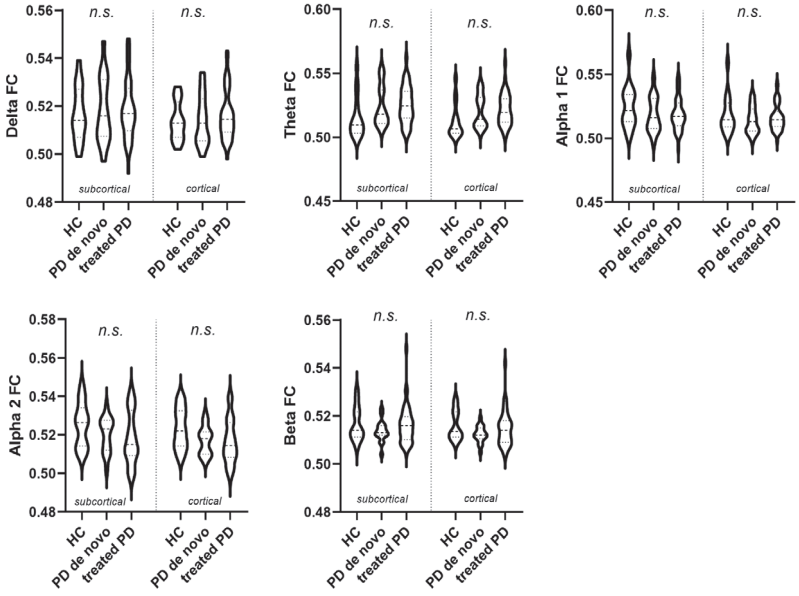

B) Longitudinal changes

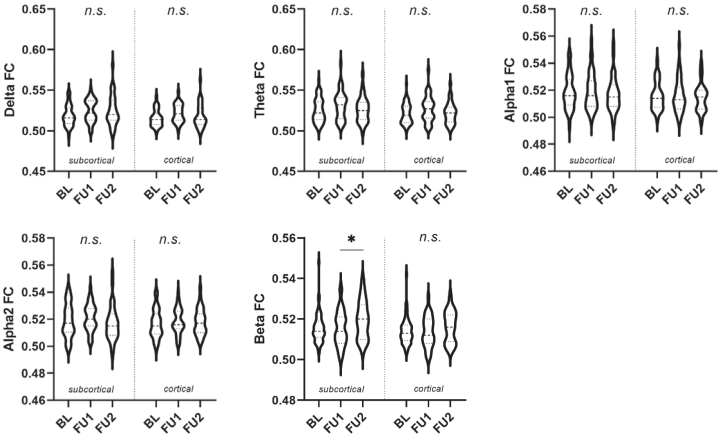

Supplementary Figure 2 Functional connectivity

A) Violin plots summarizing the baseline comparison between three groups; Healthy controls (HC), 'de novo' untreated PD patients, and later stage treated PD patients. Linear mixed models were performed and a significance level of 0.05/6 (Bonferroni correction) was applied.

B) Violin plots summarizing the longitudinal analysis. Statistical testing was performed using linear mixed models with a significance level of 0.05/6.

n.s., non-significant; FU1, follow-up 1; FU2, follow-up 2

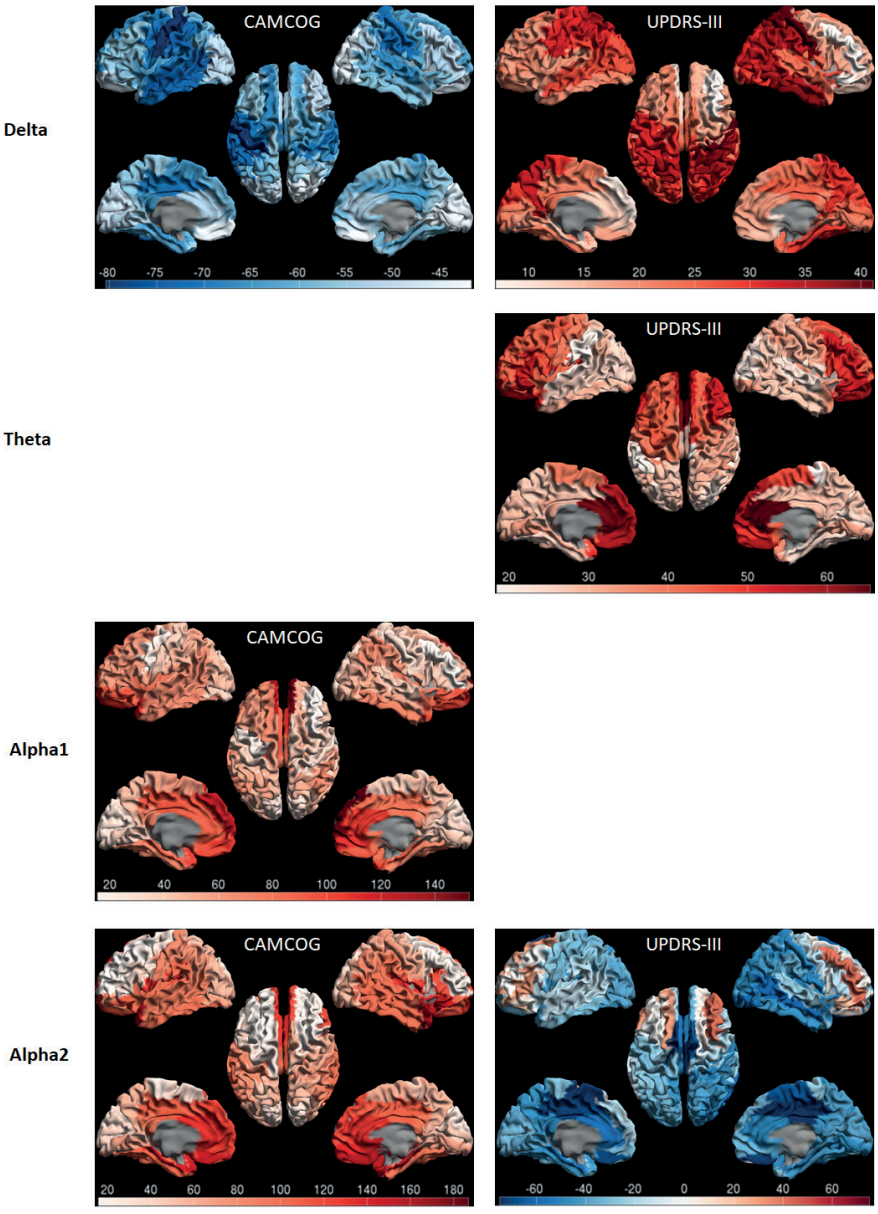

Supplementary Figure 3
Post-hoc analysis analyzing the distribution of longitudinal associations between relative delta-alpha2 band power of the cortical brain regions and CAMCOG (left column) and UPDRS-III (right column). Post-hoc visualization was only performed for the frequency bands that had a significant association with the clinical measure (CAMCOG or UDPRS-III).
Associations are expressed as the estimated regression coefficient and displayed as a color-coded map on a parcellated template brain viewed from, in clockwise order, the left, top, right, right-midline and left-midline

Supplementary Table 3

CAMCOG	Estimated regression coefficients				
AAL region	**Delta**	**Alpha1**	**Alpha2**	**Beta**	**Peak frequency**
79 Hippocampus L	-62.5	66.3	128.7	52.8	3.1
80 Hippocampus R	-60.9	73.2	128.3	54.7	3.3
81 Amygdala L	-67.2	100.0	146.2	49.9	3.0
82 Amygdala R	-67.0	90.8	190.0	46.6	3.3
83 Caudate nucleus L	-65.7	92.3	109.0	44.0	2.5
84 Caudate nucleus R	-64.6	86.9	151.7	45.9	2.8
85 Putamen L	-68.8	80.3	126.0	45.0	2.8
86 Putamen R	-62.4	87.2	156.8	43.3	3.7
87 Pallidum L	-69.4	81.5	143.4	45.0	2.8
88 Pallidum R	-66.9	90.1	186.0	47.2	3.4
89 Thalamus L	-63.9	73.4	125.6	36.2	2.7
90 Thalamus R	-66.7	80.4	150.2	39.7	3.2

UPDRS-III	Estimated regression coefficients		
AAL region	**Theta**	**Beta**	**Peak frequency**
79 Hippocampus L	27.6	-32.7	-2.1
80 Hippocampus R	23.8	-40.9	-1.6
81 Amygdala L	39.5	-32.2	-1.9
82 Amygdala R	29.5	-26.0	-1.8
83 Caudate nucleus L	47.0	-26.0	-1.8
84 Caudate nucleus R	45.2	-27.2	-2.1
85 Putamen L	40.9	-22.9	-2.4
86 Putamen R	35.5	-20.1	-2.4
87 Pallidum L	35.4	-22.5	-2.2
88 Pallidum R	34.7	-20.6	-2.0
89 Thalamus L	30.0	-16.1	-2.3
90 Thalamus R	38.4	-25.2	-2.3

Post-hoc analyses analyzing the distribution of longitudinal associations between relative spectral power (delta-beta band) and peak frequency of the subcortical brain regions with A) CAMCOG B) UPDRS-III. The post-hoc analyses were only performed for the frequency bands that had a significant association with the clinical measure. R/L; right/left

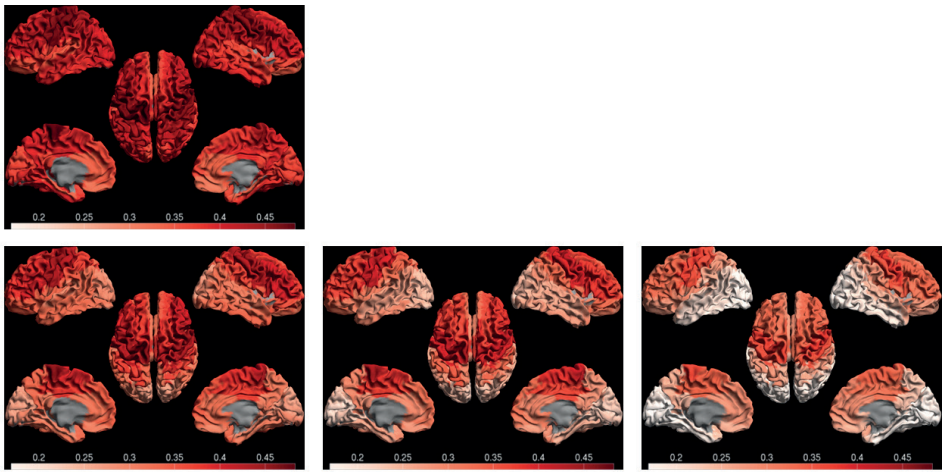

Supplementary Figure 4
Relative beta band power at baseline (healthy controls and PD), follow-up 1 and follow-up 2. Power values are displayed as a color-coded map on a parcellated template brain viewed from, in clockwise order, the left, top, right, right-midline and left-midline. Note that sensorimotor beta power remains largely intact on top of a general cortical slowing, especially at baseline (i.e. compare PD and HC at baseline).

3.2

CHAPTER 4

Changes in resting-state directed connectivity in cortico-subcortical networks correlate with cognitive function in Parkinson's disease

Lennard I Boon, Arjan Hillebrand, Kim TE Olde Dubbelink, Cornelis J Stam, Henk W Berendse

Clinical Neurophysiology 2017:1319-1326
DOI: 10.1016/j.clinph.2017.04.024

Abstract

Objective The pathophysiological mechanisms underlying Parkinson's disease (PD)-related cognitive decline and conversion to PD dementia are poorly understood. In the healthy human brain, stable patterns of posterior-to-anterior cortical information flow have recently been demonstrated in the higher frequency bands using magnetoencephalograpy (MEG). In this study we estimated PD-related changes in information flow patterns, as well as the contribution of subcortical regions.

Methods Resting-state MEG recordings were acquired in moderately advanced PD patients (n=34; mean Hoehn and Yahr-stage 2.5) and healthy controls (n=12). MEG signals were projected to both cortical and subcortical brain regions, following which we estimated the balance between incoming and outgoing information flow per region.

Results In PD patients, compared to controls, preferential beta band information outflow was significantly higher for the basal ganglia and frontotemporal cortical regions, and significantly lower for parieto-occipital regions. In addition, in patients, low preferential information outflow from occipital regions correlated with poor global cognitive performance.

Conclusions In the PD brain, a shift in balance towards more anterior-to-posterior beta band information flow takes place and is associated with poorer cognitive performance.

Significance Our results indicate that a reversal of the physiological posterior-to-anterior information flow may be an important mechanism in PD-related cognitive decline.

Introduction

Parkinson's disease (PD) is a progressive neurodegenerative disorder characterized by prominent motor symptoms, as well as a wide range of non-motor disturbances in early disease stages, among which cognitive dysfunction.[1,2] Over time, dementia develops in up to 75% of PD patients,[3] contributing significantly to an impaired quality of life and putting a heavy burden on caregivers.[4,5] The pathophysiological mechanisms underlying cognitive decline and conversion to PD dementia (PDD) are not well understood. Although there is increasing evidence that neuropathological changes extending beyond the nigrostriatal system are critically involved in cognitive decline, this relationship is not straightforward.[2,6,7] A better understanding of PD-related changes in brain function could help in translating molecular and cellular changes to clinical symptoms.

Normal cognitive function relies on the coordination and integration of neuronal activity in distinct brain regions.[8,9] Functional interactions between brain regions can be derived from the statistical dependencies between spatially distributed time series of neuronal activity obtained using electroencephalography (EEG), magnetoencephalography (MEG) and functional magnetic resonance imaging (fMRI).[10-13] In recent years, the study of spontaneous brain activity in the absence of external stimuli, so-called resting-state brain activity, has contributed enormously to our understanding of human brain function in health and disease.[14] It has been demonstrated that disruptions of resting-state functional connectivity are an important factor in the development of cognitive decline in PD. Resting-state MEG studies have shown pathologically increased cortico-cortical functional connectivity in PD, both in early and late disease stages.[15-17] By contrast, PD-related cognitive decline and dementia are associated with a loss of resting-state functional connectivity, which has most consistently been reported for frontotemporal brain regions.[17-19]

Previous MEG studies have focused on cortico-cortical functional connectivity. However, by building on methodological advances in beamforming,[20-22] MEG signals can be projected onto an atlas-based source space encompassing both cortical and subcortical regions.[23] This enabled us to now explore the contribution of disease-related changes in both cortico-*subcortical*- and cortico-*cortical* interactions to cognitive dysfunction. This is highly important considering the possible contribution of subcortical structures to large-scale functional integration across brain networks in general[24] and, more specifically, the alleged role of the basal ganglia in frontostriatal cognitive deficits in PD patients.[25-27]

Furthermore, while functional connectivity describes the strength of connections between brain regions**,** an evaluation of changes in the directionality of connectivity between brain regions may yield crucial information about the mechanisms underlying cognitive dysfunction. Using a newly developed measure of directed phase transfer entropy (dPTE),[28,29] MEG's excellent temporal resolution now enables us to study macroscopic changes in the direction of preferential information flow. In previous resting-state studies

from our research group in healthy volunteers, stable patterns of posterior-to-anterior information flow were observed in the higher frequency bands (alpha1, alpha2, beta), while an opposite pattern of information flow was found in the theta band.[30,31]

Beta band interactions between posterior and frontal brain regions are considered as general building blocks for cognition as these interactions are involved in decision making and top-down attention, whereas gamma band interactions are considered to be important during bottom-up directed sensorimotor processing.[32] The brain networks underlying these patterns of information flow consist of posteriorly located highly connected regions, the so-called hubs [33,34]. Selective damage to such hubs by a general mechanism called 'hub overload' might be a final common pathway in several neurodegenerative diseases.[35]

In the present study, eyes-closed resting-state MEG data from moderately advanced PD patients and healthy controls were projected to source space, including both cortical and subcortical regions. Subsequently, dPTE was used to characterize differences in the preferential direction of information flow in relationship to clinical measures of disease severity. We hypothesized that, in line with the 'hub overload' theory, posteriorly located hubs would be selectively damaged in PD patients. This may result in a disruption of information flow from these hubs, thereby leading to a reversal of the dominant posterior-to-anterior pattern of information flow in the higher frequency bands in association with lower global cognitive scores.

Methods

Participants

As part of a prospective longitudinal study over a period of 7 years, a cohort of 70 non-demented PD patients (disease duration 0-13 years at baseline) and 21 healthy controls, matched to the *de novo* PD patients in the cohort, was recruited.[16] Participants underwent motor and cognitive assessments, as well as resting-state MEG recordings at baseline, at 4 years and at 7 years after inclusion. MEG data obtained at the first two time points have been analyzed for previous publications,[17,36,37] but this is the first study using MEG data obtained at the third time point and the first study investigating directed connectivity in cortical as well as subcortical regions.

A total of 47 PD patients and 13 controls participated in the second follow-up evaluation, 7 years from baseline. Of the remaining participants, eight PD patients and one control had relatively severe artefacts in the MEG recordings, three PD patients had an MRI that was of poor quality, MEG data for one patient were not available due to technical problems, and clinical data for one patient were incomplete. Therefore, these subjects were excluded from further analysis. This led to a final group of 34 PD patients and 12 healthy controls, which we studied in a cross-sectional analysis.

The research protocol was approved by the medical ethical committee of the VU University Medical Center. Ethics review criteria conformed to the Helsinki declaration. After careful explanation of the procedures, all participants gave written informed consent.

Participant characteristics

Disease duration was calculated on the basis of the patients' estimation of the onset of the classical PD motor symptoms. Unified Parkinson's Disease Rating Scale motor ratings (UPDRS-III)[38] were obtained in the 'ON'-medication state by a trained physician. Global cognitive function was assessed using the CAMbridge COGnitive Examination (CAMCOG).[39] Level of education was determined using the International Standard Classification of Education (ISCED) (UNESCO, 1997).[40] At each follow-up visit, conversion to PDD was assessed according to the clinical criteria recommended by the Movement Disorder Society Task Force [41], in which the Mini Mental State Examination (MMSE) criterion was substituted with a reliable change index (RCI)[42] of the CAMCOG score over time. Both the rationale for this substitution and the calculation of the RCI in this longitudinal cohort have been described previously.[37] The total dose of dopamine replacement therapy was converted to a so-called levodopa equivalent dose (LEDD), as described previously.[36] Levodopa was always used in combination with a peripheral decarboxylase inhibitor. In addition to this, 12 patients used a catechol-O-methyltransferase inhibitor and 22 patients used a dopamine agonist. Rasagiline was used by 2 patients; amantadine, rivastigmine and selegiline were each used by 1 patient.

The sections 'Data acquisition', 'Beamforming' and 'Phase transfer entropy' have been described in detail in a previous publication.[30] We therefore provide the details as Supplementary Material, and summarize the approach below.

Data acquisition

MEG data were recorded using a 306-channel whole-head system (Elekta Neuromag, Oy, Helsinki, Finland) in an eyes-closed resting-state condition for five minutes with a sample frequency of 1250 Hz and online anti-aliasing (410 Hz) and high-pass (0.1 Hz) filters, while subjects were in the 'ON'-medication state. Anatomical images of the head were obtained on a 3.0T whole body MRI scanner (Magnetic Resonance Imaging; GE Signa HDxt, Milwaukee, WI, USA). Patients' MEG data were co-registered to their structural MRIs using a surface-matching procedure, with an estimated resulting accuracy of 4 mm.[43]

Data pre-processing

MEG channels that were malfunctioning, for example due to excessive noise, were removed after visual inspection of the data (KTEOD/LIB, mean number of excluded channels was 6, range: 2-11), after which the temporal extension of Signal Space Separation (tSSS) in MaxFilter software (Elekta Neuromag Oy, version 2.2.15) was applied

to remove artefacts.[44] The automated anatomical labelling (AAL) atlas was used to label the voxels in 78 cortical and 12 subcortical regions of interest (ROIs) in a subject's co-registered MRI.[45,46] Each ROI in the atlas contains many voxels and the number of voxels per ROI differs. In order to obtain a single time-series for a ROI we used each ROI's centroid as representative for that ROI, with the centroid defined here as the voxel within the ROI that is nearest, in terms of Euclidean distance, to all other points in the ROI.[30] An atlas-based beamformer approach[22] sequentially projected sensor signals to source space, i.e. the time-series of neuronal activity were reconstructed for these centroid voxels.

The beamformer approach resulted in broad-band (0.5-48 Hz) time-series for each centroid of the 90 ROIs. Subsequently, twenty artefact free epochs, containing 4096 samples (3.2768 s), were selected per subject (KTEOD/LIB). These time-series were then filtered in six classical EEG/MEG frequency bands (delta (0.5–4 Hz), theta (4–8 Hz), alpha1 (8–10 Hz), alpha2 (10–13 Hz), beta (13–30 Hz), and lower gamma (30–48 Hz)) and analyses of information flow were performed using in-house software (BrainWave, version 0.9.152.1.23; CJS, available from http://home.kpn.nl/stam7883/brainwave.html).

Information flow

The information flow between ROIs was estimated using the Phase Transfer Entropy (PTE), which was introduced by Paluš et al.,[29] reanalyzed by Lobier and colleagues[28] and adjusted by our group (for details see).[30] The PTE was normalized to a scale between 0 and 1, since the PTE does not have a meaningful upper bound.[28] The resulting directed PTE (dPTE) indicates whether information flow is mainly 'incoming' ($0 \leq dPTE < 0.5$) or 'outgoing' ($0.5 < dPTE \leq 1$) for a ROI in relation to another ROI. In case of no preferential direction of information flow: $dPTE = 0.5$.

Statistical analysis

Participant characteristics

Both continuous variables (age and CAMCOG) passed Kolmogorov-Smirnov tests of normality, and group differences between PD patients (N = 34) and healthy controls (N = 12) were evaluated using two-sided *t*-tests. Evaluation of categorical variables (sex distribution and ISCED) was performed by means of chi-square tests.

Information flow

For each subject and frequency band separately, dPTE matrices (90x90) were averaged over 20 epochs. Mean dPTE-values *per ROI*, meaning the average preferential information flow from one region to all other regions, were compared between groups using permutation tests (in-house software, developed for Matlab). Permutation tests do not require an assumption of normality about the reference distribution as this distribution can be derived from any test statistic of the data.[47,48] In this study, group differences were

expressed as *t*-values and permutation tests were performed separately for each of the 90 ROIs in each frequency band (N = 50000; $p < .05$). Furthermore, permutation tests can account for the multiple comparisons problem by using the maximum statistic.[47-50] Instead of the maximum statistic the 'false discovery rate' (FDR) can also be used to control for false positives.[51] For this explorative study we used the FDR-controlling procedure (each restricted to the individual frequency bands; *q*-value 0.05), as it results in higher power as compared to using the maximum statistic, at the cost of a weaker control of the false positive rate.[51,52]

Subsequently, group differences in dPTE-values *for individual connections* between ROIs, meaning the preferential flow of information from one region to another region, were compared by performing permutation tests (N = 50000; $p < .05$) on all individual connections of those ROIs for which the mean dPTE values per ROI were significantly different between PD patients and controls in the first analysis. The number of comparisons was therefore: 32*31/2 + 32*58 = 2352. An FDR correction for multiple comparisons took place for these post-hoc analyses.

Relationship between information flow and clinical measures of disease severity

Within the group of PD patients (N = 34) the relations between mean dPTE values for a group of selected ROIs (see below) and clinical measures of disease severity (UPDRS-III and CAMCOG) were analyzed using linear regression models. The use of parametric regression models was justified by normality of the standardized residuals of the dependent variables (measures of disease severity) and linearity of the dPTE values with the dependent variables. In order to reduce the number of possible regressions, we selected anatomically adjacent ROIs (see Results section for details). Mean dPTE values for these combined regions were averaged for each subject. The obtained dPTE values were used as independent variables in separate linear regression models, in which either UPDRS-III (measure of motor disease severity) or CAMCOG (measure of global cognitive function) were treated as dependent variables. Sex, age and LEDD (dichotomized) were added as covariates in all analyses, as was level of education (ISCED) in the CAMCOG regression models.[53,54,55]

Statistics on participant characteristics and linear regression analyses were performed at a significance level of 5% (two-tailed) using the IBM SPSS Statistics 20.0 software package (IBM Corporation, New York, U.S.A.).

Table 1 Participant characteristics

	Healthy controls (n=12)	PD Patients (n=34)	Statistic	*P*-value
Sex (M/F)	8/4	19/15	X^2 (1, 46) = 0.425	.514
Age (years)	66.8 (9.39)	68.6 (6.15)	t(44) = -.736	.465
ISCED (1-2 / 3-4 / 5-6)	1/2/9	12/12/10	X^2 (2, 46) = 7.76	.019
CAMCOG	99.0 (2.9)	91.4 (13.9)	t(44) = 4.24	<.001
UPDRS-III "ON"	n/a	33.8 (9.02)	n/a	n/a
Disease duration	n/a	11.85 (3.8)	n/a	n/a
Hoehn and Yahr-score "ON" (0 / 1 / 2 / 2.5 / 3 / 4 / 5)	n/a	0/0/13/10/10/1/0	n/a	n/a
LEDD total dose (mg)	n/a	1108 (549)	n/a	n/a

Values are expressed as mean (SD), unless otherwise specified.
PD, Parkinson's disease; M/F, male/female; ISCED, International Standard Classification of Education; CAMCOG, CAMbridge COGnitive examination; UPDRS-III, Unified Parkinson's Disease Rating Scale motor ratings; LEDD, Levodopa Equivalent Daily Dose; n/a, non-applicable

Results

Participant characteristics

Participant characteristics are summarized in Table 1. There were no significant differences in age or sex distribution. Mean disease duration was 11.85 years and mean Hoehn and Yahr-stage in the 'ON'-medication state was 2.5 for the PD group. PD patients had a significantly lower level of education and scored significantly lower on the CAMCOG than controls. Six PD patients fulfilled clinical diagnostic criteria for PDD.[37]

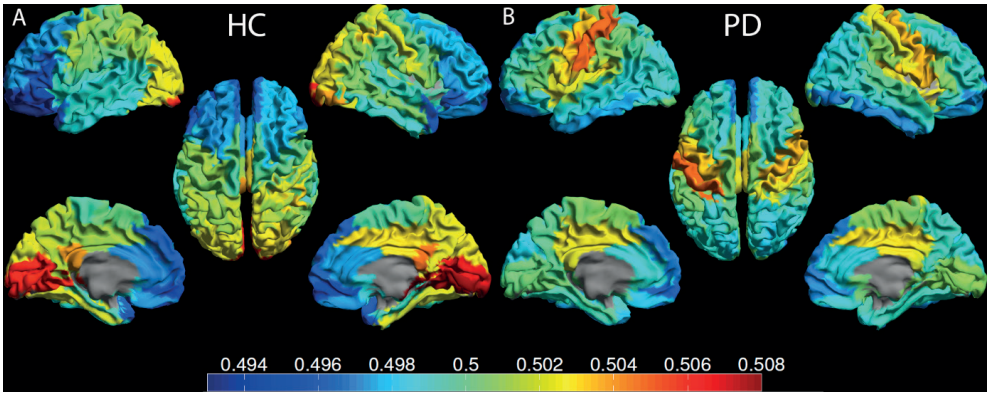

Figure 1 Distribution of beta band mean dPTE values
dPTE values for each region of interest (ROI) are displayed as a color-coded map on a parcellated template brain viewed from, in clockwise order, the left, top, right, right-midline and left-midline.
Panel a depicts the healthy control (HC) group and panel b depicts the Parkinson's Disease (PD) group. Hot and cold colors indicate preferential information outflow and inflow, respectively. For visualization purposes, preferential information flow for only the 78 cortical brain regions is shown.
Note the pattern of preferential information outflow from posterior brain regions in the controls, whereas in PD the pattern of preferential information flow is dominated by outflow from pre- and postcentral gyri.

Information flow

Before any statistics had been performed, convincing differences between PD patients and healthy subjects in beta band information outflow were already manifest. Fig. 1 displays the mean dPTE values for each cortical ROI in the beta band. In controls, a global pattern of preferential information outflow from posterior brain regions was seen, whereas in PD patients this pattern was absent. Instead, the pattern of preferential cortical information flow in PD patients was dominated by outflow from pre- and postcentral gyri.

To assess group differences in preferential information outflow *per ROI,* permutation tests with false discovery rate (FDR) correction were performed for the 90 ROIs in six frequency bands. Significant differences were found in the beta band for 32 ROIs, as listed in Supplementary Table 1 and visualized in Fig. 2: As compared to controls, in PD patients preferential information outflow was significantly higher for 16 frontotemporal and subcortical ROIs and preferential information outflow was significantly lower for 16 parieto-occipital ROIs. The latter differences seemed to be most conspicuous in the right hemisphere. However, the observed asymmetry was not associated with a lateralization in the degree of motor symptoms (Supplementary Table 2). In the PD patients, 17 of the 32 ROIs that displayed significant group differences in the beta band changed roles and 'flipped' from being a relative 'sender' to being a relative 'receiver' of information and vice versa (Supplementary Table 1). The 16 ROIs in which we found significantly lower preferential information outflow in PD patients included the right precuneus and the right posterior cingulate gyrus, both considered as functional hubs in the default mode network (DMN). No significant group differences in mean dPTE values were found in the delta, theta, alpha1, alpha2 or gamma band. Therefore, further analyses were performed in the beta band only.

In order to determine which *individual connections* contributed most to the differences in preferential beta band information flow, a post-hoc analysis with FDR-correction was performed on the dPTE values of all individual connections of those ROIs that had shown significantly different mean dPTE values between the groups. Of the significantly different individual connections ($p < .05$; $t > 1.99$, after correction for multiple comparisons $t > 2.60$) only those with the most significant differences ($t > 4.17$) are depicted in Fig. 2. The latter threshold was set for visualization purposes, as a lower threshold would lead to an unclear figure. All of the connections that reached this latter threshold were between the 32 ROIs that had shown significantly different mean dPTE values (except for a single connection linked to the (non-significant) right middle temporal gyrus), and seemed to be particularly prevalent in the right parieto-occipital regions.

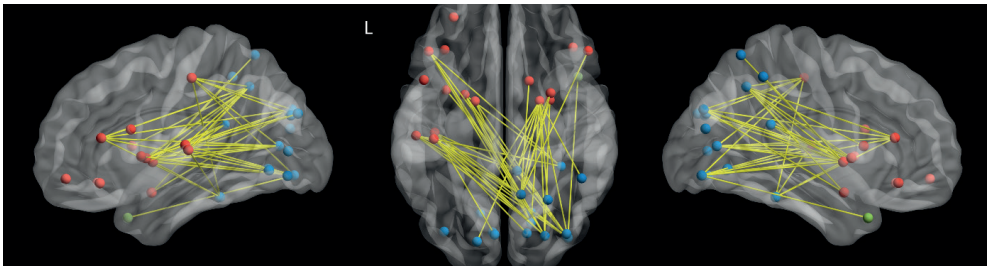

Figure 2 Significant differences in information flow between Parkinson's disease (PD) patients and healthy controls (HC)
Nodes represent brain regions, where the colors indicate significantly higher (red), significantly lower (blue) or no significant difference (green) in preferential information flow (mean dPTE) in patients relative to the control group. Left lateral (left panel), top (middle panel) and right lateral (right panel) views of a template brain are shown [56]. Names of the relevant brain regions are displayed in Supplementary Figure 1.
Note that compared to the healthy controls, in PD the frontotemporal and subcortical regions consistently display a significantly higher preferential information outflow, while the parieto-occipital regions show a significantly lower preferential information outflow. The latter is most pronounced for the right hemisphere.

Significantly different individual connections between ROIs are displayed in yellow (threshold: t = 2.60). For visualization purposes, only links with an absolute t-value larger than 4.17 are shown. Note that all but one connection are between ROIs that had shown significantly different mean dPTE values between the groups in the first analysis. Furthermore, the parieto-occipital regions displayed a right-sided dominance in differences in individual connections.

Relationship between information flow and clinical measures of disease severity

To evaluate the relationship between beta band directed connectivity and clinical measures of disease severity, we created four linear regression models in the PD group. Dependent variables were CAMCOG (measure of global cognitive function) and UPDRS-III scores (measure of motor function). Independent variables were the mean dPTE-values for two groups of anatomically adjacent ROIs. The first group included a selection of the ROIs that had shown significantly higher preferential information outflow in PD and consisted of the bilateral basal ganglia (caudate nucleus, putamen and globus pallidus). The second group comprised a selection of ROIs that had shown significantly lower preferential information outflow in PD and consisted of the bilateral occipital ROIs, i.e. the superior/middle/inferior occipital gyrus, calcarine area, cuneus, lingual gyrus and fusiform gyrus.

The results of the linear regression analyses are summarized in Table 2. We observed a significant correlation between low mean occipital dPTE values and decreased CAMCOG scores. No significant correlation was found between mean bilateral basal ganglia dPTE values and CAMCOG, nor between UPDRS-III scores and mean dPTE values for occipital cortical ROIs or the bilateral basal ganglia.

Table 2 Correlations between clinical measures of disease severity and beta band dPTE values

Brain regions	Clinical measures of disease severity	
	CAMCOG	**UPDRS-III**
Occipital*	***β*= .429, t(29) = 2.31, *p*= .029**	*β*= -.230, t(30) = -1.216 *p*= .234
Basal ganglia**	*β*= .139 t(29) = .731, *p*= .471	*β*= .019, t(30) = .102, *p*= .919

CAMCOG, Cambridge Cognitive Examination; UPDRS-III, Unified Parkinson's Disease Rating Scale motor ratings
* Superior/middle/inferior occipital gyrus, calcarine area, cuneus, lingual gyrus and fusiform gyrus (all bilateral)
** Caudate nucleus, putamen, globus pallidus (bilateral)

Beta coefficients are standardized to facilitate the interpretation

Discussion

In the present resting-state MEG study, we found robust changes in the preferential direction of beta band information flow in PD patients relative to healthy controls. In the patient group, preferential information outflow was significantly higher for basal ganglia and frontotemporal regions and significantly lower for parieto-occipital regions. In addition, the individual connections with the most prominent group differences were the connections between these same basal ganglia-frontotemporal and parieto-occipital brain regions. This underlines that an actual reversal in the physiological back-to-front information flow pattern may be present. Moreover, in patients low preferential information outflow from occipital cortical regions correlated with poor global cognitive performance.

Previous analyses of MEG data in PD, both in the current[16,17] and in another cohort,[18,19] focused on the *strength* of cortico-cortical functional connectivity. In the present study we assessed *directionality* of connectivity, or rather, preferential information flow. In addition, extension of beamforming to subcortical brain regions enabled us to also study cortico-subcortical interactions. Theoretical, simulation and experimental studies have demonstrated the beamformer's ability to project sensor-space data to deeper brain structures,[23,57-59] in spite of the reduction in signal-to-noise ratio (SNR) with depth.[60] Prior application of the dPTE in healthy subjects by our research group revealed a dominant posterior-to-anterior cortico-cortical flow of information in, among others, the beta band.[30] In the present study, we reproduced these observations in a different group of healthy controls and, more importantly, for the first time demonstrated a strong tendency towards anterior-to-posterior and basal ganglia-to-posterior patterns of preferential beta band information flow in PD patients. Moreover, 17 of the 32 ROIs that displayed significant group differences in the beta band changed roles from being a relative 'sender' to being a relative 'receiver' of information or vice versa.

The observed lower preferential information outflow from parieto-occipital brain regions is in accordance with electrophysiological, fMRI- and PET-studies that have revealed decreases in alpha rhythm peak frequency,[36] beta band power,[37,61] functional connectivity[62] and metabolic activity[63] in posterior cortical brain regions of PD patients,

predicting conversion to PDD. These results are paralleled by longitudinal clinical studies involving neuropsychological assessments, in which progression to PDD could be predicted by cognitive deficits that are assumed to have a posterior cortical basis.[64,65] From these studies, conversion to PDD would appear to be related to the addition of 'posterior cortical type' cognitive deficits on top of initial dopamine-related *frontostriatal* executive impairments.[27] Based on our observation that lower preferential beta band information outflow from the occipital cortex correlates with lower global cognitive scores, it is tempting to suggest that a reduction in occipital beta band information outflow may underlie this *posterior cortical syndrome.*[66] Analysis of longitudinal data is necessary to further substantiate the hypothesized role of changes in directed information flow in the conversion of PD to PDD and dementia risk profiling.

At present, our knowledge of the specific function of beta band oscillations in the posterior cortex is limited.[67] One proposed function is the organization of top-down (endogenously generated) attention. Therefore, preserved cognitive function has been linked to the integrity of top-down attention in the beta band.[32] Previous studies have consistently demonstrated beta-band interactions between posterior and frontal cortical regions during top-down attention. However, some studies indicate that posteriorly located brain regions 'drive' anteriorly located brain regions in top-down attention,[68] whereas other studies suggest the opposite pattern.[69]

At a network level, posterior-to-anterior information flow in the higher frequency bands might result from important functional hubs being located in the posterior parts of the brain, of which the posterior DMN is a well-known example.[70] A recent study in the mouse brain has revealed that hub regions have more distributional rather than integrational connections,[71] thereby providing a network basis for the long-range back-to-front pattern of information flow.[30] We observed a strong preferential beta band information outflow from important posterior hubs in healthy controls, which disappeared in PD patients in DMN hubs: the right precuneus and the right posterior cingulate gyrus (see Results section). This is in line with the theory that hub nodes are particularly vulnerable to damage in multiple (neurodegenerative) brain diseases, referred to as the 'hub overload' theory.[35] Therefore, one could speculate that the lower preferential information outflow from posteriorly located hubs in PD leads to a loss of top-down attention and thus might be a mechanism underlying cognitive decline in PD.

In our study, as the normalized measure dPTE represents the *relative* flow of information, we cannot determine with certainty whether the lower parieto-occipital information outflow in PD patients is a primary change or the direct consequence of increased inflow from the basal ganglia and frontotemporal regions. However, bearing in mind the PD-related posterior cortical changes that have been reported previously in other studies, we consider the lower information outflow from the parieto-occipital regions to be the most likely primary change. An open question remains whether the higher

preferential fronto-temporal- and basal ganglia information outflow plays any additional role in the pathophysiology of cognitive decline in PD or merely represents a secondary phenomenon, induced by the reduction in parieto-occipital information outflow. The surprising finding that preferential basal ganglia outflow did not correlate with motor disease severity could be taken as an argument supporting the assumption that the higher preferential basal ganglia outflow we observed is a secondary phenomenon. Future analysis of longitudinal data, including early disease stages, is necessary to reveal the primary changes in directed information flow in PD. In addition, the interplay between the basal ganglia and the posterior cortex could be further explored by studying interactions between multiple layers of functional networks, organized as multiplex networks.[72] This type of approach can be used to study cross-frequency relationships, i.e. the information flow across different frequency bands, which in the case of PD could reveal the relationship between subcortical dominant beta rhythms and the cortically dominant alpha rhythm.[28,73]

Interestingly, the decrease in parieto-occipital information outflow was asymmetrical and more conspicuous in the right hemisphere. Although we have not found an explanation for this observation (Supplementary Table 2), the observation is in line with the results of metabolic imaging studies in which the right-hemisphere circuitry was more affected in PD, for example in patients suffering from freezing of gait.[74,75]

In parallel with the lower parieto-occipital preferential information outflow, we confirmed the presence of significantly lower parieto-occipital beta band power in PD patients (Supplementary Fig. 2 and reported previously).[17] Since lower band power may lead to changes in SNR, we cannot fully rule out a role for SNR variations in the observed differences in information flow. However, since the higher relative theta band power we observed in PD patients (Supplementary Fig. 2) was *not* accompanied by significantly higher dPTE values in the theta band, it is unlikely that SNR differences constitute the sole explanation for our results. Moreover, dPTE is a phase-based measure and should therefore be relatively insensitive to band power differences.[28,30,76]

A number of potential limitations of our study deserve consideration. First, seven patients (10% of the initial cohort) withdrew from the study because increasing disease-related impairments prevented them from further participation. However, as they were clinically more severely affected their drop-out can only have led to an underestimation of true disease effects. Second, despite matching at baseline, the controls in our study scored higher on 'level of education'. Therefore, we corrected for the difference in 'level of education' by adding this as a covariate to the linear regression models involving the CAMCOG scores. Third, the PD patients in our study were on dopaminergic medication and had their MEG registrations and clinical assessments in the ON state. Electrophysiological studies indicate that levodopa administration can have effects on functional connectivity measures,[77] although effects on the preferential direction of information flow have not

been studied so far. Either way, since we added LEDD as a covariate in all linear regression models we expect that the influence of dopaminergic medication on the correlation between preferential information outflow and clinical measures of disease severity can only have been minimal. Fourth, no correction for multiple testing was performed for the four linear regression models on the relationship between preferential information flow and clinical parameters of disease severity, since the low number of observations in our regression models (n = 34) provided us with a low statistical power. Therefore, any significant correlation we found in our regression models must be based on an inherently strong correlation. A correction for multiple testing would make the occurrence of false-negatives in this situation very likely. In addition, the wide range of CAMCOG values (range 61-103) we have observed in the PD group of our study stresses the clinical relevance of the significant correlation between information flow from posterior brain regions and CAMCOG scores.

Major strengths of our study are the use of a novel measure of phase transfer entropy to assess differences in the preferential direction of information flow in the PD brain, as well as incorporating cortico-subcortical electrophysiological interactions, in addition to cortico-cortical interactions.

In conclusion, we found robust changes in the preferential direction of beta band information flow in PD patients, involving both cortical and subcortical regions. Compared to healthy subjects, preferential beta band information outflow was higher in frontotemporal and subcortical brain regions, whilst it was lower in parieto-occipital brain regions. Moreover, reduced preferential information outflow from occipital cortical regions correlated with poor global cognitive performance in PD patients. Our observations suggest that cognitive decline in PD is characterized by a primary posterior cortical dysfunction that has secondary effects on preferential fronto-temporal- and basal ganglia information outflow.

Acknowledgements

We would like to thank all patients and controls for their participation. We would also like to thank Karin D van Dijk, MD PhD, for her help in clinical (UPDRS-III) testing. We thank Ndedi Sijsma, Irene Ris-Hilgersom, Karin Plugge, Marlous van den Hoek, Nico Akemann and Peter-Jan Ris for the MEG acquisitions. We thank Victor Strijbis and Bob van Dijk, PhD, for their preliminary analysis on a different group of PD patients. Finally, we thank Jos WR Twisk, PhD and Meichen Yu, MSc for their advice on statistical issues.

References

1. Chaudhuri KR, Healy DG, Schapira AH. Non-motor symptoms of Parkinson's disease: diagnosis and management. Lancet Neurol. 2006;5(3):235-45.
2. Dickson DW, Fujishiro H, Orr C, et al. Neuropathology of non-motor features of Parkinson disease. Parkinsonism Relat Disord. 2009;15 Suppl 3:S1-5.
3. Aarsland D, Kurz MW. The epidemiology of dementia associated with Parkinson's disease. Brain pathol (Zurich, Switzerland). 2010;20(3):633-9.
4. Aarsland D, Larsen JP, Karlsen K, et al. Mental symptoms in Parkinson's disease are important contributors to caregiver distress. Int J Geriatr Psychiatry. 1999;14(10):866-74.
5. Schrag A, Hovris A, Morley D, et al. Caregiver-burden in parkinson's disease is closely associated with psychiatric symptoms, falls, and disability. Parkinsonism Relat Disord. 2006;12(1):35-41.
6. Braak H, Rub U, Gai WP, et al. Idiopathic Parkinson's disease: possible routes by which vulnerable neuronal types may be subject to neuroinvasion by an unknown pathogen. J Neural Transm (Vienna). 2003;110(5):517-36.
7. Lim SY, Fox SH, Lang AE. Overview of the extranigral aspects of Parkinson disease. Arch Neurol. 2009;66(2):167-72.
8. Schnitzler A, Gross J. Normal and pathological oscillatory communication in the brain. Nat Rev Neurosci. 2005;6(4):285-96.
9. Bullmore E, Sporns O. The economy of brain network organization. Nat Rev Neurosci. 2012;13(5):336-49.
10. Varela F, Lachaux JP, Rodriguez E, et al. The brainweb: phase synchronization and large-scale integration. Nat Rev Neurosci. 2001;2(4):229-39.
11. Fries P. A mechanism for cognitive dynamics: neuronal communication through neuronal coherence. Trends Cogn Sci. 2005;9(10):474-80.
12. Friston KJ. Functional and effective connectivity: a review. Brain Connect. 2011;1(1):13-36.
13. Kelso JA, Dumas G, Tognoli E. Outline of a general theory of behavior and brain coordination. Neural Netw. 2013;37:120-31.
14. Fox MD, Greicius M. Clinical applications of resting state functional connectivity. Front Syst Neurosci. 2010;4:19.
15. Silberstein P, Pogosyan A, Kuhn AA, et al. Cortico-cortical coupling in Parkinson's disease and its modulation by therapy. Brain. 2005;128(Pt 6):1277-91.
16. Stoffers D, Bosboom JL, Deijen JB, et al. Increased cortico-cortical functional connectivity in early-stage Parkinson's disease: an MEG study. Neuroimage. 2008;41(2):212-22.
17. Olde Dubbelink KT, Stoffers D, Deijen JB, et al. Resting-state functional connectivity as a marker of disease progression in Parkinson's disease: A longitudinal MEG study. Neuroimage Clin. 2013;2:612-9.
18. Bosboom JL, Stoffers D, Wolters E, et al. MEG resting state functional connectivity in Parkinson's disease related dementia. J Neural Transm (Vienna). 2009;116(2):193-202.
19. Ponsen MM, Stam CJ, Bosboom JL, et al. A three dimensional anatomical view of oscillatory resting-state activity and functional connectivity in Parkinson's disease related dementia: An MEG study using atlas-based beamforming. Neuroimage Clin. 2012;2:95-102.
20. Hillebrand A, Singh KD, Holliday IE, et al. A new approach to neuroimaging with magnetoencephalography. Hum Brain Mapp. 2005;25(2):199-211.
21. Hillebrand A, Barnes GR. Beamformer analysis of MEG data. Int Rev Neurobiol. 2005;68:149-71.
22. Hillebrand A, Barnes GR, Bosboom JL, et al. Frequency-dependent functional connectivity within resting-state networks: an atlas-based MEG beamformer solution. Neuroimage. 2012;59(4):3909-21.

23. Hillebrand A, Nissen IA, Ris-Hilgersom I, et al. Detecting epileptiform activity from deeper brain regions in spatially filtered MEG data. Clin Neurophysiol. 2016;127(8):2766-9.
24. Bell PT, Shine JM. Subcortical contributions to large-scale network communication. Neurosci Biobehav Rev. 2016;71:313-22.
25. Owen AM, Doyon J, Dagher A, et al. Abnormal basal ganglia outflow in Parkinson's disease identified with PET. Implications for higher cortical functions. Brain. 1998;121 (Pt 5):949-65.
26. Owen AM, James M, Leigh PN, et al. Fronto-striatal cognitive deficits at different stages of Parkinson's disease. Brain. 1992;115 (Pt 6):1727-51.
27. Pagonabarraga J, Kulisevsky J, Llebaria G, et al. Parkinson's disease-cognitive rating scale: a new cognitive scale specific for Parkinson's disease. Mov Disord. 2008;23(7):998-1005.
28. Lobier M, Siebenhuhner F, Palva S, et al. Phase transfer entropy: a novel phase-based measure for directed connectivity in networks coupled by oscillatory interactions. Neuroimage. 2014;85 Pt 2:853-72.
29. Palus M, Vejmelka M. Directionality of coupling from bivariate time series: how to avoid false causalities and missed connections. Phys Rev E Stat Nonlin Soft Matter Phys. 2007;75(5 Pt 2):056211.
30. Hillebrand A, Tewarie P, van Dellen E, et al. Direction of information flow in large-scale resting-state networks is frequency-dependent. Proc Natl Acad Sci U S A. 2016;113(14):3867-72.
31. Dauwan M, van Dellen E, van Boxtel L, et al. EEG-directed connectivity from posterior brain regions is decreased in dementia with Lewy bodies: a comparison with Alzheimer's disease and controls. Neurobiol Aging. 2016;41:122-9.
32. Siegel M, Donner TH, Engel AK. Spectral fingerprints of large-scale neuronal interactions. Nat Rev Neurosci. 2012;13(2):121-34.
33. Buckner RL, Andrews-Hanna JR, Schacter DL. The brain's default network: anatomy, function, and relevance to disease. Ann N Y Acad Sci. 2008;1124:1-38.
34. Tomasi D, Volkow ND. Association between functional connectivity hubs and brain networks. Cereb Cortex. 2011;21(9):2003-13.
35. Stam CJ. Modern network science of neurological disorders. Nat Rev Neurosci. 2014;15(10):683-95.
36. Olde Dubbelink KT, Stoffers D, Deijen JB, et al. Cognitive decline in Parkinson's disease is associated with slowing of resting-state brain activity: a longitudinal study. Neurobiol Aging. 2013;34(2):408-18.
37. Olde Dubbelink KT, Hillebrand A, Twisk JW, et al. Predicting dementia in Parkinson disease by combining neurophysiologic and cognitive markers. Neurology. 2014;82(3):263-70.
38. Fahn, Elton, Committee. amotUD. The Unified Parkinson's Disease Rating Scale. Recent Developments in Parkinson's Disease. 2 ed Florham Park, NY:Macmillan Healthcare Information. 1987;1987:153-163.
39. Roth M, Tym E, Mountjoy CQ, et al. CAMDEX. A standardised instrument for the diagnosis of mental disorder in the elderly with special reference to the early detection of dementia. Br J Psychiatry. 1986;149:698-709.
40. UNESCO. International Standard Classification of Education 1997.: In. Montreal: UNESCO Institute of Statistics.
41. Dubois B, Burn D, Goetz C, et al. Diagnostic procedures for Parkinson's disease dementia: recommendations from the movement disorder society task force. Mov Disord. 2007;22(16):2314-24.
42. Jacobson NS, Truax P. Clinical significance: a statistical approach to defining meaningful change in psychotherapy research. J Consult Clin Psychol. 1991;59(1):12-9.
43. Whalen C, Maclin EL, Fabiani M, et al. Validation of a method for coregistering scalp recording locations with 3D structural MR images. Hum Brain Mapp. 2008;29(11):1288-301.

44. Taulu S, Hari R. Removal of magnetoencephalographic artifacts with temporal signal-space separation: demonstration with single-trial auditory-evoked responses. Hum Brain Mapp. 2009;30(5):1524-34.
45. Tzourio-Mazoyer N, Landeau B, Papathanassiou D, et al. Automated anatomical labeling of activations in SPM using a macroscopic anatomical parcellation of the MNI MRI single-subject brain. Neuroimage. 2002;15(1):273-89.
46. Gong G, He Y, Concha L, et al. Mapping anatomical connectivity patterns of human cerebral cortex using in vivo diffusion tensor imaging tractography. Cereb Cortex. 2009;19(3):524-36.
47. Nichols TE, Holmes AP. Nonparametric permutation tests for functional neuroimaging: a primer with examples. Hum Brain Mapp. 2002;15(1):1-25.
48. Maris E, Oostenveld R. Nonparametric statistical testing of EEG- and MEG-data. J Neurosci Methods. 2007;164(1):177-90.
49. Singh KD, Barnes GR, Hillebrand A. Group imaging of task-related changes in cortical synchronisation using nonparametric permutation testing. Neuroimage. 2003;19(4):1589-601.
50. Chau W, McIntosh AR, Robinson SE, et al. Improving permutation test power for group analysis of spatially filtered MEG data. Neuroimage. 2004;23(3):983-96.
51. Benjamini Y, Hochberg Y. Controlling the False Discovery Rate: A Practical and Powerful Approach to Multiple Testing. J R Stat Soc Series B Stat Methodol1995;57(1):289-300.
52. Lage-Castellanos A, Martinez-Montes E, Hernandez-Cabrera JA, et al. False discovery rate and permutation test: an evaluation in ERP data analysis. Stat Med. 2010;29(1):63-74.
53. Huppert FA, Brayne C, Gill C, et al. CAMCOG--a concise neuropsychological test to assist dementia diagnosis: socio-demographic determinants in an elderly population sample. Br J Clin Psychol. 1995;34 (Pt 4):529-41.
54. Haaxma CA, Bloem BR, Borm GF, et al. Gender differences in Parkinson's disease. J Neurol Neurosurg Psychiatry. 2007;78(8):819-24.
55. Taravari A, Medziti F, Grunevska B, et al. Correlation of age and severity of clinical manifestation assessed by UPDRS in patients with idiopathic Parkinson's disease. Med Arch. 2014;68(1):44-6.
56. Xia M, Wang J, He Y. BrainNet Viewer: a network visualization tool for human brain connectomics. PLoS One. 2013;8(7):e68910.
57. Mills T, Lalancette M, Moses S, et al. Techniques for Detection and Localization of Weak Hippocampal and Medial Frontal Sources Using Beamformers in MEG. Brain Topogr. 2012;25(3):248-63.
58. Quraan MA, Moses SN, Hung Y, et al. Detection and localization of hippocampal activity using beamformers with MEG: a detailed investigation using simulations and empirical data. Hum Brain Mapp. 2011;32(5):812-27.
59. Tenney JR, Fujiwara H, Horn PS, et al. Focal corticothalamic sources during generalized absence seizures: A MEG study. Epilepsy Res. 2013;106(1–2):113-22.
60. Hillebrand A, Barnes GR. A quantitative assessment of the sensitivity of whole-head MEG to activity in the adult human cortex. Neuroimage. 2002;16(3 Pt 1):638-50.
61. Klassen BT, Hentz JG, Shill HA, et al. Quantitative EEG as a predictive biomarker for Parkinson disease dementia. Neurology. 2011;77(2):118-24.
62. Olde Dubbelink KT, Schoonheim MM, Deijen JB, et al. Functional connectivity and cognitive decline over 3 years in Parkinson disease. Neurology. 2014;83(22):2046-53.
63. Bohnen NI, Koeppe RA, Minoshima S, et al. Cerebral glucose metabolic features of Parkinson disease and incident dementia: longitudinal study. J Nucl Med. 2011;52(6):848-55.
64. Williams-Gray CH, Evans JR, Goris A, et al. The distinct cognitive syndromes of Parkinson's disease: 5 year follow-up of the CamPaIGN cohort. Brain. 2009;132(Pt 11):2958-69.
65. Kehagia AA, Barker RA, Robbins TW. Neuropsychological and clinical heterogeneity of cognitive impairment and dementia in patients with Parkinson's disease. Lancet Neurol. 2010;9(12):1200-13.

66. Kehagia AA, Barker RA, Robbins TW. Cognitive impairment in Parkinson's disease: the dual syndrome hypothesis. Neurodegener Dis. 2013;11(2):79-92.
67. Engel AK, Fries P. Beta-band oscillations--signalling the status quo? Curr Opin Neurobiol. 2010;20(2):156-65.
68. Saalmann YB, Pigarev IN, Vidyasagar TR. Neural mechanisms of visual attention: how top-down feedback highlights relevant locations. Science. 2007;316(5831):1612-5.
69. Buschman TJ, Miller EK. Top-down versus bottom-up control of attention in the prefrontal and posterior parietal cortices. Science. 2007;315(5820):1860-2.
70. Raichle ME, Snyder AZ. A default mode of brain function: a brief history of an evolving idea. Neuroimage. 2007;37(4):1083-90; discussion 97-9.
71. Henriksen S, Pang R, Wronkiewicz M. A simple generative model of the mouse mesoscale connectome. eLife 2016;5:e12366.
72. Akam T, Kullmann DM. Oscillatory multiplexing of population codes for selective communication in the mammalian brain. Nat Rev Neurosci. 2014;15(2):111-22.
73. Hohlefeld FU, Ehlen F, Tiedt HO, et al. Correlation between cortical and subcortical neural dynamics on multiple time scales in Parkinson's disease. Neuroscience. 2015;298:145-60.
74. Bartels AL, de Jong BM, Giladi N, et al. Striatal dopa and glucose metabolism in PD patients with freezing of gait. Mov Disord. 2006;21(9):1326-32.
75. Bartels AL, Leenders KL. Brain imaging in patients with freezing of gait. Mov Disord. 2008;23 Suppl 2:S461-7.
76. Muthukumaraswamy SD, Singh KD. A cautionary note on the interpretation of phase-locking estimates with concurrent changes in power. Clin Neurophysiol. 2011;122(11):2324-5.
77. Stoffers D, Bosboom JL, Wolters E, et al. Dopaminergic modulation of cortico-cortical functional connectivity in Parkinson's disease: an MEG study. Exp Neurol. 2008;213(1):191-5.

Supplementary materials

For details of sections 'Data acquisition', 'Beamforming' and 'Phase transfer entropy', we refer the reader to DOI: *10.1016/j.clinph.2017.04.024* or the original article by Hillebrand et al. [2016].

Supplementary Table 1 Significant differences in beta band dPTE values per region of interest

a. dPTE of PD patients > dPTE of healthy controls
Regions with an * 'flipped' from being a relative 'receiver'- to being a relative 'sender' of information
The sixth column represents the (raw) p-values obtained using permutation tests based on 50000 reassignments. The last column represents the FDR-corrected p-values, in which the p-values are corrected for 90 comparisons.
L, left; R, right; AAL, Automated Anatomical Labelling; PD, Parkinson's disease; HC, healthy control

b. dPTE of healthy controls > dPTE of PD patients
Regions with an * 'flipped' from being a relative 'sender'- to being a relative 'receiver' of information

a) Anatomical region	L/R	AAL atlas abbreviations	dPTE (PD)	dPTE (HC)	*P-value*	*FDR corrected p-value*
Middle frontal gyrus, orbital part	L	ORBmid.L	0.498	0.494	0.0136	0.0408
Inferior frontal gyrus, orbital part	L	ORBinf.L	0.499	0.495	0.0118	0.0366
Inferior frontal gyrus, opercular part*	L	IFGoperc.L	0.503	0.499	0.0114	0.0365
Inferior frontal gyrus, triangular part*	L	IFGtriang.L	0.501	0.496	0.0013	0.0178
Postcentral gyrus	L	PoCG.L	0.505	0.501	0.0013	0.0178
Heschl's gyrus	L	HES.L	0.503	0.500	0.0048	0.0276
Superior temporal gyrus*	L	STG.L	0.502	0.499	0.0111	0.0365
Insula	L	INS.L	0.503	0.500	0.0053	0.0277
Inferior frontal gyrus, orbital part	R	ORBinf.R	0.499	0.497	0.0147	0.0420
Inferior frontal gyrus, triangular part*	R	IFGtriang.R	0.501	0.498	0.0020	0.0180
Amygdala*	R	AMYG.R	0.501	0.498	0.0035	0.0241
Caudate nucleus	R	CAU.R	0.502	0.500	0.0069	0.0311
Lenticular nucleus, putamen*	L	PUT.L	0.503	0.499	7.2e-4	0.0166
Lenticular nucleus, putamen	R	PUT.R	0.504	0.500	0.0019	0.0180
Lenticular nucleus, pallidum	L	PAL.L	0.503	0.500	0.0049	0.0276
Lenticular nucleus, pallidum*	R	PAL.R	0.504	0.499	2.0e-5	0.0018

b) Anatomical region	L/R	AAL atlas abbreviations	dPTE (HC)	dPTE (PD)	*P-value*	*FDR corrected p-value*
Superior occipital gyrus*	L	SOG.L	0.503	0.499	0.0055	0.0277
Inferior occipital gyrus*	L	IOG.L	0.503	0.498	0.0107	0.0365
Calcarine fissure and surrounding cortex	L	CAL.L	0.507	0.500	0.0038	0.0242
Cuneus*	L	CUN.L	0.503	0.498	0.0035	0.0241
Lingual gyrus	L	LING.L	0.506	0.501	0.0097	0.0365
Superior parietal gyrus*	R	SPG.R	0.502	0.498	0.0149	0.0420
Inferior parietal gyrus	R	IPL.R	0.503	0.500	0.0101	0.0365

b) Anatomical region	L/R	AAL atlas abbreviations	dPTE (HC)	dPTE (PD)	*P-value*	*FDR corrected p-value*
Precuneus*	R	PCUN.R	0.503	0.499	5.0e-4	0.0166
Superior occipital gyrus*	R	SOG.R	0.503	0.498	0.0014	0.0178
Middle occipital gyrus*	R	MOG.R	0.503	0.499	0.0112	0.0365
Inferior occipital gyrus*	R	IOG.R	0.504	0.497	9.2e-4	0.0166
Calcarine fissure and surrounding cortex	R	CAL.R	0.507	0.501	8.0e-4	0.0166
Cuneus*	R	CUN.R	0.503	0.499	0.0064	0.0301
Lingual gyrus	R	LING.R	0.508	0.501	0.0026	0.0213
Fusiform gyrus*	R	FFG.R	0.503	0.499	0.0079	0.0339
Posterior cingulate cortex	R	PCG.R	0.505	0.502	0.0109	0.0365

Supplementary Table 2 Differences in left- versus right dominant Parkinson's disease
CAMCOG, Cambridge Cognitive Examination; UPDRS-III, Unified Parkinson's Disease Rating Scale motor ratings; n/a, non-applicable; n/s, non-significant.

	Left dominant (n=16)	Right dominant (n=18)	*t*-value	p-value
Disease duration (years)	13.44 (3.79)	10.53 (3.19)	2.47	**.019***
dPTE significant right parietal regions**	0.497 0.500 0.503 0.508	0.498 0.502 0.504 0.508	n/a	n/s** n/s n/s n/s
CAMCOG	93.1 (7.56)	89.9 (10.6)	0.979	.335*
UPDRS-III	34.0 (10.0)	33.6 (8.35)	0.124	.902*

*Independent-samples *t*-test;
**Regions of interest (ROI) with a significant group difference in mean dPTE values: inferior/superior parietal gyrus, precuneus, posterior cingulate gyrus (all right side). dPTE values per ROI were expressed as mean. Statistical analysis was performed using permutation testing (N = 5000; $p < .05$) with FDR correction for multiple comparisons.

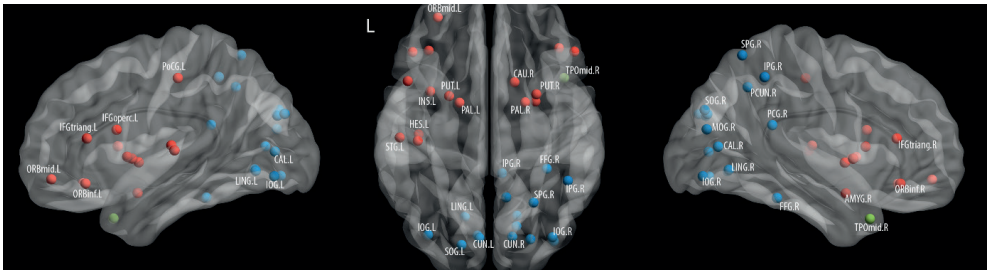

Supplementary Figure 1 Significant differences in dPTE values per region of interest between Parkinson's disease (PD) patients and healthy controls (HC)
Nodes represent brain regions, where the colors indicate significantly higher (red), significantly lower (blue) or no significant difference (green) in preferential information flow (mean dPTE) between the groups. Left lateral (left panel), top (middle panel) and right lateral (right panel) views of a template brain are shown [56]. Abbreviations of the names of relevant brain regions are displayed. A list of abbreviations is provided in Supplementary Table 1.

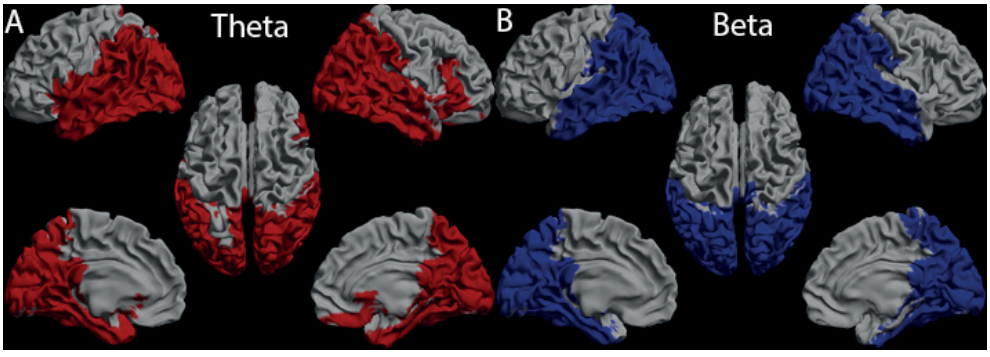

Supplementary Figure 2 Regional distribution of significant differences in band power in the Parkinson's disease (PD) group versus healthy controls (HC).
Significant differences are displayed as a color-coded map on a parcellated template brain viewed from, in clockwise order, the left, top, right, right-midline and left-midline.
Group differences were expressed as *t*-values and permutation tests (N = 5000; $p < .05$) were performed separately for each region of interest (ROI). We accounted for multiple comparisons by using the maximum statistic across ROIs. Panel **A** and **B** depict significant theta and beta band relative power differences, respectively. Red and blue indicate increases and decreases in PD (compared to HC), respectively. Note that significant decreases in beta band power are accompanied by significant increases in theta band power in the posterior ROIs.

CHAPTER 5

Functional connectivity between resting-state networks reflects decline in executive function in Parkinson's disease: a longitudinal fMRI study

Lennard I Boon, Dagmar H Hepp, Linda Douw, Noëlle van Geenen, Tommy AA Broeders, Jeroen JG Geurts, Henk W Berendse, Menno M Schoonheim

Neuroimage Clinical 2020:102468
DOI: 10.1016/j.nicl.2020.102468

Abstract

Background Deficits in cognitive functioning are a common yet poorly understood symptom in Parkinson's disease (PD). Recent studies have highlighted the importance of (dynamic) interactions between resting-state networks for cognition, which remains understudied in PD. We investigated how altered (dynamic) functional interactions between brain networks relate to cognitive dysfunction in PD patients.

Methods In this fMRI study, 50 PD patients (mean age 65.5 years ±6.27) on dopaminergic medication were studied cross-sectionally, and of this cohort 31 PD patients were studied longitudinally. MRI imaging and neuropsychological testing was performed at two time points, with a follow-up duration of approximately three years. Functional connectivity within and between seven resting-state networks was calculated (both statically and dynamically) and correlated with four neuropsychological test scores; a combined score of (four) executive tasks, a motor perseveration, memory, and category fluency task. Cognitive dysfunction was determined based on a longitudinal sample of age-matched healthy controls (n=13).

Results PD patients showed dysfunction on six out of seven cognitive tasks when compared to healthy controls. Severity of executive dysfunction was correlated with higher static and lower dynamic functional connectivity between deep gray matter regions and the frontoparietal network (DGM-FPN). Over time, declining executive function was related to increasing static DGM-FPN connectivity, together with changes of connectivity involving the dorsal attention network (amongst others with the ventral attention network). Static functional connectivity between the ventral and dorsal attention network correlated with motor perseveration.

Conclusions Our findings demonstrate that in PD patients, dysfunctional communication between (i) subcortical, fronto-parietal and attention networks mostly underlies worsening of executive functioning, (ii) attention networks are involved in motor perseveration.

Introduction

Cognitive impairment is a common non-motor symptom of Parkinson's disease (PD) that negatively impacts daily functioning and quality of life.[1] Cognitive impairment in non-demented PD patients is typically dominated by attentional, visuospatial and executive deficits, with strong heterogeneity between patients.[1] An executive syndrome in PD (deficits in cognitive flexibility, planning, working memory, and learning) is possibly related to suboptimal dopamine levels: both excesses and deficits of dopamine in the frontostriatal pathways have been associated with impairments in task performance,[2] as was demonstrated by pharmacological,[3] pharmacogenomics,[4] and neuroimaging research.[5]

Importantly, executive deficits can occur at any stage of the disease and can be progressive, but are not predictive of the development of PD dementia.[6] Progressive executive and general cognitive decline in PD may reflect complex brain pathology and involvement of other non-dopaminergic neurotransmitter systems,[7] indicating global network disruptions, which remain understudied.

Previous research in PD indicated disturbances of connectivity patterns of the default mode network (DMN) in relation to global cognitive dysfunction.[8] Domain-specific cognitive dysfunction in PD has been related to other networks, such as the attention networks (dorsal attention network, DAN; ventral attention network, VAN) and the bilateral frontoparietal networks (FPN).[9,10] In addition, recent technological advances have allowed for the evaluation of time-varying fluctuations in functional connectivity, the so-called dynamic connectivity, for instance showing that the reconfiguration between frontoparietal and frontotemporal brain networks is related to executive functioning.[11].

As such, there are strong indications that PD features extensive cortical network dysfunction in addition to the classical dopaminergic systems, possibly driven by a loss of dynamic interplay between networks. In this study, we longitudinally investigated cognitive dysfunction, in particular executive dysfunction, and functional connectivity (FC) within and between RSNs. We hypothesized that more dispersed network interactions, in addition to connections between the deep gray matter and fronto-parietal network, would be involved in the development of executive deficits as well as other cognitive domains in PD.

Methods

Participants

In this retrospective study, data of idiopathic PD patients and healthy controls was used, obtained in the context of a longitudinal study cohort. Exclusion criteria for PD patients were stereotactic surgery in the past and extensive white matter lesions or other abnormalities at MRI (see also Stoffers et al. (2007)[12] for details on recruitment and inclusion). At initial inclusion, the patients did not receive fMRI scans; all fMRI and

neuro(psycho)logical data used in this manuscript was acquired at 4 ("first timepoint") and 7 year ("second timepoint") follow-up visits (between 2008 and 2012) in the outpatient clinic of the Amsterdam UMC, locatie VUmc. For an overview of the timeline of the data acquisition, see Figure 1. All examinations were performed in the dopamine "ON" state". All patients and healthy controls have been reported in previous analyses on this dataset in which functional connectivity differences were linked to global cognitive decline and visual hallucinations,[13,14] but these studies did not specifically assess (dynamic) RSN connectivity in relation to domain-specific cognitive dysfunction.

Unified PD Rating Scale motor ratings were obtained by a trained physician. Global cognitive functioning was assessed using the Cambridge Cognitive Examination scale. The total dose of dopaminomimetics was converted to a so-called levodopa equivalent daily dose (LEDD) using a previously described conversion rate, see Olde Dubbelink et al. (2013)[15] for other definitions.
All participant gave written informed consent to the research protocol, which was approved by the local medical ethical committee conform the Helsinki declaration.

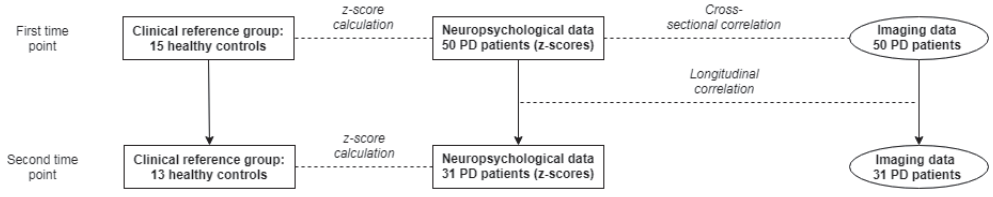

Figure 1 Overview of data analysis
At the first time point, a cross-sectional correlation was performed between (dynamic) functional connectivity of resting-state networks and neuropsychological data for the Parkinson's disease (PD) group (n=50). The neuropsychological data of the PD patients were converted to z-scores, based on the scores of healthy controls. Next, for the 31 PD patients who had undergone a second study visit, longitudinal correlations were made between the change in functional (dynamic) connectivity and the change in neuropsychological performance (expressed as z-scores).

Neuropsychological evaluation

Neuropsychological function was assessed using the Cambridge Neuropsychological Test Automated Battery (Eclipse 2.0, Cambridge, England). Executive tests included spatial working memory (outcome measure: strategy), stockings of Cambridge, spatial span length (partly a working memory test, hence executive function), and intra- extra dimensional set-shifting (outcome measure: number of stages completed). Memory was tested using the pattern recognition memory test, motor perseveration using the Vienna perseveration task, and verbal fluency using the one-minute category verbal fluency test (animals) from the CAMCOG. Cognitive scores were converted to z-scores based on the scores of the healthy controls at each time point as (Dutch) norm scores were not available for all tests, and in order to account for learning effects.[16,17] Negative z-scores

represent poorer performance on that particular neuropsychological test. The z-scores were used as clinical input for the relationship with (dynamic) functional connectivity. Subjects with a z-value <-1.5 were considered to be impaired.

MRI data acquisition

3T-MR scans (GE Signa HDXT, V15M) included a sagittal three-dimensional T1-weighted fast spoiled gradient-echo sequence (repetition time 7.8ms, echo time 3.0ms, inversion time 450ms, flip angle 12, 1.0 x 0.9 x 0.9mm voxel size, 170 slices in sagittal plane). Functional MRI included 202 volumes of axial echo-planar images, of which the first two were discarded (repetition time 1800ms, echo time 35ms, flip angle 90, 3.3mm isotropic voxel size, 33 slices in axial plane). Both in the structural and functional recordings, full-brain coverage was reached. Recordings took place in an eyes-closed, resting-state condition.

Image processing

Resting-state fMRI images were pre-processed by MMS, DH, and LIB (neuroscientist and medical doctors with respectively 10, 5 and 4 years of experience) using standard FSL-5 software (FMRIB Software Library, Oxford, England; http://www.fmrib.ox.ac.uk.fsl) and custom built scripts in bash and Matlab, version 2012a (Mathworks, Natick, MA, USA). We used an independent component analysis-based strategy for Automatic Removal of Motion Artifacts (ICA-AROMA, v0.4-beta 2017, Nijmegen, the Netherlands).[18] Cortical regions of interest (ROIs) were derived from the Brainnetome atlas[19] and deep gray matter (DGM) ROIs were derived from FIRST (part of FSL). All cortical ROIs were non-linearly registered to 3D-T1 space with inverted FNIRT parameters and multiplied with grey matter segmentation maps of SIENAX, while using FIRST ROIs for DGM areas.

Subsequently, all ROIs were combined into one atlas (225 ROIs) and this combined atlas was registered to fMRI using inverted boundary-based registration parameters and masked with a custom-made fMRI mask to remove any residual nonbrain tissue and to reduce the effect of echo planar imaging disortions. After this masking, not all atlas-based brain regions had sufficient numbers of voxels in order to be representative. We therefore included only those regions with at least 30% voxels remaining in at least 90% of the subjects.[20] On the basis of these criteria, 29 regions were excluded (bilateral orbital gyrus, nucleus accumbens, parahippocampal gyrus, and inferior temporal gyrus). The final atlas therefore segmented the fMRI sequence into 196 regions for which mean time series were obtained.

To define resting-state networks, fMRI scans were registered to standard space using aforementioned parameters, where an independent component analysis was run using the MELODIC pipeline (part of FSL). The concatenated fMRI dataset was decomposed into 30 components, which led to seven visually identified RSNs: DAN, DMN, bilateral FPN, sensorimotor network (SMN), DGM, VAN, and visual network) (Figure 2; Supplementary

Table 1; see Supplementary Table 2 for the location of the peak coordinates of each component). RSNs identified were visually inspected (by MMS, LIB) to match with previous literature.[21] Each brain region was assigned to one network only, based on maximum overlap. The localization of RSNs was based on an independent component analysis of 50 PD patients (based only on the first time point of the study).

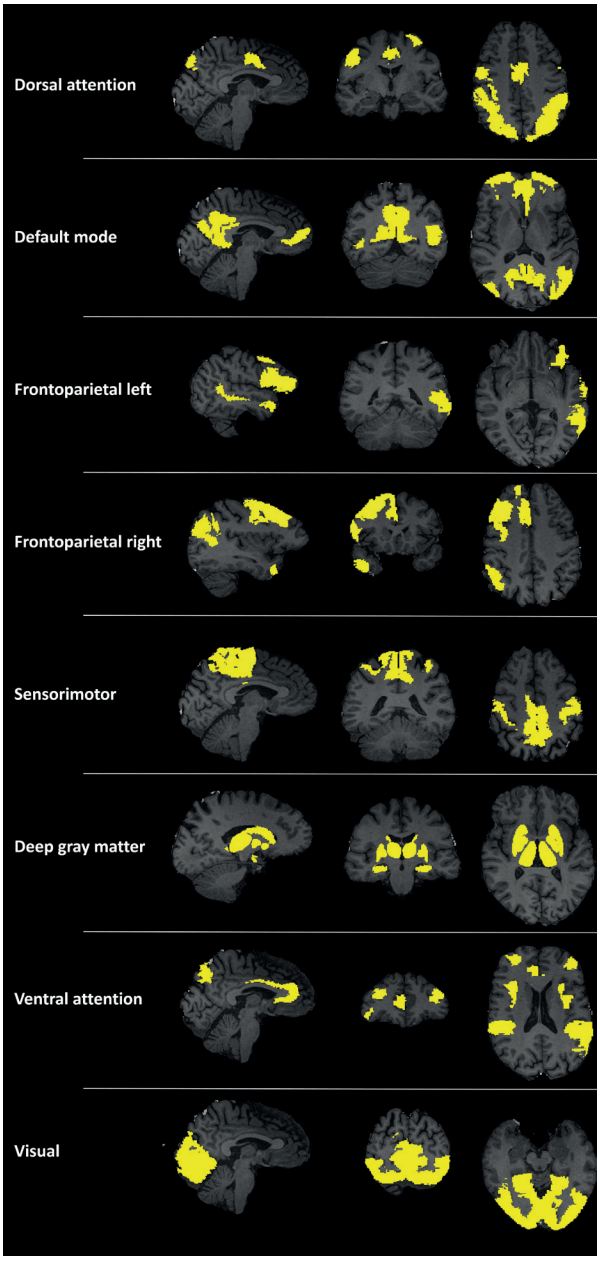

Figure 2 Brain regions involved in the resting-state networks (RSNs) of interest Sagittal, coronal and transverse views are shown. The allocation of regions of interest to RSNs can also be found in Supplementary Table 1.

FC analysis

For each participant, Pearson correlation coefficients were calculated between time series of all 196 brain regions to construct connectivity matrices. Negative correlations were converted to absolute values. Next, we calculated the average connectivity of each of the seven RSNs with the rest of the brain, as well as within- and between-RSN connectivity.

Dynamic FC analysis

In addition to static analyses, Pearson correlation coefficients were calculated per window per subject, with a window length of 48.6 seconds (27x repetition time), resulting in 34 sliding windows, using a shift of 10 seconds. The choice of the window length and # windows was based on an earlier study.[22] The standard deviation over time for each functional connection was calculated and normalized for the average FC across time of that connection, which resulted in the calculation of the coefficients of variation of each connection. Subsequently, within- and between-RSN dynamic FC was calculated.

Dynamic FC interactions that were significantly correlated with neuropsychological test performance were compared with null-models to assess whether the effects were due to random noise. These models were created using phase-randomization of our (Fourier-transformed) data.[23] Next, we averaged dynamic FC over 50 randomization runs and compared empirical- with randomized dynamic FC values.

Statistical analysis

Statistical analyses were performed in IBM SPSS version 22 (Chicago, IL, USA), $p<0.05$ was considered significant. Clinical characteristics of participants were compared using independent samples t-tests. Normality of all variables was assessed with Kolmogorov-Smirnov tests and histogram inspection. As static FC did not meet this criterion, it was transformed using an inversion transformation (1/x), resulting in normality (the sign of resulting beta values was flipped because of this transformation). Longitudinal changes in neuropsychological performance and functional connectivity were assessed using paried t-tests. To test the association between (dynamic) FC and cognition, a hierarchical linear regression using a backward elimination method was performed *per cognitive outcome measure* (in which averaged executive performance was treated as one outcome measure). Note that multiple functional connections were tested within the same regression model. Covariates in the regression models included age, sex, education level (dichotomized at level 3), disease duration and LEDD. Residuals were normally distributed for all regression analyses, justifying the use of parametric regression models.

To limit the number of networks analyzed, FC between one RSN and the rest of the brain was used as input for the first (cross-sectional) regression model and only those RSNs showing a main effect with the rest of the brain were explored further.

In the longitudinal regression models, longitudinal cognitive change was related to change in FC. Longitudinal FC scores were normalized by the individual mean overall FC, to exclude the possibility that global connectivity changes over time (e.g. a physiological and/or technical explanation) affected the results.

Dynamic FC values were compared to null models using paired t-tests.

Results

Study participants

A total of 59 patients were included at the first time point, who all had undergone imaging and neuropsychological assessments. 15 Healthy controls were included with neuropsychological assessments. Four patients had severe motion artifacts during fMRI registration and for 5 patients neuropsychological data was not available (due to incomplete cognitive evaluations), leading to an analysis of 50 patients (as opposed to 55 PD patients in previous studies on this cohort).[13,14] For the second time point (~3 years later), imaging data was available for 37 patients. The reason for not partcipating in the follow-up evaluation varied and included deep brain stimulation placement, death, strong clinical worsening and refusal to undergo an MRI scan. Of the 37 patients, six were excluded due to motion artefacts or the absence of neuropsychological data, leaving 31 PD patients with longitudinal data. In addition, 13 healthy controls had longitudinal neuropsychological measurements. Table 1 summarizes the clinical characteristics of all participants. At the first time point, PD patients did not differ from the healthy controls on age ($t(63)=0.403$; $p=0.688$) and sex ($X^2(1, 65)= 0.093$; $p=0.761$). Furthermore, PD patients showed lower global cognitive performance than healthy controls ($t(63)= 2.62$; $p=0.011$). The groups studied cross-sectionally and longitudinally (both in case of the controls and PD patients) did not differ significantly with respect to age, sex, disease duration, LEDD, global cognitive function, and neuropsychological function (all seven tests were compared separately; statistics not shown).

PD patients scored significantly lower than healthy controls on all but one of the specific neuropsychological tests (Stockings of Cambridge, an executive test, which was retained in the average executive z-score) (Table 1 and Figure 3A).

Longitudinal assessment of clinical parameters in PD patients showed a decrease in global cognitive performance ($t(30)=2.25$; $p=0.034$) and in motor performance ($t(30)=5.31$; $p<0.001$), and an increase in LEDD ($t(30)=7.28$; $p<0.001$). PD patients longitudinally declined on three neuropsychological tests; spatial working memory (between errors; $t(30)=5.43$; $p<0.001$), spatial span length ($t(30)=2.95$; $p=0.006$) and pattern recognition memory test (correct responses; $t(30)=2.47$; $p=0.020$) (Table 1 and Figure 3B). The raw scores of neuropsychological performance can be found in Supplementary Table 3.

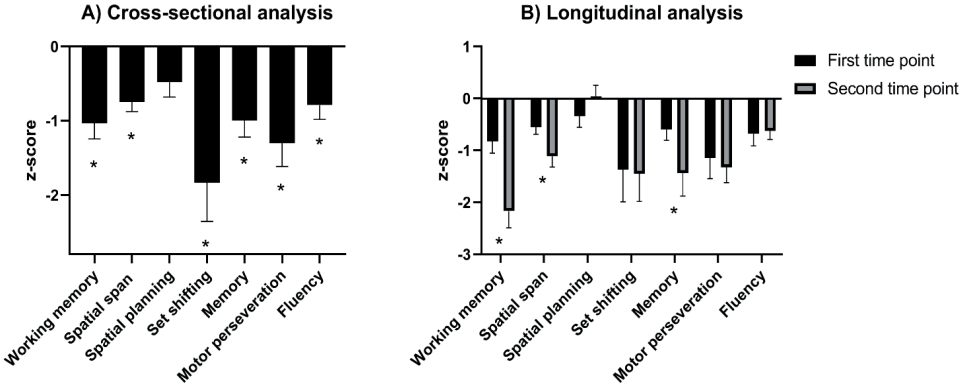

Figure 3 Z-scores of individual neuropsychological tests of Parkinson's disease patients.
Negative z-scores represent poorer performance on a particular cognitive test.

A) Cross-sectional analysis of neuropsychological performance of 50 Parkinson's disease (PD) patients, compared with a reference group of healthy controls (n=15). PD patients scored significantly lower on six out of seven neuropsychological tests (*; p<0,05).

B) Longitudinal analysis of neuropsychological performance of 31 PD patients. Z-scores were based on cross-sectional comparisons between PD patients and a group of healthy controls (first time point, n=15; second time point, n=13). Over time, performance of the PD-group significantly worsened for three out of seven tests (*; p<0,05).

Working memory, Spatial Working Memory (between errors); Spatial planning, Stockings of Cambridge; Set shifting, Intra- Extra Dimensional Set-shifting; Memory, Pattern Recognition Memory (correct responses); Motor perseveration, Vienna perseveration task redundancy; Fluency, Semantic Fluency (no. of words).

Table 1 Baseline and longitudinal demographic and cognitive measures of study sample

	Cross-sectional analysis			Longitudinal analysis		
				PD (n = 31)		
	Controls (n = 15)	PD (n = 50)		Time point 1	Time point 2	
Sex (M/F)	10/5	26/24		14/17		
Age (years)	64.4 (8.65, range 48-79))	65.5 (6.27, range 50-77)		66.2 (5.62, range 54-77)	69.1 (6.04, range 57-80)	
ISCED (0/1/2/3/4/5/6)	0/0/2/3/1/8/1	0/0/20/15/2/13/0		0/0/15/8/1/7/0		
Disease duration (years)	n/a	9.20 (3.63)		8.87 (3.75)	11.87 (3.75)	
UPDRS-III	n/a	26.1 (8.64)		25.7 (8.55)	36.44 (9.82)**	
LEDD total dose	n/a	795 (543)		675 (424)	964 (485) **	
Cambridge Cognitive Examination	99.2 (1.93)	93.3 (8.04)*		93.8 (7.53)	89.80 (14.71)**	
Specific neuropsychological evaluation						
Executive tests			*Z<-1.5; n=*		*Z<-1.5; n=*	*Z<-1.5; n=*
Working memory	0 (1)	-1.03 (1.48)*	15	-0.821 (1.26)	-2.17 (1.75)**	19
Spatial span	0 (1)	-0.745 (0.924)*	8	-0.549 (0.764)	-1.11 (1.14)**	14
Spatial planning	0 (1)	-0.481 (1.40)	9	-0.340 (1.07)	0.043 (1.06)	4
Set shifting	0 (1)	-1.83 (3.65)*	17	-1.368 (3.39)	-1.45 (2.92)	9
Other domains						
Memory	0 (1)	-0.996 (1.57)*	14	-0.598 (1.14)	-1.43 (2.48)**	12
Motor perseveration	0 (1)	-1.30 (2.17)*	16	-1.15 (2.22)	-1.32 (1.64)	11
Fluency	0 (1)	-0.851 (1.41)*	15	-0.678 (1.31)	-0.621 (0.929)	7

Values are expressed as mean (SD) unless otherwise indicated.
Disease duration was calculated on the basis of the estimated onset of first motor symptoms. Education level was determined using the International Standard Classification. PD, Parkinson's disease; ISCED, International Standard Classification of Education; UPDRS-III, Unified Parkinson's Disease Rating Scale motor ratings; LEDD, Levodopa Equivalent Daily Dose; Working memory, Spatial Working Memory (between errors); Spatial planning, Stockings of Cambridge; Set shifting, Intra- Extra Dimensional Set-shifting; Memory, Pattern Recognition Memory (correct responses); Motor perseveration, Vienna perseveration task redundancy; Fluency, Semantic Fluency (no. of words); n/a, non-applicable. * significant difference in cross-sectional analysis (p<0.05); ** significant difference in longitudinal analysis (p<0.05). Z<-1.5; number of subjects with a Z-score <-1,5 below average

Static functional connectivity

Global functional connectivity did not significantly change between baseline and follow-up (Figure 4A; 0.270 at baseline, 0.281 at FU1 (t(30)= -0.734; p=0.469)). However, longitudinal changes in (normalized) functional connectivity between RSNs did show significant changes, as summarized in Figure 4B. Over time, functional connectivity with the rest of the brain significantly increased for the DMN, DGM and VAN, and significantly decreased for the visual network. No changes were observed for DAN, FPN and SMN.

Executive cognition and static FC

The cross-sectional regression analysis with *executive tests* (average of four executive function tests) as dependent variable identified FC of DGM with the rest of the brain as important, as well as DAN with the rest of the brain. The subsequent regional analysis revealed a negative correlation between executive functioning at baseline and DGM-FPN FC, indicating higher FC in patients with dysfunction (see Table 2A for statistical values). However, patients with impaired executive functioning (z-value<-1.5) did not show significantly higher FC than non-impaired patients (z-value>-1.5; Figure 5). The DAN did not show additional cross-network correlations with executive functioning.

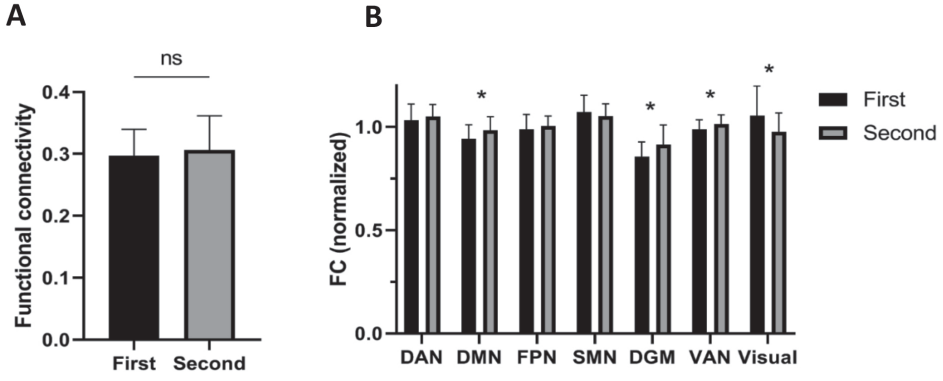

Figure 4 Longitudinal changes in functional connectivity

A) Global functional connectivity over time between the first and second time point (n=31 Parkinson's disease (PD) patients), which was not significantly different.

B) Functional connectivity (normalized) between resting-state networks and the rest of the brain. DAN-rest *t*(30)=1.12 p=0.272; DMN-rest *t*(30)=2.93 p=0.006; FPN-rest *t*(30)=0.826 p=0.415; SMN-rest *t*(30)=-1.37 p=0.180; DGM-rest *t*(30)=2.33 p=0.027; VAN-rest *t*(30)=3.013 p=0.005; Visual-rest *t*(30)=-2.693 p=0.011. (*; p<0,05).

DAN, dorsal attention network; DMN, default-mode network; FPN, frontoparietal network; SMN, sensorimotor network; DGM, deep gray matter; VAN, ventral attention network.

Table 2A Cross-sectional correlations between cognitive functioning and RSN functional connectivity in PD

Cognitive tests	R^2	RSNs involved	RSN interactions involved	Unstandardized Beta	Standardized Beta	*p*-value
Executive tests ǂ	0.247					
		DAN-rest		0.859	0.374	0.050
		DGM-rest		-1.035	-0.596	0.006*
	0.325					
			DAN-Visual	0.290	0.239	0.076
			DGM-FPN	-0.561	-0.402	0.004*
Visuospatial	-	-	-	-	-	-
Motor perseveration	0.155					
		DAN-rest		1.307	0.394	0.003*
	0.175					
			DAN-VAN	1.294	0.419	0.001*
Semantic Fluency	-	-	-	-	-	-

Linear hierarchical regression analyses were performed with a backward elimination method per cognitive outcome measure, corrected for age, sex, education, disease duration, and LEDD. First, global functional connectivity between all individual RSNs and the rest of the brain was correlated with cognitive function (second column). Next, interactions between individual RSNs were assessed (based on the significant correlations on whole-brain interactions) and correlated with cognitive function (third column). Note that multiple functional connections were tested within the same regression model. R^2 values are displayed in the second column as a single value for each separate regression model.
RSN, resting-state network; DGM, Deep Gray Matter; DAN, Dorsal Attention Network; FPN, Frontoparietal Network; PRM, Pattern Recognition Memory; VPT, Vienna Perseveration Test; VAN, Ventral Attention Network.
ǂ Average of Spatial Working Memory, Spatial Span, Stockings of Cambridge and Intra- Extra Dimensional Set-shifting. * significant correlation ($p<0.05$).

Next, longitudinal changes in cognitive function were correlated with longitudinal RSN FC measurements. Over time, change in executive functioning correlated positively with DGM-DMN connectivity changes, whereas it correlated negatively with DGM-FPN and DGM-DGM connectivity changes (Table 2B). In addition, executive cognitive decline was negatively correlated with DAN-SMN FC, while it was positively correlated with DAN-VAN connectivity changes (Table 2B).

Table 2B Longitudinal correlations between cognitive functioning and functional connectivity between RSNs in PD

Cognitive tests	R^2	RSN interactions involved	Unstandardized Beta	Standardized Beta	*p*-value
Executive tests	0.620				
		DAN-SMN	-12.825	-1.312	0.002*
		DAN-VAN	6.545	0.793	0.015*
		DAN-Visual	2.612	0.474	0.072
		DGM-DMN	6.171	0.871	0.007*
		DGM-FPN	-3.100	-0.591	0.035*
		DGM-DGM	-5.742	-0.647	0.020*
		DGM-Visual	-1.537	-0.354	0.098
Motor perseveration	-	-	-	-	-

Linear hierarchical regression analyses were performed with a backward elimination method per cognitive outcome measure, corrected for age, sex, education, disease duration, and LEDD. Selection of functional connectivity interactions between RSNs was based on RSNs deemed to be important based on Table 2A. Note that multiple functional connections were tested within the same regression model. R^2 values are displayed in the second column as a single value for each separate regression model.

Executive cognition and dynamic FC

Only connections showing effects of static connectivity were also explored using dynamic connectivity, thus only RSN interactions concerning the DGM and the DAN. A regression analysis with executive tests as dependent variable showed a positive correlation with DGM-FPN dynamic FC and a negative correlation with DAN-VAN dynamic FC. Both interactions showed significantly higher dynamic connectivity than the null models (DGM-FPN: real data 0.616±0.032, surrogate data 0.609±0.036; $t(48)=3.17$; $p=0.003$, DAN-VAN: real data 0.593±0.032, surrogate data 0.585±0.033; $t(48)=2.67$; $p=0.010$).

No significant longitudinal correlation with dynamic RSN interactions was found.

Other cognitive domains and FC

Using a similar approach, visuospatial function, verbal fluency, and motor perseveration were investigated. In the cross-sectional analysis, visuospatial function and semantic fluency did not correlate with FC of any of the RSNs and these neuropsychological tests were excluded for further analysis. Dysfunctional motor perseveration correlated with lower FC between the DAN and the rest of the brain. In the subsequent regression analysis, dysfunctional motor perseveration correlated with lower DAN-VAN FC only (Table 2A). In accordance, DAN-VAN FC was significantly different between patients with motor perseveration (z-value <-1.5, hence impaired) and non-impaired patients (z-value >-1.5; Figure 5).

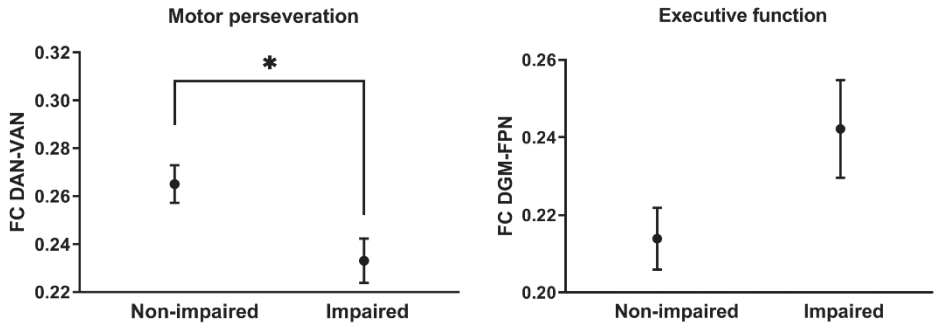

Figure 5 Plots show mean functional connectivity (FC; non-transformed; with standard error of the mean depicted as error bars). As depicted on the left, FC between the deep gray matter (DGM) and the frontoparietal networks (FPN) was non-significantly higher for PD patients impaired (z-value <-1.5) on executive tests ((t(48)=1.651; p=0.106). As depicted on the right, FC between the dorsal attention network (DAN) and ventral attention network (VAN) was significantly lower for PD patients impaired (z-value <-1.5) on motor perseveration (t(48)=2.582; p=0.013).

No longitudinal correlations were observed for motor perseveration (Table 2B).

Again, only connections showing effects of static connectivity were also explored using dynamic connectivity, thus only RSN interactions concerning the DAN were correlated with motor perseveration. Dysfunctional motor perseveration correlated with higher DAN-SMN dynamic FC (Table 2C). DAN-SMN showed significantly higher dynamic connectivity than the null model (real data 0.555±0.053, surrogate data 0.545±0.051; *t*(48)=2.76; *p*=0.008). No longitudinal correlation was found between motor perseveration and dynamic RSN interactions.

Table 2C Cross-sectional correlations between cognitive functioning and dynamic functional connectivity between RSNs in PD

Cognitive tests	R^2	RSN interactions involved	Unstandardized Beta	Standardized Beta	*p*-value
Executive tests	0.323				
		DAN-VAN	-18.815	-0.471	0.007*
		DGM-DMN	10.399	0.294	0.098
		DGM-FPN	14.185	0.383	0.049*
Motor perseveration	0.140				
		DAN-FPN	-19.57	-0.401	0.053
		DAN-SMN	-11.93	-0.294	0.030*
		DAN-DGM	17.80	0.358	0.080

Linear hierarchical regression analyses were performed with a backward elimination method per cognitive outcome measure, corrected for age, sex, education, disease duration, and LEDD. Selection of functional connectivity interactions between RSNs was based on RSNs deemed to be important based on Table 2A. Note that multiple functional connections were tested within the same regression model. R^2 values are displayed in the second column as a single value for each separate regression model.

Discussion

Our results showed that PD patients displayed deficits in almost all cognitive domains, which worsened over time. Furthermore, we found relative increases in functional connectivity with the rest of the brain for the DGM, DMN and VAN and decreases for the visual network.

Next, we observed a cross-sectional correlation between executive dysfunction and increased static, but decreased dynamic DGM-FPN FC. Longitudinally, only static FC changes were related to decline in executive function, and this included RSN-interactions in addition to DGM-FPN, especially highlighting the role of the DAN. The DAN was also related to cross-sectional deficits in motor perseveration.

We found that higher static connectivity between DGM and the FPN was related to poorer executive functioning, possibly reflecting frontostriatal dysfunction with a dopaminergic basis. However, executive dysfunction did not correlate with the LEDD (β=-0.179; p=0.179), and DGM-FPN connectivity did not correlate with motor dysfunction (β=0.049; p=0.688), nor with the LEDD (β=-0.059; p=0.666). In spite of the lack of these correlations, and the fact that we added LEDD as covariate in our analyses, in line with previous studies, we hypothesize that dopaminergic therapy could still have impacted the correlations observed, by lowering frontostriatal FC[24] and simultaneously having beneficial effects on executive functioning.[3] Since individual patients may have different baseline levels of dopamine they may exhibit a differential sensitivity to the positive and negative effects of dopaminergic medication, which may interfere with LEDD correlations.[4] Interestingly, increases in FC within the basal ganglia[25] and sensorimotor[26] network have been observed upon a dopaminergic challenge in PD patients. Hence, it remains to be determined whether a *hyper*dopaminergic state, in line with the so-called 'dopamine-overdose hypothesis',[4] or a *hypo*dopaminergic state explains the correlations observed. This knowledge would be a prerequisite for better clinical management of executive dysfunction.

Our longitudinal regression models suggest that not only FC of the DGM or FPN, but also FC of the DAN is involved in executive dysfunction. Over time, performance on executive tests correlated with FC changes not restricted to the DGM-FPN, involving a negative correlation with DAN-SMN connectivity and a positive correlation with DAN-VAN connectivity. The DAN and VAN are attention networks, involved in reorienting attention towards salient stimuli in the healthy brain.[27] Previous work has shown that as PD progresses, such networks may become involved to maintain optimal performance on executive tests,[7] as also suggested by studies on (healthy) aging.[28] A recent study has confirmed that reduced FC between the DAN and insular brain regions (the latter being part of the VAN) is associated with worse performance on attention/executive tasks.[10] Furthermore, in another study cognitively impaired PD patients had reduced insular dopaminergic D2 receptors, which was associated with worse executive functioning.[5]

Apart from executive dysfunction, our study investigated several additional cognitive testss, of which only motor perseveration showed relations with FC of brain networks. Motor perseveration (when one is instructed to demonstrate random motor behavior) has been demonstrated to occur in early stages of PD[29] and was related to lower DAN FC, especially DAN-VAN connectivity. The generation of random motor behavior is considered to involve retention of information, suppression of habitual responses, and switching of production strategies,[30] all of which are attention demanding processes. Therefore, lower connectivity between the attention networks may play a role in perseverative tendencies such as motor perseveration. The primary cause of attentional network dysfunction remains unclear hower, but is thought to revolve around cholinergic deficits.[31]

In addition to static FC, we have added dynamic FC, which has recently been shown to be important for cognitive functioning in PD.[22,32] Accumulating evidence indicates that functional connectivity between brain regions is nonstationary and alternates between periods of low and high functional coupling over time.[33] In our study, dynamic FC was expressed as the variability (coefficient of variation) of functional connectivity over a number of time windows, in which more variability/fluctuation represents higher dynamic FC. The results of our dynamic FC analysis did not simply mirror static FC results, as demonstrated by correlations involving DAN-VAN (executive dysfunction) and DAN-SMN (Vienna perseveration task) dynamic FC. At the same time, the role of DGM-FPN dynamic FC in executive dysfunction was confirmed, although in this case higher DGM-FPN dynamics seems to be beneficial rather than disadvantageous for cognitive functioning. Together, these results support the notion that the balance of excitation and inhibition, a fundamental feature of brain network activity,[34] may be disturbed in PD, thereby leading to dynamic FC changes. Our longitudinal analysis adds to the recent (cross-sectional) dynamic functional connectivity work in PD showing that PD patients with dementia dwell longer in segregated between-network states,[32] and dynamic functional connectivity of the DMN correlated with visuospatial memory disturbances.[22]

This study has several limitations. First, several subjects were lost to follow-up, leading to the possibility that only PD patients with a relatively mild disease course were included in the longitudinal analysis. However, there were no significant differences between the group studied cross-sectionally and the group studied longitudinally (sex, age, ISCED, disease duration, UPDRS-III, LEDD total dose, and CAMCOG were tested; statistics not shown). Moreover, clinically relevant correlations were still identified in the longitudinal analysis. Second, the patients were in the dopamine "ON" state during the MRI acquisition, which at the time was decided to minimize head motion and thus motion-related artefacts. This may have influenced resting-state functional connectivity, but the clinical assessments were also in the dopamine "ON" state. Therefore, our conclusions only apply to PD patients in the dopamine "ON" state. Third, we chose to study only those RSNs showing a main effect with the rest of the brain in the first cross-sectional analysis (DGM and DAN). We are aware that using this approach, we may have missed relevant interactions

between RSNs. However, we think this study did not have sufficient statistical power to study the multitude of all RSN interactions. Future studies with larger sample sizes may be able to identify additional connections relevant for cognitive decline in PD. Importantly, the method we have used allowed us to find an a-priori hypothesized result (link between executive functioning and DGM-FPN FC). Fourth, as dynamic FC has only recently been introduced, its biological correlate remains to be established. Therefore, assessing whether observed time-varying fluctuations in FC are due to statistical uncertainty/noise or reflect *true* changes in FC is important.[35] Therefore, in our study we have confirmed that the observed fluctuations in FC (of relevant interactions) significantly deviated from surrogate data/null models. Fifth, spatial span length is sometimes considered to be a visuospatial rather than a working memory test. In our study, by reasoning from the latter, working memory was included as part of the executive functioning spectrum that we aimed to measure. Future research is necessary to make well-grounded choices for the allocation of neuropsychological tests into specific domains.

In summary, we demonstrated that worse executive functioning in PD on dopaminergic medication is associated with higher static, but lower dynamic, FC between deep gray matter areas and the FPN. Over time, worsening executive function was associated with further connectivity changes between RSNs not restricted to the DGM-FPN, centered around attention networks. In addition, attentional network changes were also implicated in motor perseveration. These findings suggest that the pathophysiological mechanisms of executive dysfunction are not merely driven by dopaminergic mechanisms, but also by attention network effects.

Acknowledgements

We thank all patients and control subjects for their participation. We thank K.T.E. Olde Dubbelink MD PhD for the collection of data and her help in preprocessing of the imaging data.

References

1. Aarsland D, Creese B, Politis M, et al. Cognitive decline in Parkinson disease. Nature reviews Neurology. 2017;13(4):217-31.
2. Kehagia AA, Barker RA, Robbins TW. Cognitive impairment in Parkinson's disease: the dual syndrome hypothesis. Neurodegener Dis. 2013;11(2):79-92.
3. Gotham AM, Brown RG, Marsden CD. 'Frontal' cognitive function in patients with Parkinson's disease 'on' and 'off' levodopa. Brain. 1988;111 (Pt 2):299-321.
4. Cools R. Dopaminergic modulation of cognitive function-implications for L-DOPA treatment in Parkinson's disease. Neurosci Biobehav Rev. 2006;30(1):1-23.
5. Christopher L, Marras C, Duff-Canning S, et al. Combined insular and striatal dopamine dysfunction are associated with executive deficits in Parkinson's disease with mild cognitive impairment. Brain. 2014;137(Pt 2):565-75.
6. Williams-Gray CH, Evans JR, Goris A, et al. The distinct cognitive syndromes of Parkinson's disease: 5 year follow-up of the CamPaIGN cohort. Brain. 2009;132(Pt 11):2958-69.
7. Bassetti CL. Nonmotor disturbances in Parkinson's disease. Neurodegener Dis. 2011;8(3):95-108.
8. Tessitore A, Esposito F, Vitale C, et al. Default-mode network connectivity in cognitively unimpaired patients with Parkinson disease. Neurology. 2012;79(23):2226-32.
9. Baggio HC, Sala-Llonch R, Segura B, et al. Functional brain networks and cognitive deficits in Parkinson's disease. Hum Brain Mapp. 2014;35(9):4620-34.
10. Baggio HC, Segura B, Sala-Llonch R, et al. Cognitive impairment and resting-state network connectivity in Parkinson's disease. Hum Brain Mapp. 2015;36(1):199-212.
11. Braun U, Schafer A, Walter H, et al. Dynamic reconfiguration of frontal brain networks during executive cognition in humans. Proc Natl Acad Sci U S A. 2015;112(37):11678-83.
12. Stoffers D, Bosboom JL, Deijen JB, et al. Slowing of oscillatory brain activity is a stable characteristic of Parkinson's disease without dementia. Brain. 2007;130(Pt 7):1847-60.
13. Hepp DH, Foncke EMJ, Olde Dubbelink KTE, et al. Loss of Functional Connectivity in Patients with Parkinson Disease and Visual Hallucinations. Radiology. 2017;285(3):896-903.
14. Olde Dubbelink KT, Schoonheim MM, Deijen JB, et al. Functional connectivity and cognitive decline over 3 years in Parkinson disease. Neurology. 2014;83(22):2046-53.
15. Olde Dubbelink KT, Stoffers D, Deijen JB, et al. Cognitive decline in Parkinson's disease is associated with slowing of resting-state brain activity: a longitudinal study. Neurobiol Aging. 2013;34(2):408-18.
16. Frank R, Wiederholt WC, Kritz-Silverstein DK, et al. Effects of sequential neuropsychological testing of an elderly community-based sample. Neuroepidemiology. 1996;15(5):257-68.
17. Rabbitt P, Diggle P, Smith D, et al. Identifying and separating the effects of practice and of cognitive ageing during a large longitudinal study of elderly community residents. Neuropsychologia. 2001;39(5):532-43.
18. Pruim RHR, Mennes M, van Rooij D, et al. ICA-AROMA: A robust ICA-based strategy for removing motion artifacts from fMRI data. Neuroimage. 2015;112:267-77.
19. Fan L, Li H, Zhuo J, et al. The Human Brainnetome Atlas: A New Brain Atlas Based on Connectional Architecture. Cereb Cortex. 2016;26(8):3508-26.
20. Meijer KA, Eijlers AJC, Douw L, et al. Increased connectivity of hub networks and cognitive impairment in multiple sclerosis. Neurology. 2017;88(22):2107-14.
21. Smith SM, Fox PT, Miller KL, et al. Correspondence of the brain's functional architecture during activation and rest. Proc Natl Acad Sci U S A. 2009;106(31):13040-5.
22. Engels G, Vlaar A, McCoy B, et al. Dynamic Functional Connectivity and Symptoms of Parkinson's Disease: A Resting-State fMRI Study. Front Aging Neurosci. 2018;10:388.

23. Prichard D, Theiler J. Generating surrogate data for time series with several simultaneously measured variables. Phys Rev Letters. 1994;73(7):951-4.
24. Kwak Y, Peltier S, Bohnen NI, et al. Altered resting state cortico-striatal connectivity in mild to moderate stage Parkinson's disease. Front Syst Neurosci. 2010;4:143.
25. Szewczyk-Krolikowski K, Menke RA, Rolinski M, et al. Functional connectivity in the basal ganglia network differentiates PD patients from controls. Neurology. 2014;83(3):208-14.
26. Esposito F, Tessitore A, Giordano A, et al. Rhythm-specific modulation of the sensorimotor network in drug-naive patients with Parkinson's disease by levodopa. Brain. 2013;136(Pt 3):710-25.
27. Fox MD, Corbetta M, Snyder AZ, et al. Spontaneous neuronal activity distinguishes human dorsal and ventral attention systems. Proc Natl Acad Sci U S A. 2006;103(26):10046-51.
28. Reuter-Lorenz P. New visions of the aging mind and brain. Trends Cogn Sci. 2002;6(9):394.
29. Stoffers D, Berendse HW, Deijen JB, et al. Motor perseveration is an early sign of Parkinson's disease. Neurology. 2001;57(11):2111-3.
30. Nagano-Saito A, Leyton M, Monchi O, et al. Dopamine depletion impairs frontostriatal functional connectivity during a set-shifting task. J Neurosci. 2008;28(14):3697-706.
31. Sarter M, Albin RL, Kucinski A, et al. Where attention falls: Increased risk of falls from the converging impact of cortical cholinergic and midbrain dopamine loss on striatal function. Exp Neurol. 2014;257:120-9.
32. Fiorenzato E, Strafella AP, Kim J, et al. Dynamic functional connectivity changes associated with dementia in Parkinson's disease. Brain. 2019.
33. Hutchison RM, Womelsdorf T, Allen EA, et al. Dynamic functional connectivity: promise, issues, and interpretations. Neuroimage. 2013;80:360-78.
34. Dehghani N, Peyrache A, Telenczuk B, et al. Dynamic Balance of Excitation and Inhibition in Human and Monkey Neocortex. Sci Rep. 2016;6:23176.
35. Hindriks R, Adhikari MH, Murayama Y, et al. Can sliding-window correlations reveal dynamic functional connectivity in resting-state fMRI? Neuroimage. 2016;127:242-56.

Supplemental materials

Supplementary Table 1 Allocation of regions of interest to resting-state networks

Resting-state network	Brain region	Sub-region
Dorsal attention network	Superior Frontal Gyrus	Left dorsolateral area 6
	Middle Frontal Gyrus	Right ventral area 9/46
		Left ventrolateral area 6
	Inferior Frontal Gyrus	Left dorsal area 44
		Right dorsal area 44
		Left inferior frontal sulcus
		Right inferior frontal sulcus
		Right rostral area 45
		Right ventral area 44
	Precentral Gyrus	Left caudal dorsolateral area 6
		Right caudal dorsolateral area 6
		Left area 4(upper limb region)
		Right area 4(upper limb region)
		Right caudal ventrolateral area 6
	Inferior Temporal gyrus	Left extreme lateroventral area 37
	Fusiform Gyrus	Left lateroventral area 37
	Superior Parietal Lobule	Left caudal area 7
		Right caudal area 7
		Left lateral area 5
		Right lateral area 5
		Left intraparietal area 7
		Right intraparietal area 7
	Inferior Parietal Lobule	Left rostrodorsal area 39
		Left rostrodorsal area 40
		Right_A40rd, rostrodorsal area 40
	Postcentral Gyrus	Left area 2
		Right area 2
		Left area1/2/3 (trunk region)
	Cingulate Gyrus	Left caudodorsal area 24
		Right caudodorsal area 24
	Lateral Occipital Cortex	Left lateral superior occipital gyrus
		Right lateral superior occipital gyrus
Default Mode Network	Superior Frontal Gyrus	Left dorsolateral area 8
	Middle Frontal Gyrus	Left dorsal area 9/46
		Left ventrolateral area 8

Resting-state network	Brain region	Sub-region
		Left lateral area 10
		Right lateral area 10
	Orbital Gyrus	Left medial area 14
		Right medial area 14
		Right orbital area 12/47
		Left lateral area 11
	Superior Temporal Gyrus	Right medial area 38
	Fusiform Gyrus	Right rostroventral area 20
	Parahippocampal Gyrus	Left lateral posterior parahippocampal gyrus
		Right lateral posterior parahippocampal gyrus
	Inferior Parietal Lobule	Left caudal area 39
		Right caudal area 39
		Left rostroventral area 39
	Precuneus	Left dorsomedial parieto-occipital sulcus
		Right dorsomedial parieto-occipital sulcus
		Left area 31
		Right area 31
	Insular Gyrus	Right ventral agranular insula
	Cingulate Gyrus	Left dorsal area 23
		Right dorsal area 23
		Left ventral area 23
		Right ventral area 23
		Left subgenual area 32
Frontoparietal Network (Left)	Superior Frontal Gyrus	Left medial area 8
		Right medial area 8
		Left lateral area 9
		Left medial area 6
		Left medial area 9
		Left medial area 10
		Right medial area 10
	Middle Frontal Gyrus	Left inferior frontal junction
		Left area 46
	Inferior Frontal Gyrus	Left caudal area 45
		Left rostral area 45
		Left opercular area 44
		Left ventral area 44
	Orbital Gyrus	Left orbital area 12/47
		Left lateral area 12/47

Resting-state network	Brain region	Sub-region
	Middle Temporal Gyrus	Left rostral area 21
		Left dorsolateral area 37
		Left anterior superior temporal sulcus
	Inferior Temporal Gyrus	Right rostral area 20
	Posterior Superior Temporal Sulcus	Left rostroposterior superior temporal sulcus
		Left caudoposterior superior temporal sulcus
	Cingulate Gyrus	Left pregenual area 32
Frontoparietal Network (Right)	Superior Frontal Gyrus	Right dorsolateral area 8
		Right lateral area 9
		Right medial area 9
	Middle Frontal Gyrus	Right dorsal area 9/46
		Right inferior frontal junction
		Right ventrolateral area 8
		Right ventrolateral area 6
	Inferior Frontal Gyrus	Right caudal area 45
	Middle Temporal Gyrus	Right rostral area 21
		Right dorsolateral area37
	Inferior Parietal Lobule	Right rostrodorsal area 39
		Right caudal area 40
		Right rostroventral area 39
	Cingulate Gyrus	Right pregenual area 32
Sensorimotor network	Superior Frontal Gyrus	Right dorsolateral area 6
		Right medial area 6
	Precentral Gyrus	Left area 4 (head and face region)
		Right area 4 (head and face region)
		Left area 4 (trunk region)
		Right area 4 (trunk region)
		Left area 4 (tongue and larynx region)
		Right area 4 (tongue and larynx region)
		Left caudal ventrolateral area 6
	Paracentral Lobule	Left area 1/2/3 (lower limb region)
		Right area 1/2/3 (lower limb region)
		Left area 4 (lower limb region)
		Right area 4 (lower limb region)
	Precuneus	Left medial area 5
		Right medial area 5
	Postcentral Gyrus	Left area 1/2/3 (upper limb, head and face region)
		Right area 1/2/3 (upper limb, head and face region)

Resting-state network	Brain region	Sub-region
		Left area 1/2/3 (tongue and larynx region)
		Right area 1/2/3 (tongue and larynx region)
		Right area1/2/3 (trunk region)
	Insula	Left hypergranular insula
		Right hypergranular insula
		Left dorsal granular insula
		Right dorsal granular insula
	Cingulate gyrus	Left caudal area 23
		Right caudal area 23
Subcortical Network	Subcortical brain regions	Left thalamus
		Left caudate nucleus
		Left putamen
		Left pallidum
		Left hippocampus
		Left amygdala
		Right thalamus
		Right caudate nucleus
		Right putamen
		Right pallidum
		Right Hippocampus
		Right amygdala
Ventral Attention Network	Middle Frontal Gyrus	Right area 46
		Left ventral area 9/46
	Inferior Frontal Gyrus	Right opercular area 44
	Orbital Gyrus	Right lateral area 12/47
	Superior Temporal Gyrus	Left medial area 38
		Left area 41/42
		Right area 41/42
		Left TE1.0 and TE1.2
		Right TE1.0 and TE1.2
		Left caudal area 22
		Right caudal area 22
		Left lateral area 38
		Right lateral area 38
		Left rostral area 22
		Right rostral area 22
	Middle Temporal Gyrus	Right anterior superior temporal sulcus
	Inferior Temporal Gyrus	Left ventrolateral area 37

Resting-state network	Brain region	Sub-region
	Parahippocampal Gyrus	Left medial PPHC
		Right medial PPHC
	Posterior Superior Temporal Sulcus	Right rostroposterior superior temporal sulcus
		Right caudoposterior superior temporal sulcus
	Superior Parietal Lobule	Left rostral area 7
		Right rostral area 7
		Left postcentral area 7
		Right postcentral area 7
	Inferior Parietal Lobule	Left caudal area 40
		Left rostroventral area 40
		Right rostroventral area 40
	Precuneus	Left medial area 7
		Right medial area 7
	Insula	Left ventral agranular insula
		Left dorsal agranular insula
		Right dorsal agranular insula
		Left ventral dysgranular and granular insula
		Right ventral dysgranular and granular insula
		Left dorsal dysgranular insula
		Right dorsal dysgranular insula
	Cingulate Gyrus	Left rostroventral area 24
		Right rostroventral area 24
		Right subgenual area 32
Visual Network	Inferior Temporal Gyrus	Right ventrolateral area 37
	Fusiform Gyrus	Left medioventral area37
		Right medioventral area37
		Right lateroventral area37
	Medioventral Occipital Cortex	Left caudal lingual gyrus
		Right caudal lingual gyrus
		Left rostral cuneus gyrus
		Right rostral cuneus gyrus
		Left caudal cuneus gyrus
		Right caudal cuneus gyrus
		Left rostral lingual gyrus
		Right rostral lingual gyrus
		Left ventromedial parieto-occipital sulcus
		Right ventromedial parieto-occipital sulcus

Resting-state network	Brain region	Sub-region
	Lateral Occipital Cortex	Left middle occipital gyrus
		Right middle occipital gyrus
		Left area V5/MT+
		Right area V5/MT+
		Left occipital polar cortex
		Right occipital polar cortex
		Left inferior occipital gyrus
		Right inferior occipital gyrus
		Left medial superior occipital gyrus
		Right medial superior occipital gyrus

Supplementary Table 2 Location of components of resting-state networks
Allocation of each of the 30 components obtained by the independent component analysis to resting-state networks and the location of its peak voxels. Note that components 2, 3, 8, 12, 14, 18, 20, 21, 23, 24, 25, 26, 27, 28, 29 and 30 were considered to be noise.

Network	Component number	Number of voxels	Coordinates peak voxel (x y z)	Atlas region peak voxel
Visual	1	1915	20 15 20	Intracalcarine cortex (right)
	4	1991	14 10 22	Lateral occipital cortex (right)
	22	1522	26 7 18	Occipital pole (left)
Default-mode	5	726	25 17 21	Precuneus (left)
		481	33 15 26	Lateral occipital cortex (left)
		285	10 15 25	Lateral occipital cortex (right)
		253	28 37 29	Superior frontal gyrus (left)
		225	23 46 18	Frontal pole (left)
	6	1923	20 39 17	Anterior cingulate gyrus (right)
	7	1333	20 17 26	Precuneus (right)
Dorsal attention	9	1749	14 18 29	Superior parietal lobule (right)
		436	34 33 27	Middle frontal gyrus (left)
		297	10 34 28	Middle frontal gyrus (right)
		196	29 33 32	Superior frontal gyrus (left)
		140	34 16 17	Lateral occipital cortex (left)
		115	9 19 16	Middle temporal gyrus (right)
	15	1188	32 21 30	Superior parietal lobule (left)
		707	11 23 30	Supramarginal gyrus (right)
Frontoparietal left	10	2182	34 38 16	Frontal orbital cortex (left)
		655	24 38 33	Superior frontal gyrus (left)
		140	10 23 18	Superior temporal gyrus (right)
		100	10 34 12	Temporal pole (right)
Frontoparietal right	11	842	10 17 29	Lateral occipital cortex
		737	11 35 30	Middle frontal gyrus (right)
		163	33 17 30	Angular cortex (left)
Ventral attention	13	1436	37 22 26	Supramarginal gyrus, anterior division (left)
		385	8 24 27	Supramarginal gyrus (right)
		98	37 33 20	Precentral gyrus (left)
		73	32 43 26	Frontal pole (left)
	17	980	33 33 17	Insular cortex (left)
		856	11 31 18	Insular cortex (right)
		215	21 41 19	Cingular gyrus (right)
Sensorimotor	16	954	37 30 24	Postcentral gyrus (left)
		673	9 30 26	Precentral gyrus (right)
	19	1441	20 23 31	Postcentral gyrus (right)

Supplementary Table 3 Raw scores of neuropsychological performance

	Cross-sectional analysis		Controls (n=13)	Longitudinal analysis PD (n=31)	
Specific neuropsychological evaluation	**Controls (n=15)**	**PD (n=50)**	**Time point 2**	**Time point 1**	**Time point 2**
Executive tests					
Working memory (errors)	23.3 (14.1)	37.9 (20.9)	18.3 (11.4)	37.0 (18.6)	40.5 (23.2)
Spatial span	5.6 (1.1)	4.7 (1.2)	5.7 (0.95)	4.9 (0.89)	4.59 (1.09)
Spatial planning	8.0 (1.5)	7.3 (2.1)	8.2 (1.9)	7.2 (1.7)	7.83 (2.6)
Set shifting	8.8 (0.62)	7.3 (2.7)	8.4 (0.97)	7.8 (2.0)	6.9 (2.9)
Other domains					
Memory	22.5 (1.7)	20.9 (2.7)	22.7 (1.12)	21.4 (2.0)	21.0 (2.9)
Motor perseveration	19.5 (4.7)	25.6 (10.2)	14.2 (8.3)	25.5 (10.5)	24.7 (13.3)
Fluency	23.9 (4.8)	19.8 (6.8)	24.8 (7.2)	21.3 (6.9)	20.2 (6.9)

Values are expressed as mean (SD). In case of working memory and motor perseveration, higher scores represented worse performance; worse performance was converted to negative z-scores.
Note that the scores of healthy controls in the cross-sectional analysis were used as time point 1 scores in the longitudinal analysis.
PD, Parkinson's disease

CHAPTER 6.1

Motor effects of deep brain stimulation correlate with increased functional connectivity in Parkinson's disease: An MEG study

Lennard I Boon, Arjan Hillebrand, Wouter V Potters, Rob MA de Bie, Naomi Prent, Maarten Bot, P Richard Schuurman, Cornelis J Stam, Anne-Fleur van Rootselaar, Henk W Berendse

Neuroimage Clinical 2020:102225
DOI: 10.1016/j.nicl.2020.102225

Abstract

Background Deep brain stimulation (DBS) of the subthalamic nucleus (STN) is an established symptomatic treatment in Parkinson's disease, yet its mechanism of action is not fully understood. Locally in the STN, stimulation lowers beta band power, in parallel with symptom relief. Therefore, beta band oscillations are sometimes referred to as "anti-kinetic". However, in recent studies functional interactions have been observed beyond the STN, which we hypothesized to reflect clinical effects of DBS.

Methods Resting-state, whole-brain magnetoencephalography (MEG) recordings and assessments on motor function were obtained in 18 Parkinson's disease patients with bilateral STN-DBS, on and off stimulation. For each brain region, we estimated source-space spectral power and functional connectivity with the rest of the brain.

Results Stimulation led to an increase in average peak frequency and a suppression of absolute band power (delta to low-beta band) in the sensorimotor cortices. Significant changes (decreases and increases) in low-beta band functional connectivity were observed upon stimulation. Improvement in bradykinesia/rigidity was significantly related to increases in alpha2 and low-beta band functional connectivity (of sensorimotor regions, the cortex as a whole, and subcortical regions). By contrast, tremor improvement did not correlate with changes in functional connectivity.

Conclusions Our results highlight the distributed effects of DBS on the resting-state brain and suggest that DBS-related improvements in rigidity and bradykinesia, but not tremor, may be mediated by an increase in alpha2 and low-beta functional connectivity. Beyond the local effects of DBS in and around the STN, functional connectivity changes in these frequency bands might therefore be considered as "pro-kinetic".

Introduction

Deep brain stimulation (DBS) of the subthalamic nucleus (STN) is an established and effective symptomatic treatment for the disabling medication-related response fluctuations in the motor symptoms of Parkinson's disease.[1,2] Tremor relief most likely involves different neuronal mechanisms than the reductions in bradykinesia and rigidity.[3,4] Local field potential (LFP) studies have demonstrated that excessive beta band synchronized oscillatory activity in the basal ganglia is a hallmark of Parkinson's disease and that DBS-induced suppression of these oscillations in the STN goes hand in hand with improvement of both bradykinesia and rigidity.[5-7] Beta band oscillations have therefore been labelled as "anti-kinetic"[8] (see also McGregor and Nelson (2019) for a recent discussion on this topic).[9]

Recent observations suggest that DBS-related neurophysiological effects extend beyond the major components of the classical motor system[10-16] (for reviews on this topic see).[17,18] A better understanding of these effects is not only necessary to explain the neurophysiological mechanisms of DBS but might also aid in the development of an in-vivo biomarker for short and long-term therapeutic effects.

At the cortical level, STN-DBS can modulate oscillatory brain activity in several frequency bands. In two recent studies, STN-DBS lowered theta, alpha and low-beta band power in (source-space)[13] and over (sensor-space)[14] the sensorimotor cortex, but without a correlation with motor improvement.[13,14] Other studies demonstrated that an alpha and beta power suppression over right temporal brain regions correlated positively with DBS-related global motor improvement,[11] whereas the average frequency of cortical oscillations seemed to increase upon stimulation.[10,12]

Neural circuits involved in Parkinson's disease symptoms can be subdivided into different parallel circuits that generally concern cortico-subcortical interactions.[9,19] STN-DBS might have opposing functional effects on these circuits as well as their elements. In an fMRI study, dynamic causal modelling revealed a reduction in effective connectivity of the hyperdirect pathway, whereas effective connectivity of the direct, cortico-striatal and thalamo-cortical pathways was increased upon stimulation.[16] Oswal and co-workers confirmed that stimulation of the STN suppressed upper-beta band coherence between the STN and cortical motor areas, possibly reflecting the hyperdirect pathway. However, these changes did not correlate with clinical improvement, whereas suppression of low-beta band power in the STN did.[15]

Using magnetoencephalography (MEG), Parkinson's disease related oscillatory activity can be studied with an excellent spatial and temporal resolution.[15,20] MEG data can even be recorded successfully during DBS, in spite of the contamination of recordings by hardware and stimulation artefacts.[21,22] To date, no studies have reported on the influence of DBS on whole-brain functional connectivity including cortico-subcortical connections.

Here we investigated this influence using MEG in order to study the alleged anti-kinetic nature of beta band oscillations and to elucidate the neurophysiological correlates of DBS motor-effects.

We used the Amplitude Envelope Correlation (AEC; the correlation between the temporal evolution of spectral power in different regions) as a measure of functional connectivity [23]. The AEC is dissociated from local oscillatory processes, and therefore complementary to band power analysis.[24] In addition, the AEC has shown similarities with fMRI connectivity,[25] thereby allowing a direct comparison with fMRI data. Spurious correlations can be accounted for by using an orthogonalisation method.[24,26]

In line with previous whole-brain studies,[10-12,16,27] we expected the DBS-effects to extend beyond the 'classical' motor system. In addition, since DBS has been shown to influence oscillations in the alpha and low-beta band[13,14] and functional connectivity in the low and high-beta band,[15] we hypothesized that alpha and beta band functional connectivity changes would reflect symptom relief upon DBS in Parkinson's disease. We therefore performed resting-state MEG recordings with and without STN-DBS stimulation, at least six months after DBS electrode placement. In addition, we assessed whether functional connectivity changes correlated with improvement in motor function, measured using the motor part of the Unified Parkinson's Disease Rating Scale (MDS-UPDRS-III).

Materials and methods

Patients

Parkinson's disease patients who had undergone bilateral implantation of STN DBS electrodes between 2016 and 2018 at Amsterdam UMC, location AMC, were included in this study. Eligibility for STN DBS placement has been described previously.[28] In the context of standard clinical care, the active contacts, voltage, pulse width and frequency of stimulation were individually determined for optimal therapeutic efficacy. Inclusion criteria for the study were: bilateral Boston Scientific Vercise Directed (Valencia, CA, USA) stimulation system (as pilot results demonstrated that this stimulation system was most compatible with our MEG system with respect to the head position estimation; when using a Medtronic Activa PC system (Minneapolis, Minnesota, USA) the noise introduced by the stimulator was such that the head position indicator coils could not be localised by the MEG system), DBS placement at least six months before the MEG recordings, and monopolar stimulation. Exclusion criteria were treatment with levodopa continuous intestinal gel or subcutaneous apomorphine, and permanent post-operative structural damage following DBS electrode placement that could affect the MEG results (apart from the DBS-placement itself).

Disease duration was calculated on the basis of the patients' estimation of the onset of the classical Parkinson's disease motor symptoms. The total dose of dopamine

replacement therapy was converted to the levodopa equivalent daily dose (LEDD), as described previously.[29] The research protocol was approved by the medical ethical committee of the Amsterdam UMC, location VUmc. Ethics review criteria conformed to the Helsinki declaration. After careful explanation of the procedures, all patients gave written informed consent.

Data acquisition

MEG data were recorded using a 306-channel whole-head system (Elekta Neuromag Oy, Helsinki, Finland) in an eyes-closed resting-state condition, with a sample rate of 1250 Hz, and online anti-aliasing (410 Hz) and high-pass (0.1 Hz) filters. Anatomical T1-weighted images of the head were obtained using a 3T MRI scanner (Philips Ingenia, Best, the Netherlands) in the context of standard clinical care before DBS placement. The study visit took place after an overnight withdrawal of dopaminergic medication (practically defined OFF state). The head position relative to the MEG sensors was recorded continuously using the signals from five head position indicator (HPI) coils. The HPI positions were digitized before each recording, as well as the outline of the patient's scalp (~500 points), using a 3D digitizer (Fastrak, Polhemus, Colchester, VT, USA). For each patient total MEG recording time was 55 minutes, consisting of 11 trials of 5 minutes each in which different stimulation settings were explored. At the beginning of each individual trial, localization of the HPI coils was performed in the DBS OFF condition, following which one of the researchers, who monitored the patient inside the magnetically shielded room, changed the DBS-settings and recordings were started. During the recordings, the programming device was kept (offline) in the magnetically shielded room on a stable underground, at approximately 2.5 meters distance from the MEG helmet. The experimental setup can be appreciated from Figure 1.

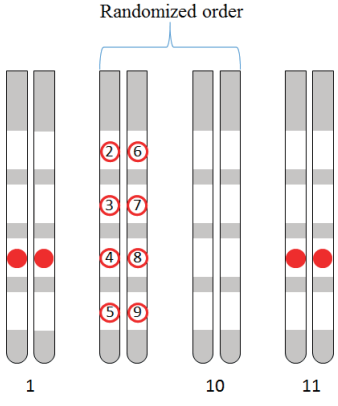

Figure 1 Experimental setup
Overview of the different DBS settings during the MEG recordings. The bilateral electrodes, each having four contact points are depicted (the two middle contact points consisted of triplets of segments, together used as one contact point). During the first MEG recording (1) both electrodes were stimulated in the optimal settings of the patient. The second to tenth MEG recordings took place in a randomized order, during which each of the eight individual contact points were stimulated once (2 & 6, dorsal; 3 & 7, dorsomedial; 4 & 8, ventromedial; 5 & 9 ventral; outside the scope of this study), and one recording took place during DBS OFF (10). During the last MEG recording, both electrodes were, again, stimulated in the optimal settings of the patient (11).

The first recording was during stimulation with the standard (optimal) DBS settings of the individual patient (DBS ON). Then, nine recordings took place in randomized order, eight of which were during unilateral stimulation of one of the eight individual contact points (data not shown), and one recording during DBS OFF. The last recording was, again, during stimulation with the standard DBS settings of each individual patient (DBS ON2; data analyzed as supplementary analysis). The time between recordings, including change of DBS settings and localization of the HPI coils, was at least 2 minutes.

MDS-UPDRS-III scores were measured during DBS ON and OFF on a separate day by trained nurses, approximately six months after DBS-placement. In accordance with the MEG-recordings, these scores were obtained in the dopamine OFF-state.

Data pre-processing

MEG channels that were malfunctioning, for example due to excessive noise, were removed after visual inspection of the data. Thereafter, the temporal extension of Signal Space Separation (tSSS)[30,31] in MaxFilter software (Elekta Neuromag Oy, version 2.2.15) was applied with a sliding window of 10s, origin (0,0,40), and harmonic expansions of 8 respectively 3 for the internal and external signals (all default settings), as well as subspace correlation-limit of 0.8 to suppress the strong magnetic artefacts, which has previously been demonstrated to result in satisfactory data quality without suppression of brain signals.[30,32-34] An example of the effect of tSSS on MEG data recorded in our study is depicted in Supplementary Figure 1. Patient's MEG data were co-registered to their structural MRIs using a surface-matching procedure, with an estimated resulting accuracy of 4 mm.[35] A single sphere was fitted to the outline of the scalp as obtained from the co-registered MRI, which was used as a volume conductor model for the beamformer approach described below.

The automated anatomical labelling (AAL) atlas was used to label the voxels in 78 cortical and 12 subcortical regions of interest (ROIs).[36,37] We used each ROI's most central voxel (centroid) as the representative for that ROI.[38] Subsequently, an atlas-based beamformer approach was used to project broad-band (0.5-48 Hz) filtered sensor signals to these centroid voxels,[39] resulting in broad-band time-series for each centroid of the 90 ROIs. MEG data were visually inspected (by LIB) for tremor-, motion- and stimulation-related artefacts and drowsiness. In addition, for each recording, the 50% epochs with the slowest peak frequency were discarded in order to make the occurrence of drowsiness in the selected data even more unlikely. Epochs contained 4096 samples (3.28 s), and for each condition, 20 epochs with the best quality recordings were selected for further analysis. Spectral and functional connectivity analyses were performed using in-house software (BrainWave, version 0.9.152.12.26; CJS, available from https://home.kpn.nl/stam7883/brainwave.html). For frequency band specific analyses, epochs were filtered in six frequency bands (delta (0.5-4 Hz), theta (4-8 Hz), alpha1 (8-10 Hz), alpha2 (10-13 Hz; as the distinction between alpha1 and alpha2 oscillations does have functional significance),[40] low-beta (13-22 Hz) and high-beta (22-30 Hz), using a fast Fourier Transform.

2.4 Data analysis

We estimated the overall absolute spectral power (0.5-48 Hz) averaged over all ROIs and normalised based on the maximum power peak (Figure 2), as well as the absolute spectral power for each frequency band and ROI separately (Figure 3). Peak frequency values were estimated within the 4-13 Hz frequency range.

For each epoch, frequency-band specific functional connectivity was estimated using the corrected cAEC, an implementation of the AEC[23] corrected for volume conduction/field spread, using a symmetric orthogonalisation procedure.[23,24] The cAEC was calculated for all possible pairs of ROIs, leading to a 90 x 90 adjacency matrix that contained the functional connectivity values between all ROI pairs.

Statistical analysis

For each patient, stimulation condition and frequency band separately, absolute power and cAEC matrices were averaged over 20 epochs. Both mean absolute power and mean cAEC per ROI, hence, functional connectivity of one ROI with the rest of the brain, were compared between the ON and OFF stimulation condition using permutation tests (N = 10000; p < 0.05).[41,42] Correction for false positives was performed using the 'false discovery rate' (FDR), separately for each frequency band, with a p-value for each of the 90 ROIs as input.[43]

The correlations between DBS-related improvement in motor function and changes in functional connectivity were estimated using Spearman tests (without correction for multiple comparisons due to the exploratory nature of the analysis), where percentage improvement in total MDS-UPDRS-III, bradykinesia/rigidity (items 3-7) and tremor (items 15-18) scores were used as measures of motor improvement. Functional connectivity changes were obtained for all six frequency bands averaged over ROIs in i) the sensorimotor cortices (bilateral pre and post-central gyri), ii) all cortical regions, and iii) all subcortical regions. Only patients who had tremor during DBS OFF were selected for correlation analyses on tremor improvement.

Results

Patients

Twenty-one Parkinson's disease patients participated in this study and underwent MEG recordings at Amsterdam UMC, location VUmc, at least 6 months after DBS placement (range 6-15 months). Three patients were excluded from further analysis since their MEG data had too many dysfunctional channels during stimulation (>~13 channels, caused by excessive noise), which prevented the use of tSSS. This led to a final group of 18 Parkinson's disease patients treated with DBS (mean age 58.4 y, SD 8.3), whose characteristics are summarized in Table 1. Thirteen patients suffered from tremor and were used for correlations between functional connectivity changes and tremor effects of DBS. The mean number of excluded MEG channels was 9 for DBS ON recordings (range: 5-13) and 6 for DBS OFF recordings (range: 2-12).

Table 1 Patient characteristics

Patient	Age (years)	Sex	Disease duration (years)	Stimulation parameters (stimulation side; contact point on electrode; intensity (mA))	Pulse width and stimulation frequency	Levodopa equivalent dose (mg/day)		Motor MDS-UPDRS (III)			Tremor subscore (MDS-UPDRS (III))	
						Pre-DBS	Post-DBS	Med OFF/ pre-DBS	Med OFF/ DBS OFF	Med OFF/ DBS ON	Med OFF/ DBS OFF	Med OFF/ DBS ON
1	38	M	8	L; DM; 2.9 R; VM; 3.4	60 µs 179 Hz	1644	996	73	54	31	9	4
2	63	F	5	L; DM; 1.7 R; DM; 1.7	60 µs 130 Hz	495	567	43	16	11	0	0
3	65	F	27	L; VM; 2.7 R; DM; 1.5	60 µs 130 Hz	500	400	33	20	19	4	3
4	49	F	10	L; D; 1.9 R; D; 2.5	60 µs 130 Hz	797	536	35	37	22	1	0
5	69	M	12	L; DM; 2.1 R; DM; 2.1	60 µs 130 Hz	1830	150	56	24	14	2	0
6	60	M	8	L; DM; 3.2 R; DM; 1.3	60 µs 179 Hz	1200	300	57	65	38	8	0
7	53	M	11	L; DM; 2.9 R; DM; 1.9	60 µs 130 Hz	1567	1043	60	44	30	4	3
8	66	F	8	L; VM; 2.2 R; DM; 1.8	60 µs 130 Hz	1226	753	47	37	33	11	6
9	45	M	5	L; D; 1.7 R; DM; 1.7	60 µs 130 Hz	1410	283	50	80	44	12	2
10	70	F	25	L; DM; 2.1 R; DM; 2.4	60 µs 130 Hz	1590	555	46	33	15	0	0
11	66	M	10	L; DM; 2.5 R; DM; 1.8	60 µs 149 Hz	750	575	38	54	27	7	3
12	55	M	8	L; DM; 2.7 R; DM; 2.6	60 µs 130 Hz	950	775	42	31	15	0	0
13	57	M	11	L; VM; 1.6 R; VM; 1.6	60 µs 130 Hz	1134	606	38	21	7	0	0

Patient	Age (years)	Sex	Disease duration (years)	Stimulation parameters (stimulation side; contact point on electrode; intensity (mA))	Pulse width and stimulation frequency	Levodopa equivalent dose (mg/day)		Motor MDS-UPDRS (III)			Tremor subscore (MDS-UPDRS (III))	
						Pre-DBS	Post-DBS	Med OFF/ pre-DBS	Med OFF/ DBS OFF	Med OFF/ DBS ON	Med OFF/ DBS OFF	Med OFF/ DBS ON
14	61	M	7	L; VM; 1.5 R; VM; 2.1	60 µs 130 Hz	1000	375	30	27	11	2	0
15	60	M	14	L; DM; 2.0 R; VM; 2.5	60 µs 130 Hz	1073	425	55	27	7	3	1
16	57	M	12	L; VM; 3.1 R; VM; 2.3	60 µs 130 Hz	1380	720	80	52	26	5	3
17	61	M	8	L; DM; 1.8 R; DM; 2.3	60 µs 130 Hz	1726	946	56	52	21	8	1
18	56	M	12	L; DM; 1.4 R; VM; 1.3	60 µs 130 Hz	2131	1245	45	20	10	0	0
Mean (SD)	58 (8)	M, 13; F, 5	11 (6)	L: 2.2 (0.54) R: 2.0 (0.52)		1245 (456)	625 (294)	49 (13)	39 (18)	21 (11)	4 (4)	1 (2)

mA, milliampere; µs, microseconds; LEDD, Levodopa Equivalent Daily Dose; MDS-UPDRS-III, Movement Disorders Society Unified Parkinson's Disease Rating Scale motor ratings; DBS, Deep Brain Stimulation; M/F, male/female; L/R, left/right; D/DM/VM, Dorsal/Dorsomedial/Ventromedial; Med, medication.

Spectral power

Figure 2 shows global stimulation-related normalized spectral power for all Parkinson's disease patients. The peak frequency was significantly (and, for all but one patient, consistently) higher during stimulation ON compared to stimulation OFF (DBS ON 8.79 Hz ± 0.69; DBS OFF 8.54 ± 0.64 Hz; t(17)= 5.16; p <0.001). Two stimulation-related spectral peaks were not removed by tSSS and beamforming. For all patients, these peaks were present around 27 Hz and 35 Hz. Figure 3 displays significant differences in absolute power per frequency band between DBS ON and DBS OFF. During DBS ON, a decrease in (mostly occipital) power was observed in the delta and theta band, and an increase in band power was observed in the alpha2, low-beta and high-beta band. This suggests a spectral shift towards the higher frequencies. The sensorimotor cortices were hardly involved in this shift, and even showed a right-sided suppression of band power in the frequency range between 0.5 and 22 Hz.

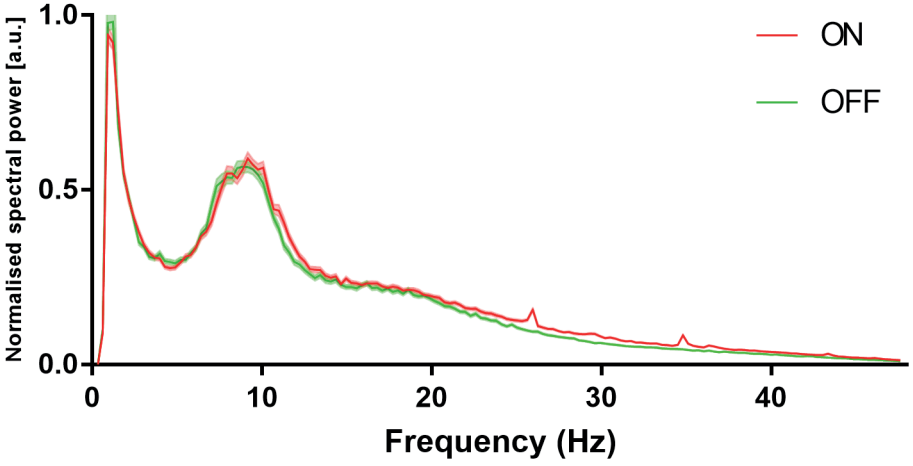

Figure 2 Overall power spectrum
Average of normalised frequency spectra for all patients (*n* = 18) and all regions of interest (*n* = 90), shaded areas indicate standard error of the means. Despite tSSS filtering and the beamforming approach, stimulation artefact peaks remained present at 27 Hz and 35 Hz during DBS ON (red).
DBS, deep brain stimulation; tSSS, spatiotemporal Signal Space Separation.

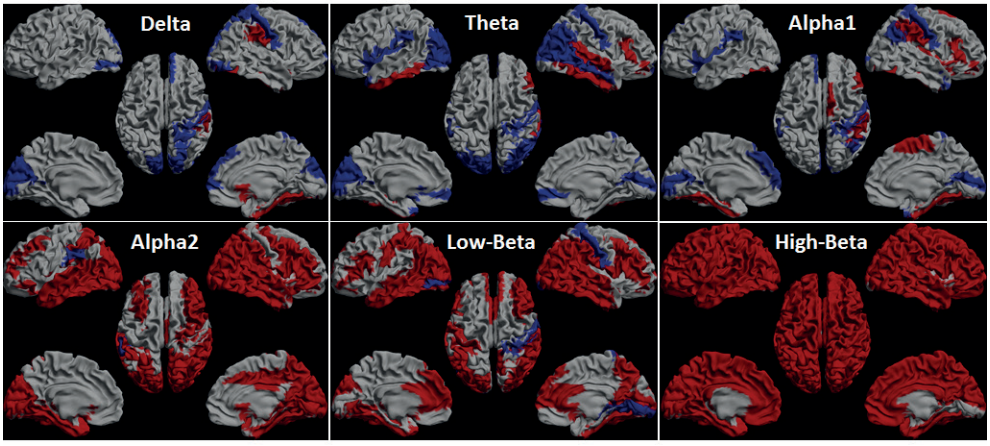

Figure 3 Regional band power changes
Distribution of significant differences (p <0.05, FDR corrected) in absolute band power between DBS ON and DBS OFF. Significant increases (decreases) are displayed in red (blue) on a parcellated template brain viewed from, in clockwise order, the left, top, right, left-midline and right-midline. For visualisation purposes, only cortical brain regions are displayed. During DBS ON, a decrease in (mostly occipital) power was observed in the delta and theta band, and an increase in band power was observed in the alpha2, low-beta and high-beta band, suggesting a spectral shift towards the higher frequencies during DBS ON. Note that the sensorimotor regions were hardly involved in this shift and, instead, showed a decrease in absolute band power for the delta, theta, alpha1, alpha2 and low-beta band.

Functional connectivity

To assess differences in average functional connectivity *per ROI* between DBS ON and DBS OFF, permutation tests were performed for all 90 ROIs in the six frequency bands. Significant differences in cAEC were found for the low-beta band (ten ROIs) and also for the alpha2 band (one ROI) and are listed in Table 2 (as well as visualized in Supplementary Figure 2). The regions that showed the largest increases in functional connectivity following stimulation were mainly located in bilateral frontobasal brain regions, whereas regions that showed significant decreases followed a more dispersed pattern (frontal, parietal and temporal lobes, bilaterally).

Table 2 Significant differences in average cAEC values per region of interest

Frequency band	Anatomical region	L/R	cAEC (DBS ON)	cAEC (DBS OFF)	↑ or ↓	P-value (FDR-corrected)
Alpha2	Middle temporal gyrus	L	0.504	0.499	↑	0.0090
	Gyrus rectus	L	0.514	0.511	↑	0.0210
	Olfactory cortex	L	0.515	0.512	↑	0.0210
	Superior frontal gyrus, orbital part	L	0.513	0.510	↑	0.0210
	Inferior frontal gyrus, triangular part	L	0.511	0.515	↓	0.0210
	Superior frontal gyrus	L	0.510	0.514	↓	0.0090
Low-beta	Superior parietal gyrus	L	0.509	0.513	↓	0.0090
	Anterior cingulate gyrus	L	0.511	0.514	↓	0.0461
	Gyrus rectus	R	0.512	0.510	↑	0.0475
	Superior frontal gyrus, orbital part	R	0.511	0.509	↑	0.0399
	Superior temporal pole	R	0.510	0.512	↓	0.0475
	Thalamus	L	0.518	0.512	↑	0.0475

Comparison between the DBS ON state and the DBS OFF state. Significance threshold $p<0.05$
L, Left; R, Right; cAEC, corrected Amplitude Envelope Correlation; DBS, Deep Brain Stimulation; FDR, False Discovery Rate.

Relationship between clinical motor improvement and functional connectivity changes

A significant positive correlation was found between total DBS-related motor improvement (MDS-UPDRS-III) and low-beta cAEC change in the sensorimotor cortices ($r\text{-}_{SM}\,(16)= 0.58$, $p = 0.011$), the whole cortex ($r\text{-}_{WC}\,(16)= 0.50$, $p = 0.035$), and all subcortical regions ($r\text{-}_{SC}\,(16)= 0.62$, $p = 0.006$) (Figure 4). When only the MDS-UPDRS-III subscores for bradykinesia and rigidity were considered, the correlations with low-beta band cAEC change were even stronger (respectively: $r\text{-}_{SM}\,(16)= 0.61$, $p = 0.007$; $r\text{-}_{WC}\,(16)= 0.70$, $p = 0.001$; $r\text{-}_{SC}\,(16)= 0.76$, $p < 0.001$) (Figure 4). In addition, a significant positive correlation was found between bradykinesia/rigidity subscores and alpha2 band cAEC changes ($r\text{-}_{SM}\,(16)= 0.57$, $p = 0.014$; $r\text{-}_{WC}\,(16)= 0.72$, $p = 0.001$; $r_{\text{-}SC}\,(16)= 0.68$, $p = 0.002$) (Supplementary Table 1). cAEC changes did not correlate significantly with tremor improvement (Figure 4; Supplementary Table 1).

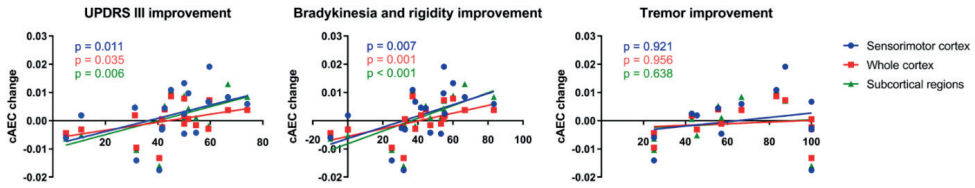

Figure 4 Correlation of functional connectivity changes with improvement in motor scores
Scatter plots of clinical improvement values and low-beta functional connectivity changes (averaged for respectively the sensorimotor cortices, whole cortex and subcortical regions). Left: Significant correlations between MDS-UPDRS-III improvement (% comparing ON versus OFF-DBS) and cAEC changes (absolute difference ON versus OFF-DBS). Sensorimotor cortices (r_{SM} *(16)*= 0.58, p = 0.011), whole cortex (r_{WC} *(16)*= 0.50, p = 0.035), and all subcortical regions (r_{SC} *(16)*= 0.62, p = 0.006). Middle: Significant correlations between bradykinesia/rigidity improvement and cAEC changes (r_{SM} *(16)*= 0.61, p = 0.007; r_{WC}*(16)*= 0.70, p = 0.001; r_{SC} *(16)*= 0.76, p < 0.001). Right: Tremor improvement (n= 13 patients) and cAEC change, no significant correlation. All correlations tested can be found in Supplementary Table 1.
cAEC, corrected Amplitude Envelope Correlation; MDS-UPDRS-III, Movement Disorders Society Unified Parkinson's Disease Rating Scale motor ratings.

Discussion

In this study, we investigated stimulation effects of STN DBS on whole-brain functional connectivity in 18 Parkinson's disease patients. We found that increases in alpha2 and low-beta band functional connectivity were correlated with DBS-related improvements in bradykinesia and rigidity, but not with tremor relief. This suggests that the alleged *anti-kinetic* role of beta band oscillations[6,44-46] does not apply when large-scale cortico-cortical and cortico-subcortical functional interactions are taken into account. In addition, and in accordance with previous studies,[12-14] we found a suppression of sensorimotor cortical oscillatory activity (ranging from delta to low-beta band) against a background of widespread stimulation-related increases in oscillatory brain activity involving the higher frequencies.

6.1

Band power

Our present observations confirm previous results on band power changes associated with DBS. Firstly, during DBS ON, throughout the cerebral cortex, higher absolute band powers were observed for the higher frequencies (10-30 Hz), whereas lower absolute band powers were found for the lower frequencies (0.5-8 Hz), which could be interpreted as an overall acceleration of oscillatory brain activity. Furthermore, during DBS ON the alpha peak frequency was significantly higher than during DBS OFF. However, since the DBS ON recording was always the first recording of the day, we cannot exclude the possibility that the order of recordings (for example due to increased drowsiness in subsequent recordings) added to the observed spectral shift. Therefore, we additionally studied spectral power in the ON2 recording, which always took place as the last recording. In Supplementary Figure 3 we illustrate the band power differences between ON2 and DBS OFF (n = 17, data for one patient was excluded due to excessive noise of the ON2 recording): Again, stimulation led to an increase in band power for the higher frequencies (8-30 Hz), and a higher frequency of the alpha peak (DBS ON2 8.64, SD 0.69 vs DBS OFF

8.55, SD 0.65; *t(16)*= 2.06, *p* = 0.056). Hence, we conclude that the observed acceleration of oscillatory brain activity is stimulation related, which is in line with the results of an earlier study [12]). This effect has previously been attributed to a non-specific increase in intrinsic alertness, independent of motor function.[47,48] Alternatively, it may reflect a stimulation-related "release" of the thalamus, which affects cortical brain rhythms.[49] However, we cannot exclude the possibility that noise from the stimulator changes the aperiodic "background" 1/f component of the neural power spectrum, thereby causing a peak frequency shift towards the faster frequencies.[50] Secondly, we confirmed alpha and beta band suppression in the sensorimotor regions which was previously observed after DBS in Parkinson's disease patients[13,14] and following transcranial direct current stimulation over the sensorimotor cortex in healthy controls,[51] although this effect was less distinct in our study. Perhaps the fact that our recordings took place in an eyes-closed condition, during which the posterior dominant alpha rhythm is stronger than during an eyes-open condition, may have "blurred" these specific effects.

Functional connectivity

The presently observed correlation between increases in functional connectivity and improvements in bradykinesia and rigidity scores is in contradiction with the observations reported by Silberstein and co-workers, who were the first (and up to now the only) to study the effect of DBS on whole-brain functional connectivity.[46] They used coherence analysis of (scalp-recorded) EEG data, obtained in DBS-patients with and without stimulation and found reductions in 10-35 Hz coherence between EEG channels that correlated with overall MDS-UPDRS-III improvement. A potential explanation for the discrepancy with our results is the sensitivity of coherence analysis to volume conduction and band power changes (and thereby signal-to-noise ratio (SNR) changes).[52,53] Indeed, the authors observed positive correlations between therapy-induced power and coherence changes. Hence, taking into account the reduction of (mostly alpha and beta band) power around the sensorimotor cortex due to DBS [13,14], the correlations between reduced coherence and improvement of motor function reported by Silberstein et al. may have been influenced by band power changes. In addition, although unlikely to be the sole explanation for the discrepancy between the two studies, MEG and EEG measure different components of the electromagnetic fields generated by neuronal activity, resulting in different sensitivity profiles.[54,55] Importantly, although cortico-subcortical functional connections do seem to matter (Supplementary Figure 4C), the correlations we observed between increases in functional connectivity and clinical improvement cannot fully be explained by the inclusion of subcortical brain regions in our study, since this correlation remained after excluding cortico-subcortical interactions from our analyses (results not shown).

So far, two MEG-studies have assessed the influence of an acute dopaminergic challenge on whole-brain functional connectivity. Stoffers et al. demonstrated, upon levodopa administration, increases in both short-distance functional connectivity (averaging connectivity values for all possible sensor pairs overlying a lobe; 4-30 Hz) and long-

range functional connectivity (averaging values for all possible sensor pairs between two lobes; 13-30 Hz), assessed using the synchronization likelihood (SL). In patients with a strong dopamine-related improvement in motor scores, motor improvement was associated with *decreases* in local beta band SL.[56] Although we have confirmed the range of effects of DBS on functional connectivity in this study, *i.e.* both decreases and increases, strongest bradykinesia and rigidity improvement were related to *increases* in functional connectivity in our study. Again, volume conduction might have played a role in this partial discrepancy, since SL is sensitive to volume conduction/field spread and the functional connectivity analysis was performed in sensor space. Volume conduction/field spread leads to multiple recording sites picking up signals from a single source, which may result in erroneous estimates of functional connectivity.[53] The fact that only *local* beta band SL showed the discrepancy described supports the notion that volume conduction/field spread might have affected the relationship that was found. In accordance with this line of reasoning, using a functional connectivity measure that is insensitive to the effects of volume conduction/field spread (phase lag index; PLI) others have also found a positive correlation between functional connectivity changes in the left parietal area and improvement in motor function after a dopamine challenge.[57]

In contrast with the aforementioned studies, our main results are not based on an acute DBS stimulation challenge, but rather compares DBS ON with DBS OFF. We did however record acute stimulation data in the optimal settings of the patient at the end of each experiment, namely during condition DBS ON2. Although this recording started immediately after switching on the DBS and stimulation effects may not have been maximally present yet, we again found a significant correlation between functional connectivity increases in the subcortical regions and bradykinesia/rigidity improvement ($r_{SC}(15)$= 0.57, p = 0.017), as well as positive trends for the sensorimotor regions ($r_{SM}(15)$= 0.43, p = 0.088) and the cortex as a whole ($r_{WC}(15)$= 0.36, p = 0.152). Therefore, we conclude that the order of stimulation (first DBS ON recording and then the DBS OFF recording, or the other way around) has not influenced the observed direction of correlations found.

In the present study, a differential effect of DBS on alpha2 and low-beta functional connectivity was found. As shown in Supplementary Figure 4, in Parkinson's disease patients who had a modest clinical response to DBS we observed a decrease in whole-brain functional connectivity, whereas in Parkinson's disease patients who had a good clinical response we observed an increase, involving cortico-subcortical connections (Supplementary Figure 4C). We propose the possibility of a technical as well as a physiological explanation for the observed effect.

The technical explanation involves the potential effect of stimulation artefacts in the DBS ON condition, and thereby the addition of 'noise', onto the reconstructed neuronal signals. The effect of the resulting changes in SNR on source level functional connectivity is complex, but stimulation-related noise may have had a lowering effect on functional connectivity (see Schoffelen et al.[53] for further reading). Along this line of reasoning,

stimulation could have led to a lowering in global functional connectivity for *all* DBS-patients, on top of which small increases in functional connectivity co-occurred with slight clinical improvement (but were covered by noise-related functional connectivity decreases) and large increases in functional connectivity co-occurred with strong clinical improvement (which became apparent as functional connectivity increases). In Supplementary Figure 5 we show that the addition of spatially correlated white noise onto brain signals of two of our DBS-patients during DBS OFF indeed leads to a global decrease in estimated low-beta cAEC. This illustrates that the extra noise introduced by deep brain stimulation (simulated here as spatially correlated white noise) could have led to a reduction in estimated functional connectivity values. However, the addition of spatially correlated white noise hardly affected theta cAEC values in one patient. Hence, this effect seems frequency-dependent, and is perhaps related to the more prominent presence of amplitude envelope correlations in the alpha and beta band.[24]

An alternative, physiological, explanation for the observed differential effect may lie in the complex balance between the different cortico-subcortical functional circuits that converge in the STN. Stimulation in and around the STN can affect cortical brain regions antidromically via axonal stimulation, and can also have downstream effects on the cortico-striato-thalamic loop. We hypothesize that a shift in balance from antidromic axonal towards downstream effects might play a role in the link between better clinical effects and increases in functional connectivity. An overview of the hypothesis can be found in Figure 5 and reads as follows:

Antidromic stimulation effects of axons (en route to other structures, or of axons that terminate in the STN) can affect the motor cortex via the hyperdirect pathway, but can also affect a wide variety of other cortical brain regions.[58,59] Stimulation effects downstream from the stimulated STN affect the cortico-striato-thalamic loop. The net effect on functional connectivity might not be the same for antidromic axonal and downstream stimulation effects. A dynamic causal modelling study demonstrated that upon DBS, the effective functional connectivity strength of the hyperdirect and indirect (striato-STN and STN-thalamus) pathway decreased, whereas the strength of the direct cortico-striato-pallido-thalamic pathway increased,[16] the latter being suggested by an empirical fMRI study,[60] as well as by our own additional visualizations in patients with a good clinical response, who had increases in cortico-subcortical functional connectivity (Supplementary Figure 4C; although we lack the spatial resolution to draw conclusions on the functional connectivity profiles of individual subcortical brain regions). Via downstream effects, effective modulation of the STN could reduce the indirect inhibitory drive from the subthalamic nucleus to the thalamus, which would "release" the thalamus to communicate with cortical brain regions.[19,49] Furthermore, beneficial effects of stimulation on the resting motor system were better explained by strengthening the coupling along the direct pathway, and not by reducing coupling along the hyperdirect pathway.[16,19] This observation was supported by an MEG study by Oswal et al., who found

that a stimulation-related decrease in functional connectivity of the hyperdirect pathway was not related to clinical improvement.[15]

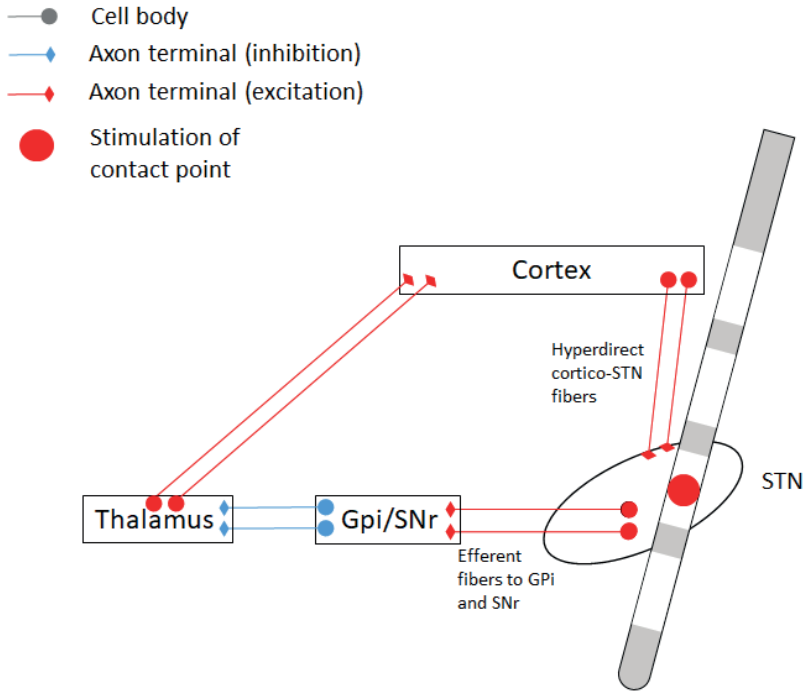

Figure 5 Model of antidromic and downstream effects in STN-DBS
Stimulation effects in the antidromic direction take place upon stimulation of axons of the hyperdirect pathway. These stimulation effects may cause a suppression of band power in frontal cortical brain regions, as well as a lowering of functional connectivity between the frontal cortex and the STN (see also [13-15]). At the same time, stimulation can have downstream effects through the indirect cortico-striato-pallido-thalamic pathway. Downstream stimulation effects may lead to an increase in cortical functional connectivity via disinhibition of the thalamus.[19,60]
Gpi, internal globus pallidus; SNr, substantia nigra pars reticulate; STN, subthalamic nucleus; DBS, deep brain stimulation.

We expect the individual anatomy of white matter tracts, as well as the exact stimulation site in and around the STN (illustrated in Supplementary Figure 6 and Supplementary Table 2), to play a crucial role in the balance between antidromic axonal and downstream effects. Clearly, our hypothesis will have to be substantiated in future studies that combine local stimulation effects with whole-brain effects, such as LFP recordings combined with MEG recordings. In addition, the MEG data recorded in our study during stimulation of each individual contact point (data not shown), will be analyzed in future studies and may shed further light on this matter.

Methodological issues

Several methodological issues deserve consideration. i) In our study, DBS was off for several minutes before we started the 5 minutes recording. We expect that stronger DBS-related effects could have been observed if the period between turning off the DBS and the start of the MEG-recording had been longer. During epoch selection, we prioritized epochs from later parts of the recordings. However, considering that at least 50% of the total clinical change seems to occur within 5 minutes after the DBS is turned off,[61] and since we did observe significant changes in brain activity in parallel with a clinical correlate, we believe that our experimental setup was effective. ii) The MDS-UPDRS-III assessments were always performed 6 months after DBS-placement, whereas the MEG recordings took place between six and fifteen months after surgery. The six months' time period made sure that the patients were measured in a clinically stable state. In one patient the stimulation was switched to a more dorsal contact point in the period between clinical assessments and the MEG recordings, due to non-motor side effects (patient 4). In all other patients, clinical assessments and MEG recordings took place during stimulation of the same contact points and with approximately the same stimulation strength (mean difference left-sided contact points 0.12 mA SD 0.25; right-sided contact points 0.05 mA SD 0.21). Although this separation in time may have affected our results, the correlation between clinical improvement and functional connectivity changes would probably have been even stronger if the MEG recordings and clinical assessments had taken place on the same day. iii) The use of the temporal extension of tSSS[30,31] allowed us to study brain signals during DBS. Despite the ability of tSSS and beamforming to effectively suppress artefacts[62] (see also Supplementary Figure 7 for the effect of tSSS on magnetometers and gradiometers separately), two sharp stimulation-related peaks were seen in the power spectrum (Fig. 1), in line with previous research.[12] We are aware that monopolar stimulation is associated with stronger artefacts than bipolar stimulation, but we chose to stimulate in the monopolar setting in our study as this represented the clinical setting of our patients. The peaks appeared not to affect the frequency range below 22 Hz, which encouraged us to separately consider the low-beta band and the high-beta band, and to refrain from analysing the gamma band. The observed relationship between alpha2 and low-beta functional connectivity changes and clinical improvement seem to confirm the validity of our recording and analysis approach. Obviously, the high-beta band results should be interpreted with caution and the stimulation-related increase in high-beta band power (Fig. 3) may be related to a stimulation artefact; In addition, the lack of a clinical correlate with high-beta band functional connectivity could also mean that stimulation artefacts affected the reconstruction of the brain signals too much in this band or, alternatively, that high-beta band functional connectivity does not reflect DBS-related clinical improvement. iv) Methodological advances in beamforming[63,64] allow MEG signals to be projected onto an atlas-based source space encompassing both cortical and subcortical brain regions.[65,66] In the present study, this approach enabled us to study large scale cortico-subcortical interactions six months after surgery when 'stun effects' of the DBS placement have disappeared, instead of directly after surgery

using LFP analysis with externalised DBS leads. Previous LFP studies have analyzed fine-grained interactions between the STN and the cortex (e.g. [15,67-70]), whereas our study lacks this spatial resolution. We were therefore not able to draw conclusions regarding individual subcortical regions, yet our coarser approach is complementary to the existing literature. v) The lack of a correlation between functional connectivity changes and tremor improvement may reflect a difference in pathophysiological mechanisms underlying bradykinesia/rigidity on the one hand and tremor on the other hand. However, we cannot exclude the possibility of a false-negative finding, since the number of patients suffering from tremor was lower than the number of patients suffering from bradykinesia/rigidity (n=13 versus n=18, respectively). In addition, the lack of correlation may be driven by the patients with 100% tremor improvement, who demonstrated an unexpected lowering of functional connectivity upon stimulation (considering the results for patients with less improvement). However, we do not have a plausible explanation for this observation. vi) Lastly, the correlations between clinical improvement and functional connectivity changes might have been affected by the stimulation strength or the dopaminergic state of the patients. However, we did not correct for this, since these parameters did not correlate with clinical improvement (correlation LEDD and bradykinesia/rigidity improvement $r(16)=0.340$, $p=0.168$; correlation stimulation strength and bradykinesia/rigidity improvement $r(16)=0.012$, $p=0.961$).

Conclusion

In conclusion, we found a DBS-related suppression of sensorimotor cortical oscillatory activity against a background of widespread stimulation-related increases in oscillatory brain activity involving the higher frequencies. Increases in alpha2 and low-beta functional connectivity were correlated with bradykinesia/rigidity improvement, but not with tremor improvement. Our results provide new insights in the mechanism of action of DBS as they complement the alleged "anti-kinetic" effect of beta band oscillations, and suggest a "pro-kinetic" effect when large-scale cortico-cortical and cortico-subcortical functional interactions are taken into consideration.

Acknowledgements

We would like to thank all patients for their participation. We thank Gosia Iwan, Miranda Postma, Marije Scholten, Rosanne Prins, and Sharon Stoker-van Dijk for the MDS-UPDRS-III assessments, as well as their help with patient inclusions. We also thank Karin Plugge, Nico Akemann and Marieke Alting Siberg for the MEG acquisitions, and Pelle Wilbers for help with pre-processing and preliminary analyses.

References

1. Benabid AL, Koudsie A, Benazzouz A, et al. Deep brain stimulation of the corpus luysi (subthalamic nucleus) and other targets in Parkinson's disease. Extension to new indications such as dystonia and epilepsy. J Neurol. 2001;248 Suppl 3:Iii37-47.
2. Deuschl G, Schade-Brittinger C, Krack P, et al. A randomized trial of deep-brain stimulation for Parkinson's disease. N Engl J Med. 2006;355(9):896-908.
3. Helmich RC. The cerebral basis of Parkinsonian tremor: A network perspective. Mov Disord. 2018;33(2):219-31.
4. Louis ED, Tang MX, Cote L, et al. Progression of parkinsonian signs in Parkinson disease. Arch Neurol. 1999;56(3):334-7.
5. Brown P, Williams D. Basal ganglia local field potential activity: character and functional significance in the human. Clin Neurophysiol. 2005;116(11):2510-9.
6. Hammond C, Bergman H, Brown P. Pathological synchronization in Parkinson's disease: networks, models and treatments. Trends Neurosci. 2007;30(7):357-64.
7. Kühn AA, Kupsch A, Schneider GH, et al. Reduction in subthalamic 8–35 Hz oscillatory activity correlates with clinical improvement in Parkinson's disease. Eur J Neurosci. 2006;23(7):1956-60.
8. Brown P. Oscillatory nature of human basal ganglia activity: relationship to the pathophysiology of Parkinson's disease. Mov Disord. 2003;18(4):357-63.
9. McGregor MM, Nelson AB. Circuit Mechanisms of Parkinson's Disease. Neuron. 2019;101(6):1042-56.
10. Cao C, Li D, Jiang T, et al. Resting state cortical oscillations of patients with Parkinson disease and with and without subthalamic deep brain stimulation: a magnetoencephalography study. J Clin Neurophysiol. 2015;32(2):109-18.
11. Cao CY, Zeng K, Li DY, et al. Modulations on cortical oscillations by subthalamic deep brain stimulation in patients with Parkinson disease: A MEG study. Neurosci Lett. 2017;636:95-100.
12. Airaksinen K, Butorina A, Pekkonen E, et al. Somatomotor mu rhythm amplitude correlates with rigidity during deep brain stimulation in Parkinsonian patients. Clin Neurophysiol. 2012;123(10):2010-7.
13. Abbasi O, Hirschmann J, Storzer L, et al. Unilateral deep brain stimulation suppresses alpha and beta oscillations in sensorimotor cortices. Neuroimage. 2018;174:201-7.
14. Luoma J, Pekkonen E, Airaksinen K, et al. Spontaneous sensorimotor cortical activity is suppressed by deep brain stimulation in patients with advanced Parkinson's disease. Neurosci Lett. 2018;683:48-53.
15. Oswal A, Beudel M, Zrinzo L, et al. Deep brain stimulation modulates synchrony within spatially and spectrally distinct resting state networks in Parkinson's disease. Brain. 2016;139(Pt 5):1482-96.
16. Kahan J, Urner M, Moran R, et al. Resting state functional MRI in Parkinson's disease: the impact of deep brain stimulation on 'effective' connectivity. Brain. 2014;137(Pt 4):1130-44.
17. Boon LI, Geraedts VJ, Hillebrand A, et al. A systematic review of MEG-based studies in Parkinson's disease: The motor system and beyond. Hum Brain Mapp. 2019;40(9):2827-48.
18. Harmsen IE, Rowland NC, Wennberg RA, et al. Characterizing the effects of deep brain stimulation with magnetoencephalography: A review. Brain stimulation. 2018;11(3):481-91.
19. Nambu A, Tokuno H, Takada M. Functional significance of the cortico-subthalamo-pallidal 'hyperdirect' pathway. Neurosci Res. 2002;43(2):111-7.
20. Baillet S. Magnetoencephalography for brain electrophysiology and imaging. Nat Neurosci. 2017;20(3):327-39.
21. Oswal A, Jha A, Neal S, et al. Analysis of simultaneous MEG and intracranial LFP recordings during Deep Brain Stimulation: a protocol and experimental validation. J Neurosci Methods. 2016;261:29-46.

22. Abbasi O, Hirschmann J, Schmitz G, et al. Rejecting deep brain stimulation artefacts from MEG data using ICA and mutual information. J Neurosci Methods. 2016;268:131-41.
23. Brookes MJ, Woolrich MW, Barnes GR. Measuring functional connectivity in MEG: a multivariate approach insensitive to linear source leakage. Neuroimage. 2012;63(2):910-20.
24. Hipp JF, Hawellek DJ, Corbetta M, et al. Large-scale cortical correlation structure of spontaneous oscillatory activity. Nat Neurosci. 2012;15(6):884-90.
25. Brookes MJ, Woolrich M, Luckhoo H, et al. Investigating the electrophysiological basis of resting state networks using magnetoencephalography. Proc Natl Acad Sci U S A. 2011;108(40):16783-8.
26. Colclough GL, Brookes MJ, Smith SM, et al. A symmetric multivariate leakage correction for MEG connectomes. Neuroimage. 2015;117:439-48.
27. Hill KK, Campbell MC, McNeely ME, et al. Cerebral blood flow responses to dorsal and ventral STN DBS correlate with gait and balance responses in Parkinson's disease. Exp Neurol. 2013;241:105-12.
28. Contarino MF, Bour LJ, Verhagen R, et al. Directional steering: A novel approach to deep brain stimulation. Neurology. 2014;83(13):1163-9.
29. Olde Dubbelink KT, Stoffers D, Deijen JB, et al. Cognitive decline in Parkinson's disease is associated with slowing of resting-state brain activity: a longitudinal study. Neurobiol Aging. 2013;34(2):408-18.
30. Taulu S, Hari R. Removal of magnetoencephalographic artifacts with temporal signal-space separation: demonstration with single-trial auditory-evoked responses. Hum Brain Mapp. 2009;30(5):1524-34.
31. Taulu S, Simola J. Spatiotemporal signal space separation method for rejecting nearby interference in MEG measurements. Phys Med Biol. 2006;51(7):1759-68.
32. Carrette E, De Tiege X, Op De Beeck M, et al. Magnetoencephalography in epilepsy patients carrying a vagus nerve stimulator. Epilepsy research. 2011;93(1):44-52.
33. Medvedovsky M, Taulu S, Bikmullina R, et al. Fine tuning the correlation limit of spatio-temporal signal space separation for magnetoencephalography. J Neurosci Methods. 2009;177(1):203-11.
34. Boring MJ, Jessen ZF, Wozny TA, et al. Quantitatively validating the efficacy of artifact suppression techniques to study the cortical consequences of deep brain stimulation with magnetoencephalography. Neuroimage. 2019;199:366-74.
35. Whalen C, Maclin EL, Fabiani M, et al. Validation of a method for coregistering scalp recording locations with 3D structural MR images. Hum Brain Mapp. 2008;29(11):1288-301.
36. Gong G, He Y, Concha L, et al. Mapping anatomical connectivity patterns of human cerebral cortex using in vivo diffusion tensor imaging tractography. Cereb Cortex. 2009;19(3):524-36.
37. Tzourio-Mazoyer N, Landeau B, Papathanassiou D, et al. Automated anatomical labeling of activations in SPM using a macroscopic anatomical parcellation of the MNI MRI single-subject brain. Neuroimage. 2002;15(1):273-89.
38. Hillebrand A, Tewarie P, van Dellen E, et al. Direction of information flow in large-scale resting-state networks is frequency-dependent. Proc Natl Acad Sci U S A. 2016;113(14):3867-72.
39. Hillebrand A, Barnes GR, Bosboom JL, et al. Frequency-dependent functional connectivity within resting-state networks: an atlas-based MEG beamformer solution. Neuroimage. 2012;59(4):3909-21.
40. Klimesch W, Schack B, Sauseng P. The functional significance of theta and upper alpha oscillations. Exp Psychol. 2005;52(2):99-108.
41. Maris E, Oostenveld R. Nonparametric statistical testing of EEG- and MEG-data. J Neurosci Methods. 2007;164(1):177-90.
42. Nichols TE, Holmes AP. Nonparametric permutation tests for functional neuroimaging: a primer with examples. Hum Brain Mapp. 2002;15(1):1-25.

43. Benjamini Y, Hochberg Y. Controlling the False Discovery Rate: A Practical and Powerful Approach to Multiple Testing. J R Stat Soc Series B Stat Methodol1995;57(1):289-300.
44. Levy R, Ashby P, Hutchison WD, et al. Dependence of subthalamic nucleus oscillations on movement and dopamine in Parkinson's disease. Brain. 2002;125(6):1196-209.
45. Heinrichs-Graham E, Kurz MJ, Becker KM, et al. Hypersynchrony despite pathologically reduced beta oscillations in patients with Parkinson's disease: a pharmaco-magnetoencephalography study. J Neurophysiol. 2014;112(7):1739-47.
46. Silberstein P, Pogosyan A, Kühn AA, et al. Cortico-cortical coupling in Parkinson's disease and its modulation by therapy. Brain. 2005;128(6):1277-91.
47. Jech R, Ruzicka E, Urgosik D, et al. Deep brain stimulation of the subthalamic nucleus affects resting EEG and visual evoked potentials in Parkinson's disease. Clin Neurophysiol. 2006;117(5):1017-28.
48. Fimm B, Heber IA, Coenen VA, et al. Deep brain stimulation of the subthalamic nucleus improves intrinsic alertness in Parkinson's disease. Mov Disord. 2009;24(11):1613-20.
49. DeLong MR, Wichmann T. Circuits and circuit disorders of the basal ganglia. Arch Neurol. 2007;64(1):20-4.
50. Haller M, Donoghue T, Peterson E, et al. Parameterizing neural power spectra. Nat Neurosci. 2020 Dec;23(12):1655-1665.
51. Pellegrino G, Maran M, Turco C, et al. Bilateral Transcranial Direct Current Stimulation Reshapes Resting-State Brain Networks: A Magnetoencephalography Assessment. Neural plasticity. 2018;2018:2782804.
52. Palva S, Palva JM. Discovering oscillatory interaction networks with M/EEG: challenges and breakthroughs. Trends Cogn Sci. 2012;16(4):219-30.
53. Schoffelen JM, Gross J. Source connectivity analysis with MEG and EEG. Hum Brain Mapp. 2009;30(6):1857-65.
54. Goldenholz DM, Ahlfors SP, Hamalainen MS, et al. Mapping the signal-to-noise-ratios of cortical sources in magnetoencephalography and electroencephalography. Hum Brain Mapp. 2009;30(4):1077-86.
55. Muthuraman M, Hellriegel H, Hoogenboom N, et al. Beamformer source analysis and connectivity on concurrent EEG and MEG data during voluntary movements. PLoS One. 2014;9(3):e91441.
56. Stoffers D, Bosboom JL, Wolters EC, et al. Dopaminergic modulation of cortico-cortical functional connectivity in Parkinson's disease: an MEG study. Exp Neurol. 2008;213(1):191-5.
57. Cao C, Li D, Zeng K, et al. Levodopa Reduces the Phase lag Index of Parkinson's Disease Patients: A Magnetoencephalographic Study. Clin EEG Neurosci. 2018:1550059418781693.
58. Whitmer D, de Solages C, Hill B, et al. High frequency deep brain stimulation attenuates subthalamic and cortical rhythms in Parkinson's disease. Front Hum Neurosci. 2012;6:155.
59. Accolla EA, Herrojo Ruiz M, Horn A, et al. Brain networks modulated by subthalamic nucleus deep brain stimulation. Brain. 2016;139(Pt 9):2503-15.
60. Mueller K, Jech R, Ruzicka F, et al. Brain connectivity changes when comparing effects of subthalamic deep brain stimulation with levodopa treatment in Parkinson's disease. Neuroimage Clin. 2018;19:1025-35.
61. Little S, Pogosyan A, Neal S, et al. Adaptive deep brain stimulation in advanced Parkinson disease. Ann Neurol. 2013;74(3):449-57.
62. Hillebrand A, Fazio P, de Munck JC, et al. Feasibility of clinical magnetoencephalography (MEG) functional mapping in the presence of dental artefacts. Clin Neurophysiol. 2013;124(1):107-13.
63. Hillebrand A, Singh KD, Holliday IE, et al. A new approach to neuroimaging with magnetoencephalography. Hum Brain Mapp. 2005;25(2):199-211.
64. Hillebrand A, Barnes GR. Beamformer analysis of MEG data. Int Rev Neurobiol. 2005;68:149-71.
65. Boon LI, Hillebrand A, Dubbelink KTO, et al. Changes in resting-state directed connectivity in

cortico-subcortical networks correlate with cognitive function in Parkinson's disease. Clin Neurophysiol. 2017;128(7):1319-26.

66. Hillebrand A, Nissen I, Ris-Hilgersom I, et al. Detecting epileptiform activity from deeper brain regions in spatially filtered MEG data. Clin Neurophysiol. 2016;127(8):2766-9.
67. Hirschmann J, Hartmann CJ, Butz M, et al. A direct relationship between oscillatory subthalamic nucleus-cortex coupling and rest tremor in Parkinson's disease. Brain. 2013;136(Pt 12):3659-70.
68. Hirschmann J, Ozkurt TE, Butz M, et al. Distinct oscillatory STN-cortical loops revealed by simultaneous MEG and local field potential recordings in patients with Parkinson's disease. Neuroimage. 2011;55(3):1159-68.
69. Hirschmann J, Ozkurt TE, Butz M, et al. Differential modulation of STN-cortical and cortico-muscular coherence by movement and levodopa in Parkinson's disease. Neuroimage. 2013;68:203-13.
70. Litvak V, Jha A, Eusebio A, et al. Resting oscillatory cortico-subthalamic connectivity in patients with Parkinson's disease. Brain. 2011;134(Pt 2):359-74.
71. Xia M, Wang J, He Y. BrainNet Viewer: a network visualization tool for human brain connectomics. PLoS One. 2013;8(7):e68910.
72. Horn A, Li N, Dembek TA, et al. Lead-DBS v2: Towards a comprehensive pipeline for deep brain stimulation imaging. Neuroimage. 2019;184:293-316.
73. Prent N, Potters WV, Boon LI, et al. Distance to white matter tracts is associated with deep brain stimulation motor outcome in Parkinson's disease. J Neurosurg. 2019:1-10.

Supplementary materials

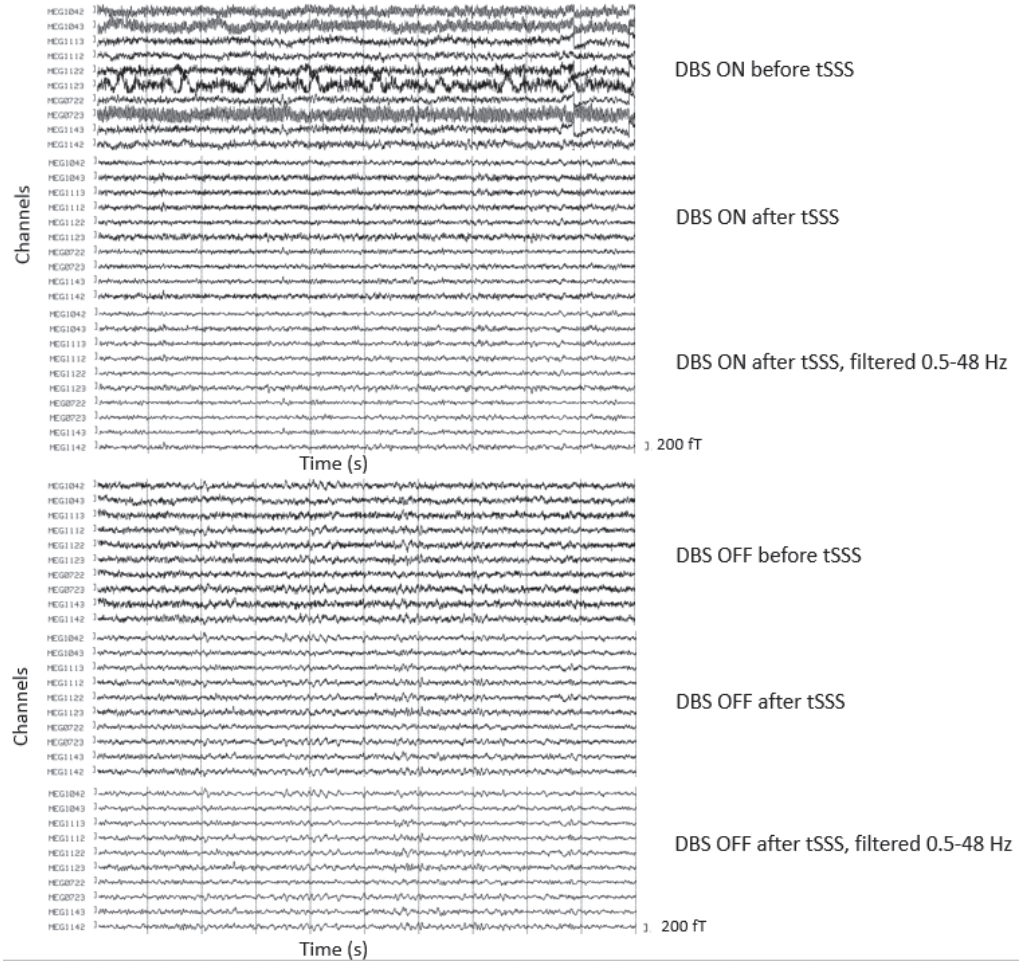

Supplementary Figure 1 Raw MEG data of a representative PD patient with STN-DBS, before tSSS, after tSSS, and after tSSS and broadband filtering (0.5-48 Hz). A selection of right parietal gradiometers are depicted, both during DBS ON- and OFF. The amplitude of the raw data at DBS ON is higher than the data after tSSS, indicating that artefacts from electrical stimulation are discarded by the tSSS algorithm. 10 seconds of recording is depicted.

MEG, magnetoencephalography; PD, Parkinson's disease; STN-DBS, subthalamic deep brain stimulation; tSSS, temporal Signal Space Separation; fT, femtoTesla

Supplementary Table 1 Correlation of functional connectivity changes with improvement in motor scores

Spearman's rho		UPDRS-III total	UPDRS-III Bradykinesia and Rigidity	UPDRS-III Tremor
Theta	Sensorimotor cortex	0.08 (p = 0.741)	0.41 (p = 0.090)	-0.18 (p = 0.572)
	Whole cortex	-0.25 (p = 0.319)	0.07 (p = 0.785)	-0.38 (p = 0.221)
	Subcortical regions	-0.22 (p = 0.375)	0.09 (p = 0.717)	-0.32 (p = 0.303)
Alpha1	Sensorimotor cortex	-0.23 (p = 0.353)	-0.11 (p = 0.657)	-0.19 (p = 0.549)
	Whole cortex	-0.16 (p = 0.514)	-0.34 (p = 0.893)	-0.15 (p = 0.642)
	Subcortical regions	-0.12 (p = 0.623)	0.02 (p = 0.945)	-0.35 (p = 0.271)
Alpha2	Sensorimotor cortex	0.29 (p = 0.293)	**0.57 (p = 0.014)**	-0.24 (p = 0.455)
	Whole cortex	0.43 (p = 0.072)	**0.72 (p = 0.001)**	-0.42 (p = 0.169)
	Subcortical regions	0.42 (p = 0.080)	**0.68 (p = 0.002)**	-0.47 (p = 0.126)
Low-beta	Sensorimotor cortex	**0.58 (p = 0.011)**	**0.61 (p = 0.007)**	-0.03 (p = 0.921)
	Whole cortex	**0.50 (p = 0.035)**	**0.70 (p = 0.001)**	-0.02 (p = 0.956)
	Subcortical regions	**0.62 (p = 0.006)**	**0.76 (p < 0.001)**	0.13 (p = 0.638)
High-beta	Sensorimotor cortex	0.02 (p = 0.951)	-0.04 (p = 0.861)	0.24 (p = 0.448)
	Whole cortex	0.00 (p = 0.997)	-0.04 (p = 0.880)	-0.32 (p = 0.309)
	Subcortical regions	0.21 (p = 0.403)	0.15 (p = 0.559)	-0.51 (p = 0.090)

Spearman correlations between the change in clinical scores (UPDRS-III total, bradykinesia/rigidity sub score, and tremor sub score) and the change in cAEC upon stimulation. The correlations with a p-value lower than 0.05 are marked in bold.
cAEC, corrected Amplitude Envelope Correlation; UPDRS-III, Unified Parkinson's Disease Rating Scale motor ratings.

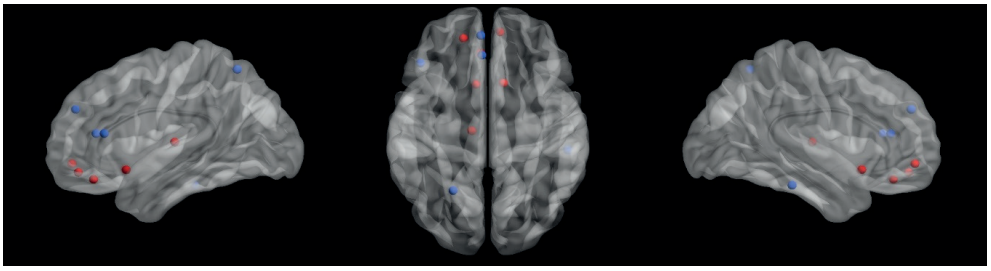

Supplementary Figure 2 Stimulation-related significant differences in functional connectivity (low-beta band) between DBS-ON and DBS-OFF

Nodes represent brain regions, where the colors indicate significantly higher (red), or significantly lower (blue) functional connectivity of that node with the rest of the brain. Left lateral (left panel), top (middle panel) and right lateral (right panel) views of a template brain are shown.[71] Names of the relevant brain regions can be appreciated from Table 2.

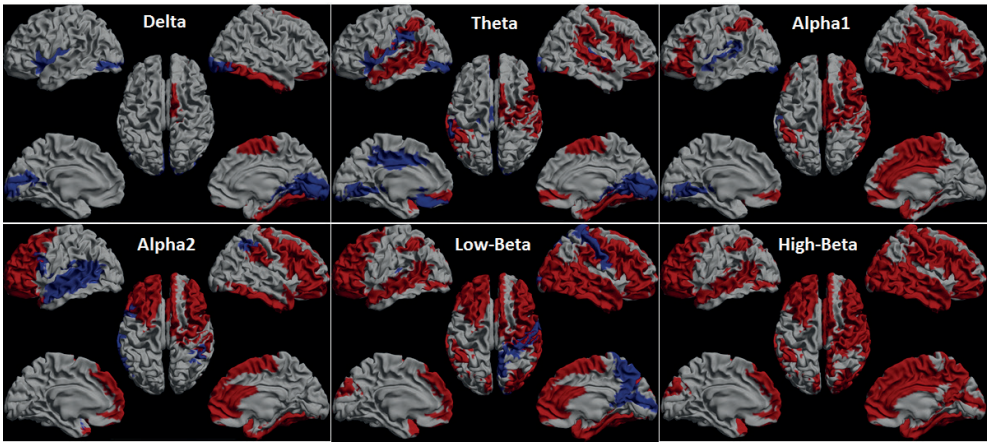

Supplementary Figure 3 Distribution of significant differences in absolute band power between the second DBS-ON recording (ON2) and DBS-OFF. Significant increases (decreases) are displayed in red (blue) on a parcellated template brain viewed from, in clockwise order, the left, top, right, left-midline and right-midline. An absolute power increase of the faster frequencies (alpha1, alpha2, low-beta, high-beta) was found during DBS-ON2, similar as for the comparison between DBS-ON and DBS-OFF (see Figure 3).

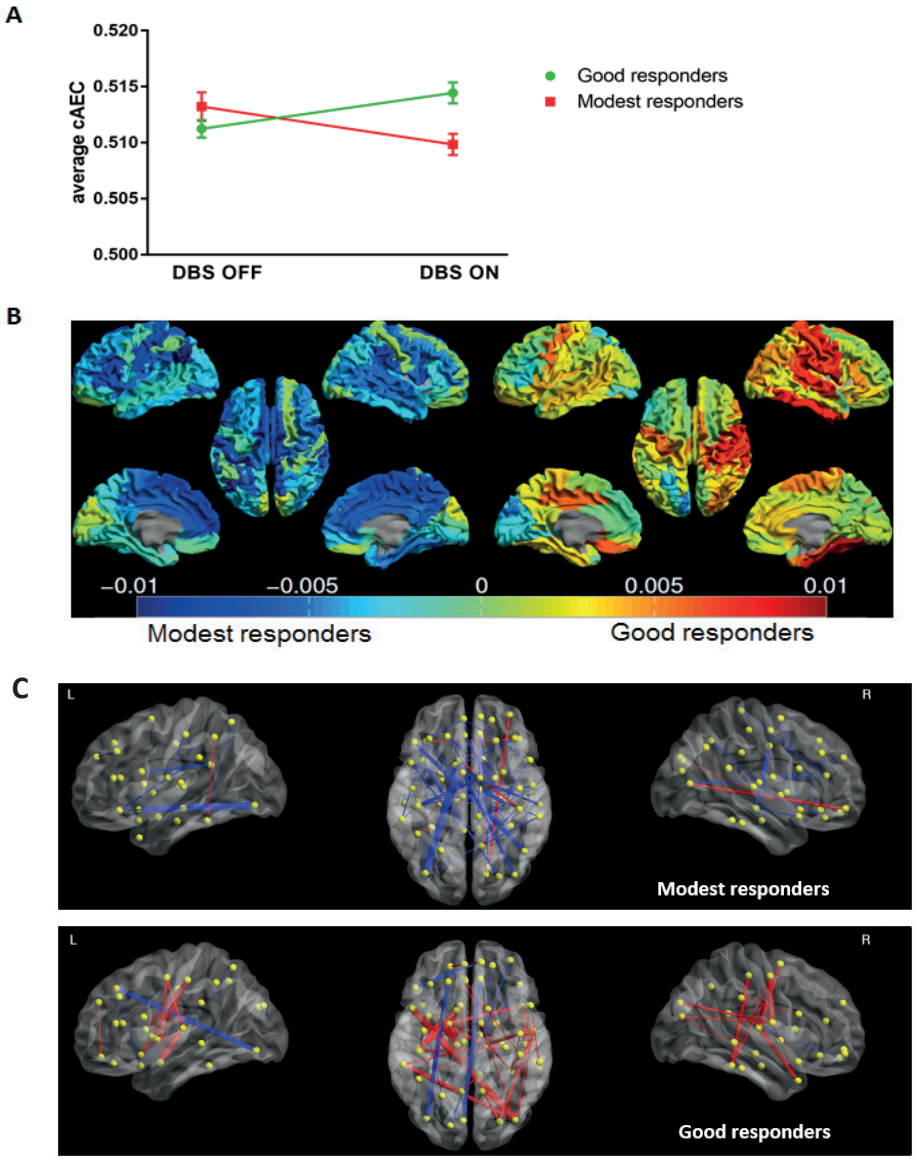

Supplementary Figure 4 Group-specific functional connectivity changes
Plots showing the effect of stimulation on low-beta band cAEC (DBS ON versus DBS OFF) for modest responders (<40% bradykinesia/rigidity improvement, n = 8) and for good responders (>40% bradykinesia/rigidity improvement, n = 10). A) Overall average (and standard error) of cAEC values for DBS OFF and DBS ON for both groups. Although no significant group differences were found (DBS OFF $t(16)$, $p = 0.744$; DBS ON $t(16)$, $p = 0.404$), during DBS ON average cAEC values diverged. B) Distribution of cAEC differences (DBS ON versus DBS OFF) for each region for both groups, displayed as a color-coded map on a parcellated template brain viewed from, in clockwise order, the left, top, right, left-midline, and right-midline. Hot and cold colors indicate cAEC increases and decreases, respectively. For visualisation purposes, only cortical brain regions are displayed. C) Distribution of cAEC differences (DBS ON versus DBS OFF) for each individual connection for both groups. Nodes represent brain regions, red (blue) connections represent a stimulation-related increase (decrease) in functional connectivity. Left lateral (connections within left hemisphere), top, and right panel (connections within right hemisphere) views of

a template brain are shown.[71] For visualization purposes, only links with an absolute t-value larger than 3.17 are shown (arbitrary threshold, thicker lines represent larger t-values). Note that for the good responders, stimulation-related *increases* in functional connectivity can be seen, involving cortico-subcortical connections including connections with the sensorimotor cortex (left and right lateral views).

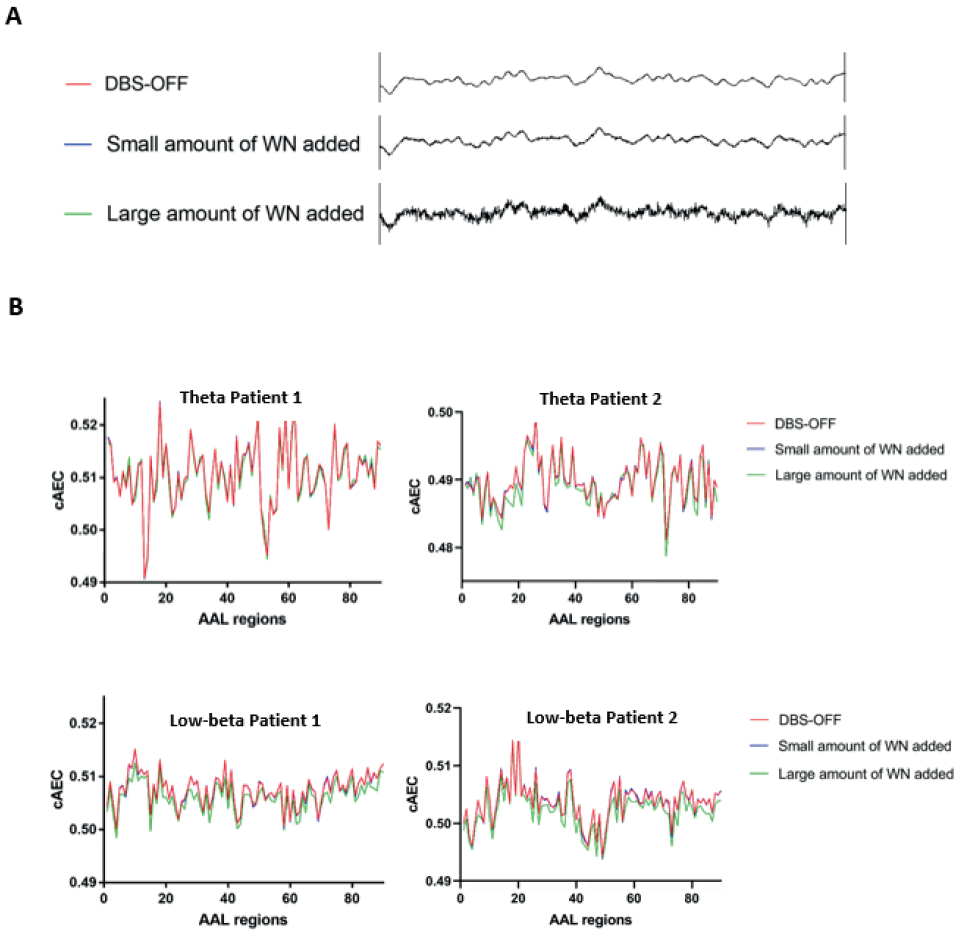

Supplementary Figure 5 Effect of noise addition on functional connectivity estimation
Effect of addition of spatially correlated white noise (WN) to DBS-OFF data on A) MEG data, and B) Functional connectivity estimation.
Zero-mean WN was spatially correlated between individual regions of interest (ROIs), that is, the white noise from one region of interest (ROI) was added to that of another ROI, scaled by the distance between the ROIs (smaller distance led to a higher correlation). In one situation, a small amount of WN was added (σ=1) and in another situation, a large amount of WN was added to the data (σ=5).
After noise addition to the DBS-OFF data, average functional connectivity was again estimated for each ROI. Theta band functional connectivity (upper panel) was hardly affected by WN addition in patient 1, whereas low-beta FC was lowered by the addition of noise in both patients (in green). This illustrates that the extra noise introduced by deep brain stimulation (simulated here as spatially correlated white noise) could lead to a reduction in estimated functional connectivity values, although this effect may be frequency-dependent.

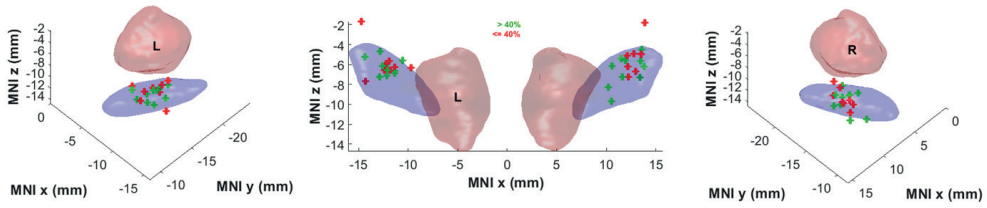

Supplementary Figure 6
Patient-specific localization of active contact points in MNI-space (viewed from respectively dorsolateral left, posterior, and dorsolateral right). The subthalamic nucleus is shown in blue, the red nucleus (added for reference purposes) in red. Good responders (bradykinesia/rigidity-improvement >40%) are depicted in green, modest responders (bradykinesia/rigidity-improvement ≤=40%) in red. Coregistration of the pre-operative MRI-scan and post-operative CT-scan took place using LEAD-DBS[72] and implemented as described by Prent and colleagues.[73]
MNI, Montreal Neurological Institute; R, right; L, left.

Supplementary Table 2

Patient	Right active contact point			Left active contact point		
	X	Y	Z	X	Y	Z
1	-12.2	-11.7	-7.1	13.4	-10.2	-7.3
2	-10.6	-10.9	-5.6	10.6	-11.8	-6.1
3	-11.8	-11.0	-6.5	13.4	-11.4	-4.9
4	-14.8	-12.4	-1.7	13.9	-12.4	-1.8
5	-11.3	-12.1	-6.3	12.8	-11.0	-4.9
6	-9.7	-11.8	-6.3	12.1	-13.2	-5.1
7	-13.9	-11.4	-12.5	12.8	-9.3	-11.7
8	-12.2	-14.0	-5.9	13.5	-12.9	-5.0
9	-11.9	-12.8	-5.7	12.2	-11.0	-6.2
10	-12.1	-13.7	-6.6	11.9	-11.9	-5.6
11	-11.4	-10.9	-6.6	13.4	-11.7	-5.6
12	-12.6	-14.6	-6.2	13.6	-12.4	-4.5
13	-12.9	-12.0	-7.2	13.8	-12.5	-6.2
14	-12.4	-13.4	-6.6	12.2	-12.5	-7.2
15	-11.4	-12.4	-6.9	10.2	-13.5	-8.3
16	-12.3	-13.1	-6.1	11.6	-13.2	-7.2
17	-12.8	-12.0	-4.7	11.5	-13.4	-5.4
18	-14.3	-12.4	-5.2	10.5	-10.4	-9.7

Patient-specific MNI-coordinates for each active contact point. Coregistration of pre operative MRI-scan and post-operative CT-scan took place using LEAD-DBS,[72] and implemented as described by Prent and colleagues (see also Supplementary Figure 5).[73]

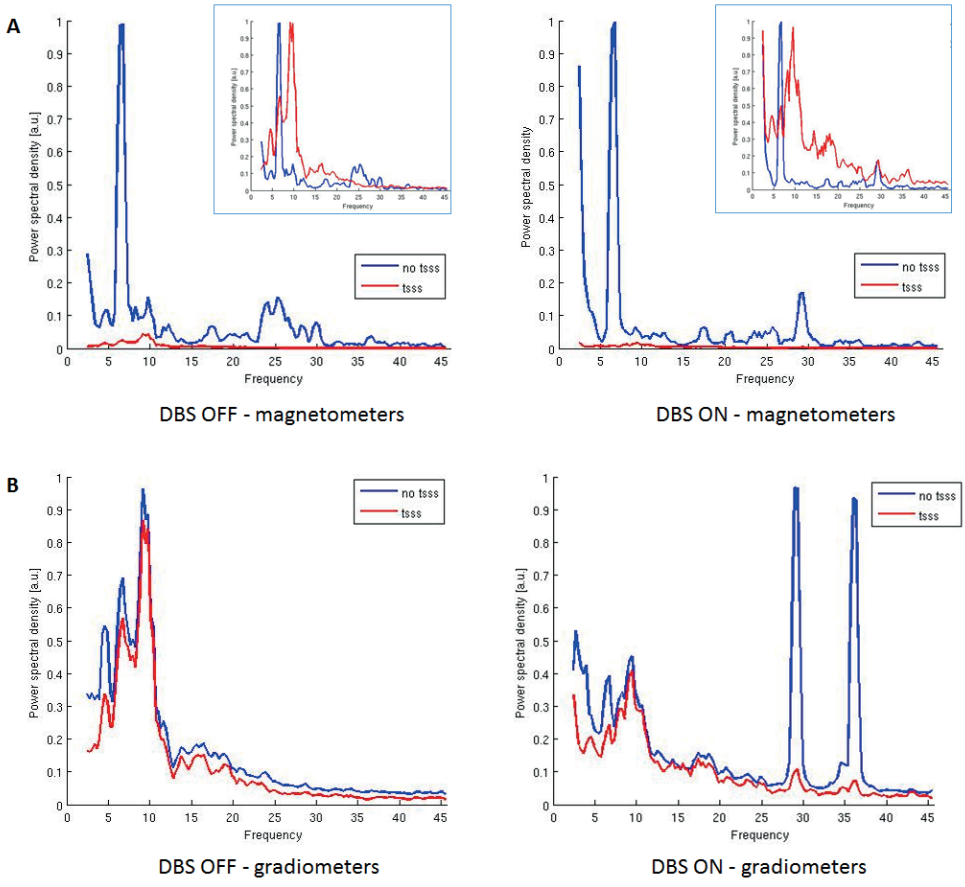

Supplementary Figure 7 Influence of the temporal extension of Signal Space Separation (tSSS) on average sensor-space power spectra (2 to 45 Hz). Magnetometers (A) and gradiometers (B) are depicted separately during stimulation OFF (left figures) and stimulation ON (right figures). Data for one illustrative patient (patient 1; 4096 samples) was used. For each of the four figures, power spectra were *jointly* normalized to 1, based on the maximum peak in the figure. In case of the insets (magnetometers - A), spectra within the same figure were normalized *individually*, for visualization purposes.
As shown in the figure, removal of noise with tSSS reveals the alpha peak in magnetometer data. Moreover, tSSS drastically lowers the amplitude of environmental noise, as well as stimulation artefacts.

CHAPTER 6.2

Structural and functional correlates of subthalamic deep brain stimulation-induced apathy in Parkinson's disease

Lennard I Boon, Wouter V Potters, Thomas JC Zoon, Odile A van den Heuvel, Naomi Prent, Rob MA de Bie, Maarten Bot, P Richard Schuurman, Pepijn van den Munckhof, Gert J Geurtsen, Arjan Hillebrand, Cornelis J Stam, Anne-Fleur van Rootselaar, Henk W Berendse

Brain Stimulation 2021:192-201
DOI: 10.1016/j.brs.2020.12.008

Abstract

Background Notwithstanding the large improvement in motor function in Parkinson's disease (PD) patients treated with deep brain stimulation (DBS), apathy may increase. Postoperative apathy cannot always be related to a dose reduction of dopaminergic medication and stimulation itself may play a role.

Objective We studied whether apathy in DBS-treated PD patients could be a stimulation effect.

Methods In 26 PD patients we acquired apathy scores before and >6 months after DBS of the subthalamic nucleus (STN). Magnetoencephalography recordings (ON and OFF stimulation) were performed ≥6 months after DBS placement. Change in apathy severity was correlated with (i) improvement in motor function and dose reduction of dopaminergic medication, (ii) stimulation location (merged MRI and CT-scans) and (iii) stimulation-related changes in functional connectivity of brain regions that have an alleged role in apathy.

Results Average apathy severity significantly increased after DBS (p<0.001) and the number of patients considered apathetic increased from two to nine. Change in apathy severity did not correlate with improvement in motor function or dose reduction of dopaminergic medication. For the right hemisphere, increase in apathy was associated with a more dorsolateral stimulation location (p=0.010). The increase in apathy severity correlated with a decrease in alpha1 functional connectivity of the dorsolateral prefrontal cortex (p=0.006), but not with changes of the medial orbitofrontal or the anterior cingulate cortex.

Conclusions The present observations suggest that apathy after STN-DBS is not necessarily related to dose reductions of dopaminergic medication, but may be an effect of the stimulation itself. This highlights the importance of determining optimal DBS settings based on both motor and non-motor symptoms.

Introduction

Deep brain stimulation (DBS) of the subthalamic nucleus (STN) is an effective treatment for Parkinson's disease (PD) patients with disabling fluctuations in motor symptoms.[1-3] Despite excellent effects on motor symptoms, emotional, behavioural and cognitive disturbances associated with STN-DBS have been reported.[4-7] Apathy is a frequently observed symptom after STN-DBS in PD (prevalence ~25%) and is associated with a decrease in the quality of life.[8-11]

Apathy can be defined by a lack of motivation, diminished goal-directed behaviour and decreased emotional involvement.[12] Apathy after DBS has been attributed to mesolimbic denervation[10] and dose reductions in dopaminergic medication,[13] although a consistent correlation with the latter has not been found.[10,14,15] The results of a recent animal study suggest that impaired motivation may be an effect of the brain stimulation itself.[16] Moreover, in DBS-treated PD patients apathy scores correlated with the position of active DBS contacts,[4,17,18] as well as with DBS-related changes in cortical glucose metabolism.[15] However, a study in which the functional effects of deep brain stimulation (DBS-ON versus DBS-OFF) are related to apathy scores is currently lacking.

In the current study, we selected three bilateral brain regions that have an alleged role in apathy: the dorsolateral prefrontal cortex (dlPFC), the anterior cingulate cortex (antCC) and the medial orbitofrontal cortex (medORB). Functional changes in the antCC and the medORB appear to be related to emotional-affective apathy,[10,19] whereas functional changes in the dlPFC are associated with cognitive apathy (mostly via executive cognitive dysfunction).[20,21]

In a previous magnetoencephalography (MEG) study, we demonstrated that DBS has widespread effects on oscillatory brain activity and functional connectivity and that changes in the latter correlate with DBS-related improvement in motor scores.[22] Based on this observed correlation between functional connectivity changes and motor effects, we decided to study apathy-related functional connectivity changes. Specifically, in this MEG study using a DBS ON-OFF setup, we aimed to determine whether change in pre-to-post-DBS apathy score correlated with (i) the dose reduction of dopaminergic medication, (ii) the stimulation location and (iii) changes in functional connectivity of the three pre-selected bilateral cortical brain regions. In line with a previous case-report from our group,[4] we hypothesized that postoperative apathy can be an effect of stimulation of the ventral (limbic) STN, affecting brain regions involved in emotional-affective processing.

Materials and methods

Patients

A total of 33 PD patients who had undergone bilateral STN-DBS implantation between 2016 and 2018 at Amsterdam UMC, location AMC, participated in this study (after consecutively approaching eligible patients) and underwent MEG recordings at least 6 months after DBS electrode placement (range 6-17 months; median 7 months). Inclusion and exclusion criteria were previously described.[22] In the context of standard clinical care, the stimulation parameters were individually determined for optimal therapeutic efficacy (regarding motor effects) and monopolar stimulation was applied. All patients were implanted with a Boston Scientific Vercise directional stimulation system (Valencia, CA, USA). Of the 33 PD patients included in this study, five patients were excluded from further analysis due to excessive noise in more than ~13 MEG channels during the ON-stimulation recording, which prevented the use of the temporal extension of Signal Space Separation (tSSS; see MEG data preprocessing). One patient was excluded because of missing clinical data (pre-DBS apathy score) and one patient as a consequence of excessive tremor during the OFF-stimulation recording. This led to a final study sample of 26 patients. The research protocol describing the MEG, psychiatric and neuropsychological data collection was approved by the medical ethical committee of Amsterdam UMC, location VUmc. Ethics review criteria conformed to the Helsinki declaration. All patients gave written informed consent before participation.

Data acquisition

Study visits took place after an overnight withdrawal of dopaminergic medication (practically defined off-state). MEG data were recorded using a 306-channel whole-head system (Elekta Neuromag Oy, Helsinki, Finland) in an eyes-closed resting-state condition, with a sample rate of 1250 Hz and online anti-aliasing (410 Hz) and high-pass (0.1 Hz) filters. The head position relative to the MEG sensors was recorded continuously using the signals from five head position indicator (HPI) coils. For each subject, the total MEG recording time was 55 minutes, consisting of 11 trials of 5 minutes. In each trial different DBS stimulation settings were used. The first recording was during bilateral stimulation with the standard DBS-settings of the individual patient (DBS-ON). Subsequently, nine recordings took place in randomized order, eight of which consisted of unilateral stimulation using a single electrode contact (data not presented) and one recording during DBS-OFF. The eleventh and last recording was, again, performed during stimulation using the standard DBS-settings of the individual patient (DBS-ON2; data not presented). Further details on the MEG acquisition can be found in Boon et al..[22]

Anatomical images of the head were obtained in the context of standard pre-operative imaging up to 6 months before surgery using a 3T magnetic resonance imaging (MRI) scanner (Philips Ingenia, Best, the Netherlands) and a 16-channel receiver coil. We acquired post-gadolinium volumetric T1-weighted scans (TR 8.8–9.1ms; TE 4.0–4.2ms;

flip angle (FA) 8°; field of view (FOV) 256×256mm; slice thickness 1.0mm; 1.0×1.0mm; 169 slices) and T2-weighted scans using a slab covering the brain from the superior cerebellar peduncle to the top of the lateral ventricles (TR 4000.0–5233.2ms; TE 80.0–87.7ms; FA 90°; FOV 432×432/560×560mm; slice thickness 2mm; 0.5×0.5mm; 46–80 slices). For 21 patients, on the postoperative day, a multidetector CT-scan of the head was acquired (Philips Medical System, Best, The Netherlands; slice thickness 1–2mm; FOV 512×512mm; 56–169 slices). For the five remaining participants, an intra-operative CT-scan was acquired using a Medtronic O-arm O2 (high definition mode; 20 cm FOV; 192 slices; 120 kV; 150 mAs; Medtronic Inc., Minneapolis, MN, USA).

Apathy scores reflecting the last 4 weeks[23] were obtained from the patient (helped by the patient's relative or caregiver, if possible) using the patient-based version of the Starkstein apathy scale,[24] both at baseline (several days before DBS placement) and after DBS placement (several days before the study visit) with patients on medication and ON stimulation in the standard settings of the individual patient. This validated apathy scale ranges from 0 to 42 and patients with an apathy score $\geq$14 were considered apathetic.[24] Hamilton Depression Scores and Hamilton Anxiety Scores[25] were also obtained at baseline and during the study visit. Neuropsychological tests of executive functioning (Trail Making Test A and B; Stroop Test 1-3) were performed before DBS placement and after six months of DBS therapy by a licensed clinical neuropsychologist on medication and ON stimulation. Motor function was scored by trained nurses using the motor part of the Movement Disorders Society Unified Parkinson's Disease Rating Scale (MDS-UPDRS-III) both at baseline and, approximately six months after DBS placement, during DBS-ON and DBS-OFF, off medication.

Data processing

MEG data

MEG channels that were malfunctioning or noisy were ignored after visual inspection of the data. Thereafter, the temporal extension of Signal Space Separation (tSSS)[26,27] in MaxFilter software (Elekta Neuromag Oy, version 2.2.15) was applied with a subspace correlation-limit of 0.8 to suppress the strong magnetic artefacts.[22] MEG data of each patient were co-registered to their T1 MRIs using a surface-matching procedure, with an estimated accuracy of 4mm.[28] A single sphere was fitted to the outline of the scalp as obtained from the co-registered MRI, which was used as a volume conductor model for the beamformer approach described below.

The automated anatomical labelling (AAL) atlas was used to label the voxels in 78 cortical and 12 subcortical regions of interest (ROIs).[29,30] We used each ROI's centroid as representative for that ROI.[31] Subsequently, an atlas-based beamforming approach[32] was used to project broad-band (0.5-48 Hz) filtered sensor signals to these centroid voxels, resulting in broad-band time series for each of the 90 ROIs (see Hillebrand et al.[33] for

details). The source-reconstructed MEG data were visually inspected (by LIB) for tremor-, motion- and stimulation-related artefacts and drowsiness. The MEG data were cut into ~22 epochs per (5 minute) recording. Epochs were then downsampled from 1250 Hz to 313 Hz (4x) and contained 4096 samples (13.12 s). For each recording, the 50% epochs with the lowest peak frequency (estimated within the 4-13 Hz frequency range using automatic quantification) were discarded in order to minimize the risk of including episodes with drowsiness. For each condition, 10 epochs with the best quality (visual selection based on the absence of artefacts and drowsiness) were selected for further analysis. Spectral and functional connectivity analyses were performed using BrainWave (version 0.9.152.12.26; CJS, available from https://home.kpn.nl/stam7883/brainwave.html). For frequency band-specific analyses, epochs were filtered in five frequency bands (delta (0.5-4 Hz), theta (4-8 Hz), alpha1 (8-10 Hz), alpha2 (10-13 Hz) and beta (13-30 Hz), using a Fast Fourier Transform. The gamma band was not analyzed as we had observed stimulation-related artefact peaks in this band in a previous study.[22] For each epoch, frequency band-specific functional connectivity was estimated using the corrected Amplitude Envelope Correlation (cAEC), an implementation of the AEC[34] corrected for volume conduction/field spread, using a symmetric (pairwise) orthogonalisation procedure.[34,35] The cAEC was calculated for all possible pairs of ROIs, leading to a 90x90 adjacency matrix.

Imaging data

To determine the stimulation locations after placement of the DBS system, the electrode trajectories were reconstructed using Lead-DBS (Lead-DBS, version 2.2; http://www.lead-dbs.org).[36] To this end, the post- or intra-operative CT-scan was co-registered to the pre-operative MR image using a two-stage (rigid and affine) registration as implemented in Advanced Normalization Tools (ANT).[37] In three cases in which only an intra-operative CT-scan was available, the co-registration failed using ANT. In these cases, co-registration was successfully performed using FSL FLIRT. Co-registration was followed by a semiautomatic localization of the electrode positions on the CT data in patient space.

The electrode stimulation positions were then transformed from patient space to Montreal Neurological Institute space (MNI ICBM 2009b NLIN ASYM space) to facilitate group-level analyses. The DISTAL Minimal atlas[38] was used as outline of the STN. Next, the midpoints of stimulation positions were projected on a vector running through the longitudinal axis of the STN (from ventromedial to dorsolateral), leading to one scalar value to indicate each stimulation position, where negative values indicated more ventromedial stimulation positions.

Statistical analysis

We tested the differences in proportion of apathetic patients (pre- versus post-DBS) using a chi-square test, change in apathy score, MDS-UPDRS-III score, and levodopa equivalent daily dose (LEDD)-score using paired *t*-tests (all pre-DBS versus post-DBS).

Correlations between the change in apathy score and change in LEDD, change in MDS-UPDRS-III score, stimulation positions, change in depression score, change in anxiety score, and change in executive functioning (difference in T-scores (mean of 50±10), normed by age and education) were estimated using Pearson correlations. Next, in order to explore the possibility of confounding variables explaining change in apathy scores, the abovementioned variables were combined into a single hierarchical linear regression model using a backward elimination method (in which change in apathy score functioned as dependent variable).

For each patient, stimulation condition and frequency band separately, functional connectivity matrices were averaged over 10 epochs. Next, we obtained the average functional connectivity between one ROI and the rest of the brain by averaging functional connectivity values over each column of the matrix. We then calculated the change in functional connectivity (DBS-ON versus DBS-OFF) for three pre-selected cortical brain regions, the dlPFC (AAL-region: middle frontal gyrus, as previously used by Pretus and co-workers),[39] antCC and medORB, and correlated these values with the change in pre-to-post-DBS apathy score. As the functional connectivity data was not normally distributed (despite attempts to transform the data) this was done using Spearman correlations.

All analyses were performed using the SPSS Statistics 20.0 software package (IBM Corporation, New York, USA), using a significance level of 0.05 (two-tailed). Bonferroni correction was applied for the number of seed regions in the Spearman correlations between change in apathy score and change in functional connectivity. Due to the exploratory nature of the study, we did not correct for the number of frequency bands used for the functional connectivity estimates.

Results

Patients

26 DBS-treated PD patients, whose characteristics are summarized in Table 1, were included in this study. DBS significantly improved off-dopamine motor function with a mean change of 51.2% in MDS-UPDRS-III score ($t(25)$=9.21; p<0.001) and the LEDD was significantly lowered after DBS placement ($t(25)$=8.01; p<0.001; see Table 1). The mean number of excluded MEG channels before running tSSS was 9 for DBS-ON recordings (range: 4-13) and 6 for DBS-OFF recordings (range: 2-12).

Table 1 Patient characteristics

Patient	Age (years)	Sex	Disease duration (years)	Side disease onset	Stimulation parameters (stimulation side; contact; intensity (mA))	Pulse width and frequency of stimulation	LEDD pre-DBS (mg/day)	LEDD study visit (post-DBS (mg/day))	Motor UPDRS (III)			Starkstein apathy score	
									Pre-DBS Med off	Med off / DBS-OFF	Med off / DBS-ON	Pre-DBS	Post-DBS (DBS-ON)
1	38	M	8	Right	L; DM; 2.9 R; VM; 3.4	60 µs 179 Hz	Total: 1644 DA: 320	Total: 996 DA: 80	73	54	31	3	8
2	63	F	5	Right	L; DM; 1.7 R; DM; 1.7	60 µs 130 Hz	Total: 495 DA: 150	Total: 567 DA: 315	43	16	11	2	3
3	65	F	27	Left	L; VM; 2.7 R; DM; 1.5	60 µs 130 Hz	Total: 500 DA: -	Total: 400 DA: -	33	20	19	24	25
4	49	F	10	Left	L; Dors; 1.9 R; Dors; 2.5	60 µs 130 Hz	Total: 797 DA: 240	Total: 536 DA: 120	35	37	22	12	20
5	69	M	12	Right	L; DM; 2.1 R; DM; 2.1	60 µs 130 Hz	Total: 1830 DA: 360	Total: 150 DA: -	56	24	14	12	18
6	60	M	8	Left	L; DM; 3.2 R; DM; 1.3	60 µs 179 Hz	Total: 1200 DA: 75	Total: 300 DA: -	57	65	38	4	19
7	53	M	11	Right	L; DM; 2.9 R; DM; 1.9	60 µs 130 Hz	Total: 1567 DA: 240	Total: 1043 DA: 160	60	44	30	2	6
8	66	F	8	Left	L; VM; 2.2 R; DM; 1.8	60 µs 130 Hz	Total: 1226 DA: 160	Total: 753 DA: 120	47	37	33	6	5
9	45	M	5	Left	L; Dors; 1.7 R; DM; 1.7	60 µs 130 Hz	Total: 1410 DA: -	Total: 283 DA: -	50	80	44	14	19
10	70	F	25	Left	L; DM; 2.1 R; DM; 2.4	60 µs 130 Hz	Total: 1590 DA: 450	Total: 555 DA: 37.5	46	33	15	4	12
11	66	M	10	Left	L; DM; 2.5 R; DM; 1.8	60 µs 149 Hz	Total: 750 DA: -	Total: 575 DA: -	38	54	27	6	12
12	55	M	8	Right	L; DM; 2.7 R; DM; 2.6	60 µs 130 Hz	Total: 950 DA: -	Total: 775 DA: -	42	31	15	5	15
13	57	M	11	Left	L; VM; 1.6 R; VM; 1.6	60 µs 130 Hz	Total: 1134 DA: 320	Total: 606 DA: 80	38	21	7	0	12
14	61	M	7	Left	L; VM; 1.5 R; VM; 2.1	60 µs 130 Hz	Total: 1000 DA: -	Total: 375 DA: -	30	27	11	3	16

Patient	Age (years)	Sex	Disease duration (years)	Side disease onset	Stimulation parameters (stimulation side; contact; intensity (mA))	Pulse width and frequency of stimulation	LEDD pre-DBS (mg/day)	LEDD study visit (post-DBS (mg/day))	Motor UPDRS (III)			Starkstein apathy score	
									Pre-DBS Med off	Med off / DBS-OFF	Med off / DBS-ON	Pre-DBS	Post-DBS (DBS-ON)
15	60	M	14	Left	L; DM; 2.0 R; VM; 2.5	60 µs 130 Hz	Total: 1073 DA: -	Total: 425 DA: -	55	27	7	6	14
16	57	M	12	Left	L; VM; 3.1 R; VM; 2.3	60 µs 130 Hz	Total: 1380 DA: 480	Total: 720 DA: 120	80	52	26	4	9
17	61	M	8	Left	L; DM; 1.8 R; DM; 2.3	60 µs 130 Hz	Total: 1726 DA: 360	Total: 946 DA: 80	56	52	21	3	11
18	56	M	12	Right	L; DM; 1.4 R; VM; 1.3	60 µs 130 Hz	Total: 2131 DA: 240	Total: 1245 DA: 45	45	20	10	5	6
19	58	M	16	Left	L; VM; 1.9 R; DM; 1.9	60 µs 130 Hz	Total: 2032 DA: 160	Total: 613 DA: 80	35	38	14	11	12
20	57	M	12	Left	L; VM; 3.0 R; VM; 3.2	60 µs 130 Hz	Total: 1170 DA: 150	Total: 533 DA: -	38	51	33	8	11
21	71	F	17	Right	L; VM; 1.8 R; VM; 1.7	60 µs 130 Hz	Total: 1940 DA: -	Total: 791 DA: -	56	59	42	3	9
22	57	F	14	Left	L; DM; 1.7 R; DM; 2.0	60 µs 130 Hz	Total: 1080 DA: 480	Total: 660 DA: 160	50	40	21	5	12
23	54	F	6	Left	L; DM; 2.2 R; DM; 2.4	60 µs 130 Hz	Total: 1600 DA: -	Total: 883 DA: -	71	69	44	6	4
24	55	M	12	Left	L; VM; 2.9 R; DM; 2.9	60 µs 130 Hz	Total: 1344 DA: -	Total: 679 DA: -	30	50	17	0	1
25	64	M	22	Left	L; DM; 3.7 R; DM; 3.2	60 µs 130 Hz	Total: 2100 DA: 150	Total: 780 DA: 150	59	59	39	13	27
26	48	M	6	Right	L; DM; 2.0 R; DM; 1.7	60 µs 130 Hz	Total: 990 DA: 320	Total: 110 DA: 80	14	14	12	5	10
Mean (SD)	58 (8)	M, 18; F, 8	12 (6)		L; 2.3 (0.61) R; 2.1 (0.58)		Total: 1369 (490)	Total: 627 (273)	47.6 (14.8)	41.3 (17.7)	23.2 (11.8)	6 (5)	12 (7)

mA, milliampère; µs, microseconds; LEDD, Levodopa Equivalent Daily Dose; DA, dopamine agonist; mg, milligrams; MDS-UPDRS-III, Movement Disorders Society Unified Parkinson's Disease Rating Scale motor ratings; DBS, Deep Brain Stimulation; M/F, male/female; L/R, left/right; D/DM/VM, Dorsal/Dorsomedial/Ventromedial; Med, medication.

Apathy

In 24 of the 26 PD patients apathy severity increased after DBS and the number of apathetic patients increased from 2 pre-DBS to 9 post-DBS (X^2 (1,26)=4.093, p=0.043). Apathy severity scores were significantly higher during follow-up than at baseline (pre-DBS versus post-DBS; $t(25)$=6.47, p<0.001). Increase in apathy severity did not correlate with decrease in LEDD, neither taking all dopaminergic medication into account (p=0.157; Supplementary Figure A.1), nor dopamine agonists alone (p=0.503; Supplementary Figure A.2). Change in apathy severity did not correlate with improvement in motor function (MDS-UPDRS-III; p=0.518; Supplementary Figure A.3). Change in apathy severity did also not correlate with change in depression severity (p=0.443; Supplementary Figure B.1), change in anxiety severity (p=0.710; Supplementary Figure B.2), nor with change in executive functioning (p=0.693; Supplementary Figure B.3). Lastly, as a recent paper shows that motor asymmetry can predict emotional outcome of STN-DBS [40], we compared the change in apathy score for patients with left- and right-sided onset of motor symptoms, but there was not difference ($t(25)$=0.68, p=0.501).

Apathy and DBS localization

In Figure 1A, the midpoints of the stimulation positions of all active contact points are depicted in standard MNI space relative to an atlas representation of the STN. Increases in apathy scores are color-coded, ranging from no increase (green/yellow) to a strong increase (dark red) in apathy severity. There was a significant correlation between a more dorsolateral stimulation position (along a vector) and increase in apathy severity post-DBS for the right side (p = 0.010), but not for the left side (p = 0.491; Fig.1B). In contrast, there was no relationship between stimulation position (along the same vector) and the degree of improvement in total motor score (UPDRS-III; Supplementary Fig E).

Next, we performed a hierarchical linear regression model using a backward elimination method to study the relationship between stimulation location and change in apathy score, including the following covariates: pre-to post-operative change in executive functioning, depression score, anxiety score, LEDD total, LEDD of dopamine agonist, and motor function. For the right side this resulted in the following model: R2 = 0.465; change in depression score, b(standardized) = 0.587, p = 0.039; stimulation position, b(standardized) = 0.727, p = 0.015. For the left side no statistically significant model could be fitted.

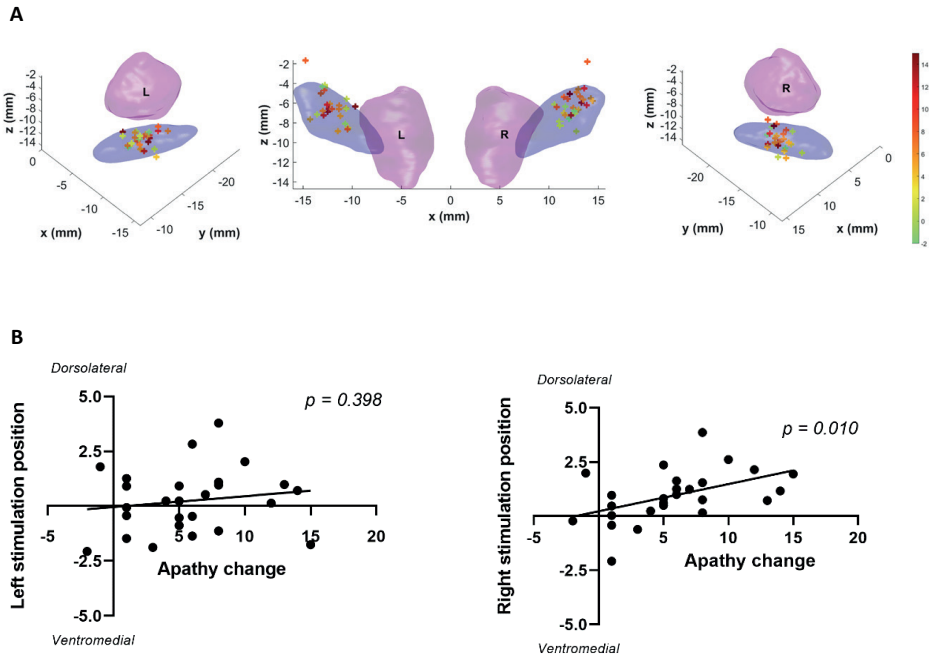

Figure 1 Stimulation locations of contact points in relation to change in apathy severity
A) Stimulation locations in MNI-space (viewed from respectively dorsolateral left, posterior and dorsolateral right). The subthalamic nucleus (blue) and red nucleus (red) were added for reference purposes. Increases in apathy severity are color-coded, ranging from no increase (green/yellow) to strong increase (dark red).
MNI, Montreal Neurological Institute; L, left; R, right.
B) Stimulation locations were projected on a vector through the longitudinal axis of the STN, where negative values indicated more ventromedial stimulation positions. There was a significant correlation between stimulation position and increase in apathy severity for the right side (r(24) = 0.498, p = 0.010), but not for the left side (r(24) = 0.141, p = 0.491).

Apathy and functional connectivity

6.2

The three *a priori* selected cortical brain regions are depicted in Figure 2A. The centroid voxel was taken as representative for each individual brain region, and its time-series was used for the estimation of functional connectivity. A significant negative correlation was found between the pre-to-post-DBS change in apathy score and the stimulation-related change in functional connectivity of the bilateral dlPFC with the rest of the brain (alpha1, p=0.006; alpha level was adjusted to 0.05/3 to correct for multiple comparisons as three seed regions were studied; Figure 2B). A reduction in stimulation-related functional connectivity was related to an increase in post-operative apathy. In contrast, no significant correlations were found for the medORB (alpha1, p=0.298), as well as for the antCC (alpha1, p=0.163). Correlations with functional connectivity in the other frequency bands can be found in Table 2.

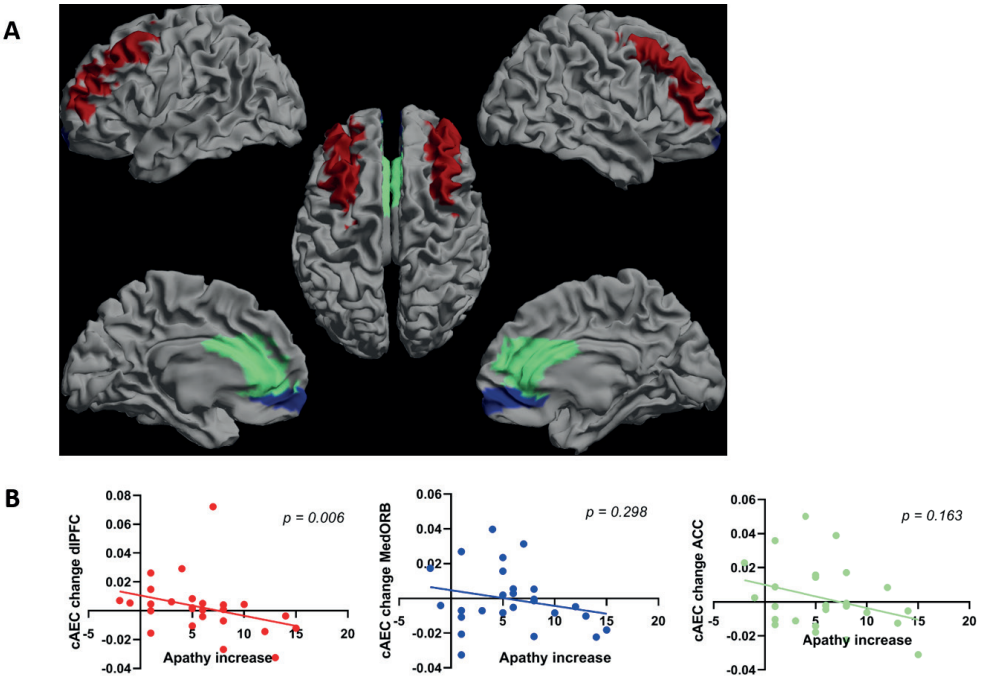

Figure 2 Correlations between regional changes in functional connectivity (alpha1) and change in apathy severity
A) Distribution of the bilateral cortical brain regions studied, the dlPFC (red), medORB (blue) and antCC (green) displayed on a parcellated template brain viewed from, in clockwise order, the left, top, right, left midline and right midline.
B) Scatter plots of pre-to-post-DBS change in apathy severity and alpha1 functional connectivity change (DBS-ON – DBS-OFF), averaged for each of the three regions of interest. Statistics can be found in Table 2.
dlPFC, dorsolateral prefrontral cortex; medORB, medial orbitofrontal cortex; antCC, anterior cingulate cortex.

Table 2 Correlations of functional connectivity changes with change in apathy severity

Region	Frequency band	Spearman's rho
Dorsolateral prefrontal cortex	Delta	0.231 (p= 0.256)
	Theta	-0.261 (p= 0.290)
	Alpha1	**-0.520 (p= 0.006)**
	Alpha2	-0.393 (p= 0.047)
	Beta	-0.241 (p= 0.235)
Medial orbitofrontal cortex	Delta	0.044 (p= 0.829)
	Theta	-0.151 (p= 0.461)
	Alpha1	-0.212 (p= 0.298)
	Alpha2	-0.124 (p= 0.545)
	Beta	-0.247 (p= 0.224)
Anterior cingulate cortex	Delta	-0.105 (p= 0.609)
	Theta	-0.110 (p= 0.593)
	Alpha1	-0.282 (p= 0.163)
	Alpha2	-0.108 (p= 0.599)
	Beta	-0.243 (p= 0.231)

Correlations between the changes in cAEC upon stimulation and increase in apathy severity (Starkstein apathy scale) between baseline (pre-DBS) and follow-up (post-DBS). The correlations are expressed as a Spearman's rho. To account for the fact that three seed regions were compared, alpha levels were adjusted such that p-values smaller than 0.05/3 (using Bonferroni correction) were considered to be statistically significant, marked in bold.
cAEC, corrected Amplitude Envelope Correlation; DBS, deep brain stimulation.

As a post-hoc visualization, both for patients with weaker (≤5) and patients with stronger (>5) increase in apathy severity (based on a median split of the data) we showed the distribution of stimulation-related changes in alpha1 functional connectivity of individual connections linked to the dlPFC (Figure 3). In line with the correlation previously shown, we observed a stimulation-related lowering in functional connectivity in patients with a stronger increase in apathy severity. Furthermore, stimulation-related functional connectivity changes in both groups mostly involved connections with frontal brain regions. Functional connectivity matrices and functional connectivity of the three seed regions (alpha1; both DBS-OFF and DBS-ON) averaged over all subjects are provided in Supplementary Figure C and D.

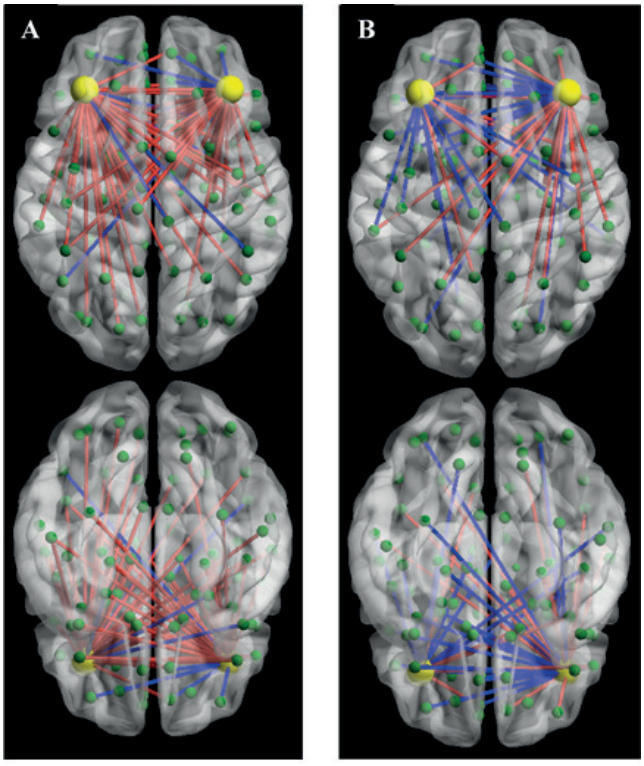

Figure 3 Functional connectivity changes induced by DBS for individual connections for patients with weaker (≤5; panel A) and with stronger (>5; panel B) increase in apathy severity. Distribution of alpha1 cAEC differences induced by DBS stimulation for each individual connection linked to the dorsolateral prefrontal cortex (yellow nodes) for patients with weaker (≤5; panel A) and with stronger (>5; panel B) increase in apathy severity. Green nodes represent brain regions, red (blue) connections represent a stimulation-related increase (decrease) in functional connectivity. Top and bottom views of a template brain are shown[41]. For visualization purposes, only links with an absolute t-value larger than 1.00 are shown (arbitrary threshold for visualization purposes).

Discussion

In this study, we investigated apathy after STN-DBS treatment in patients with PD, in particular the relationship between DBS-related increase in apathy severity and stimulation location, as well as the association between DBS-related increase in apathy severity and stimulation-induced changes in functional connectivity. Our results confirm the notion that apathy severity increases after STN-DBS in PD and that the stimulation itself may play a role in this increase.[15,17,18] The pre-to-post-DBS increase in apathy severity was associated with a more dorsolateral position of the stimulation for the right hemisphere, as well as a stimulation-related reduction in alpha1 band functional connectivity of the bilateral dlPFC with the rest of the brain. The latter could be interpreted as a stimulation-related loss in connectedness (functional communication) of this brain region with the rest of the brain in patients who became apathetic.

We found no significant correlation between the increase in pre-to-post-DBS apathy score and the degree of reduction of dopaminergic medication in the present study. Reintroduction of dopaminergic medication has previously been shown to improve post-operative apathy[13] suggesting a causal role for dopamine withdrawal in the occurrence

of apathy. However, a recent animal study has demonstrated that impaired motivation caused by deep brain stimulation itself can also be reversed by a dopamine agonist.[16] We acknowledge that post-operative apathy is a complex and multifactorial phenomenon in which adjustments of dosages of dopaminergic medication, degeneration of dopaminergic neurons,[42] as well as the stimulation itself may have a role.

The STN occupies a central role in several functionally different basal ganglia circuits and comprises specific motor (dorsolateral), associative (central) and limbic (ventromedial) regions.[43,44] The influence of the stimulation location in or around the STN on the occurrence of post-DBS apathy is as yet unclear. Two case-studies have described the induction of apathy by stimulation of the zona incerta,[13,45] located dorsally from the STN, whereas another case study demonstrated that apathy resolved by switching from a ventrally located contact point to a more dorsal contact point.[4] By contrast, in one study cohort (analyzed in two publications),[17,18] apathy scores (non-significantly) decreased in PD patients after STN-DBS placement. Above-average decreases in apathy scores were related to stimulation around the ventral border and the sensorimotor subregion of the STN and below-average decreases were related to stimulation dorsal to the STN.[17,18] A potential explanation for the fact that decreases rather than increases in apathy severity were found in the latter study is that subscores related to apathy derived from the Non Motor Symptom Scale were used as a measure of apathy, which is not recommended for the assessment of apathy in PD.[23]

We found a significant increase in apathy severity after STN-DBS. We observed a significant correlation between increase in pre-to-post DBS apathy score and a more dorsolateral stimulation location relative to the STN for the right hemisphere, but not for the left hemisphere. As the occurrence of apathy has previously not been related to laterality of DBS,[46,47] we refrain from drawing any conclusions from this left-right difference. Despite the fact that dorsolateral stimulation positions in the motor part of the STN are considered as the optimal STN target resulting in the best clinical motor effects (and hence a stronger reduction in dopaminergic medication dose),[48,49] increased apathy severity was not associated with a stronger improvement of motor symptoms. In addition, we did not find a relation between stimulation position and the degree of improvement in motor score (Supplementary Figure E), contrasting with the results of the study by Bot and coworkers.[49] Our study differed in several aspects though, including the method of localizing the electrodes (patient versus standard space), method of quantifying the stimulation location (vector through the longitudinal axis of the STN versus Euclidian distance to the medial STN border), and the motor scores used (overall UPDRS-III versus unilateral motor score).

When combining our observations with those of previous studies,[13,17,18,45] we conclude that, in contradiction with the previously proposed mechanism (and our own hypothesis),[4,50] stimulation in the ventral part of the STN (the limbic regions) does not necessarily induce apathy. Our findings even suggest that apathy may worsen by a stimulation location in

proximity to the motor region of the STN. Moreover, the fact that increase in apathy severity did not correlate with improvement in motor symptoms leads us to conclude that finding an optimal stimulation location, striking a balance between the least apathy and the best motor response, seems feasible. Future longitudinal studies using a within-subject design in which the stimulation in case of post-DBS apathy is switched to an alternative (more ventral) contact point may shed further light on this matter. In addition, studies that take into account individual differences in the division of subregions using structural connectivity profiles of the STN (using high-resolution MRI techniques) could guide the search for an optimal stimulation position.

The fact that we found stimulation-related changes in functional connectivity of the dlPFC to be associated with the pre-to-post-DBS increase in apathy severity, suggests an (executive) cognitive substrate, rather than an emotional-affective type of apathy (which is more related to the antCC and medORB). Moreover, in our study increases in apathy severity were not associated with changes in executive functioning, whereas in the multiple regression model there was a relation between improvement in depression scores and better apathy scores after surgery (in the context of right-sided stimulation). It remains to be determined whether the occurrence of apathy after DBS has a cognitive or emotional-affective basis.

Our results on stimulation-related changes in functional connectivity were most outspoken for the alpha1 band (8-10 Hz). A direct functional loop of resting-state alpha band coherence has previously been observed between the STN and the ipsilateral temporal cortex,[51-53] but not the dlPFC. This could suggest that the dlPFC is indirectly influenced by DBS via downstream effects on the thalamus, although there may also be direct antidromic stimulation effects via the hyperdirect pathway (albeit the latter mechanism would be more likely for the medial prefrontal cortex than for the dlPFC).[54,55] The complex balance between downstream (via the thalamus) and antidromic stimulation effects (hyperdirect pathway) may also explain the differential effects of stimulation; an increase in FC in some patients and a decrease in FC in others.

The present study has some limitations that need to be addressed. (i) We correlated change in apathy severity over a time interval of ≥6 months with differences in functional connectivity between ON-DBS and OFF-DBS conditions recorded on the same day. Nevertheless, we believe that studying DBS effects (ON versus OFF) on the same day offers the advantage of a better insight into the effect of brain stimulation *itself* (in which we interpret the DBS-ON setting, and not turning off, the stimulation as the intervention), without any bias of disease progression or change in the dose of (dopaminergic) medication over time. The occurrence of apathy is generally assessed over a period of four weeks and can therefore not be tested in a DBS-ON versus DBS-OFF setup.[23,24] However, since we lacked an ON-OFF paradigm in the apathy scores, we must be cautious in drawing conclusions on causality beyond the observed correlation. (ii) We correlated the change in apathy scores obtained on medication with MEG recordings

recorded off medication. The off-medication state of the subjects may have influenced the MEG signals. However, as the subjects served as their own controls in this DBS ON-OFF setup, we expect the influence of the off-medication state on our results to have been minimal. (iii) The correlation between the position of stimulation and the change in apathy severity was based on the position of the stimulation sites along a vector running through the longitudinal axis of the STN, from the ventromedial tip in a dorsolateral direction. Although this correlation analysis does not provide information on the optimal position of stimulation in 3D, it does give an intuitive idea of the different stimulation positions throughout the functional subdivision of the STN. (iv) Previously, we described the potential effects of monopolar DBS on MEG signals.[22] Despite the ability of tSSS and beamforming to effectively suppress artefacts,[56,57] two sharp peaks remained in the power spectrum during stimulation, at ~27 Hz and ~35 Hz. As the peaks did not appear to affect the alpha1 band, we consider the influence of stimulation artefacts on our results to be limited. Furthermore, the estimation of (changes in) functional connectivity may be influenced by modulation of the signal to noise ratio in the seed regions.[58] It is unlikely that our results can be explained by such modulations, since there was no relation between change in absolute alpha1 band power and change in functional connectivity in the three seed regions (Supplementary Figure D). (v) Instead of focusing on the functional effects of stimulation in all brain regions, we chose to select only three (literature-based) brain regions, which prevented us from testing an abundance of other possible correlations. In addition, our MEG analysis lacked the spatial resolution to study subcortical brain regions such as the nucleus accumbens, which has previously been associated with apathy in PD.[59] As a consequence, we may have missed brain regions that may be associated with the occurrence of apathy. However, we assume that, in accordance with a previous PET-study in DBS-patients with apathy[15] the stimulation-related change in the dlPFC specifically reflects the increased apathy severity and does not represent a global phenomenon such as stimulation-related vigilance affecting background alpha-activity. To verify this in a *negative control* brain region, we tested whether stimulation-related changes in functional connectivity of the bilateral inferior occipital lobe correlated with the change in apathy severity and this was not the case (alpha1, Spearman's $\rho(24)$=-0.227; p=0.265).

Important strengths of this study include the DBS ON-OFF setup taking place on the same day. Second, the use of MEG (instead of EEG) in source-space, in combination with a leakage-corrected connectivity measure (cAEC), offers good spatial resolution, enabling interpretation of the findings in an anatomical context. Last, the Starkstein apathy scale used in our study has very high intra- and interrater reliability.[24] Regarding the scores on post-DBS apathy, we consider our study sample as representative for the STN-DBS population, as the average apathy scores were comparable to those in a large longitudinal cohort.[11,60]

In conclusion, we found that increase in apathy severity after STN-DBS might well be an effect of the stimulation itself. Increased apathy severity scores correlated with a more dorsolateral stimulation location (right hemisphere) and with reduced functional connectivity of the dlPFC, not with decreases in dopaminergic medication dose. Hence, the occurrence of apathy after DBS might not necessarily be linked to stimulation of the limbic STN, whereas the correlation with dlPFC connectivity suggests that it may even have a cognitive substrate. To further validate this hypothesis, future prospective (within-subject) studies are necessary to determine whether switching stimulation to an alternative, more ventromedially located, contact point can resolve DBS-induced apathy, preferably without losing clinical effectiveness on motor symptoms, along with a normalization of functional connectivity of the dlPFC.

Acknowledgements

We thank all patients for their participation. We thank Gosia Iwan, Miranda Postma, Marije Scholten, Rosanne Prins and Sharon Stoker-van Dijk for their help with patient inclusions, as well as the collection of clinical data. We also thank Karin Plugge, Nico Akemann and Marieke Alting Siberg for the MEG acquisitions.

References

1. Benabid AL, Koudsie A, Benazzouz A, et al. Deep brain stimulation of the corpus luysi (subthalamic nucleus) and other targets in Parkinson's disease. Extension to new indications such as dystonia and epilepsy. J Neurol. 2001;248 Suppl 3:Iii37-47.
2. Deuschl G, Schade-Brittinger C, Krack P, et al. A randomized trial of deep-brain stimulation for Parkinson's disease. N Engl J Med. 2006;355(9):896-908.
3. Odekerken VJ, van Laar T, Staal MJ, et al. Subthalamic nucleus versus globus pallidus bilateral deep brain stimulation for advanced Parkinson's disease (NSTAPS study): a randomised controlled trial. Lancet Neurol. 2013;12(1):37-44.
4. Zoon TJ, de Bie RM, Schuurman PR, et al. Resolution of apathy after dorsal instead of ventral subthalamic deep brain stimulation for Parkinson's disease. J Neurol. 2019;266(5):1267-9.
5. Ulla M, Thobois S, Llorca PM, et al. Contact dependent reproducible hypomania induced by deep brain stimulation in Parkinson's disease: clinical, anatomical and functional imaging study. J Neurol Neurosurg Psychiatry. 2011;82(6):607-14.
6. Hatz F, Meyer A, Roesch A, et al. Quantitative EEG and Verbal Fluency in DBS Patients: Comparison of Stimulator-On and -Off Conditions. Front Neurol. 2018;9:1152.
7. Castrioto A, Lhommée E, Moro E, et al. Mood and behavioural effects of subthalamic stimulation in Parkinson's disease. Lancet Neurol. 2014;13(3):287-305.
8. Higuchi MA, Tsuboi Y, Inoue T, et al. Predictors of the emergence of apathy after bilateral stimulation of the subthalamic nucleus in patients with Parkinson's disease. Neuromodulation: 2015;18(2):113-7.
9. Barone P, Antonini A, Colosimo C, et al. The PRIAMO study: A multicenter assessment of nonmotor symptoms and their impact on quality of life in Parkinson's disease. Mov Disord. 2009;24(11):1641-9.
10. Thobois S, Ardouin C, Lhommee E, et al. Non-motor dopamine withdrawal syndrome after surgery for Parkinson's disease: predictors and underlying mesolimbic denervation. Brain. 2010;133(Pt 4):1111-27.
11. Abbes M, Lhommee E, Thobois S, et al. Subthalamic stimulation and neuropsychiatric symptoms in Parkinson's disease: results from a long-term follow-up cohort study. J Neurol Neurosurg Psychiatry. 2018;89(8):836-43.
12. Marin RS. Apathy: a neuropsychiatric syndrome. J Neuropsychiatry Clin Neurosci. 1991;3(3):243-54.
13. Czernecki V, Schupbach M, Yaici S, et al. Apathy following subthalamic stimulation in Parkinson disease: a dopamine responsive symptom. Mov Disord. 2008;23(7):964-9.
14. Drapier D, Drapier S, Sauleau P, et al. Does subthalamic nucleus stimulation induce apathy in Parkinson's disease? J Neurol. 2006;253(8):1083-91.
15. Le Jeune F, Drapier D, Bourguignon A, et al. Subthalamic nucleus stimulation in Parkinson disease induces apathy: a PET study. Neurology. 2009;73(21):1746-51.
16. Vachez Y, Carcenac C, Magnard R, et al. Subthalamic nucleus stimulation impairs motivation: Implication for apathy in Parkinson's disease. Mov Disord. 2020.
17. Petry-Schmelzer JN, Krause M, Dembek TA, et al. Non-motor outcomes depend on location of neurostimulation in Parkinson's disease. Brain. 2019;142(11):3592-604.
18. Dafsari HS, Petry-Schmelzer JN, Ray-Chaudhuri K, et al. Non-motor outcomes of subthalamic stimulation in Parkinson's disease depend on location of active contacts. Brain stimul. 2018;11(4):904-12.
19. Huang C, Ravdin LD, Nirenberg MJ, et al. Neuroimaging markers of motor and nonmotor features of Parkinson's disease: an 18f fluorodeoxyglucose positron emission computed tomography study. Dement Geriatr Cogn Dis. 2013;35(3-4):183-96.
20. Eckert T, Tang C, Eidelberg D. Assessment of the progression of Parkinson's disease: a metabolic network approach. Lancet Neurol. 2007;6(10):926-32.

21. Pagonabarraga J, Kulisevsky J, Strafella AP, et al. Apathy in Parkinson's disease: clinical features, neural substrates, diagnosis, and treatment. Lancet Neurol. 2015;14(5):518-31.
22. Boon LI, Hillebrand A, Potters WV, et al. Motor effects of deep brain stimulation correlate with increased functional connectivity in Parkinson's disease: An MEG study. Neuroimage Clin. 2020;26:102225.
23. Leentjens AF, Dujardin K, Marsh L, et al. Apathy and anhedonia rating scales in Parkinson's disease: critique and recommendations. Mov Disord. 2008;23(14):2004-14.
24. Starkstein SE, Mayberg HS, Preziosi TJ, et al. Reliability, validity, and clinical correlates of apathy in Parkinson's disease. J Neuropsychiatry Clin Neurosci. 1992;4(2):134-9.
25. Bech P, Kastrup M, Rafaelsen OJ. Mini-compendium of rating scales for states of anxiety depression mania schizophrenia with corresponding DSM-III syndromes. Acta Psychiatr Scand Suppl. 1986;326:1-37.
26. Taulu S, Hari R. Removal of magnetoencephalographic artifacts with temporal signal-space separation: demonstration with single-trial auditory-evoked responses. Hum Brain Mapp. 2009;30(5):1524-34.
27. Taulu S, Simola J. Spatiotemporal signal space separation method for rejecting nearby interference in MEG measurements. Phys Med Biol. 2006;51(7):1759-68.
28. Whalen C, Maclin EL, Fabiani M, et al. Validation of a method for coregistering scalp recording locations with 3D structural MR images. Hum Brain Mapp. 2008;29(11):1288-301.
29. Gong G, He Y, Concha L, et al. Mapping anatomical connectivity patterns of human cerebral cortex using in vivo diffusion tensor imaging tractography. Cereb Cortex. 2009;19(3):524-36.
30. Tzourio-Mazoyer N, Landeau B, Papathanassiou D, et al. Automated anatomical labeling of activations in SPM using a macroscopic anatomical parcellation of the MNI MRI single-subject brain. Neuroimage. 2002;15(1):273-89.
31. Hillebrand A, Tewarie P, van Dellen E, et al. Direction of information flow in large-scale resting-state networks is frequency-dependent. Proc Natl Acad Sci U S A. 2016;113(14):3867-72.
32. Hillebrand A, Barnes GR, Bosboom JL, et al. Frequency-dependent functional connectivity within resting-state networks: an atlas-based MEG beamformer solution. Neuroimage. 2012;59(4):3909-21.
33. Hillebrand A, Tewarie P, Van Dellen E, et al. Direction of information flow in large-scale resting-state networks is frequency-dependent. Proc Natl Acad Sci U S A. 2016;113(14):3867-72.
34. Brookes MJ, Woolrich MW, Barnes GR. Measuring functional connectivity in MEG: a multivariate approach insensitive to linear source leakage. Neuroimage. 2012;63(2):910-20.
35. Hipp JF, Hawellek DJ, Corbetta M, et al. Large-scale cortical correlation structure of spontaneous oscillatory activity. Nat Neurosci. 2012;15(6):884-90.
36. Horn A, Kuhn AA. Lead-DBS: a toolbox for deep brain stimulation electrode localizations and visualizations. Neuroimage. 2015;107:127-35.
37. Avants B, Epstein C, Grossman M, et al. Symmetric diffeomorphic image registration with cross-correlation: evaluating automated labeling of elderly and neurodegenerative brain. Med Image Anal. 2008;12:26-41.
38. Ewert S, Plettig P, Li N, et al. Toward defining deep brain stimulation targets in MNI space: A subcortical atlas based on multimodal MRI, histology and structural connectivity. Neuroimage. 2018;170:271-82.
39. Pretus C, Hamid N, Sheikh H, et al. Ventromedial and dorsolateral prefrontal interactions underlie will to fight and die for a cause. Soc Cogn Affect Neurosci. 2019;14(6):569-77.
40. Voruz P, Le Jeune F, Haegelen C, et al. Motor symptom asymmetry in Parkinson's disease predicts emotional outcome following subthalamic nucleus deep brain stimulation. Neuropsychologia. 2020;144:107494.
41. Thobois S, Hotton GR, Pinto S, et al. STN stimulation alters pallidal-frontal coupling during response selection under competition. J Cereb Blood Flow Metab 2007;27(6):1173-84.

42. Alexander GE, Crutcher MD, DeLong MR. Basal ganglia-thalamocortical circuits: parallel substrates for motor, oculomotor, "prefrontal" and "limbic" functions. Prog Brain Res. 1990;85:119-46.
43. Haynes WI, Haber SN. The organization of prefrontal-subthalamic inputs in primates provides an anatomical substrate for both functional specificity and integration: implications for Basal Ganglia models and deep brain stimulation. J Neurosci. 2013;33(11):4804-14.
44. Ricciardi L, Morgante L, Epifanio A, et al. Stimulation of the subthalamic area modulating movement and behavior. Parkinsonism Relat Disord. 2014;20(11):1298-300.
45. Kirsch-Darrow L, Zahodne LB, Marsiske M, et al. The trajectory of apathy after deep brain stimulation: from pre-surgery to 6 months post-surgery in Parkinson's disease. Parkinsonism Relat Disord. 2011;17(3):182-8.
46. Okun MS, Wu SS, Fayad S, et al. Acute and Chronic Mood and Apathy Outcomes from a randomized study of unilateral STN and GPi DBS. PLoS One. 2014;9(12):e114140.
47. Zaidel A, Spivak A, Grieb B, et al. Subthalamic span of beta oscillations predicts deep brain stimulation efficacy for patients with Parkinson's disease. Brain. 2010;133(Pt 7):2007-21.
48. Bot M, Verhagen O, Caan M, et al. Defining the Dorsal STN Border Using 7.0-T MRI: A Comparison to Microelectrode Recordings and Lower Field Strength MRI. Stereotact Funct Neurosurg. 2019;97(3):153-9.
49. Stefurak T, Mikulis D, Mayberg H, et al. Deep brain stimulation for Parkinson's disease dissociates mood and motor circuits: a functional MRI case study. Mov Disord. 2003;18(12):1508-16.
50. Irmen F, Horn A, Mosley P, et al. Left Prefrontal Connectivity Links Subthalamic Stimulation with Depressive Symptoms. Ann Neurol. 2020.
51. Hirschmann J, Ozkurt TE, Butz M, et al. Distinct oscillatory STN-cortical loops revealed by simultaneous MEG and local field potential recordings in patients with Parkinson's disease. Neuroimage. 2011;55(3):1159-68.
52. Hirschmann J, Ozkurt TE, Butz M, et al. Differential modulation of STN-cortical and cortico-muscular coherence by movement and levodopa in Parkinson's disease. Neuroimage. 2013;68:203-13.
53. Litvak V, Jha A, Eusebio A, et al. Resting oscillatory cortico-subthalamic connectivity in patients with Parkinson's disease. Brain. 2011;134(Pt 2):359-74.
54. Kelley R, Flouty O, Emmons EB, et al. A human prefrontal-subthalamic circuit for cognitive control. Brain. 2018;141(1):205-16.
55. Baláz M, Srovnalová H, Rektorová I, et al. The effect of cortical repetitive transcranial magnetic stimulation on cognitive event-related potentials recorded in the subthalamic nucleus. Exp Brain Res. 2010;203(2):317-27.
56. Hillebrand A, Fazio P, de Munck JC, et al. Feasibility of clinical magnetoencephalography (MEG) functional mapping in the presence of dental artefacts. Clin Neurophysiol. 2013;124(1):107-13.
57. Kandemir AL, Litvak V, Florin E. The comparative performance of DBS artefact rejection methods for MEG recordings. Neuroimage. 2020:117057.
58. Schoffelen JM, Gross J. Source connectivity analysis with MEG and EEG. Hum Brain Mapp. 2009;30(6):1857-65.
59. Carriere N, Besson P, Dujardin K, et al. Apathy in Parkinson's disease is associated with nucleus accumbens atrophy: a magnetic resonance imaging shape analysis. Mov Disord. 2014;29(7):897-903.
60. Lhommee E, Klinger H, Thobois S, et al. Subthalamic stimulation in Parkinson's disease: restoring the balance of motivated behaviours. Brain. 2012;135(Pt 5):1463-77.
61. Xia M, Wang J, He Y. BrainNet Viewer: a network visualization tool for human brain connectomics. PLoS One. 2013;8(7):e68910.

Supplementary materials

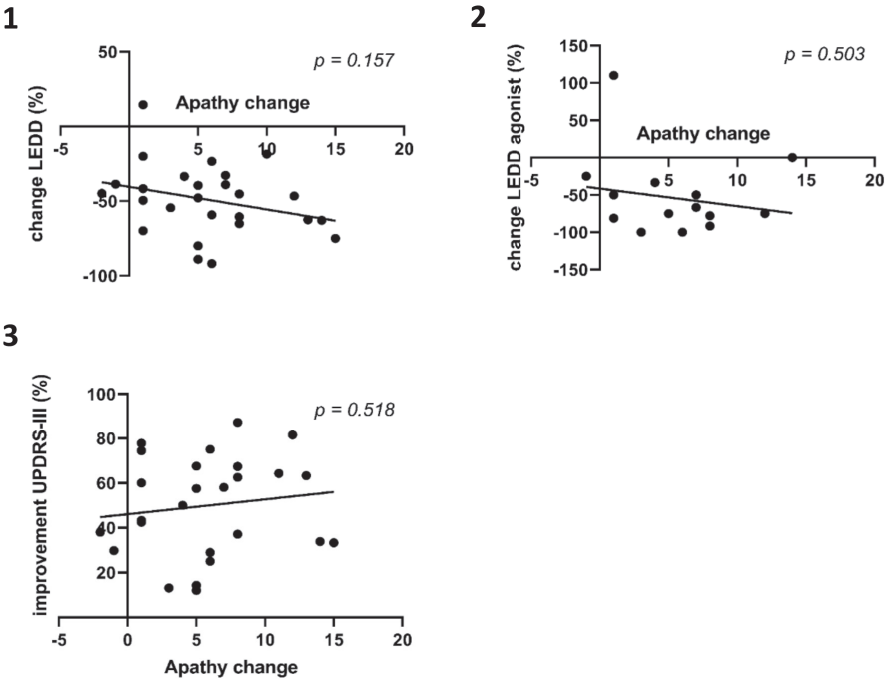

Supplementary Figure A Correlation of change in apathy score with (1) change in dopaminergic medication, (2) change in dopamine agonists, and (3) improvement in MDS-UPDRS-III scores
(1 + 2) Scatter plots of change in apathy score (pre-DBS versus post-DBS) with change in dopaminergic medication (% change of Levodopa Equivalent Daily Dose; LEDD; pre-DBS versus post-DBS). There were no significant correlations between increase in apathy score and decrease in dopaminergic medication (1) $r(24)= 0.286$, $p= 0.157$; (2) $r(14)= 0.181$, $p= 0.503$.
(3) Scatter plots of change in apathy score (pre-DBS versus post-DBS) with improvement in MDS-UPDRS-III scores (% change of improvement pre-DBS versus post-DBS, ON stimulation, dopamine OFF). There was no significant correlation $r(24)= 0.133$, $p=0.518$.
MDS-UPDRS-III, Movement Disorders Society Unified Parkinson's Disease Rating Scale motor ratings

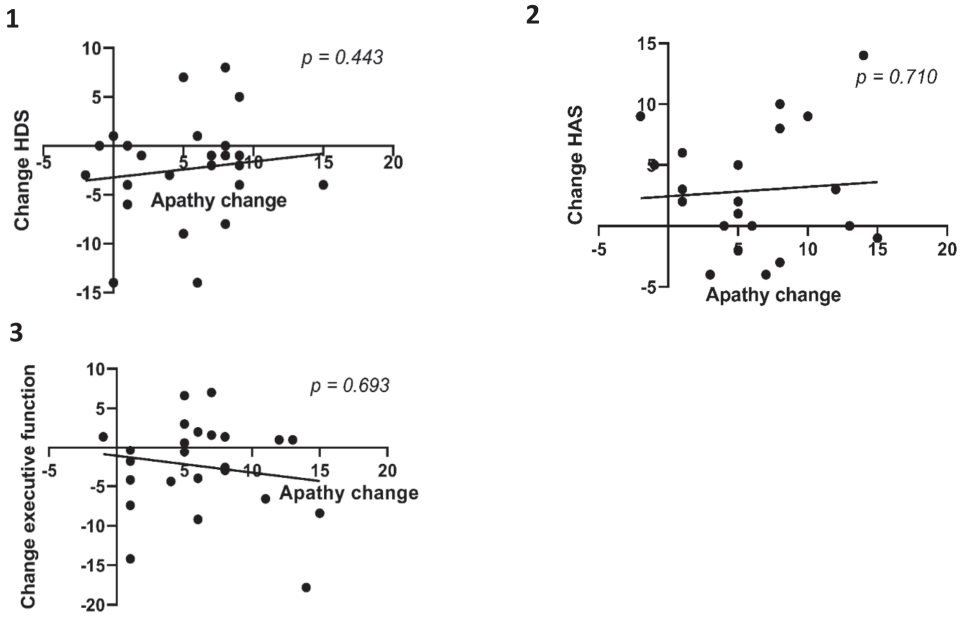

Supplementary Figure B Correlation of change in apathy score with changes in (1) depression score, (2) anxiety score, and (3) executive functioning

Scatter plots of change in apathy score (pre-DBS versus post-DBS) with (1) change in Hamilton Depression Scores (HDS; pre-DBS versus post-DBS), (2) change in Hamilton Anxiety Scores (HAS; pre-DBS versus post-DBS) and (3) average change of T-values of executive functioning (Trail Making Test A and B; Stroop Test 1-3; in which higher scores represent worse functioning). There were no significant correlations between increase in apathy score and change in (1) depression scores $r(24)= 0.160$, $p= 0.443$; (2) anxiety scores $r(24)= 0.077$, $p= 0.710$ (3) T-values of executive functioning $r(24)= -0.083$; $p= 0.693$.

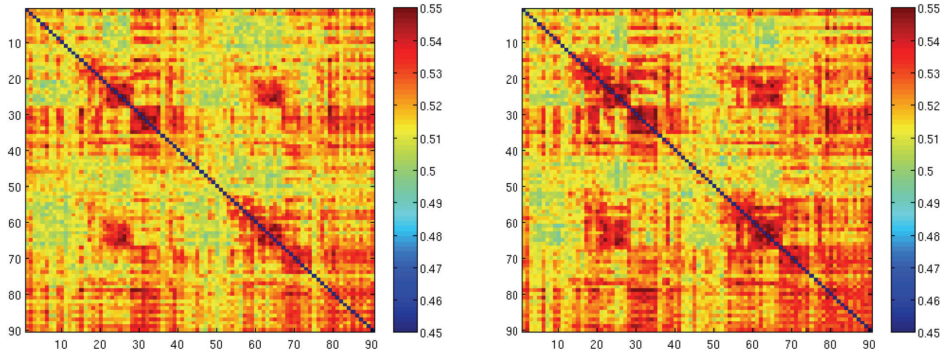

Supplementary Figure C Functional connectivity matrices (alpha1 band)
Functional connectivity matrices were averaged over all subjects. 1-39 represent left-cortical brain regions, 40-78 represent right-cortical brain regions and 79-90 represent subcortical brain regions. A more detailed explanation of the AAL regions can be found in Supplementary Table 1.

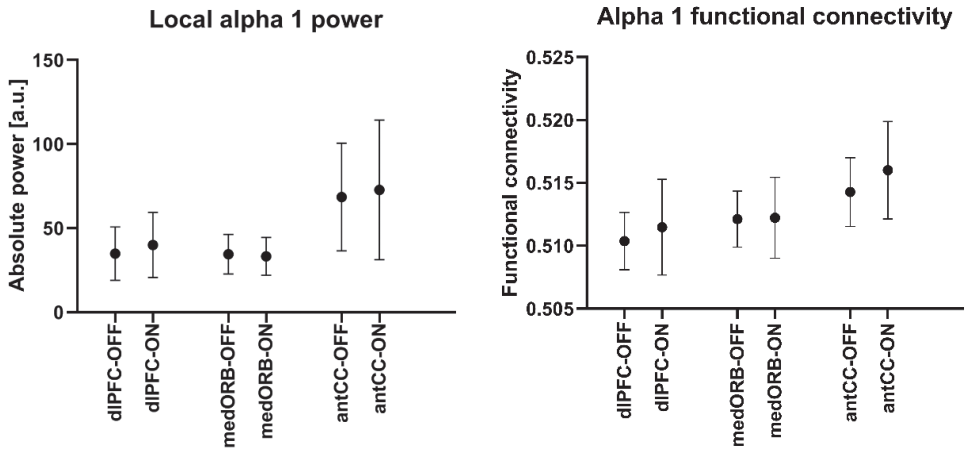

Supplementary Figure D
Local (absolute) band power (left panel) and functional connectivity (right panel) in the alpha1 band for the three seed regions, both in the DBS-OFF and DBS-ON state. Values are presented as mean (± SD). Statistics was performed on the relationship between change in local alpha1 absolute band power (surrogate marker for change in signal to noise ratio) and change in alpha1 functional connectivity using spearman correlations. None of the relationships reached statistical significance. (dlPFC, Spearman's ρ = 0.317, p = 0.107 ; medORB, Spearman's ρ = -0.057 , p = 0.776 ; antCC, Spearman's ρ = 0.284 , p = 0.151)
dlPFC, dorsolateral prefrontal cortex; medORB, medial orbitofrontal cortex; antCC, anterior cingulate cortex

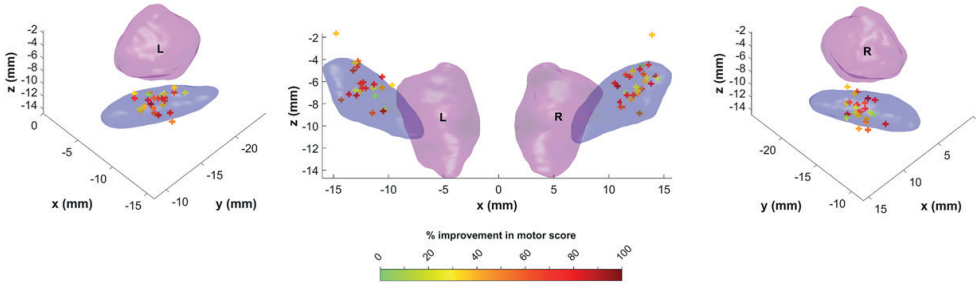

Supplementary Fig. E Stimulation locations of contact points in relation to improvement in motor score
Stimulation locations in MNI-space (viewed from respectively dorsolateral left, posterior and dorsolateral right). The subthalamic nucleus (blue) and red nucleus (red) were added for reference purposes. Improvements in motor score (% UPDRS-III, contrasting pre- versus post-DBS scores) are color-coded, ranging from no improvement (green/yellow) to strong improvement (dark red).
Next, stimulation locations were projected on a vector through the longitudinal axis of the STN, where negative values indicated more ventromedial stimulation positions. There were no significant correlations between stimulation position and improvement in motor performance; left side ($r(24)= 0.055$, $p= 0.788$); right side ($r(24)= -0.197$, $p= 0.335$).
MNI, Montreal Neurological Institute; L, left; R, right; UPDRS-III, Unified Parkinson's disease Rating Scale, motor part

Supplementary Table 1 Regions of the AAL atlas
This table can be found in the supplementary materials of Chapter 3.2

CHAPTER 6.3

Magnetoencephalography to measure the effect of contact point-specific deep brain stimulation in Parkinson's disease: a proof of concept study

Lennard I Boon, Wouter V Potters, Arjan Hillebrand, Rob MA de Bie, Maarten Bot, P Richard Schuurman, Pepijn van den Munckhof, Jos W Twisk, Cornelis J Stam, Henk W Berendse, Anne-Fleur van Rootselaar

Neuroimage Clinical 2023;38:103431
DOI: 10.1016/j.nicl.2023.10343

Abstract

Background Deep brain stimulation (DBS) of the subthalamic nucleus (STN) is an effective treatment for disabling fluctuations in motor symptoms in Parkinson's disease (PD) patients. However, iterative exploration of all individual contact points (four in each STN) by the clinician for optimal clinical effects may take months.

Objective In this proof of concept study we explored whether magnetoencephalography (MEG) may be used to noninvasively measure the effects of changing the active contact point of STN-DBS on spectral power and functional connectivity in PD patients, with the ultimate aim to aid in the process of selecting the optimal contact point, and perhaps reduce the time to achieve optimal stimulation settings.

Methods The study included 30 PD patients who had undergone bilateral DBS of the STN. MEG was recorded during stimulation of each of the eight contact points separately (four on each side). Each stimulation position was projected on a vector running through the longitudinal axis of the STN, leading to one scalar value indicating a more dorsolateral or ventromedial contact point position. Using linear mixed models, the stimulation positions were correlated with band-specific absolute spectral power and functional connectivity of i) the motor cortex ipsilateral tot the stimulated side, ii) the whole brain.

Results At group level, more dorsolateral stimulation was associated with lower low-beta absolute band power in the ipsilateral motor cortex (p = .019). More ventromedial stimulation was associated with higher whole-brain absolute delta (p = .001) and theta (p = .005) power, as well as higher whole-brain theta band functional connectivity (p = .040). At the level of the individual patient, switching the active contact point caused significant changes in spectral power, but the results were highly variable.

Conclusions We demonstrate for the first time that stimulation of the dorsolateral (motor) STN in PD patients is associated with lower low-beta power values in the motor cortex. Furthermore, our group-level data show that the location of the active contact point correlates with whole-brain brain activity and connectivity. The results in individual patients were too variable to draw conclusions regarding the potential use of MEG in the selection of the optimal DBS contact point.

Introduction

Deep brain stimulation (DBS) of the subthalamic nucleus (STN) is an effective treatment in case of disabling fluctuations in motor symptoms of Parkinson's disease (PD) patients.[1-3] In addition to the excellent effects on motor symptoms, DBS may positively or negatively affect non-motor symptoms, such as neuropsychological and neuropsychiatric functioning.[4-6] DBS electrodes are implanted bilaterally and each DBS electrode generally contains multiple contact points. After DBS placement, the stimulation settings have to be iteratively explored by the clinician during a rather long period, often spanning months, to find the optimal stimulation settings. Optimal contact point selection is important, because motor and non-motor outcomes seem to depend on the location of the active contact point in the STN and its surrounding white matter.[7-9]

STN target identification is based on T2 magnetic resonance imaging (MRI) coordinates.[10] Post-operative refinements of stimulation parameters are mainly based on the clinical effects of the stimulation. In theory, the expected clinical effects of stimulation could be based on the anatomical position of contact points in relation to their surrounding structural networks, obtained using coregistered pre- and post-operative images.[11] However, this does not offer insight into the effects on *functional* brain networks, which have gained increasing attention over the years. A better understanding of the effects of DBS on functional brain networks may provide insight in the underlying mechanisms and can help to optimize treatment effects.[12]

Magnetoencephalography (MEG) has been used for the in-vivo assessment of the modulatory effect of stimulation of the STN on neural networks involving both the cerebral cortex and subcortical brain regions. To date, this has only been studied in a DBS ON versus OFF design in which only one contact point (with clinically optimal effect) per hemisphere was stimulated[13-18]. In our own studies, we have found that DBS, using the optimal contact point, led to a whole-brain acceleration of neuronal oscillations and to a suppression of absolute band power (delta to low-beta power) in the sensorimotor cortices.[13] Furthermore, changes in functional connectivity correlated with improvement in motor function[13] and with the occurrence of the non-motor side effect apathy[18]. Two studies from other research groups found a lowering effect of STN-DBS on alpha and low-beta band power in the sensorimotor cortices.[14,15]

In this proof of concept study, we tested for the first time the functional effects of stimulating *different* DBS contact points in the STN within individual patients using MEG. If differential effects would prove to be observable, MEG recordings could potentially aid in the process of selecting the optimal contact point, and perhaps reduce the time to achieve optimal stimulation settings. We first analyzed the effect of stimulation on the ipsilateral motor cortex. Based on previous studies,[13-15] we expected that stimulation in the dorsolateral STN would lead to a suppression of absolute alpha2 and low-beta band power and functional connectivity. This suppression may occur via stimulation

of the hyperdirect pathway that structurally connects the dorsolateral STN with the motor cortex, which may lead to desynchronization of cortical neurons.[19,20] Next, we analyzed the effect of stimulating different contact points on whole-brain spectral power and functional connectivity. The ventral STN has recently been demonstrated to have functional loops with the cerebral cortex via theta and alpha oscillations,[21,22] so we expected ventral stimulation to affect these oscillations. Finally, we set out to analyse whether an acute change in stimulation position would lead to consistent changes in brain activity and connectivity in individual patients.

Materials and methods

Patients

A total of 30 PD patients participated in this study after we consecutively approached eligible PD patients who had undergone bilateral DBS implantation between 2016 and 2018 at Amsterdam UMC, location AMC. All patients were implanted with a bilateral Boston Scientific Vercise directional stimulation system (Valencia, CA, USA). Inclusion and exclusion criteria were previously described.[13] In all patients, monopolar stimulation in so-called ring mode at one of four available depths was used, with the implantable pulse generator set positive and (deepest) contact point 1, contact points 2-4, contact points 5-7 or (upper) contact point 8 set negative (Supplementary Figure 1).

The study protocol was approved by the medical ethical committee of the Amsterdam UMC, location VUmc. All patients gave written informed consent before participation.

Data acquisition

Patients underwent MEG recordings at least 6 months after DBS placement (range 6-17 months; median 7 months), after an overnight withdrawal of dopaminergic medication (practically defined OFF-medication state). MEG data were recorded using a 306-channel whole-head system (Elekta Neuromag Oy, Helsinki, Finland) in an eyes-closed resting-state condition, with a sample rate of 1250 Hz and online anti-aliasing (410 Hz) and high-pass (0.1 Hz) filters. The head position relative to the MEG sensors was recorded continuously using the signals from five head position indicator (HPI) coils. The HPI positions were digitized before each recording, as well as the outline of the patient's scalp (~500 points), using a 3D digitizer (Fastrak, Polhemus, Colchester, VT, USA).

For each patient, the total MEG recording time was 55 minutes, consisting of 11 trials of 5 minutes. A different DBS stimulation setting was used for each trial with a 'wash-out' period of approximately one minute. The first and eleventh (last) recording were performed during bilateral stimulation using the standard DBS-settings of the individual patient (DBS-ON; results presented previously).[13,18] In between, nine recordings took place in randomized order, eight of which consisted of unilateral stimulation using a single contact point, and

one recording during DBS OFF (results previously presented).[13,18] For each individual participant, unilateral stimulation was performed within the limits of the results of the initial threshold screening for effects and adverse effects of stimulating each contact point. This threshold screening was obtained in the context of standard care, two to four weeks after DBS placement, and indicated the maximally tolerable stimulation strength for each contact point. In the first 13 patients of the study, stimulation strength differed between recordings, but in patients that were recorded later in the project we aimed to keep the stimulation strength more equal between contact points. The stimulation frequency and pulse width we used were the same as during bilateral stimulation (standard settings). After each individual recording, we asked whether patients experienced discomfort. If so, then we limited the number of recordings. Further details on the experimental set-up can be found in our previous publications on this study cohort.[13,18]

Anatomical images of the head were obtained in the context of standard pre-operative imaging up to 6 months before surgery using a 3T MRI scanner (Philips Ingenia, Best, the Netherlands) and a 16-channel receiver coil. Further details on the MRI parameters have been described previously[13,18]. Up to 1 day after surgery, a CT scan of the head was acquired (slice thickness 1–2mm; FOV 512×512 mm; number of slices 56–169). For 25 patients, on the postoperative day, a multidetector CT-scan of the head was acquired (Philips Medical System, Best, The Netherlands; slice thickness 1–2 mm; FOV 512×512mm; 56–169 slices). For the five remaining participants, an intra-operative CT-scan was acquired (O-arm O2, Medtronic Inc., Minneapolis, MN, USA) with a 20 cm FOV (high definition mode; 192 slices; 120 kV; 150 mAs).

Data processing

MEG data

MEG channels that were malfunctioning or noisy were ignored after visual inspection of the data. Thereafter, the temporal extension of Signal Space Separation (tSSS)[23,24] in MaxFilter software (Elekta Neuromag Oy, version 2.2.15) was applied with a subspace correlation-limit of 0.8 to suppress the strong magnetic artefacts; see also[13] for an example of the effect of tSSS on MEG data recorded during DBS). MEG data of each patient were co-registered to their structural MRI using a surface-matching procedure, with an estimated accuracy of 4 mm.[25] A single sphere was fitted to the outline of the scalp as obtained from the co-registered MRI, which was used as a volume conductor model for the beamformer approach described below.

The automated anatomical labelling (AAL) atlas was used to label the voxels in 78 cortical and 12 subcortical regions of interest (ROIs).[26,27] We used each ROI's centroid as representative for that ROI[28]. Subsequently, an atlas-based beamforming approach[29] was used to project broad-band (0.5-48 Hz) filtered sensor signals to these centroid voxels, resulting in broad-band time-series for each of the 90 ROIs (see[28] for details). The source-reconstructed MEG data were downsampled from 1250 Hz to 312.5 Hz (4x) and

cut into epochs containing 4096 samples (13.11 s). The epochs were visually inspected (by LIB) for tremor-, motion- and stimulation-related artefacts and drowsiness. In addition, for each recording, the 50% epochs with the lowest peak frequency (frequency with maximum power within the 4-13 Hz frequency range) were discarded in order to make the occurrence of drowsiness in the selected data even more unlikely. Finally, the 10 epochs with the best quality were selected for further analysis. Spectral and functional connectivity analyses were performed using in-house software (BrainWave, version 0.9.152.12.26; CJS, available from https://home.kpn.nl/stam7883/brainwave.html). For frequency band-specific analyses, epochs were filtered in five frequency bands (delta (0.5-4 Hz), theta (4-8 Hz), alpha1 (8-10 Hz), alpha2 (10-13 Hz), and low-beta (13-22 Hz), using a Fast Fourier Transform. The high-beta and gamma bands were not analyzed as we observed stimulation-related artefact peaks in this frequency range (22-48 Hz) in our previous study.[13] For each epoch, frequency band-specific functional connectivity was estimated using the corrected Amplitude Envelope Correlation (AEC-c), an implementation of the AEC[30,31] corrected for volume conduction/field spread, using a symmetric (pairwise) orthogonalisation procedure applied to each epoch.[30,32] To adjust for any negative correlations, 1 was added to the raw AEC values and this sum was subsequently divided by 2, leading to values between 0 and 1, with 0.5 indicating absence of functional connectivity. The AEC-c was calculated for all possible pairs of ROIs, leading to a 90x90 adjacency matrix for each frequency band. We obtained region-specific functional connectivity of one ROI with the rest of the brain by taking the average of each of the 90 columns of the matrix.

Imaging data

To determine the stimulation locations after placement of the DBS system, the electrode trajectories were reconstructed. To this end, the post-operative CT-scan was co-registered to the pre-operative MR image using a two-stage (rigid and affine) registration as implemented in Advanced Normalization Tools (ANT).[33] For the five patients of whom only an intra-operative CT-scan was available, the co-registration failed using ANT. In these cases, co-registration was successfully performed using FSL FLIRT. The co-registration was followed by a semiautomatic localization of the electrode positions in the CT data in patient space (Lead-DBS, version 2.2; http://www.lead-dbs.org).[34]

The electrode stimulation positions were then transformed from patient space to Montreal Neurological Institute space (MNI ICBM 2009b NLIN ASYM space) to facilitate group-level analyses. We used the DISTAL Minimal atlas[35] as an outline of the STN. Next, in line with our previous analysis on stimulation positions in this study cohort,[18] stimulation positions were projected on a vector running through the longitudinal axis of the STN (from ventromedial to dorsolateral), leading to one scalar value to indicate each stimulation position, where negative values indicated more ventromedial stimulation positions (see Figure 1A for a schematic display, in which the 25% most dorsolateral and 25% most ventrolateral contact points have been indicated).

Statistical analysis

Group analyses

For each stimulation condition and frequency band separately, neurophysiological results were averaged over 10 epochs. Next, we obtained i) alpha2 and low-beta band absolute band power and functional connectivity of the motor cortex ipsilateral to the stimulated hemisphere and ii) absolute band power and functional connectivity per frequency band, averaged for the brain as a whole (all 90 AAL regions).

We used linear mixed models to evaluate the association between the (scalarized) stimulation locations and neurophysiological measures. Linear mixed models can account for the dependency of the observations within the patient (by adding a random intercept) and the fact that not all patients had complete data. The neurophysiological measures were used as dependent variables and stimulation locations as independent variables. The side of stimulation, age, gender, post-operative use of dopaminergic medication (expressed as levodopa equivalent dose; LEDD),[36] disease duration, and stimulation strength (mA) were included in the model as covariates. In the models that focused on the motor cortex, we added the Unified Parkinson's disease Rating Scale (UPDRS-III) motor score (during DBS and levodopa OFF) as additional covariate.

All analyses were performed using the SPSS Statistics 20.0 software package (IBM Corporation, New York, USA), and a significance level of 0.05 (two-tailed). Results of linear mixed models are expressed as standardized effect sizes.

Post-hoc visualizations of group analysis

We visualized the distribution of the neurophysiological measures that were significantly associated with stimulation location in the linear mixed model analyses and compared dorsolateral with ventromedial stimulation. For this, we compared the results of stimulation of the 25% most dorsolateral contact points with stimulation of the 25% most ventrolateral contact points of each hemisphere. We also compared the results of these 'extreme' contact point locations (25% most dorsolateral and ventromedial) with the results of the DBS OFF condition using analysis of variance (ANOVA) to study the direction of change that caused the observed associations.

Individual subjects

Next, we analyzed whether a change in stimulation position within individual patients would lead to consistent changes in brain activity, again for the neurophysiological measures that had a significant relationship with stimulation positions in the linear mixed model analyses. Therefore, for each individual patient, we calculated the correlation coefficient between the (scalarized) stimulation locations and the neurophysiological measures, without taking covariates into account.

We also explored within one randomly selected patient how the measures of absolute spectral power evolved during the recording session, with the aim to observe distinct changes in neurophysiological patterns upon change of the stimulation position.

Table 1 Patient characteristics

Patient	Age	Sex	Disease duration (years)	Range of stimulation strengths (mA)	Pulse width and frequency of stimulation	LEDD post-DBS (mg/day)	#datasets available/ #recordings
1	38	M	8	L; 2.5-3.5 R; 1.5-3.5	60 µs; 179 Hz	996	8/8
2	70	F	25	L;1.5-3.5 R; 2.0	60 µs; 130 Hz	567	8/8
3	66	M	10	L; 2.5-3.5 R; 1.5-3.0	60 µs; 149 Hz	575	8/8
4	55	M	8	L; 2.0-2.5 R; 2.0-3.0	60 µs; 130 Hz	775	7/8
5	57	M	11	L; 3.0 R; 1.0-2.0	60 µs; 130 Hz	606	8/8
6	61	M	7	L; 1.5-3.5 R; 1.5-3.0	60 µs; 130 Hz	375	8/8
7	60	F	10	L; 2.5 R; 3.0	60 µs; 179 Hz	350	6/7
8	60	M	14	L; 1.5-3.0 R; 1.0-2.0	60 µs; 130 Hz	425	5/8
9	63	F	5	L; 2.0 R; 2.0	60 µs; 130 Hz	567	8/8
10	65	F	27	L; 2.5-3.0 R; 2.0-2.5	60 µs; 130 Hz	400	8/8
11	49	F	10	L; 1.5-2.0 R; 1.5-2.0	60 µs; 130 Hz	536	4/5
12	57	M	12	L; 2.5 R; 2.0-2.5	60 µs; 130 Hz	720	5/5
13	69	M	12	L; 2.0 R; 1.0-1.5	60 µs; 130 Hz	150	7/8
14	61	M	8	L; 2.0 R; 1.5	60 µs; 130 Hz	946	6/8
15	60	M	8	L; 1.5 R; 1.5	60 µs; 179 Hz	300	7/8
16	56	M	12	L; 2.5 R; 2.5	60 µs; 130 Hz	1245	7/8
17	56	M	14	L; 2.5 R; 2.5	60 µs; 130 Hz	783	3/3
18	53	M	11	L; 2.0 R; 2.0	60 µs; 130 Hz	1043	6/7
19	66	F	8	L; 2.0-2.5 R; 2.5	60 µs; 130 Hz	753	7/8
20	45	M	5	L; 2.5 R; 2.5	60 µs; 130 Hz	283	7/8
21	58	M	16	L; 3.0 R; 3.0	60 µs; 130 Hz	613	6/6
22	55	F	20	L; 2.0 R; 1.3	60 µs; 130 Hz	558	8/8
23	57	M	12	L; 3.5 R; 3.5	60 µs; 130 Hz	533	4/4
24	65	F	18	L; 1.5 R; 1.5	60 µs; 130 Hz	500	8/8
25	57	F	14	L; 2.5 R; 2.5	60 µs; 130 Hz	660	8/8
26	63	F	11	L; 2.0 R; 2.0	60 µs; 130 Hz	887	6/8
27	53	F	5	L; - R; 3.0	60 µs; 130 Hz	883	3/4
28	55	M	12	L; 1.5 R; 1.5	60 µs; 130 Hz	679	8/8
29	64	M	22	L; 3.0 R; 3.0	60 µs; 130 Hz	780	7/8
30	48	M	6	L; 1.0-1.5 R; 1.5-2.0	60 µs; 130 Hz	110	7/8
Mean (SD)	58.1 (6.9)	M, n=19; F, n=11	12.0 (5.6)			620 (260)	

mA, milliampère; µs, microseconds; LEDD, Levodopa equivalent daily dose; mg, milligrams, M/F, male/female, L/R left/right; SD, standard deviation; Hz, Hertz

Results

Patients

30 DBS-treated PD patients, whose characteristics are summarized in Table 1, were included in this study. The median number of MEG-recordings performed for each subject was 8 (range 3-8) out of 8 possible recordings. 9% of these recordings could not be used for further analysis due to insufficient quality, leading to a median number of 7 recordings per patient (range 3-8) and a total of 199 recordings (27.1% (deepest) contact point 1, 23.6% contact points 2-4, 25.1% contact points 5-7, 24.1% (upper) contact point 8)). Of the data that had sufficient quality, the median number of excluded MEG channels before running tSSS was 9 (range 3-12).

Associations between stimulation location and neurophysiological measures

The stimulation positions are depicted in Figure 1A, in standard MNI space relative to an atlas representing the STN. Using linear mixed models, we analyzed the associations between the (scalarized) stimulation locations and absolute spectral power as well as functional connectivity values. An overview of the results can be found in Table 2.

The analysis of the motor cortex ipsilateral to the stimulated STN demonstrated a significant association between more dorsolateral stimulation and lower (absolute) low-beta band power (standardized effect size -0.112; p = .019). There were no significant associations for absolute alpha2 power or alpha2 and low-beta functional connectivity.

The whole-brain analysis showed a significant association between more ventromedial stimulation and higher (absolute) delta and theta power (standardized effect sizes -0.154; p = .001 and -0.059; p = .005 respectively). In addition, more ventromedial stimulation was associated with higher whole-brain theta functional connectivity (standardized effect size -0.125; p = .040). Scatter plots of the neurophysiological measures that had a significant association with stimulation positions are shown in Supplementary Figure 2.

Table 2 Associations between location of stimulated contact point and brain activity/connectivity

Absolute power	**Standardized effect size**	**95% CI (standardized)**	***p* value**
Motor cortex			
Alpha2	-0.045	-0.146 to 0.057	.421
Low-beta	**-0.112**	**-0.206 to -0.018**	**.019**
Whole brain			
Delta	**-0.154**	**-0.247 to -0.061**	**.001**
Theta	**-0.059**	**-0.100 to -0.018**	**.005**
Alpha1	0.015	-0.043 to 0.072	.614
Alpha2	-0.01275	-0.054 to 0.028	.540
Low-beta	-0.014	-0.061 to 0.032	.548

Functional connectivity	**Standardized effect size**	**95% CI (standardized)**	***p* value**
Motor cortex			
Alpha2	-0.0432	-0.155 to 0.068	.483
Low-beta	-0.0139	-0.126 to 0.099	.870
Whole brain			
Delta	-0.101	-0.234 to 0.033	.140
Theta	**-0.125**	**-0.243 to -0.006**	**.040**
Alpha1	-0.011	-0.109 to 0.087	.820
Alpha2	-0.019	-0.106 to 0.068	.669
Low-beta	-0.054	-0.147 to 0.038	.249

The location of the stimulated contact point was obtained by projecting the stimulation position on a vector following the longitudinal axis of the STN, leading to one scalar value for each stimulation position. The following variables were included in the model as covariates: Side of stimulation, age, gender, levodopa equivalent daily dose (LEDD), disease duration, and stimulation strength (mA). In the models regarding the motor cortex, we added the Unified Parkinson's disease Rating Scale (UPDRS-III) motor score (during DBS and levodopa OFF) as additional covariate.
Significant associations are indicated in bold.
CI, 95% confidence interval

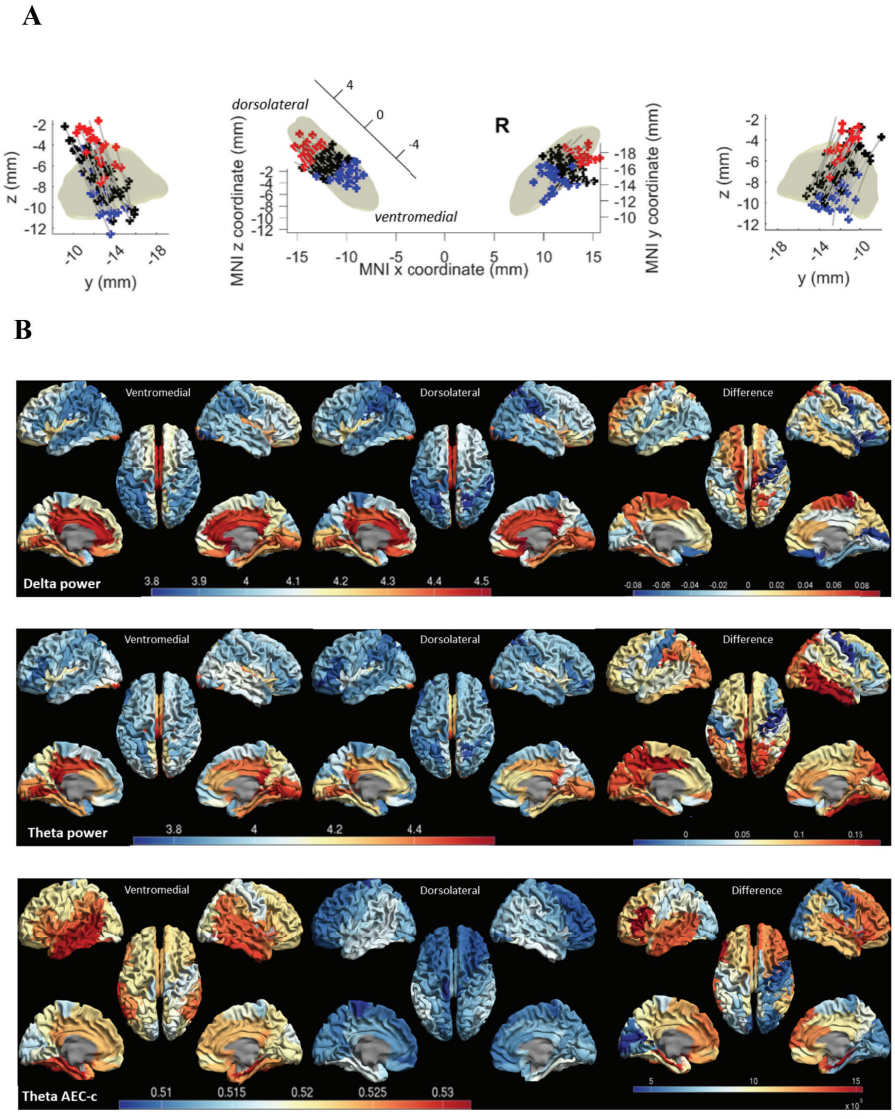

Figure 1 Visualization of ventromedial versus dorsolateral stimulation and their effects on neurophysiological parameters

A Stimulation locations in MNI-space, viewed from lateral left, ventral-posterior and lateral right, and projected on a standard subthalamic nucleus. Parallel to the left STN (middle panel), the longitudinal axis containing scalarized values is indicated. The 25% most dorsolateral contact points (positive values) are depicted in red, the 25% most ventromedial contact points are depicted in blue (negative values). The black dots indicate the remaining 50% of the contact points.

MNI, Montreal Neurological Institute; R, right

B Topographic distribution of absolute spectral power and functional connectivity values for; Left panel, the 25% most ventromedial contact points; Middle panel, the 25% most dorsolateral contact points; Right panel, difference between both conditions. We present neurophysiological measures that had a significant association on a whole-brain scale. Logarithmic absolute power/difference values are visualized as a color-coded map on a parcellated template brain viewed from, in clockwise order, the left, top, right, right-midline and left-midline.

Post-hoc visualizations

We selected the data obtained by stimulation of the 25% most dorsolateral and 25% most ventromedial contact points. We visualized the distribution of absolute delta power, theta power and theta band functional connectivity (as these measures showed a significant association with contact point position in the linear mixed model analyses), for both selections separately. Furthermore, we visualized the difference between both selections (Figure 1B). As can be appreciated from Figure 1B, when comparing ventromedial stimulation positions with dorsolateral stimulation positions, higher absolute delta power values were mainly present in frontal brain regions, higher absolute theta power values in occipitotemporal brain regions and higher theta band functional connectivity in frontotemporal brain regions.

Next, we compared the values obtained by stimulating the 25% most dorsolateral and ventromedial contact points with the values in the DBS OFF condition, to assess the direction of change of the neurophysiological measures following stimulation. The absolute low-beta band power in the motor cortex was higher compared to the DBS OFF condition with a (log) low-beta power in the ipsilateral motor cortices of 4.19 for dorsolateral stimulation and 4.20 for ventromedial stimulation versus 4.15 in the bilateral motor cortices for DBS OFF (p = .472). Average whole-brain absolute delta power was comparable for the three conditions ((log) delta power ~4.22; p = .858). For absolute whole-brain theta power, values during DBS OFF were in between those obtained during the 25% most dorsolateral and ventromedial stimulation (dorsolateral whole-brain absolute (log) theta power 4.09; DBS OFF 4.12; ventromedial 4.19; p = .036). This was also the case for whole-brain theta band functional connectivity (dorsolateral whole-brain theta band functional connectivity 0.513; DBS OFF 0.516; ventromedial 0.524; p = .001).

Acute switch in individual patients

The range of correlation coefficients between contact point positions and absolute (log) low-beta band power in the motor cortex of individual patients was -0.878 to 0.997 with a median of -0.003; for whole-brain absolute (log) delta power -0.988 to 0.614, median -0.421; for whole-brain absolute (log) theta power -0.997 to 0.634, median -0.331; for whole-brain theta band functional connectivity -0.895 to 0.740, median -0.070. All ranges of correlations were normally distributed. From this, we concluded that there was no consistent direction of correlations at the level of individual patients.

We visualized the evolution of absolute spectral power over epochs and conditions (in chronological order) within a single randomly selected patient. Although significant changes in absolute spectral power were present between different stimulation conditions (DBS-OFF condition was not included in the statistical analyses), we could not distinguish a clear pattern in the evolution of neurophysiological measures during the recording session (Supplementary Figure 3).

Discussion

In this proof of concept MEG study in 30 PD patients with DBS of the STN we explored whether MEG recordings might aid in the selection of the optimal contact point for stimulation, by analysing the effects of stimulating different DBS contact points on neurophysiological brain activity within the same patient. In our group analysis, we confirmed the hypothesis that more dorsolateral STN stimulation is associated with lower absolute low-beta band power in the ipsilateral motor cortex compared to more ventromedial stimulation. In addition, more ventromedial stimulation was associated with higher whole-brain absolute delta and theta power, as well as higher whole-brain functional connectivity in the theta band. At the level of the individual patient, we observed significant changes in absolute spectral power when we switched the active contact point, but the results were too variable to draw conclusions on.

We found an association between more dorsolateral stimulation positions and lower absolute low-beta band power in the motor cortex ipsilateral to stimulation. Our previous study[13] as well as other MEG studies[14,15] demonstrated a suppressing effect of DBS on alpha2 and beta power in the motor cortex and we hypothesized that stimulation of the motor part of the STN (in comparison to other parts of the STN) would lead to stronger suppression of beta band power in the motor cortex via the hyperdirect pathway. We could partly confirm this hypothesis, but in the post-hoc analysis we found stimulation of the (25%) most ventromedial and dorsolateral contact points to both lead to *higher* absolute low-beta band power values in the motor cortex compared to DBS OFF. The observation that band power in higher frequency bands, including low-beta power, increased in general upon stimulation therefore suggests that the net result of dorsolateral stimulation was not so much a 'suppression', but rather 'less activation' of the motor cortex. As discussed in our previous work,[13] the general increase in high-frequency band power could be an effect of a stimulation-related "release" of the thalamus,[37] increased intrinsic alertness upon stimulation,[38] and/or an increase in background noise from the stimulator. This general increase may have been superimposed by a local suppression of absolute low-beta band power in the motor cortex. The clinical implication of this local suppression of low-beta band power is yet unknown, as a lowering effect of stimulation on low-beta band power was not associated with clinical motor improvement in previous studies.[14,15]

More ventromedial stimulation was associated with higher whole-brain absolute delta and theta band power, as well as higher theta band functional connectivity. As we learned from the comparison with DBS-OFF (see paragraph "post-hoc visualizations" including figure 1B), this was partly accompanied by a lowering effect of dorsolateral stimulation on these measures. Nonetheless, in case of absolute theta power and theta band functional connectivity, the most pronounced effect of stimulation was an increase in spectral power/functional connectivity for ventromedial stimulation. In case of absolute delta power, the effect of ventromedial and dorsolateral stimulation did not differ from DBS OFF in the post-hoc analysis, therefore we cannot be sure of the direction of this effect.

Increases in absolute theta power upon ventromedial stimulation would be in line with the literature, as theta/alpha band interactions between the STN and cortex are more frequently located ventrally in the STN than beta band interaction, which is located in the dorsolateral STN.[21,22] The function of theta/alpha band interactions with the STN is not well understood, but these interactions may be involved in emotional and cognitive processes.[22] Another possible explanation for the increases in absolute delta and theta power is a reduced effect on intrinsic alertness when stimulating ventromedial versus a stronger level of arousal when stimulating in dorsolateral STN regions.[39] To exclude another optional explanation, we have tested whether the observed relationship between stimulation position and whole-brain absolute theta power may have been influenced by an adequate (in case of dorsolateral stimulation) or inadequate (in case of ventromedial stimulation) suppression of tremor. When we added tremor severity during DBS OFF as a covariate in the mixed model, the model still led to significant associations between stimulation location and whole-brain neurophysiological measures (absolute delta power p = .001; standardized effect size -0.149; absolute theta power p = .005 (-0.059); theta functional connectivity p = .033 (-0.135)). Therefore, a confounding effect of tremor is highly unlikely.

Although we found statistically significant changes in brain activity and connectivity in our group-level analyses, in individual patients we were unable to find any consistent pattern of change resulting from an acute switch of stimulation location. We assumed a linear relationship between stimulation location and functional effects of stimulation in our analyses. However, the implantation trajectory of a DBS electrode usually does not follow the dorsolateral to ventromedial axis of the STN. Ideally, the dorsolateral sensorimotor part of the STN is targeted, resulting in two (middle) contact points within, the upper contact just above and the deepest contact just below the dorsolateral STN. In less ideally implanted electrodes, all contact points end up more medially or even ventromedially in/around the STN. Switching of the active contact points may then have no effect or a different (non-linear) effect for each individual, which may be a factor contributing to the inconsistent effects in individuals. In the group level analysis using linear mixed models, the sum of these individual effect still led to significant observations. We expect that the within-subject analysis can be improved by including individual (high-resolution) anatomical information, which was lost in the group analysis that we performed in MNI space.

In an exemplary case (Supplementary Figure 3), we did observe significant differences in absolute spectral power upon switching stimulation locations, but the amount of variation within conditions was rather high and we could not observe a consistent pattern of stimulation effects in this case either. Possibly, the significant differences in spectral power in this single case were caused by other factors unrelated to the stimulation, such as variations in intrinsic alertness or natural fluctuation of brain signals over time. As factors unrelated to the stimulation may obscure subtle effects of stimulation in individual patients, analysing stimulation effects at group level may 'average-out' these variations and significant patterns may appear.

We believe that the data acquisition protocol can be further optimized to reveal the full potential of MEG for the assessment of the effects of changes in stimulation location in individual DBS-patients. I) We used a 'wash-out' period for stimulation effects of approximately one minute, which is rather short. The wash-out period for motor effects is highly variable between patients,[40] but five minutes on average.[41] Furthermore, stimulation effects on brain networks may take time to stabilize. By mainly selecting data from the last part of the recordings, we think we have partly accounted for this, but longer wash-out periods and longer recordings may be necessary to both obtain stronger group-level results and to be able to draw conclusions regarding the effects of stimulation in individual patients. II) Optimization of artefact rejection and/or artefact correction may improve the signal-to-noise ratio and hence the study results.[16]

There are several other methodological factors that deserve attention. Firstly, in the initial 13 patients the stimulation strength differed between contact points, as we stimulated at the maximally tolerable strength based on the threshold screening. In patients we included later in the study, the stimulation strength used was more comparable between contact points, in order to reduce the possibility of bias, given that stimulation strength itself may influence the neurophysiological results. However, there were no significant differences in stimulation strength between contact points (contact point 1 (deepest) average 2.22 mA, contact points 2-4 2.28 mA, contact points 5-7 2.32 mA, contact point 8 (upper) 2.25 mA; ANOVA; p = .850). Moreover, we added stimulation strength as a covariate in our analyses. Secondly, ideally we would have correlated the brain activity and connectivity resulting from stimulating different contact points with clinical measures of motor and/or non-motor functioning. Unfortunately it was not possible to obtain data on the clinical effect for each stimulated contact point during the MEG recordings, nor was the data of the threshold screening (two to four weeks after DBS placement) sufficient to perfom analyses with, but we have previously demonstrated the capability of MEG to capture clinically meaningful DBS-effects.[13,18] Thirdly, we did not perform a correction for multiple comparisons in this explorative study. We aimed to reduce the number of statistical tests by preselecting frequency bands (alpha2 and beta band analyses involving the motor cortex) and analysing global spectral power and functional connectivity (whole-brain analyses). However, we cannot exclude the possibility of false positive findings in our analyses.

In conclusion, in this proof of concept study, we explored whether MEG could be used to measure the effects of DBS on brain activity and connectivity in PD patients, which could be a stepping-stone towards the use of MEG recordings in the process of selecting the optimal contact point for stimulation. The group-level data showed that a change in stimulation location produces measurable changes in brain activity and connectivity. More dorsolateral stimulation led to lower absolute low-beta band power in the ipsilateral motor cortex, whereas ventromedial stimulation led to higher whole-brain absolute delta and theta band power, as well as higher whole-brain theta band functional connectivity. The clinical implications of these findings are currently unknown, but our results suggest

that functional mapping of the STN using MEG is feasible at a group level. However, as we did not find consistent intra-individual patterns, MEG is currently not useful in the selection of the optimal DBS contact point. Optimizations in the acquisition (both MRI and MEG) and analysis protocols may improve the potential of this approach in individual patients.

Acknowledgements

We thank all patients for their participation. We also thank Karin Plugge, Nico Akemann and Marieke Alting Siberg for the MEG acquisitions.

Study funding

This study was supported by Amsterdam Neuroscience; 05 Amsterdam Neuroscience Alliantieproject – ND 2016. The funding source had no involvement in the study design, collection, analysis and interpretation of the data, writing of the report, and in the decision to submit the article for publication.

References

1. Benabid AL, Koudsie A, Benazzouz A, et al. Deep brain stimulation of the corpus luysi (subthalamic nucleus) and other targets in Parkinson's disease. Extension to new indications such as dystonia and epilepsy. J Neurol. 2001;248 Suppl 3:Iii37-47.
2. Deuschl G, Schade-Brittinger C, Krack P, et al. A randomized trial of deep-brain stimulation for Parkinson's disease. N Engl J Med. 2006;355(9):896-908.
3. Odekerken VJ, van Laar T, Staal MJ, et al. Subthalamic nucleus versus globus pallidus bilateral deep brain stimulation for advanced Parkinson's disease (NSTAPS study): a randomised controlled trial. Lancet Neurol. 2013;12(1):37-44.
4. Ulla M, Thobois S, Llorca PM, et al. Contact dependent reproducible hypomania induced by deep brain stimulation in Parkinson's disease: clinical, anatomical and functional imaging study. J Neurol Neurosurg Psychiatry. 2011;82(6):607-14.
5. Hatz F, Meyer A, Roesch A, et al. Quantitative EEG and Verbal Fluency in DBS Patients: Comparison of Stimulator-On and -Off Conditions. Front Neurol. 2018;9:1152.
6. Castrioto A, Lhommée E, Moro E, et al. Mood and behavioural effects of subthalamic stimulation in Parkinson's disease. Lancet Neurol. 2014;13(3):287-305.
7. Bot M, Verhagen O, Caan M, et al. Defining the Dorsal STN Border Using 7.0-T MRI: A Comparison to Microelectrode Recordings and Lower Field Strength MRI. Stereotact Funct Neurosurg. 2019;97(3):153-9.
8. Dafsari HS, Petry-Schmelzer JN, Ray-Chaudhuri K, et al. Non-motor outcomes of subthalamic stimulation in Parkinson's disease depend on location of active contacts. Brain stim. 2018;11(4):904-12.
9. Petry-Schmelzer JN, Krause M, Dembek TA, et al. Non-motor outcomes depend on location of neurostimulation in Parkinson's disease. Brain. 2019;142(11):3592-604.
10. Aviles-Olmos I, Kefalopoulou Z, Tripoliti E, et al. Long-term outcome of subthalamic nucleus deep brain stimulation for Parkinson's disease using an MRI-guided and MRI-verified approach. J Neurol Neurosurg Psychiatry. 2014;85(12):1419-25.
11. Garcia-Garcia D, Guridi J, Toledo JB, et al. Stimulation sites in the subthalamic nucleus and clinical improvement in Parkinson's disease: a new approach for active contact localization. J Neurosurg. 2016;125(5):1068-79.
12. Boutet A, Madhavan R, Elias GJB, et al. Predicting optimal deep brain stimulation parameters for Parkinson's disease using functional MRI and machine learning. Nat Commun. 2021;12(1):3043.
13. Boon LI, Hillebrand A, Potters WV, et al. Motor effects of deep brain stimulation correlate with increased functional connectivity in Parkinson's disease: An MEG study. Neuroimage Clin. 2020;26:102225.
14. Abbasi O, Hirschmann J, Storzer L, et al. Unilateral deep brain stimulation suppresses alpha and beta oscillations in sensorimotor cortices. Neuroimage. 2018;174:201-7.
15. Luoma J, Pekkonen E, Airaksinen K, et al. Spontaneous sensorimotor cortical activity is suppressed by deep brain stimulation in patients with advanced Parkinson's disease. Neurosci Lett. 2018;683:48-53.
16. Litvak V, Florin E, Tamás G, et al. EEG and MEG primers for tracking DBS network effects. Neuroimage. 2021;224:117447.
17. Cao C, Li D, Jiang T, et al. Resting state cortical oscillations of patients with Parkinson disease and with and without subthalamic deep brain stimulation: a magnetoencephalography study. J Clin Neurophysiol. 2015;32(2):109-18.
18. Boon LI, Potters WV, Zoon TJC, et al. Structural and functional correlates of subthalamic deep brain stimulation-induced apathy in Parkinson's disease. Brain stimulation. 2021;14(1):192-201.
19. Brunenberg EJ, Moeskops P, Backes WH, et al. Structural and resting state functional connectivity of the subthalamic nucleus: identification of motor STN parts and the hyperdirect pathway. PLoS One. 2012;7(6):e39061.

20. Li S, Arbuthnott GW, Jutras MJ, et al. Resonant antidromic cortical circuit activation as a consequence of high-frequency subthalamic deep-brain stimulation. J Neurophysiol. 2007;98(6):3525-37.
21. van Wijk BCM, Neumann WJ, Kroneberg D, et al. Functional connectivity maps of theta/alpha and beta coherence within the subthalamic nucleus region. Neuroimage. 2022:119320.
22. Rappel P, Grosberg S, Arkadir D, et al. Theta-alpha oscillations characterize emotional subregion in the human ventral subthalamic nucleus. Mov Disord. 2020;35(2):337-43.
23. Taulu S, Hari R. Removal of magnetoencephalographic artifacts with temporal signal-space separation: demonstration with single-trial auditory-evoked responses. Hum Brain Mapp. 2009;30(5):1524-34.
24. Taulu S, Simola J. Spatiotemporal signal space separation method for rejecting nearby interference in MEG measurements. Phys Med Biol. 2006;51(7):1759-68.
25. Whalen C, Maclin EL, Fabiani M, et al. Validation of a method for coregistering scalp recording locations with 3D structural MR images. Hum Brain Mapp. 2008;29(11):1288-301.
26. Gong G, He Y, Concha L, et al. Mapping anatomical connectivity patterns of human cerebral cortex using in vivo diffusion tensor imaging tractography. Cereb Cortex. 2009;19(3):524-36.
27. Tzourio-Mazoyer N, Landeau B, Papathanassiou D, et al. Automated anatomical labeling of activations in SPM using a macroscopic anatomical parcellation of the MNI MRI single-subject brain. Neuroimage. 2002;15(1):273-89.
28. Hillebrand A, Tewarie P, van Dellen E, et al. Direction of information flow in large-scale resting-state networks is frequency-dependent. Proc Natl Acad Sci U S A. 2016;113(14):3867-72.
29. Hillebrand A, Barnes GR, Bosboom JL, et al. Frequency-dependent functional connectivity within resting-state networks: an atlas-based MEG beamformer solution. Neuroimage. 2012;59(4):3909-21.
30. Brookes MJ, Woolrich MW, Barnes GR. Measuring functional connectivity in MEG: a multivariate approach insensitive to linear source leakage. Neuroimage. 2012;63(2):910-20.
31. Bruns A, Eckhorn R, Jokeit H, et al. Amplitude envelope correlation detects coupling among incoherent brain signals. Neuroreport. 2000;11(7):1509-14.
32. Hipp JF, Hawellek DJ, Corbetta M, et al. Large-scale cortical correlation structure of spontaneous oscillatory activity. Nat Neurosci. 2012;15(6):884-90.
33. Avants B, Epstein C, Grossman M, et al. Symmetric diffeomorphic image registration with cross-correlation: evaluating automated labeling of elderly and neurodegenerative brain. Med Image Anal. 2008;12:26-41.
34. Horn A, Kuhn AA. Lead-DBS: a toolbox for deep brain stimulation electrode localizations and visualizations. Neuroimage. 2015;107:127-35.
35. Ewert S, Plettig P, Li N, et al. Toward defining deep brain stimulation targets in MNI space: A subcortical atlas based on multimodal MRI, histology and structural connectivity. Neuroimage. 2018;170:271-82.
36. Olde Dubbelink KT, Stoffers D, Deijen JB, et al. Cognitive decline in Parkinson's disease is associated with slowing of resting-state brain activity: a longitudinal study. Neurobiol Aging. 2013;34(2):408-18.
37. DeLong MR, Wichmann T. Circuits and circuit disorders of the basal ganglia. Arch Neurol. 2007;64(1):20-4.
38. Fimm B, Heber IA, Coenen VA, et al. Deep brain stimulation of the subthalamic nucleus improves intrinsic alertness in Parkinson's disease. Mov Disord. 2009;24(11):1613-20.
39. Serranová T, Sieger T, Růžička F, et al. Topography of emotional valence and arousal within the motor part of the subthalamic nucleus in Parkinson's disease. Sci Rep. 2019;9(1):19924.
40. Cooper SE, McIntyre CC, Fernandez HH, et al. Association of deep brain stimulation washout effects with Parkinson disease duration. JAMA Neurol. 2013;70(1):95-9.

41. Little S, Pogosyan A, Neal S, et al. Adaptive deep brain stimulation in advanced Parkinson disease. Ann Neurol. 2013;74(3):449-57.
42. Ten Brinke, T.R., Arnts H., Schuurman P.R. and van den Munckhof P., *Directional sensory thalamus deep brain stimulation in poststroke refractory pain.* BMJ Case Rep, 2020. **13**(8).

Supplementary materials

Supplementary Figure 1 Schematic representation of the implanted eight-segment DBS electrode (Cartesia, Boston Scientific, Marlborough, Massachusetts, USA).
Adapted from Ten Brinke et al. (2020)[42] with permission from the authors

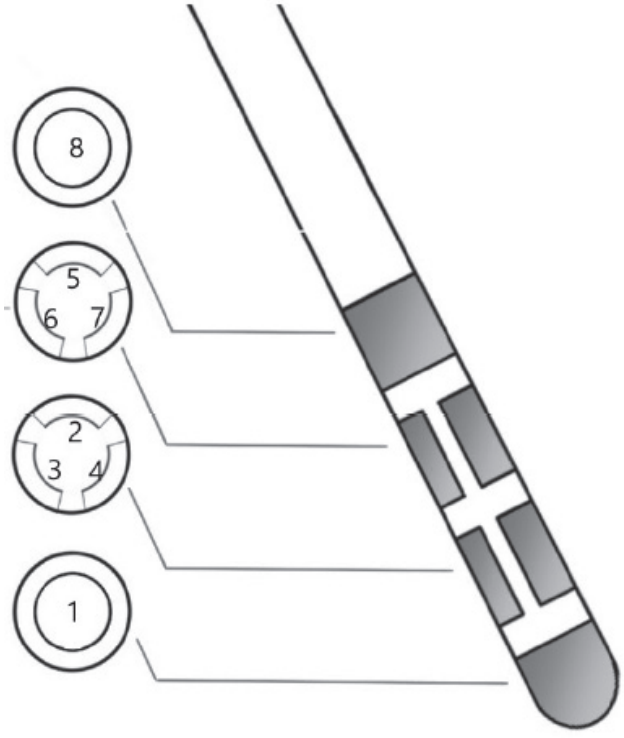

Supplementary Figure 2 Stimulation location plotted against the neurophysiological measures

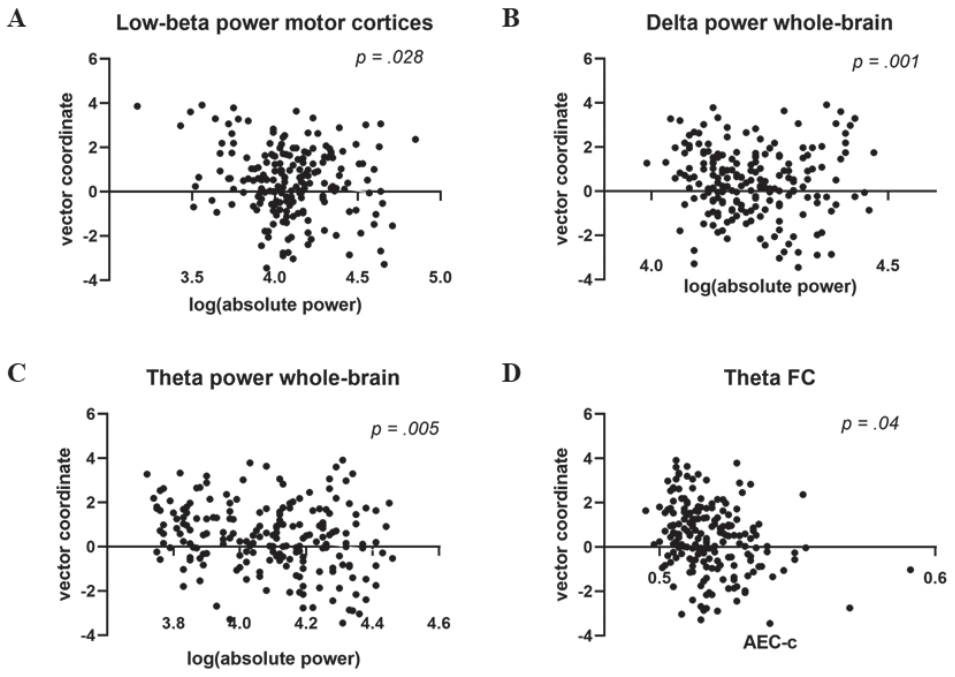

Scatter plots of four neurophysiological measures plotted against the stimulation location of the active contact point they were significantly associated with. As the analysis was performed using linear mixed models, the intercept is influenced by covariates in the model. Therefore, we did not draw a line indicating the direction of association.
FC, functional connectivity; AEC-c, corrected amplitude envelope correlation

Supplementary Figure 3 Evolution of absolute spectral power in an individual patient
Visualization of the evolution of absolute spectral power over all epochs in a recording session of a single patient. Absolute band power is depicted as logarithmic on the y-axis and each individual epoch (ten selected epochs per condition, in chronological order) on the x-axis. The condition labels are indicated; Red vertical lines indicate a change in stimulation condition. Contact point 1 represents the deepest (most ventral) contact point, contact point 8 the upper (most dorsal) contact point (see Supplementary Figure 1).
It is clear that the amount of variation *within* the same stimulation condition is high and we cannot distinguish a general pattern over time. We have analyzed whether there were significant differences in spectral power *between* conditions using repeated-measure ANOVA's (excluding the OFF condition). For all frequency bands, these analyses were statistically significant, indicating a significant difference between at least two of the conditions; Alpha2 motor cortex, $p = .001$; Low-beta power motor cortex, $p < .001$; Whole brain: Delta power, $p < .001$; Theta, $p = .029$; Alpha1 power, $p < .001$; Alpha2 power, $p = .002$; Low-beta power, $p < .001$.
A.U., arbitrary units

Alpha2 power motor cortex

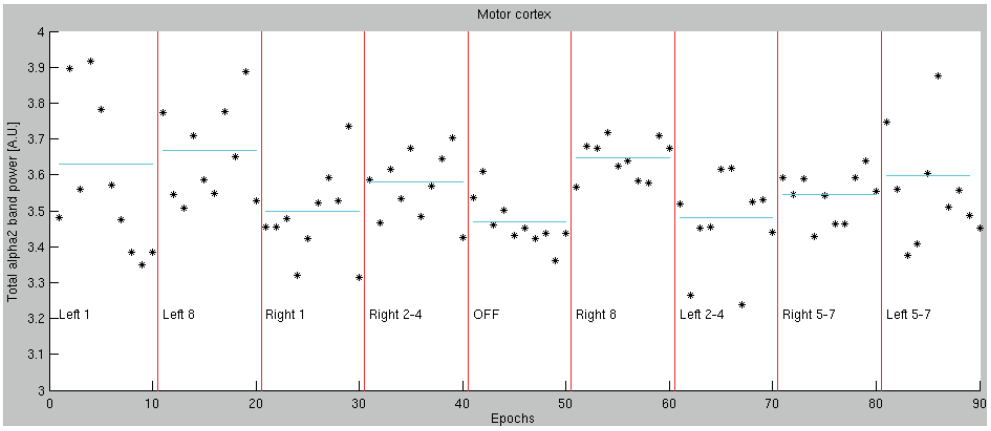

Low-beta power motor cortex

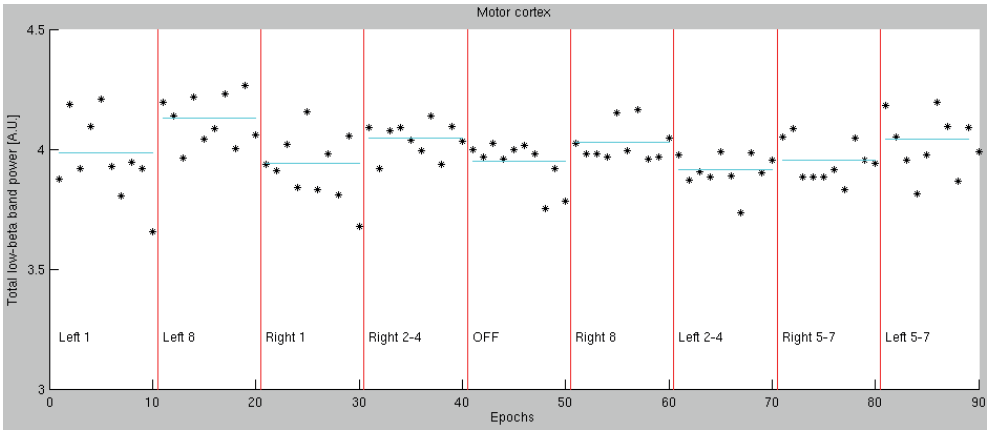

Delta power whole-brain

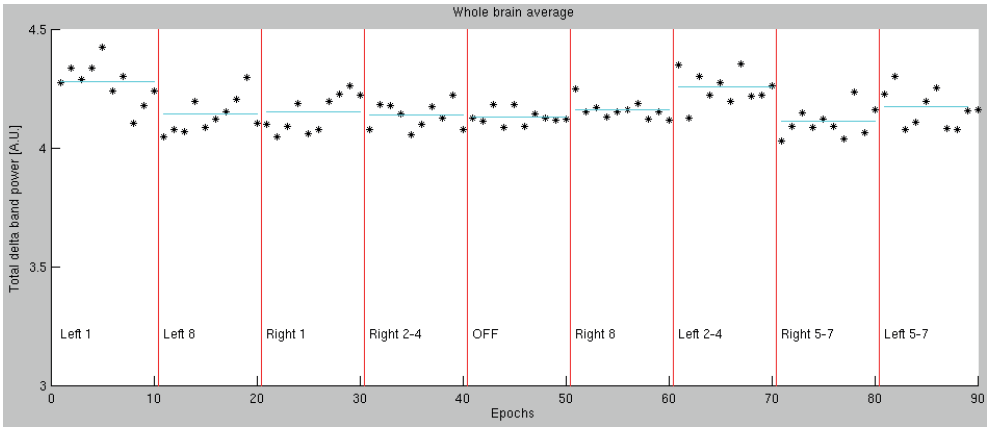

Theta power whole-brain

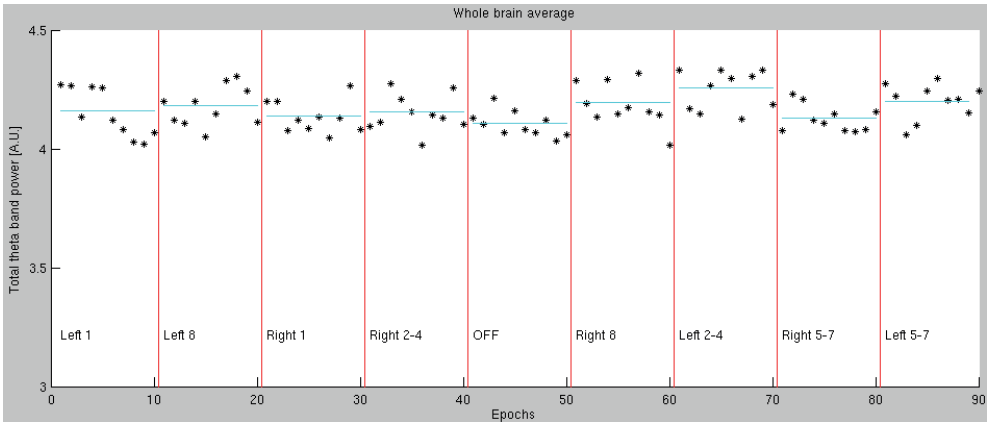

Alpha1 power whole-brain

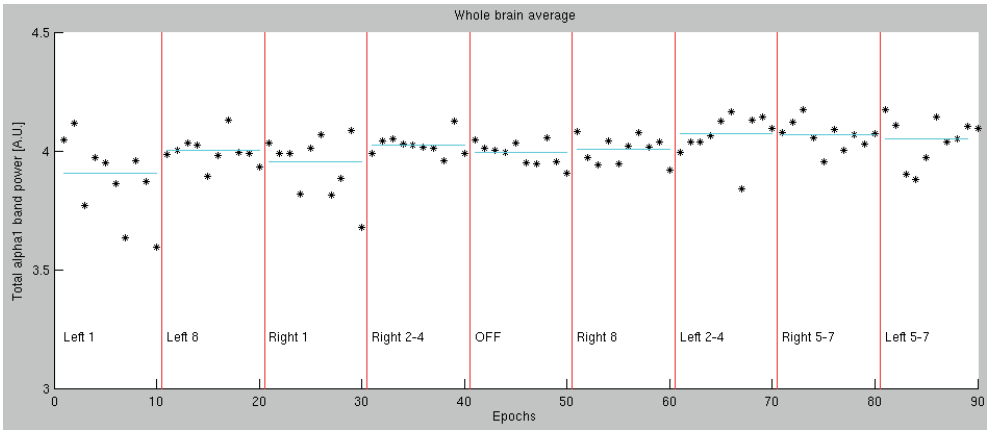

Alpha2 power whole-brain

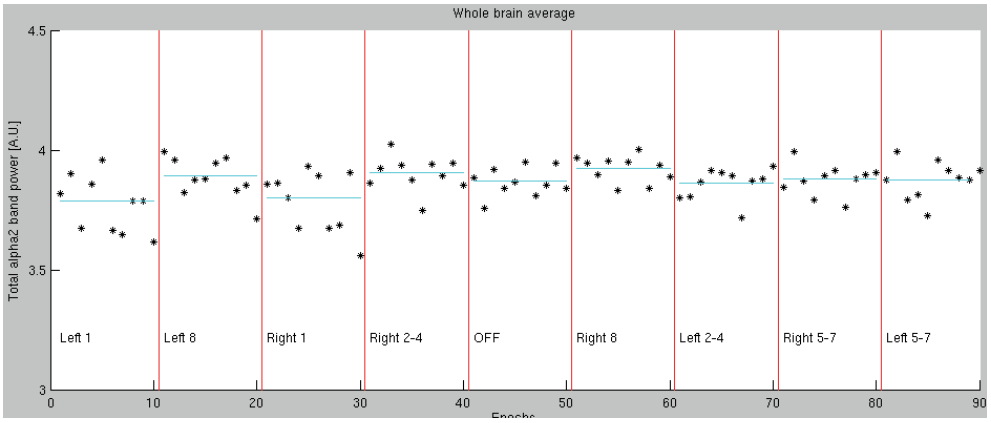

Low-beta power whole brain

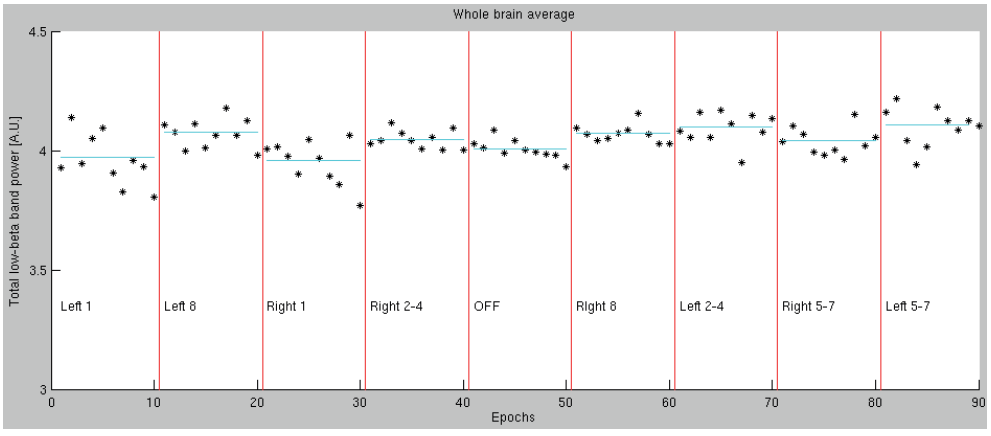

6.3

CHAPTER 7

Summary and general discussion

The main objectives of this thesis were to gain more insight into the functional brain mechanisms related to motor and non-motor symptoms in PD, as well as its progression over the course of the disease, both from a cortical and subcortical perspective. In addition, we studied the neurophysiological effects of DBS on the PD brain in relation to motor and non-motor functioning. We aimed to answer the question whether MEG can be used to measure DBS effects on brain activity and connectivity. In this chapter, we will summarize the main conclusions of the chapters in this thesis and discuss these in four parts.

Reviews of the EEG and MEG literature in PD

In **chapter 2.1** we reviewed the EEG literature in PD to determine whether quantitative EEG measures reflect clinical measures of disease severity and progression in PD. Based on the available evidence, slowing of the power spectrum correlates with clinical disease progression, mainly cognitive decline, and appears to be a robust non-invasive biomarker of the disease process. In addition, we concluded that functional connectivity and network analyses may have utility as additional biomarkers of the disease process, but have to be further explored in future studies.

In **chapter 2.2** we reviewed the MEG literature in PD, which can roughly be subdivided into whole-brain studies, mainly focused on cortical brain regions, and motor-network studies, mainly focused on the motor cortex, in some studies combined with deep brain stimulation and/or micro-electrode recordings of the STN. Based upon our review of the literature, we concluded that i) whole-brain disease processes, such as slowing of oscillatory activity or loss of functional connectivity, may affect local motor network findings and should therefore be taken into account in the interpretation of the results of motor network studies, and ii) changes in cortical brain activity may find their origin in subcortical brain regions. Hence, treatments that target subcortical brain structures such as dopaminergic medication or deep brain stimulation can have diffuse effects on the brain as a whole.

Changes in neurophysiological measures over the course of PD

In the study described in **chapter 3.1** we addressed the question whether it is feasible to perform a longitudinal analysis of MEG data recorded using two different MEG systems. We performed this analysis on MEG data obtained in eight healthy controls who had undergone recordings at three time points over a period of seven years. We hypothesized that neurophysiological measures of brain activity, i.e. spectral power and functional connectivity, in healthy controls would remain stable over time. In our analysis, we did not observe significant changes in spectral power or functional connectivity over the seven-year period. This observation opened up the possibility of a longitudinal analysis in our cohort of PD patients in whom we had performed MEG recordings on two different MEG systems as well. The results of this longitudinal study are described in **chapter 3.2**. We assessed MEG-derived measures of spectral power and functional connectivity for cortical and subcortical brain regions. At baseline, we included 61 non-demented

PD patients, including 17 early-stage PD patients who were not yet on dopaminergic medication. At the second time point, after four years, we could include 39 of the PD patients who had previously been recorded, and at the third time point, after seven years, 35 PD patients. The early-stage, unmedicated PD patients already showed spectral slowing in both subcortical and cortical brain regions at baseline, most pronounced for the cortical brain regions. Spectral slowing entailed a decrease in peak frequency, (relative) power increases for 'slower frequencies', mainly theta power, and (relative) power decreases for 'higher' frequencies such as alpha2 and beta power. Thanks to the multiple longitudinal design of the study, in which PD patients with a variety of disease durations were included at baseline, we were able to establish that over a period of 20 years disease duration, spectral slowing progresses in both subcortical and cortical brain regions and is strongly (positively) associated with clinical deterioration (cognitive and motor). In contrast, we were unable to detect significant changes in band-specific functional connectivity over time. This may have been a result of methodological choices (such as the connectivity measure use, a whole-brain analysis) or imply that functional connectivity changes were hardly present in our study cohort. This is further discussed in the methodology section of this final chapter. The results of our study confirm and extend previous observations that spectral slowing of cortical brain activity in PD is a robust indicator of disease progression and cognitive decline throughout the course of the disease.[1,2] In addition, we were able to demonstrate that subcortical brain regions are involved in this process from the earliest clinical motor stage of the disease.

Discussion of results in chapter 2 and 3

Against our expectation, spectral slowing in subcortical brain regions did not precede slowing in cortical brain regions in our study cohort. Perhaps, subcortical spectral slowing precedes cortical slowing only at the *premotor* stage, as dopaminergic deficits (and hence subcortical functional changes) are already present at the premotor stage.[3] Furthermore, we cannot exclude the possibility that some of the early subcortical changes were too local to be picked up by MEG, as the spatial resolution for deeply located brain regions is not as good as the resolution at the cortical level.[4,5]

The origin of spectral slowing in subcortical and cortical brain regions in early-stage PD patients remains to be determined and seems to involve multiple mechanisms. Slowing of cortical brain activity has also been observed in other diseases that lead to mild cognitive impairment and dementia, such as Alzheimer's disease[6,7] and Lewy Body dementia (DLB).[8,9] In all three diseases, spectral slowing has been attributed to cholinergic deficits.[7,10] Spectral slowing is most pronounced in patients with DLB, which may not be surprising considering the more severe cholinergic deficits in this disease.[8,11] Acetylcholine has an excitatory effect on the rhythmic firing of the thalamus and several cortical layers. Loss of cholinergic input may induce a change in the balance between excitation and inhibition that leads to a slowing of the background rhythm.[12,13] In line with these observations, oscillatory slowing in PD can partly be reversed by cholinergic medication in parallel

with an improvement in cognitive functioning.[14] However, dysfunction of the cholinergic system is not the only possible explanation for the observed relationship between cognitive decline and spectral slowing. First, cholinergic blocking in healthy subjects does not lead to cognitive symptoms.[15] Second, slowing of cortical and subcortical brain activity in relation to cognitive decline has also been demonstrated in other brain diseases that do not involve the cholinergic system, such as multiple sclerosis.[16,17]

As an alternative to the cholinergic hypothesis, spectral slowing may represent a 'final common pathway' resulting from a range of pathophysiological changes, ultimately leading to a slowing of background rhythms. Contributing factors may include i) changes in corticothalamic connectivity due to local neuropathological changes in subcortical structures, so-called 'corticothalamic dysrhythmia',[18] ii) impaired synaptic plasticity or synaptic dysfunction at a cortical level due to local neuropathological changes, as previously observed in Alzheimer's disease in relation to amyloid-β and Tau pathology,[19] iii) selective degeneration of highly connected brain regions, so-called 'hubs', e.g. the thalamus, precuneus and posterior cingulate gyrus; these hubs are important in maintaining the background rhythm, but are also vulnerable to an overload of brain activity and consequential damage.[20,21] It is unlikely that dopaminergic deficits play a major role in the correlation between cognitive decline and spectral slowing, as in our study the recordings were performed in the normal medicated state of the patients. Moreover, dopaminergic medication appears to be unable to reverse cortical oscillatory slowing.[22]

Rather unexpectedly, subcortical slowing and changes in beta band power in the sensorimotor cortex were only weakly associated with motor dysfunction, whereas widespread cortical slowing was associated strongly with motor dysfunction. The latter has only incidentally been reported previously[23] and could not be confirmed in other studies.[24,25] The lack of a strong association between changes in subcortical brain activity and motor impairment might be explained by the fact that the MEG recordings took place in a medicated (dopaminergic treatment) state. The dopaminergic treatment may have normalized both motor function and beta oscillations in the subcortical brain regions. Another option we discussed in our MEG-review (chapter 2.2) is that neuronal oscillations may only correlate with motor impairment when recorded during a motor task, but not during the resting-state. Thus, spectral power data derived from resting-state recordings may reflect the disease process rather than pose a mechanistic explanation for motor symptoms.

A closer look at the role of cortico-subcortical interactions in PD-related cognitive decline

In **chapter 4** we studied the involvement of subcortical brain regions in global cognitive functioning in 34 late-stage PD patients (mean disease duration 12 years) and 12 healthy controls at the third time point of our longitudinal study cohort, seven years from baseline. Using the connectivity measure directed phase transfer entropy (dPTE), we observed that in PD patients compared to healthy controls, the balance in information

flow was changed from a preferential posterior-to-anterior flow of information in the beta band to a more anterior-to-posterior information flow; i.e. from the subcortical and frontal brain regions towards the posterior brain regions. In addition, lower outflow from the posterior cortical brain regions correlated with a global measure of cognitive decline, which suggests that dysfunction of the posterior cortical brain regions rather than the subcortical brain regions underlies the observed shift in the balance of information flow.

In **chapter 5** we described a study in which we focused on domain-specific cognitive functioning in relation to longitudinally studied resting-state networks derived from fMRI scans that were performed at the second and third time points of our longitudinal study cohort. The study included 50 PD patients at time of the first fMRI scan (four years after inclusion at baseline) and 31 PD patients at time of the second fMRI scan (seven years after inclusion at baseline). At both study visits and in all PD patients and healthy controls, an array of seven cognitive tests was administered, which focused on the following cognitive domains: executive functioning (four tests), memory, motor perseveration, and verbal fluency. At time of the first fMRI scan, patients showed dysfunction on six out of seven tests compared to a sample of 15 healthy controls. Executive dysfunction correlated with stronger static functional connectivity and weaker dynamic functional connectivity between the subnetworks 'subcortical brain regions' and the frontoparietal network. Over a three-year period, further decline in executive function correlated with a further increase in static functional connectivity between these subnetworks. Furthermore, a decline in functional connectivity within the subcortical brain regions and a decline in functional connectivity between the dorsal attention network and the rest of the brain correlated with further deterioration in executive dysfunction. We concluded that dysfunctional communication between the subcortical, frontoparietal and dorsal attention networks is related to impaired executive functioning in PD.

Discussion of results in chapter 4 and 5

In the studies described in chapter 4 and 5, we have explored the interaction between the basal ganglia and cortical brain regions in relation to cognitive dysfunction in PD patients. We were able to capture the two phenomena that fit into the so-called 'dual syndrome' hypothesis of cognitive decline in PD. This states that dopaminergic deficits in fronto-striatal circuits underlie executive dysfunction, whereas cholinergic denervation or local cortical spreading of alpha-synuclein pathology causes 'posterior cortical' deficits, such as visuospatial and memory deficits.[26] Patients with the latter clinical profile are considered to be at a higher risk for future development of PD dementia than patients exhibiting a frontal-executive dysfunction.[27] The neurophysiological changes involving the posterior cortex in our study on global cognitive decline (chapter 4) signal a higher risk for the development of PD dementia. This notion is strengthened by the fact that lower beta band power in posterior cortical brain regions is predictive for the subsequent development of PD dementia.[28] Moreover, a loss of beta band power is also a feature of Alzheimer's disease[4] and may therefore suggest the involvement of a cholinergic deficit.

The results of our study in chapter 5 suggest that subcortical brain regions, as well as their interactions with the frontoparietal network, are involved in executive dysfunction. The application of dynamic functional connectivity is relatively new in the field of neuroscience and several analytical pitfalls should be taken into consideration.[29] Our finding of lower dynamic functional connectivity between the basal ganglia and the frontoparietal network may reflect impaired flexibility due to hypersynchronization, restricting the 'functional repertoire', an idea put forward in a recent MEG-study.[30] The influence of dopaminergic medication on frontostriatal functional interactions and executive dysfunction is complex. On average, dopaminergic medication appears to lower frontostriatal functional connectivity and thus relieve hypersynchronization[31] and improve executive dysfunction.[32] However, as individual patients have different baseline levels of dopamine in individual subcortical structures, these structures may exhibit a differential sensitivity to the positive and negative effects of dopaminergic medication, the so-called 'overdose theory';[33] i.e. within a given patient, one subcortical structure involved in a certain cognitive task can be dysfunctional due to a lack of dopamine in the unmedicated state, but will start to function properly upon the administration of dopaminergic medication. Within the same patient, another subcortical structure involved in another cognitive task may function properly in an unmedicated state as there is sufficient dopamine present, but will dysfunction when dopaminergic medication is administered ('overdose').

The effects of deep brain stimulation on the PD brain

In **chapter 6.1** we studied the effect of DBS on brain activity and connectivity in PD patients as well as its relationship with improvement in motor function. We performed MEG recordings ON and OFF stimulation in eighteen PD patients who had undergone DBS placements at least six months earlier. Scores of motor function (Unified Parkinson's Disease Rating Scale, UPDRS-III) were obtained before and six months after surgery. We found that DBS led to a global acceleration of neuronal oscillations, combined with a suppression of absolute band power (0.5-22 Hz) in the sensorimotor cortical brain regions. Improvement of bradykinesia and rigidity was significantly related to increases in alpha2 and low-beta band (10-13 and 13-22 Hz) functional connectivity. This was the case for the brain as a whole, for subcortical and cortical brain regions separately, and when we focused on the sensorimotor cortices. Tremor improvement did not correlate with changes in functional connectivity. We concluded that we are able to record clinically relevant neurophysiological phenomena when combining MEG and DBS.

In **chapter 6.2** we aimed to answer the question whether apathy, which is often observed after DBS, could be a stimulation effect, superimposed upon the effect of disease progression and/or the dose reduction of dopaminergic medication that often takes place after surgery. We performed MEG recordings in 26 PD patients, at least six months after surgery, ON and OFF stimulation. In addition, we obtained apathy scores (Starkstein apathy scale)[34] before surgery as well as on the day of the MEG recordings. We correlated

the DBS-related changes in functional connectivity of three preselected cortical brain regions (known from the literature to be involved in apathy) with the change in apathy scores. We observed a large increase in overall apathy scores after surgery (assessed during stimulation). Moreover, the number of patients that fulfilled clinical criteria for a diagnosis of apathy increased from two to nine after DBS. Change in apathy score did not correlate with improvement in motor function or dose reduction of dopaminergic medication. For the right hemisphere, an increased apathy score was associated with a more dorsolateral stimulation location. Furthermore, the increase in apathy severity correlated with a decrease in alpha1 functional connectivity of the dorsolateral prefrontal cortex. We concluded that, both from a structural (stimulation location) and functional perspective, increased apathy in PD patients with DBS can at least partly be related to the stimulation itself.

In **chapter 6.3** we used MEG recordings in 30 PD patients with DBS (population overlapping with chapter 6.1 and 6.2) to determine whether an acute switch of the active contact point would lead to measurable changes in brain activity and connectivity. We observed that, at a group-level, more dorsolateral stimulation was associated with lower whole-brain delta and theta power, as well as lower whole-brain theta band functional connectivity. In addition, more dorsolateral stimulation correlated with lower low-beta power (13-22 Hz) in the motor cortex ipsilateral to the stimulated STN. Within-subject findings were too variable to draw conclusions at the individual level. We concluded that the group-level data show that in PD patients on DBS a change in stimulation location produces measurable changes in brain activity and connectivity.

Discussion of results in chapter 6

Our observations demonstrate that DBS in PD patients has whole-brain effects, mainly an acceleration of neuronal oscillations upon stimulation. Three possible mechanisms may have contributed to these findings. First, the acceleration of brain activity may reflect an increase in intrinsic alertness or arousal, as suggested previously.[35,36] Second, an overactive STN in PD patients in the context of local hypersynchrony in the beta band range may put a 'brake' on the thalamus. Stimulation of the STN may then lead to a 'release' of the thalamus, which results in an acceleration of cortical brain rhythms (Figure 1).[37,38] Third, although we did not observe stimulation artefacts in the power spectrum for the frequencies we studied, we cannot exclude the possibility that noise originating from the stimulator changed the composition of the 'aperiodic' background rhythms, thereby causing an apparent shift in frequency towards faster frequencies.[39] We do not expect the latter to be the sole explanation, as we found i) functional connectivity changes to correlate with changes in clinical functioning (motor and apathy), ii) the stimulation location to correlate with spectral measures (whole brain delta and theta band power), which suggests that we recorded brain activity instead of noise.

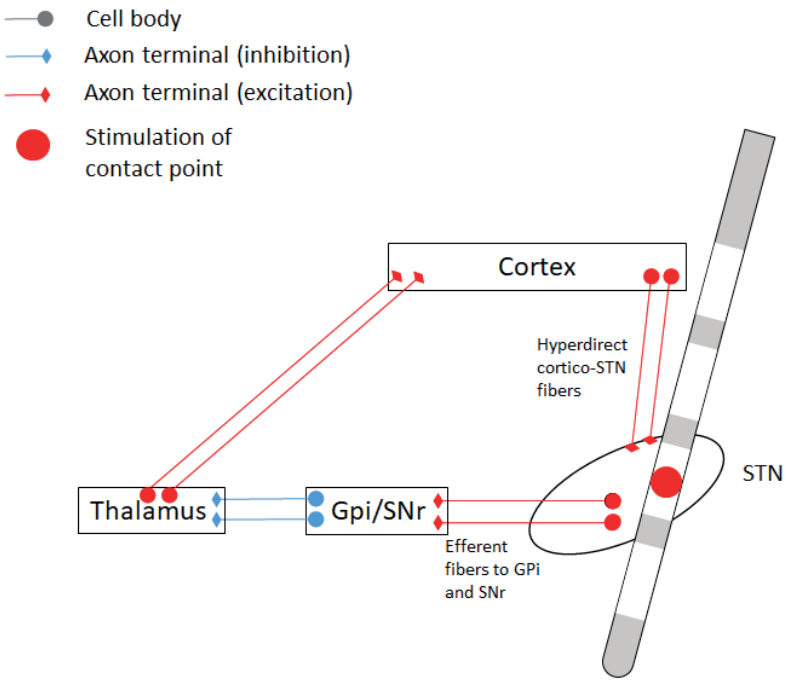

Figure 1 Model of antidromic and downstream effects in STN-DBS
Stimulation effects in the antidromic/backward direction affect the axons involved in the hyperdirect pathway, connecting the STN with the motor cortex. Orthodromic/downstream effects on the STN may ultimately lead to a 'release' of the thalamus and thereby increase large scale cortico-cortical connectivity.
Gpi, internal globus pallidus; SNr, substantia nigra pars reticulate; STN, subthalamic nucleus
Figure adapted from chapter 6.1

Since we described a global spectral slowing in relation to cognitive decline in the first part of the thesis, an obvious question would be: could DBS have positive cognitive effects through reversal of the slowing of brain activity? Among several factors contributing to cortical slowing, cortico-thalamic dysrhythmia is the factor most likely to respond to DBS, whereas local cortical Lewy pathology and cholinergic denervation are less likely to be reversed by DBS. Cognitive function generally declines rather than improves after chronic DBS, which not necessarily implies an effect of DBS, but may also reflect natural disease progression.[40] As there is generally no improvement in cognitive function after DBS, it is most likely that the whole-brain acceleration of neuronal oscillations related to DBS is an epiphenomenon independent from clinical effects: DBS can have localized effects on the basal ganglia system or on specific cortical brain regions, whilst at the same time, by increasing arousal, lead to whole-brain changes in spectral power. On the other hand, in our study in chapter 6.1, DBS-related motor improvements strongly correlated with widespread increases in alpha2 and low-beta functional connectivity (10-13 and 13-22 Hz), which makes it less likely that the observed functional connectivity

changes represent an epiphenomenon. As long as it remains unclear whether the whole-brain changes in brain activity and connectivity are a physiological effect or represent a non-specific epiphenomenon, DBS-studies should not only focus on the 'classical' motor network, but include whole-brain analyses to avoid missing relevant changes in brain activity and connectivity at a distance.

Many studies suggest that beta oscillations play an 'anti-kinetic' role, at least within the network involving the STN and the motor cortex, two brain areas that are directly connected via a white matter tract, the 'hyperdirect pathway' (Figure 1). Higher beta band power within the STN correlates with bradykinesia and rigidity in PD[41] and can be reduced by dopaminergic medication,[42] as well as stimulation of the STN.[43] Moreover, beta-band cortico-cortical functional connectivity over the motor cortices is reduced by stimulation of the STN, although due to the nature of the connectivity measure that was used it cannot be excluded that these observed changes are a reflection of power differences.[44] Lastly, non-invasive transcranial alternating stimulation (tACS) of the motor cortex with a frequency of around 25 Hz (beta band) worsened bradykinesia in PD patients.[45] Our findings of correlations between *increased* large-scale cortico-cortical and cortico-subcortical alpha2 and low-beta band functional connectivity and *improvements* in motor function may seem to be at odds with the results of the aforementioned studies, as they imply that beta band interactions can be 'pro-kinetic' in some situations, dependent on the network that is studied. We believe that such different expressions of beta band oscillations may be caused by the complex interactions that subcortical brain structures have with one another, through inhibition and excitation (Figure 1). The net result of stimulation of the STN on cortical beta band interactions may differ depending on the direction of its effects on the STN. DBS may exert its influence in an antidromic way, i.e. inhibiting the motor cortex through backward propagation from the STN via the hyperdirect pathway, or in an orthodromic way, from the STN to the internal globus pallidus, thereby 'releasing the brake' on thalamocortical projections and increasing large-scale cortico-cortical interactions. The differential effects of DBS on measures of brain function are reminiscent of the effects of dopamine, which can reduce beta band functional connectivity both locally within the STN as well as between the STN and the cortex through the hyperdirect pathway, but also evoke an increase in cortico-cortical functional connectivity.[46]

The results of the study described in chapter 6.2 suggest that post-operative apathy could at least partly be a side effect of the stimulation itself. The fact that the depression scores of the patients correlated positively with the increase in apathy scores suggests an emotional-affective basis of apathy. In addition, dorsolateral stimulation may lead to inclusion of the zona incerta in the stimulated area, which may lead to mood disturbances that relate to apathy.[47] In contrast, leakage of stimulation into the associative (ventrolateral) areas of the STN may also lead to apathy, in that case related to executive dysfunction[48] (see Figure 2 for an overview of the different subregions of the STN). In previous case series,

stimulation-related apathy developed upon stimulating ventral to the STN and improved upon switching to a more dorsal contact point.[49,50] We conclude that STN-targeted DBS that is either too ventral or too dorsal can induce apathy by leakage of current into regions involved in mood and executive function, respectively. According to the literature, the dorsolateral STN is considered to be the optimal target to improve PD-related motor symptoms.[51] In our study, increased apathy severity did not correlate with a better effect on motor symptoms. The latter observation indicates that it should be possible to find a stimulation location that strikes a balance between avoiding apathy whilst retaining a large effect on motor symptoms. Since the occurrence of apathy as well as other non-motor side effects can be very unpredictable due to differences in individual anatomy, a non-invasive biomarker predictive of side-effects would be very relevant.

In the same study described in chapter 6.2, we found an association between an increase in post-operative apathy and a stimulation-related decrease in functional connectivity of the dorsolateral prefrontal cortex. The dorsolateral prefrontal cortex is a brain region known for its involvement in executive functioning[52] and its connections with associative STN regions.[53] However, increases in apathy did not correlate with executive dysfunction in our study, and the analysis relating contact point positions with post-operative apathy did not support an executive/cognitive type of apathy either. Hence, our results regarding the stimulation location and functional connectivity point at a different (cognitive and emotional-affective) type of apathy. Nonetheless, we conclude that in the search for a non-invasive biomarker of the optimal stimulation position and parameters, our neurophysiological results obtained using MEG were encouraging. In future studies, the dorsolateral prefrontal cortex could be a region to focus on. Another candidate would be the medial orbitofrontal cortex, due to its involvement in emotional-affective apathy, although functional changes in this brain region were not associated with post-operative apathy in our study.

The final question addressed in chapter 6 was whether MEG-related neurophysiological measures would be sensitive to the acute effects of changing the stimulation location during DBS. The next experiment, described in chapter 6.3, therefore involved an analysis of the effects of stimulation of different sites within the same patient. We found neurophysiological changes resulting from stimulation around the dorsolateral and ventromedial borders of the STN. More dorsolateral stimulation led to lower low-beta power in the motor cortex than was the case for ventromedial stimulation. This so-called suppression is in line with our own findings in the motor study (chapter 6.1), as well as other MEG studies[54,55] and could be an expression of stimulation of the hyperdirect pathway, which is connected to the dorsolateral STN. More ventromedial stimulation led to higher global delta (mainly frontal cortical regions) and theta power (mainly parieto-occipital brain regions). This is in line with the available literature, since theta/alpha band interactions between the STN and the cortex appear to emanate from the ventral STN and beta band interactions from the dorsolateral STN.[56,57] Another explanation for the

increase in delta and theta power may be the effect of stimulation on arousal. Potentially, in contrast to dorsolateral stimulation, stimulation of the ventromedial STN may have a lower effect on arousal[58] and give room for phenomena related to drowsiness such as delta oscillations. Our results suggest that functional mapping of the STN using MEG is possible. However, we were unable to draw conclusions on the acute DBS-effects in individual patients, as intra-individual variation was too large. Optimization of the MEG acquisition protocols may improve the potential of our approach in individual patients (see also methodological considerations).

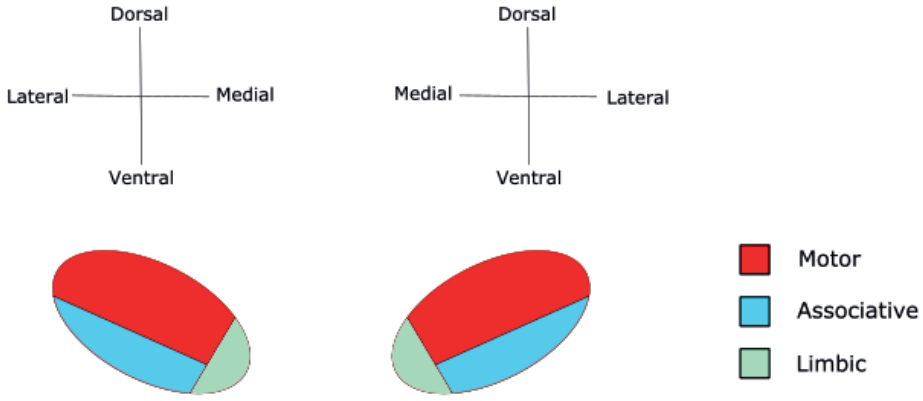

Figure 2 Frontal view of the STN
Dorsolateral and ventromedial regions are considered to represent motor and limbic regions, respectively

Methodological considerations

In the MEG-analyses described in chapter 3.2, functional connectivity measures (unexpectedly) remained unchanged over time, in spite of clinical progression of the patients. A previous analysis in the same study cohort, using a different functional connectivity measure, the phase lag index (PLI), revealed decreases in functional connectivity for several pre-selected regions over a time period of four years.[59] In addition, a recent high-density EEG study with a longitudinal design demonstrated a progressive loss of functional connectivity (using the phase locking value; PLV) in correlation with global cognitive decline and lateralization of motor symptoms.[60] In our present longitudinal analysis over a longer period of time (seven years), including three time points and two different MEG systems, we observed almost no changes in functional connectivity over time. The most obvious reason for this discrepancy is that we used a whole-brain approach (including subcortical brain regions) for the connectivity of each brain region, and may therefore have missed changes restricted to certain subsystems. Alternatively, the corrected amplitude envelop correlation (AEC-c) may not have been sensitive or stable enough to pick up subtle changes in functional communication between brain regions, since it is an amplitude-based measure in contrast to the

phase-based measures PLI and PLV. We chose the AEC-c as functional connectivity estimator as it handles volume conduction well and has previously been demonstrated to be a robust metric with a good within-subject reproducibility in the alpha band.[61,62] Furthermore, compared to other functional connectivity measures, alpha and beta band AEC-c are best able to distinguish Alzheimer's disease patients from cognitively healthy controls.[63,64] Lastly, the change of MEG system between the second and third time point may have confounded the analysis, which is in contradiction with our study in chapter 3.1 demonstrating the feasibility of performing a longitudinal analysis using two different MEG systems. The only significant change we observed in our analysis in PD patients was an increase in beta band functional connectivity between the second and third time point. However, since the same change was also present in our healthy control group (although non-significantly; chapter 3.1), it may have been related to the change from one MEG system to another.

In our DBS-study, stimulation-induced changes in alpha2 and low-beta band AEC-c correlated better with motor improvement than changes in band power. In view of the considerations in the previous paragraph this may seem rather unexpected. Perhaps the fact that i) envelope coupling measures are relatively robust against brain state changes during a long recording session (thereby being a better reflection of the effect of the stimulation itself),[65] and ii) that AEC-c is considered superior to other connectivity measures when analyzing data with a substantial amount of noise,[66] makes it useful in studies involving DBS patients.

In contrast, phase-based functional connectivity measures may be more useful when studying longitudinal (long-term) changes as we did in chapter 3.2, as its more 'volatile character' may better reflect subtle changes in brain state.[59,67]

In chapter 4 we used the directed phase transfer entropy (dPTE), with the aim to demonstrate changes in the direction of information flow. Although the dPTE is a phase-based measure,[68] it may yet have been affected by band power differences. In our study, it was striking that a lower beta band 'outflow' from the parieto-occipital brain regions in PD versus healthy controls was accompanied by lower beta band power in these brain regions. Power differences could have influenced the estimation of the dPTE either by inducing differences in signal-to-noise ratio or by the fact that some brain regions become 'lagging' instead of 'leading' due to local cortical slowing. However, for the theta band there was no relationship between band power differences and dPTE values. Also, a recent study that used dPTE for the estimation of information flow between the hippocampus and prefrontal cortex found directed functional connectivity differences without significant power differences.[69] Therefore, we conclude that band power differences cannot be the sole explanation for our beta band findings.

fMRI is an excellent technique to study subcortical brain regions in PD patients due to its high spatial resolution and would therefore have been a good addition to our analysis

of the earliest functional changes in untreated PD patients. In previous fMRI studies, a loss of functional connectivity within the basal ganglia circuit in early-stage PD has been observed[70,71] and this was paralleled by whole-brain changes in activity.[72] We were unable to investigate this, since fMRI was not performed at baseline in our study cohort.

Although we aimed to integrate fMRI and MEG results at later time points, the data are generally difficult to compare. MEG has the advantage of having higher temporal resolution; interactions between brain regions take place at a millisecond scale, which is a temporal scale that cannot be picked up by fMRI. Furthermore, MEG offers a more direct measure of neuronal activity than the hemodynamic response used in fMRI.[73] Yet, the AEC-c that we have applied in most of our MEG-studies has shown similarities with fMRI-derived measures of functional connectivity.[74] Nonetheless, a direct comparison of resting-state networks obtained using fMRI with the result of the MEG studies is challenging, although possible for the posterior 'hubs' of the brain,[75,76] and we consider these techniques to be complimentary to each other.

The use of fMRI in PD patients treated with DBS may also offer information that complements MEG-results. The use of fMRI in combination with DBS was previously considered to be hazardous because of the risk of displacing or heating the DBS system, due to the magnetic activity of the MRI-scanner in combination with metal parts of the DBS system, and hence lead to brain damage. However, studies have now confirmed the safety of fMRI during DBS under certain conditions[77,78] and it is now increasingly being used.[79,80] The use of fMRI instead of MEG in our DBS-studies could potentially have improved our ability to draw conclusions on the location of DBS-related functional changes. On the other hand, fMRI lacks the temporal resolution of MEG to record neurophysiological signals in the higher frequency ranges, such as the beta band (13-30 Hz), that are related to movement.

The within-subject MEG-recordings in chapter 6.3 were too variable to find a consistent pattern of changes in brain activity upon changing stimulation locations within individual patients. This could partly be explained by the MEG-metrics being noisy when applied within a single individual. In our study, we used a 'wash-out' period for stimulation effects of several minutes, which is rather short. The wash-out period for motor effects is highly variable between patients,[81] but five minutes on average.[82] Stimulation effects on brain networks may take time to stabilize. By mainly selecting data from the last part of the recordings, we think we have partly compensated for this, yet longer wash-out periods and longer recordings may be necessary to be able to draw conclusions on the effects of changing contact points in individual patients. Considering that the total duration of the MEG recordings in our study was already quite long, we chose not to further increase the recording time in order to avoid discomfort for the patient. Wearable MEG technology holds the potential of recording for longer time periods in a more natural and comfortable environment.[83]

In addition, the variable results at the level of a single individual may have resulted from the fact that we analyzed the contact point positions in a 'standardized' MNI space. As the actual anatomical positions of the STN differs between patients, this may have led to a variable and non-linear effect of changing the active contact point. At a group level, differences in the exact anatomical positions of the STN may level out and therefore allow significant observations. High-resolution 7 Tesla MRI scanners can be used to more precisely delineate the brain structures affected by the stimulation field, in particular including the white matter tracts surrounding the STN. We expect that a better knowledge of the inter-individual anatomical variation in and around the STN, in combination with detailed knowledge of its anatomical connections may improve the tracking of functional effects of DBS using MEG.

Future perspectives

As demonstrated in this thesis, neurophysiological measures that reflect spectral slowing of brain activity in PD may represent non-invasive markers of the ongoing disease process, read-out markers for future disease-modifying drugs and help in the identification of patients at a high risk for conversion to PD dementia (with respect to advanced care planning). For the application in clinical practice, EEG recordings seem better suitable than MEG recordings, as spectral slowing is a global phenomenon in cortical brain regions and EEG is a low-cost and readily available tool. Considering that many EEG-studies have already shown promising results,[84-86] the next step would be to design a study to establish cut-off values for spectral slowing as a predictive tool for PD dementia. Spectral slowing could be expressed as a so-called spectral ratio (theta power/(alpha1+alpha2+beta power)). PD patients visiting an outpatient clinic could be included in a longitudinal study cohort and undergo a baseline EEG. After a follow-up period of at least five years, we could identify which of the patients has developed PD dementia. Next, we could test the sensitivity and specificity of the baseline spectral ratio to predict the future development of PD dementia, as well as obtain cut-off values.

MEG-recordings remain vital for research questions that demand a more exact localization of changes in cortical brain activity and connectivity as well as for the study of subcortical brain regions. As demonstrated in chapter 4 and 5, using MEG and fMRI we were able to study the role of subcortical brain regions in (domain-specific) cognitive decline in PD.

Furthermore, MEG is useful for studying the effects of targeted therapies, so-called manipulation studies such as the DBS study in this thesis, with the aim to better understand disease mechanisms (e.g. how whole-brain phenomena may find their origin in a subcortical brain region as small as the STN), but also to improve patient outcome, as described in chapter 6.1-6.3. Furthermore, MEG-recordings could aid in finding targets for symptomatic treatments of specific PD symptoms. Non-invasive electrical modulation of brain networks is an emerging technique in PD that could be used in this approach.[87] Brain regions that display abnormal brain activity and connectivity in association with

specific PD symptoms could be selected as targets for such stimulation studies. We have already come to learn that transcranial alternating current stimulation (tACS) of the motor cortex in the gamma frequency range may relieve bradykinesia,[45] whereas stimulation of the dorsolateral prefrontal cortex may improve cognitive functioning in PD patients with mild cognitive impairment.[88]

In the studies in this thesis, we estimated oscillatory power and functional connectivity as measures of brain activity and communication. However, emerging evidence has suggested that the aperiodic (non-oscillatory) component of the neuronal signal contains valuable additional information[39] and may provide insight in, for example, the balance between cortical inhibition and excitation.[89] In a recent study in PD patients, characteristics of the aperiodic background significantly changed after a dopamine challenge.[90] The analysis of aperiodic background signals would also be an interesting addition to our DBS-studies, although it would be a challenge to distinguish between 'stimulation-related noise' and physiological changes in brain activity leading to changes in the aperiodic background signals.

We have demonstrated the feasibility of performing MEG-recordings in PD patients treated with STN-DBS, which means that recordings during directional steering of DBS[91] should also be possible. This would allow a further exploration of the neurophysiological footprint of the STN by expanding the potential number of stimulation locations within a single subject. Furthermore, MEG recordings during stimulation of other targets, such as the nucleus basalis of Meynert, in PD dementia patients are an interesting option.[92] The same holds for MEG recordings during DBS of targets for other indications such as obsessive compulsive disorders,[93] depression,[94] and disorders of consciousness.[95] Although DBS is increasingly used for these indications, the underlying mechanisms of its effect are only poorly understood. MEG recordings could be used to characterize the brain networks targeted by DBS. This may be combined with local field potential recordings of the target that is being stimulated to characterize the functional loops that are influenced by the stimulation.

The purpose of monitoring DBS-effects on brain activity and connectivity in individual patients was not met in our studies. Taking into account the methodological considerations that were mentioned in the previous section, this purpose may yet be realized. Instead of in-vivo monitoring, *in silico* computer-based network modelling may be an option to better predict the occurrence of side effects in individual patients and optimize stimulation settings. Such network models may involve oscillating models of the basal ganglia in combination with the cerebral cortex,[96-98] but can also make use of the patient's functional data recorded during or after surgery.[99]

Conclusions

In this thesis, we have studied brain activity and connectivity in PD from the earliest until the more advanced disease stages. We have focused our analyses on the activity of subcortical brain regions, their interactions with cortical brain regions, and on the effects of stimulation of a subcortical brain region, the STN, on brain activity and connectivity. Taken together, the studies in this thesis contribute to a better understanding of the changes in brain activity and connectivity that occur in PD and during treatment using DBS.

From the earliest stages of PD, the disease is characterized by a progressive slowing of both subcortical and cortical brain activity. These measurable changes in brain activity are associated with disease-related cognitive decline and increasing motor impairments. Hence, spectral power may serve as a non-invasive marker of the ongoing disease process in PD, a read-out marker for future disease-modifying drugs and as a means to identify patients at a high risk for conversion to PD dementia.

Changes in cortico-subcortical interactions, measured using MEG and fMRI in our studies, contribute to specific cognitive deficits, such as executive dysfunction, as well as global cognitive decline. The functional changes we observed in our studies represent dysfunction in two different neuropsychological profiles, frontostriatal and posterior cortical dysfunction. The distinction between these profiles is relevant, as changes in frontostriatal interactions may be sensitive to changes in dopaminergic medication, whereas posterior cortical dysfunction may be predictive for the subsequent development of PD dementia.

DBS of the STN has both local and generalized effects on brain activity and connectivity, that can be captured using MEG and are associated with clinically relevant phenomena. At a group level, we were able to measure changes in brain activity and connectivity upon varying the DBS stimulation locations, although the clinical relevance and applicability in individual patients remains to be established in future studies. Our results may be a stepping-stone towards the use of MEG in the selection of the optimal stimulation location in DBS in individual patients, with the ultimate aim to strike an optimal balance between the beneficial effects on motor function and the occurrence of non-motor side effects, such as apathy.

References

1. Caviness JN, Hentz JG, Belden CM, et al. Longitudinal EEG changes correlate with cognitive measure deterioration in Parkinson's disease. J Parkinsons Dis. 2015;5(1):117-24.
2. Cozac VV, Chaturvedi M, Hatz F, et al. Increase of EEG Spectral Theta Power Indicates Higher Risk of the Development of Severe Cognitive Decline in Parkinson's Disease after 3 Years. Front Aging Neurosci. 2016;8:284.
3. Booij J, Knol RJ. SPECT imaging of the dopaminergic system in (premotor) Parkinson's disease. Parkinsonism Relat Disord. 2007;13 Suppl 3:S425-8.
4. Hillebrand A, Barnes GR. A quantitative assessment of the sensitivity of whole-head MEG to activity in the adult human cortex. Neuroimage. 2002;16(3 Pt 1):638-50.
5. Attal Y, Schwartz D. Assessment of subcortical source localization using deep brain activity imaging model with minimum norm operators: a MEG study. PLoS One. 2013;8(3):e59856.
6. Engels M, van der Flier W, Stam C, et al. Alzheimer's disease: the state of the art in resting-state magnetoencephalography. Clin Neurophysiol. 2017.
7. Polverino P, Ajčević M, Catalan M, et al. Brain oscillatory patterns in mild cognitive impairment due to Alzheimer's and Parkinson's disease: An exploratory high-density EEG study. Clin Neurophysiol. 2022;138:1-8.
8. Briel R, McKeith I, Barker W, et al. EEG findings in dementia with Lewy bodies and Alzheimer's disease. J Neurol, Neurosurg & Psychiatry. 1999;66(3):401-3.
9. Babiloni C, De Pandis MF, Vecchio F, et al. Cortical sources of resting state electroencephalographic rhythms in Parkinson's disease related dementia and Alzheimer's disease. Clin Neurophysiol. 2011;122(12):2355-64.
10. Rea RC, Berlot R, Martin SL, et al. Quantitative EEG and cholinergic basal forebrain atrophy in Parkinson's disease and mild cognitive impairment. Neurobiol Aging. 2021;106:37-44.
11. Franciotti R, Iacono D, Della Penna S, et al. Cortical rhythms reactivity in AD, LBD and normal subjects: a quantitative MEG study. Neurobiol Aging. 2006;27(8):1100-9.
12. Détári L, Rasmusson DD, Semba K. The role of basal forebrain neurons in tonic and phasic activation of the cerebral cortex. Prog Neurobiol. 1999;58(3):249-77.
13. van Nifterick AM, Gouw AA, van Kesteren RE, et al. A multiscale brain network model links Alzheimer's disease-mediated neuronal hyperactivity to large-scale oscillatory slowing. Alzheimers Res Ther. 2022;14(1):101.
14. Bosboom JL, Stoffers D, Stam CJ, et al. Cholinergic modulation of MEG resting-state oscillatory activity in Parkinson's disease related dementia. Clin Neurophysiol. 2009;120(5):910-5.
15. Dringenberg HC. Alzheimer's disease: more than a 'cholinergic disorder' - evidence that cholinergic-monoaminergic interactions contribute to EEG slowing and dementia. Behav Brain Res. 2000;115(2):235-49.
16. Schoonhoven DN, Fraschini M, Tewarie P, et al. Resting-state MEG measurement of functional activation as a biomarker for cognitive decline in MS. Mult Scler. 2019;25(14):1896-906.
17. Van der Meer ML, Tewarie P, Schoonheim MM, et al. Cognition in MS correlates with resting-state oscillatory brain activity: An explorative MEG source-space study. Neuroimage Clin. 2013;2:727-34.
18. Llinas RR, Ribary U, Jeanmonod D, et al. Thalamocortical dysrhythmia: A neurological and neuropsychiatric syndrome characterized by magnetoencephalography. Proc Natl Acad Sci U S A. 1999;96(26):15222-7.
19. Ranasinghe KG, Cha J, Iaccarino L, et al. Neurophysiological signatures in Alzheimer's disease are distinctly associated with TAU, amyloid-β accumulation, and cognitive decline. Sci Transl Med. 2020;12(534).
20. de Haan W, Mott K, van Straaten EC, et al. Activity dependent degeneration explains hub vulnerability in Alzheimer's disease. PLoS Comput Biol. 2012;8(8):e1002582.

21. Stam CJ. Modern network science of neurological disorders. Nat Rev Neurosci. 2014;15(10):683-95.
22. Stoffers D, Bosboom JL, Deijen JB, et al. Slowing of oscillatory brain activity is a stable characteristic of Parkinson's disease without dementia. Brain. 2007;130(Pt 7):1847-60.
23. Morita A, Kamei S, Serizawa K, et al. The relationship between slowing EEGs and the progression of Parkinson's disease. J Clin Neurophysiol. 2009;26(6):426-9.
24. Geraedts VJ, Marinus J, Gouw AA, et al. Quantitative EEG reflects non-dopaminergic disease severity in Parkinson's disease. Clin Neurophysiol. 2018;129(8):1748-55.
25. Olde Dubbelink KT, Stoffers D, Deijen JB, et al. Cognitive decline in Parkinson's disease is associated with slowing of resting-state brain activity: a longitudinal study. Neurobiol Aging. 2013;34(2):408-18.
26. Kehagia AA, Barker RA, Robbins TW. Cognitive impairment in Parkinson's disease: the dual syndrome hypothesis. Neurodegener Dis. 2013;11(2):79-92.
27. Williams-Gray CH, Evans JR, Goris A, et al. The distinct cognitive syndromes of Parkinson's disease: 5 year follow-up of the CamPaIGN cohort. Brain. 2009;132(Pt 11):2958-69.
28. Olde Dubbelink KT, Hillebrand A, Twisk JW, et al. Predicting dementia in Parkinson disease by combining neurophysiologic and cognitive markers. Neurology. 2014;82(3):263-70.
29. Hindriks R, Adhikari MH, Murayama Y, et al. Can sliding-window correlations reveal dynamic functional connectivity in resting-state fMRI? Neuroimage. 2016;127:242-56.
30. Sorrentino P, Rucco R, Baselice F, et al. Flexible brain dynamics underpins complex behaviours as observed in Parkinson's disease. Sci Rep. 2021;11(1):4051.
31. Kwak Y, Peltier S, Bohnen NI, et al. Altered resting state cortico-striatal connectivity in mild to moderate stage Parkinson's disease. Front Syst Neurosci. 2010;4:143.
32. Gotham AM, Brown RG, Marsden CD. 'Frontal' cognitive function in patients with Parkinson's disease 'on' and 'off' levodopa. Brain. 1988;111 (Pt 2):299-321.
33. Cools R. Dopaminergic modulation of cognitive function-implications for L-DOPA treatment in Parkinson's disease. Neurosci Biobehav Rev. 2006;30(1):1-23.
34. Starkstein SE, Mayberg HS, Preziosi TJ, et al. Reliability, validity, and clinical correlates of apathy in Parkinson's disease. J Neuropsychiatry Clin Neurosci. 1992;4(2):134-9.
35. Fimm B, Heber IA, Coenen VA, et al. Deep brain stimulation of the subthalamic nucleus improves intrinsic alertness in Parkinson's disease. Mov Disord. 2009;24(11):1613-20.
36. Jech R, Ruzicka E, Urgosik D, et al. Deep brain stimulation of the subthalamic nucleus affects resting EEG and visual evoked potentials in Parkinson's disease. Clin Neurophysiol. 2006;117(5):1017-28.
37. DeLong MR, Wichmann T. Circuits and circuit disorders of the basal ganglia. Arch Neurol. 2007;64(1):20-4.
38. Bell PT, Shine JM. Subcortical contributions to large-scale network communication. Neurosci Biobehav Rev. 2016;71:313-22.
39. Haller M, Donoghue T, Peterson E, et al. Parameterizing neural power spectra. Nat Neurosci. 2020 Dec;23(12):1655-1665.
40. Castrioto A, Lhommée E, Moro E, et al. Mood and behavioural effects of subthalamic stimulation in Parkinson's disease. Lancet Neurol. 2014;13(3):287-305.
41. Kühn AA, Tsui A, Aziz T, et al. Pathological synchronisation in the subthalamic nucleus of patients with Parkinson's disease relates to both bradykinesia and rigidity. Experimental neurology. 2009;215(2):380-7.
42. Giannicola G, Rosa M, Marceglia S, et al. The effects of levodopa and deep brain stimulation on subthalamic local field low-frequency oscillations in Parkinson's disease. Neurosignals. 2013;21(1-2):89-98.
43. Quinn EJ, Blumenfeld Z, Velisar A, et al. Beta oscillations in freely moving Parkinson's subjects are attenuated during deep brain stimulation. Mov Disord. 2015;30(13):1750-8.

44. Silberstein P, Pogosyan A, Kühn AA, et al. Cortico-cortical coupling in Parkinson's disease and its modulation by therapy. Brain. 2005;128(6):1277-91.
45. Guerra A, Colella D, Giangrosso M, et al. Driving motor cortex oscillations modulates bradykinesia in Parkinson's disease. Brain. 2022;145(1):224-36.
46. Sharma A, Vidaurre D, Vesper J, et al. Differential dopaminergic modulation of spontaneous cortico-subthalamic activity in Parkinson's disease. eLife. 2021;10.
47. Stefurak T, Mikulis D, Mayberg H, et al. Deep brain stimulation for Parkinson's disease dissociates mood and motor circuits: a functional MRI case study. Mov Disord. 2003;18(12):1508-16.
48. Brezovar S, Pažek L, Kavčič M, et al. Personality Changes After Subthalamic Nucleus Stimulation in Parkinson's Disease. J Parkinsons Dis. 2022;12(4):1231-40.
49. Zoon TJ, de Bie RM, Schuurman PR, et al. Resolution of apathy after dorsal instead of ventral subthalamic deep brain stimulation for Parkinson's disease. J Neurol. 2019;266(5):1267-9.
50. Ricciardi L, Morgante L, Epifanio A, et al. Stimulation of the subthalamic area modulating movement and behavior. Parkinsonism Relat Disord. 2014;20(11):1298-300.
51. Bot M, Schuurman PR, Odekerken VJJ, et al. Deep brain stimulation for Parkinson's disease: defining the optimal location within the subthalamic nucleus. J Neurol Neurosurg Psychiatry. 2018;89(5):493-8.
52. Eckert T, Tang C, Eidelberg D. Assessment of the progression of Parkinson's disease: a metabolic network approach. Lancet Neurol. 2007;6(10):926-32.
53. Benarroch EE. Subthalamic nucleus and its connections: anatomic substrate for the network effects of deep brain stimulation. Neurology. 2008;70(21):1991-5.
54. Abbasi O, Hirschmann J, Storzer L, et al. Unilateral deep brain stimulation suppresses alpha and beta oscillations in sensorimotor cortices. Neuroimage. 2018;174:201-7.
55. Luoma J, Pekkonen E, Airaksinen K, et al. Spontaneous sensorimotor cortical activity is suppressed by deep brain stimulation in patients with advanced Parkinson's disease. Neurosci Lett. 2018;683:48-53.
56. van Wijk BCM, Neumann WJ, Kroneberg D, et al. Functional connectivity maps of theta/alpha and beta coherence within the subthalamic nucleus region. Neuroimage. 2022:119320.
57. Rappel P, Grosberg S, Arkadir D, et al. Theta-alpha oscillations characterize emotional subregion in the human ventral subthalamic nucleus. Mov Disord. 2020;35(2):337-43.
58. Serranová T, Sieger T, Růžička F, et al. Topography of emotional valence and arousal within the motor part of the subthalamic nucleus in Parkinson's disease. Sci Rep. 2019;9(1):19924.
59. Olde Dubbelink KT, Stoffers D, Deijen JB, et al. Resting-state functional connectivity as a marker of disease progression in Parkinson's disease: A longitudinal MEG study. Neuroimage Clin. 2013;2:612-9.
60. Yassine S, Gschwandtner U, Auffret M, et al. Functional Brain Dysconnectivity in Parkinson's Disease: A 5-Year Longitudinal Study. Mov Disord. 2022;37(7):1444-53.
61. Colclough GL, Woolrich MW, Tewarie PK, et al. How reliable are MEG resting-state connectivity metrics? Neuroimage. 2016;138:284-93.
62. Demuru M, Gouw AA, Hillebrand A, et al. Functional and effective whole brain connectivity using magnetoencephalography to identify monozygotic twin pairs. Sci Rep. 2017;7(1):9685.
63. Briels CT, Schoonhoven DN, Stam CJ, et al. Reproducibility of EEG functional connectivity in Alzheimer's disease. Alzheimers Res Ther. 2020;12(1):68.
64. Schoonhoven DN, Briels CT, Hillebrand A, et al. Sensitive and reproducible MEG resting-state metrics of functional connectivity in Alzheimer's disease. Alzheimers Res Ther. 2022;14(1):38.
65. Engel AK, Fries P. Beta-band oscillations--signalling the status quo? Curr Opin Neurobiol. 2010;20(2):156-65.
66. Yu M. Benchmarking metrics for inferring functional connectivity from multi-channel EEG and MEG: A simulation study. Chaos. 2020;30(12):123124.

67. Engel AK, Gerloff C, Hilgetag CC, et al. Intrinsic coupling modes: multiscale interactions in ongoing brain activity. Neuron. 2013;80(4):867-86.
68. Lobier M, Siebenhuhner F, Palva S, et al. Phase transfer entropy: a novel phase-based measure for directed connectivity in networks coupled by oscillatory interactions. Neuroimage. 2014;85 Pt 2:853-72.
69. Das A, Menon V. Replicable patterns of causal information flow between hippocampus and prefrontal cortex during spatial navigation and spatial-verbal memory formation. Cereb Cortex. 2022;8.
70. Rolinski M, Griffanti L, Szewczyk-Krolikowski K, et al. Aberrant functional connectivity within the basal ganglia of patients with Parkinson's disease. Neuroimage Clin. 2015;8:126-32.
71. Szewczyk-Krolikowski K, Menke RA, Rolinski M, et al. Functional connectivity in the basal ganglia network differentiates PD patients from controls. Neurology. 2014;83(3):208-14.
72. Pan P, Zhang Y, Liu Y, et al. Abnormalities of regional brain function in Parkinson's disease: a meta-analysis of resting state functional magnetic resonance imaging studies. Sci Rep. 2017;7(1):40469.
73. Hall EL, Robson SE, Morris PG, et al. The relationship between MEG and fMRI. Neuroimage. 2014;102 Pt 1:80-91.
74. Brookes MJ, Woolrich M, Luckhoo H, et al. Investigating the electrophysiological basis of resting state networks using magnetoencephalography. Proc Natl Acad Sci U S A. 2011;108(40):16783-8.
75. Shafiei G, Baillet S, Misic B. Human electromagnetic and haemodynamic networks systematically converge in unimodal cortex and diverge in transmodal cortex. PLoS Biol. 2022;20(8):e3001735.
76. Tewarie P, Hillebrand A, van Dellen E, et al. Structural degree predicts functional network connectivity: a multimodal resting-state fMRI and MEG study. Neuroimage. 2014;97:296-307.
77. Zhang F, Jiang C, Mo X, et al. Safety assessment of displacement force, torque and vibration of a deep brain stimulation system under 3T MRI. Int J Applied Electromagnetics and Mechanics. 2019;59(3):1081-6.
78. Boutet A, Hancu I, Saha U, et al. 3-Tesla MRI of deep brain stimulation patients: safety assessment of coils and pulse sequences. J Neurosurg. 2019;132(2):586-94.
79. Shen L, Jiang C, Hubbard CS, et al. Subthalamic Nucleus Deep Brain Stimulation Modulates 2 Distinct Neurocircuits. Ann Neurol. 2020;88(6):1178-93.
80. Fridgeirsson EA, Figee M, Luigjes J, et al. Deep brain stimulation modulates directional limbic connectivity in obsessive-compulsive disorder. Brain. 2020;143(5):1603-12.
81. Cooper SE, McIntyre CC, Fernandez HH, et al. Association of deep brain stimulation washout effects with Parkinson disease duration. JAMA Neurol. 2013;70(1):95-9.
82. Little S, Pogosyan A, Neal S, et al. Adaptive deep brain stimulation in advanced Parkinson disease. Ann Neurol. 2013;74(3):449-57.
83. Boto E, Hill RM, Rea M, et al. Measuring functional connectivity with wearable MEG. Neuroimage. 2021;230:117815.
84. Geraedts VJ, Koch M, Contarino MF, et al. Machine learning for automated EEG-based biomarkers of cognitive impairment during Deep Brain Stimulation screening in patients with Parkinson's Disease. Clin Neurophysiol. 2021;132(5):1041-8.
85. Geraedts VJ, Boon LI, Marinus J, et al. Clinical correlates of quantitative EEG in Parkinson disease: A systematic review. Neurology. 2018.
86. Klassen BT, Hentz JG, Shill HA, et al. Quantitative EEG as a predictive biomarker for Parkinson disease dementia. Neurology. 2011;77(2):118-24.
87. Oswal A. Towards therapeutic non-invasive electrical modulation of brain circuits in Parkinson's disease. Brain. 2022;145(1):11-3.
88. Manenti R, Brambilla M, Benussi A, et al. Mild cognitive impairment in Parkinson's disease is improved by transcranial direct current stimulation combined with physical therapy. Mov Disord. 2016;31(5):715-24.

89. Gao R, Peterson EJ, Voytek B. Inferring synaptic excitation/inhibition balance from field potentials. Neuroimage. 2017;158:70-8.
90. Wang Z, Mo Y, Sun Y, et al. Separating the aperiodic and periodic components of neural activity in Parkinson's disease. Eur J Neurosci. 2022.
91. Contarino MF, Bour LJ, Verhagen R, et al. Directional steering: A novel approach to deep brain stimulation. Neurology. 2014;83(13):1163-9.
92. Oswal A, Gratwicke J, Akram H, et al. Cortical connectivity of the nucleus basalis of Meynert in Parkinson's disease and Lewy body dementias. Brain. 2021;144(3):781-8.
93. van Westen M, Rietveld E, Bergfeld IO, et al. Optimizing Deep Brain Stimulation Parameters in Obsessive-Compulsive Disorder. Neuromodulation. 2021;24(2):307-15.
94. van der Wal JM, Bergfeld IO, Lok A, et al. Long-term deep brain stimulation of the ventral anterior limb of the internal capsule for treatment-resistant depression. J Neurol Neurosurg Psychiatry. 2020;91(2):189-95.
95. Vanhoecke J, Hariz M. Deep brain stimulation for disorders of consciousness: Systematic review of cases and ethics. Brain stim. 2017;10(6):1013-23.
96. Little S, Bestmann S. Computational neurostimulation for Parkinson's disease. Prog Brain Res. 2015;222:163-90.
97. Pirini M, Rocchi L, Sensi M, et al. A computational modelling approach to investigate different targets in deep brain stimulation for Parkinson's disease. J Comput Neurosci. 2009;26(1):91-107.
98. Alavi SM, Mirzaei A, Valizadeh A, et al. Excitatory deep brain stimulation quenches beta oscillations arising in a computational model of the subthalamo-pallidal loop. Sci Rep. 2022;12(1):7845.
99. Connolly MJ, Cole ER, Isbaine F, et al. Multi-objective data-driven optimization for improving deep brain stimulation in Parkinson's disease. J Neural Eng. 2021;18(4).

Nederlandse samenvatting

De diepte in: hersenenfuncties bij de ziekte van Parkinson in beeld

De ziekte van Parkinson is een progressieve hersenziekte die gepaard gaat met zowel motorische als niet-motorische symptomen. De typische motorische symptomen zijn beven, traagheid, stijfheid en balansproblemen. Niet-motorische symptomen zijn onder andere verlies van reukvermogen, autonome stoornissen, apathie, angstklachten, depressie, slaapproblemen, cognitieve achteruitgang en dementie.

Het doel van de onderzoeken die beschreven staan in dit proefschrift was om met functionele beeldvormende technieken (Magneto-EncefaloGrafie (MEG), functionele *Magnetic Resonance Imaging* (fMRI)) meer inzicht te verschaffen in de veranderingen in hersenfunctie die aan de motorische en niet-motorische symptomen, met name de cognitieve achteruitgang, ten grondslag liggen. Een beter begrip van deze functionele veranderingen is belangrijk voor i) de ontwikkeling van betere behandelingsmogelijkheden, ii) betere voorspelling van het beloop van de ziekte voor een individuele patiënt, iii) het monitoren van het effect van toekomstige ziekte modulerende therapieën.

Uit pathologisch onderzoek is gebleken dat de eerste veranderingen bij de ziekte van Parkinson plaatsvinden in de hersenstam en diep gelegen hersengebieden. Deze veranderingen leiden via het afsterven van dopaminerge cellen tot de kenmerkende motorische symptomen van de ziekte. Veel voorgaand onderzoek naar functionele veranderingen in de hersenen bij mensen met de ziekte van Parkinson heeft zich echter gericht op de corticale hersengebieden. Door het gebruik van MEG en fMRI was het mogelijk in onze studie ook de dieper gelegen hersengebieden te onderzoeken. In dit proefschrift ligt de nadruk op de rol van de diepgelegen hersengebieden, die wij van de vroegste tot meer gevorderde ziektestadia onderzocht hebben.

Diepe hersenstimulatie is een effectieve chirurgische behandeling om de motorische symptomen in met name latere stadia van de ziekte van Parkinson tegen te gaan. Er wordt beiderzijds diep in de hersenen, in de nucleus subthalamicus (STN), een elektrode geplaatst, met elk vier contactpunten, waarvan er per kant één gestimuleerd wordt. Naast de uitstekende effecten op de motoriek, kan diepe hersenstimulatie helaas in tot wel 25% van de patiënten niet-motorische bijwerken geven. Daarom hebben wij middels MEG het effect van diepe hersenstimulatie van de STN op de functie van de hersenen onderzocht. Wij hebben hierbij het verband met het optreden van motorische verbetering en niet-motorische bijwerkingen van deze behandeling onderzocht. Tot slot hebben we onderzocht of MEG zou kunnen functioneren als uitleesmaat (ook wel *biomarker*) voor de effecten van diepe hersenstimulatie, om zo de positieve en negatieve effecten hiervan beter te kunnen voorspellen.

De studies die wij beschreven hebben in dit proefschrift zijn uitgevoerd in twee cohorten van patiënten met de ziekte van Parkinson. Het eerste cohort bestond op het eerste tijdspunt uit 61 niet-demente Parkinson patiënten en 21 gezonde controles en werd gedurende een periode van zeven jaar gevolgd. De patiënten en controles ondergingen herhaalde metingen van het motorisch en cognitief functioneren, MEG registraties en structurele MRI scans aan het begin van de studie, na vier jaar en na zeven jaar. fMRI scans werden alleen op de laatste twee tijdspunten verricht.

Het tweede cohort bestond uit een groep van 30 Parkinson patiënten die behandeld werden met diepe hersenstimulatie. De patiënten zijn zowel voorafgaand aan- als zes maanden na de operatie klinisch beoordeeld (motorisch, psychiatrisch, cognitief). Minimaal zes maanden na de operatie ondergingen ze een MEG-meting tijdens stimulatie van beide elektrodes in hun (klinisch bepaalde) standaard instellingen, zonder stimulatie en tijdens stimulatie van elk van de individuele contactpunten afzonderlijk (vier aan elke kant; in totaal tien condities).

In **hoofdstuk 1** van het proefschrift wordt achtergrondinformatie over de ziekte van Parkinson gegeven. De motorische en niet-motorische symptomen en de neuropathologische bevindingen die hier verband mee houden worden beschreven. Vervolgens bespreken wij het grote probleem dat cognitieve achteruitgang bij de ziekte van Parkinson vormt met specifieke aandacht voor executieve dysfunctie en apathie. We beschrijven drie technieken die gebruikt worden om de functie van de hersenen te meten, namelijk elektro-encefalografie (EEG), MEG, en fMRI. MEG en fMRI hebben wij zelf toegepast in onze studies. Ook introduceren wij de verschillende maten van hersenfunctie, die grofweg ingedeeld kunnen worden in lokale activiteit (de sterkte van de hersenactiviteit; ook wel *power*) en communicatie tussen hersengebieden (functionele connectiviteit). Tot slot formuleren wij de onderzoeksvragen die de basis gevormd hebben voor de studies beschreven in dit proefschrift.

Overzicht van de EEG en MEG literatuur over de ziekte van Parkinson

Hoofdstuk 2.1 is een overzicht van de bestaande EEG literatuur, waarbij de hoofdvraag was of gekwantificeerde EEG waardes als maat van ernst en progressie van de ziekte van Parkinson kunnen functioneren. Gebaseerd op het beschikbare bewijs concludeerden we dat vertraging van hersenactiviteit correleert met ziekteprogressie, met name cognitieve achteruitgang. Dit lijkt dus een robuuste, niet-invasieve biomarker van het ziekteproces zelf te zijn. Ook maten voor de functionele interacties tussen hersengebieden en de organisatie van hersennetwerken zijn potentieel geschikt als biomarker van het ziekteproces, maar moeten nog verder onderzocht worden.

Hoofdstuk 2.2 is een overzicht van de bestaande MEG literatuur. Deze kan grofweg ingedeeld kan worden in studies gericht op de gehele hersenen, vooral de corticale

hersengebieden, en studies gericht op het motorische netwerk, vooral de motorische cortex, in sommige studies in combinatie met diepe hersenstimulatie en/of dieptemetingen in de STN. Gebaseerd op het beschikbare bewijs concludeerden we dat: i) ziekteprocessen die de hersenen als geheel treffen en leiden tot vertraging van hersenactiviteit of verlies van functionele interacties tussen hersengebieden, invloed hebben op bevindingen die lokaal in bijvoorbeeld de motorische cortex gedaan worden. Dit moet daarom bij de interpretatie van studieresultaten meegenomen worden. ii) veranderingen in corticale hersenactiviteit voort kunnen komen uit veranderingen in subcorticale hersengebieden. Derhalve kunnen behandelingen gericht op de subcorticale hersengebieden, zoals dopaminerge medicatie of diepe hersenstimulatie, invloed hebben op de gehele hersenen.

Neurofysiologische veranderingen tijdens het beloop van de ziekte van Parkinson

In **hoofdstuk 3.1** worden de resultaten beschreven van een studie waarin we onderzocht hebben of het mogelijk is een longitudinale analyse uit te voeren met MEG data gemeten op twee verschillende MEG apparaten. We hebben deze analyse verricht op MEG data verkregen bij acht gezonde controles die metingen op drie tijdspunten hebben ondergaan, over een periode van zeven jaar. We gingen er van uit dat neurofysiologische maten, namelijk de frequentie-specifieke relatieve *power*, piekfrequentie (frequentie waarbij de *power* maximaal is tussen 4 en 13 Hz) en de functionele connectiviteit, stabiel zouden blijven in deze groep. We vonden in onze analyse geen significante veranderingen in de tijd qua frequentie-specifieke relatieve *power* en functionele connectiviteit. Dit bevestigde de mogelijkheid een longitudinale analyse uit te voeren met gegevens verkregen bij patiënten met de ziekte van Parkinson door middel van metingen op twee verschillende MEG apparaten. De resultaten hiervan zijn te lezen in **hoofdstuk 3.2**. Ook in deze studie hebben wij de frequentie-specifieke relatieve *power* en functionele connectiviteit van de MEG data bepaald, voor zowel de corticale als subcorticale hersengebieden. Aan het begin van de studie zijn 61 niet-demente Parkinson patiënten geïncludeerd, waarvan 17 patiënten vroeg in de ziekte waren en nog geen dopaminerge medicatie gebruikten. Op het tweede tijdspunt, na vier jaar, vervolgden we 39 patiënten en op het derde tijdspunt, na zeven jaar, 35 patiënten. Bij de patiënten in de vroege fase van de ziekte van Parkinson, die nog geen dopaminerge medicatie gebruikten, vonden we al een vertraging van de hersenactiviteit, met name corticaal maar ook subcorticaal. De vertraging van hersenactiviteit bestond uit een daling van de piekfrequentie, een stijging van (relatieve) *power* van de langzame frequenties, vooral van de theta frequentie, en een daling van (relatieve) *power* van hogere frequenties zoals de alpha2 en beta frequenties. Dankzij de zogenaamde multipel longitudinale opzet van de studie, waarin we patiënten met een verschillende ziekteduur bij de start van de studie vervolgd hebben, konden we vaststellen dat over een ziekteperiode van ongeveer 20 jaar de vertraging van hersenactiviteit van zowel de corticale als subcorticale hersengebieden sterk (positief) gecorreleerd is met klinische verslechtering, zowel wat betreft cognitie als motoriek. Daarentegen konden we

geen significante veranderingen in (frequentieband-specifieke) functionele connectiviteit vinden. Dit kan een gevolg zijn van methodologische keuzes die we gemaakt hebben (de connectiviteitsmaat, een analyse met name gericht op de hersenen als geheel) of van het feit dat er in ons studiecohort daadwerkelijk nauwelijks veranderingen in functionele connectiviteit waren. De resultaten van onze studie bevestigen voorgaand onderzoek waarin vertraging van hersenactiviteit in het gehele beloop van de ziekte een robuuste maat voor ziekteprogressie en cognitieve achteruitgang is gebleken. Ons onderzoek voegt hier aan toe dat subcorticale hersengebieden al vanaf de eerste klinische (motorische) verschijnselen van de ziekte betrokken zijn bij deze algehele vertraging.

De rol van cortico-subcorticale interacties bij cognitieve achteruitgang gerelateerd aan de ziekte van Parkinson

In **hoofdstuk 4** onderzochten we de betrokkenheid van de subcorticale gebieden bij globale cognitieve achteruitgang bij 34 patiënten met gevorderde ziekte van Parkinson (gemiddelde ziekteduur 12 jaar) en 12 gezonde controles, gemeten op het derde tijdspunt van ons longitudinale studie cohort, zeven jaar na inclusie. We maakten hierbij gebruik van de directionele connectiviteitsmaat *directed phase transfer entropy* (dPTE). We hebben gevonden dat bij de Parkinson patiënten in vergelijking met gezonde controles de balans tussen de informatiestromen was veranderd. In plaats van een stroom van 'achter naar voren' voor de beta band was er een meer 'van voor naar achteren' patroon; dat wil zeggen, van de subcorticale en frontale hersengebieden naar de posterieure hersengebieden. Daarnaast was een lagere informatiestroom vanuit de posterieure hersengebieden gecorreleerd met een maat voor globale cognitieve achteruitgang, wat suggereert dat dysfunctie van de posterieure corticale hersengebieden, en niet de subcorticale hersengebieden, verantwoordelijk is voor de verandering van de balans in de informatiestroom.

Hoofdstuk 5 beschrijft de resultaten van een studie waarin we ons richtten op het functioneren op specifieke domeinen van cognitie, in relatie tot *resting-state* netwerken die wij middels fMRI scans longitudinaal bestudeerd hebben. De studie omvatte 50 patiënten met de ziekte van Parkinson tijdens de eerste meting; 31 patiënten hebben ook een tweede fMRI scan ondergaan. Een reeks van zeven cognitieve tests werd verricht gericht op de volgende cognitieve domeinen: executief functioneren (vier testen), geheugen, motorische perseveratie, en verbale vloeiendheid. Bij de eerste meting scoorden de patiënten op zes van de zeven testen slechter dan een groep van 15 gezonde controles. Executieve dysfunctie correleerde met een sterkere (statische) functionele connectiviteit en een zwakkere dynamische functionele connectiviteit tussen de subnetwerken 'subcorticale hersengebieden' en het frontoparietale netwerk. Een verdere verslechtering van executief functioneren over een periode van drie jaar correleerde met een toegenomen (statische) functionele connectiviteit tussen deze subnetwerken. Verder waren een daling van functionele connectiviteit binnen de subcorticale hersengebieden en een daling van functionele connectiviteit tussen het dorsale aandachtsnetwerk en

de rest van de hersenen gecorreleerd met een verdere verslechtering van executief functioneren. We concludeerden dat dysfunctionele communicatie tussen het subcorticale, frontoparietale en dorsale aandachtsnetwerk gerelateerd is aan slechter executief functioneren bij patiënten met de ziekte van Parkinson.

De effecten van diepe hersenstimulatie bij patiënten met de ziekte van Parkinson

In de studie beschreven in **hoofdstuk 6.1** bestudeerden we het effect van diepe hersenstimulatie op de hersenactiviteit van patiënten met de ziekte van Parkinson in relatie tot de verbetering van het motorisch functioneren. We voerden MEG metingen uit met de stimulator aan en uit bij achttien patiënten bij wie minimaal zes maanden daarvoor een diepe hersenstimulator geplaatst was. Scores op een schaal voor het motorisch functioneren (Unified Parkinson's Disease Rating Scale, UPDRS-III) waren zowel voor de operatie als zes maanden na de operatie bepaald. We hebben gevonden dat diepe hersenstimulatie leidt tot een globale versnelling van hersenactiviteit, in combinatie met een onderdrukking van de activiteit (0.5-22 Hz) in de sensomotorische cortex. Verbetering van de motorische symptomen bradykinesie en rigiditeit was significant gecorreleerd met een toename van de functionele connectiviteit in de alpha2 en de lage beta band (10-22 Hz). Dit was het geval voor de hersenen als geheel, voor subcorticale en corticale hersengebieden afzonderlijk, en ook wanneer we ons concentreerden op de sensomotorische cortex. Verbetering van tremor was niet gecorreleerd met een verandering van functionele connectiviteit. Wij concludeerden dat het mogelijk is klinisch relevante veranderingen in hersenactiviteit te meten wanneer MEG wordt uitgevoerd tijdens diepe hersenstimulatie.

In **hoofdstuk 6.2** wordt het onderzoek beschreven waarmee we trachtten de vraag te beantwoorden of de apathie, die vaak wordt gezien na diepe hersenstimulatie voor de ziekte van Parkinson, een effect van de stimulatie kan zijn, bovenop het effect van ziekteprogressie en/of postoperatieve verlaging van dopaminerge medicatie. We hebben MEG metingen verricht bij 26 patiënten, minimaal zes maanden na de operatie, met de stimulator aan en uit. Daarnaast hebben we apathie scores verkregen (Starkstein apathie schaal), zowel vóór de operatie als op de dag van de MEG metingen. We hebben voor drie hersengebieden die wij van tevoren hadden geselecteerd (en die volgens de literatuur betrokken zijn bij apathie) de stimulatie-geïnduceerde veranderingen in functionele connectiviteit gecorreleerd met veranderingen in de apathie scores. We zagen een grote toename van apathie scores in ons studie cohort. Bovendien steeg het aantal patiënten dat voldeed aan de klinische criteria voor apathie na de operatie van twee naar negen. De toename van apathie scores correleerde niet met de verbetering van het motorisch functioneren of de verlaging van de dosis van de dopaminerge medicatie. De toename van de apathie scores was wel geassocieerd met een meer dorsolaterale locatie van het gebruikte contactpunt, alleen voor de rechter kant. Verder correleerde een toename van de ernst van de apathie met een afname van functionele connectiviteit van de dorsolaterale

prefrontale cortex (dlPFC) in de alpha1 band. Wij concludeerden derhalve dat, zowel vanuit een structureel (stimulatie locatie) als vanuit een functioneel oogpunt, een toename van apathie bij patiënten met de ziekte van Parkinson die diepe hersenstimulatie ondergaan hebben ten minste deels gerelateerd is aan de stimulatie zelf.

In het onderzoek beschreven in **hoofdstuk 6.3** voerden we MEG metingen uit bij 30 patiënten met de ziekte van Parkinson met diepe hersenstimulatie (in een studie populatie die deels overlapte met die van hoofdstuk 6.1 en 6.2). Het doel was vaststellen of een acute verandering van het gestimuleerde contact punt zou leiden tot meetbare veranderingen van hersenactiviteit en connectiviteit. Op groepsniveau bleek een meer ventromediale positie van het gebruikte contactpunt geassocieerd te zijn met hogere delta en theta *power* over de gehele hersenen, en met een hogere functionele connectiviteit in de theta band frequentie in de gehele hersenen. Daarnaast correleerde een meer dorsolaterale stimulatie positie met lagere lage-beta *power* (13-22 Hz) in de motorische cortex ipsilateraal van de gestimuleerde STN. De bevindingen bij individuele patiënten waren onderling te sterk variabel om conclusies te kunnen trekken over de effecten binnen een individu. We concludeerden dat bij patiënten met de ziekte van Parkinson met diepe hersenstimulatie op groepsniveau een verandering van stimulatie locatie leidt tot een meetbare verandering van hersenactiviteit en connectiviteit.

In het laatste hoofdstuk (**hoofdstuk 7**) worden de belangrijkste bevindingen van dit proefschrift samengevat, geïntegreerd en bediscussieerd. Methodologische kwesties worden besproken en suggesties voor vervolgonderzoek worden gedaan.

Conclusies

Op basis van de EEG en MEG reviews (hoofdstuk 2.1 en 2.2) en de longitudinale MEG studies (hoofdstuk 3.1 en 3.2) concluderen wij dat een vertraging van hersenactiviteit vanaf de eerste fase van de ziekte van Parkinson aanwezig is, zowel in corticale als in subcorticale hersengebieden. Deze vertraging hangt samen met zowel ziekte-gerelateerde cognitieve als motorische symptomen. De vertraging van hersenactiviteit lijkt dan ook een goede weerspiegeling van het ziekteproces te zijn, die in de toekomst ingezet kan worden om het effect van ziekte remmende therapieën te monitoren of die gebruikt kan worden bij het voorspellen van het risico op het ontwikkelen van een Parkinson dementie. Aangezien de vertraging van hersenactiviteit een robuuste maat is, lijkt EEG het meest geschikt voor toepassing in de klinische praktijk, mede gezien de lage kosten en beschikbaarheid van EEG.

Voor vraagstellingen waarbij het lokaliseren van veranderingen in hersenactiviteit en connectiviteit van belang is, zijn juist MEG en fMRI uitermate geschikt. Zo passen de resultaten die wij in hoofdstuk 4 en 5 beschrijven bij twee verschillende cognitieve profielen met verschillende onderliggende oorzaken: De resultaten van hoofdstuk 4 illustreren de posterieure corticale dysfunctie in relatie tot globale achteruitgang in het

cognitief functioneren, terwijl de resultaten van hoofdstuk 5 duidelijk maken dat fronto-striatale dysfunctie gerelateerd is aan executieve stoornissen.

Blijkens de onderzoeksresultaten beschreven in hoofdstuk 6 heeft diepe hersenstimulatie van de STN zowel lokale als gegeneraliseerde effecten op de functie van de hersenen. Sommige effecten waren gecorreleerd met klinische effecten of bijwerkingen van de behandeling, maar andere effecten, zoals het versnellen van hersenactiviteit na stimulatie, leken minder specifiek te zijn. Een wisseling van het gebruikte contactpunt hing op groepsniveau samen met acute veranderingen in enkele neurofysiologische maten. De stimulatie-gerelateerde veranderingen van hersenactiviteit verschilden sterk tussen individuen, zodat de bruikbaarheid van deze maten voor het aflezen van stimulatie-effecten bij individuele patiënten nog verder onderzocht moet worden. Wij hebben suggesties gedaan voor verder onderzoek om de variabiliteit van hersenactiviteit gemeten met MEG binnen een individu te verkleinen en zo de klinische toepasbaarheid te vergroten.

List of publications

Boon LI, Hillebrand A, Schoonheim MM, Twisk JW, Stam CJ, Berendse HW. Cortical and subcortical changes in MEG activity reflect Parkinson's progression over a period of 7 years. Brain Topography 2023 Jul;36(4):566-580.

Boon LI, Potters WV, Hillebrand A, de Bie RMA, Bot M, Schuurman PR, van den Munckhof P, Twisk JW, Stam CJ, Berendse HW, van Rootselaar AF. Magnetoencephalography to measure the effect of contact point-specific deep brain stimulation in Parkinson's disease: a proof of concept study. Neuroimage Clin. 2023;38:103431

Boon LI, Potters WV, Zoon TJC, van den Heuvel OA, Prent N, de Bie RMA, Bot M, Schuurman PR, van den Munckhof P, Geurtsen GJ, Hillebrand A, Stam CJ, van Rootselaar AF, Berendse HW. Structural and functional correlates of subthalamic deep brain stimulation-induced apathy in Parkinson's disease. Brain Stim. 2021 Jan-Feb;14(1):192-201

Boon LI, Tewarie P, Berendse HW, Stam CJ, Hillebrand A. Longitudinal consistency of source-space spectral power and functional connectivity using different magnetoencephalography recording systems. Sci Rep. 2021 Aug 11;11(1):16336.

Arnts H, van Erp WS, **Boon LI**, Bosman CA, Admiraal MM, Schrantee A, Pennarts CMA, Schuurman PR, Stam CJ, van Rootselaar AF, Hillebrand A, van den Munckhof P. Awakening after a sleeping pill: Restoring functional brain networks after severe brain injury. Cortex 2020 Nov;132:135-146

Boon LI, Hepp DH, Douw L, van Geenen N, Broeders TAA, Geurts JJG, Berendse HW, Schoonheim MM. Functional connectivity between resting-state networks reflects decline in executive function in Parkinson's disease: A longitudinal MEG fMRI study. Neuroimage Clin. 2020;28:102468.

Boon LI, Hillebrand A, Potters WV, de Bie RMA, Prent N, Bot M, Schuurman PR, Stam CJ, van Rootselaar AF, Berendse HW. Motor effects of deep brain stimulation correlate with increased functional connectivity in Parkinson's disease: An MEG study. Neuroimage Clin. 2020;26:102225

Boon LI, Geraedts VJ, Hillebrand A, Tannemaat MR, Contarino MF, Stam CJ, Berendse HW. A systematic review of MEG-based studies in Parkinson's disease: The motor system and beyond. Human Brain Mapp. 2019 Jun 15;40(9):2827-2848

De Haan W, **Boon LI**, Foncke EM. Drooping eyelid after vomiting. JAMA Neurol. 2019 Jul 1;76(7):862-863

Prent N, Potters WV, **Boon LI**, Caan MWA, de Bie RMA, van den Munckhof P, Schuurman

PR, van Rootselaar AF. Distance to white matter tracts is associated with deep brain stimulation motor outcome in Parkinson's disease. J Neurosurg. 2019 Jul 26:1-10.

Geraedts VJ, **Boon LI**, Marinus J, Gouw AA, van Hilten JJ, Stam CJ, Tannemaat MR, Contarino MF. Clinical correlates of quantitative EEG in Parkinson's disease: A systematic review. Neurology 2018 Nov 6;91(19):871-883.

Boon LI, Hillebrand A, Olde Dubbelink KTE, Stam CJ, Berendse HW. Changes in resting-state directed connectivity in cortico-subcortical networks correlate with cognitive function in Parkinson's disease. Clin Neurophysiol. 2017 Jul;128(7)1319-1326.

Dankwoord

Tijdens mijn promotietraject heb ik tussen beide locaties van Amsterdam UMC gependeld en met veel mensen van allerlei vakgebieden mogen samenwerken. Het samenbrengen van verschillende expertises heb ik als een ontzettend leerzaam ervaren. Ik wil iedereen die aan de totstandkoming van dit proefschrift heeft bijgedragen bedanken.

Om te beginnen de patiënten met de ziekte van Parkinson die hebben deelgenomen aan de MEG-DBS studie. Alleen al het bestaan van een werkgroep *patiënt onderzoekers* van de Parkinson vereniging is een uitstekend voorbeeld van de betrokkenheid van deze patiënten bij wetenschappelijk onderzoek.

Mijn promotieteam, bestaande uit mijn promotoren Henk Berendse en Kees Stam, en copromotoren Arjan Hillebrand en Fleur van Rootselaar.

Henk, vanaf het eerste mailtje dat ik in 2015 stuurde op zoek naar een stage heb ik van jou vertrouwen gevoeld, tijdens mijn promotietraject, en nu ook tijdens de opleiding tot neuroloog. Jouw rol in dit eindresultaat is enorm geweest. Je hebt mijn eigen denkprocessen alle ruimte gegeven, maar kon mij door je analytisch vermogen altijd verder helpen of net even de juiste richting op sturen. Zowel in het onderzoek als in de kliniek had ik mij geen betere begeleider kunnen wensen!

Kees, dank voor je uitstekende en altijd laagdrempelige begeleiding. Wanneer ik op vrijdagmiddag een manuscript rondstuurde (in de hoop een rustig weekend tegemoet te gaan), kreeg ik 'm soms binnen een uur voorzien van commentaar terug. Je creatief denkvermogen en kennis die verder gaat dan de klinische neurofysiologie zijn indrukwekkend. Dank ook voor je pragmatisme wanneer er knopen doorgehakt moesten worden.

Arjan, je technische expertise was natuurlijk onmisbaar, maar je kritische blik heeft ook elk onderzoeksproject beter gemaakt. Je bent daarnaast een verbinder voor de onderzoeksgroep en zorgt met je droge humor voor een uitstekende sfeer.

Fleur, jij hebt alle voorwaarden gecreëerd voor een succesvolle samenwerking tussen (toen nog) twee verschillende ziekenhuizen. Dank voor je frisse kijk op de MEG resultaten waarbij je altijd de klinische relevantie op de radar hield. En tot slot bedankt dat je mij ooit op de onderzoekerskamer bij collega Sharifi hebt gezet ;).

De leden van de lees- en promotiecommissie, prof.dr. Ysbrand van der Werf, dr. Rick Helmich, prof.dr. Yolande Pijnenburg, prof.dr. Ben Schmand, prof.dr. Yasin Temel, dr. Bernadette van Wijk: Bedankt voor de tijd en moeite voor het lezen van het proefschrift en zitting te nemen in de promotiecommissie.

Dank aan alle co-auteurs voor de leerzame samenwerking en waardevolle input op de onderzoeksprojecten. Rob de Bie, Maarten Bot, Pepijn van den Munckhof, Rick Schuurman, Gert Geurtsen, Thomas Zoon, Fiorella Contarino, Martijn Tannemaat, Victor Geraedts, Jos Twisk, Linda Douw, Odile van den Heuvel, Menno Schoonheim en Wouter Potters. Menno, bedankt voor je altijd enthousiaste begeleiding, ik maakte altijd met veel plezier de 'tocht' naar het O2 gebouw! Wouter, samen hebben we hard aan het MEG-DBS project gewerkt en met toffe resultaten! Je Matlab-skills zijn ongeëvenaard, je codeert sneller dan je schaduw. Dank ook voor alle uren die je bij de MEG-metingen bent geweest, het had misschien ook wel iets meditatiefs in jouw drukke bestaan!

Ook veel dank aan de wetenschapsstage studenten voor jullie enorme inzet en waardevolle bijdrages, o.a. Naomi, Laura, Barbara, Pelle en Noelle.

'Oude garde' KNF onderzoekers Ida, Matteo, Pierpaolo, Meichen, Marjolein, Willem en Alida, en 'nieuwe garde' onderzoekers Deborah, Elliz, Ilse, Shanna, Janne, Anne en Ana. Bedankt voor alle brainstorm sessies, we zorgden er met elkaar voor dat het wiel niet steeds opnieuw uitgevonden moest worden. Bedankt ook voor alle gezelligheid (lunch stipt om 12u, heel belangrijk), zo'n internationaal gezelschap gaf altijd een leuke dynamiek!

KNF laboranten, in het bijzonder Nico, Marieke en Karin die met de arbeidsintensieve MEG metingen MEG hebben meegeholpen. Bedankt voor jullie hulp, gezelligheid en de vele cappuccino's.

Parkinson onderzoekers aan VUmc zijde op D2-135 Tom, Karin, Dagmar, en het langst met Dareia en Merijn: Bedankt voor de uitstekende sfeer en goede gesprekken. Bovendien hield ik door jullie en de wekelijkse bewegingsstoornissen MDO's altijd een voet in de kliniek! Aan AMC zijde: Timo, bedankt!

Bedankt aan alle (oud) collega's van de afdeling Neurologie, aan beide kanten van de Amstel, door jullie ga ik elke dag met veel plezier naar mijn werk!

Verder wil ik natuurlijk mijn vrienden en familie bedanken.

Mijn vrienden uit Castricum, sommigen al sinds de basisschool: De Deeldeliers (Gijs, Dirk, Zaid, Patrick en Milan) en mijn (van oorsprong) tennis maatjes Stef, Bob en Auke. Auke, in de Amsterdamse jaren hebben onze paden elkaar weer gekruist en hoe. Ik waardeer je eindeloze nieuwsgierigheid en onze (soms tot waanzin drijvende) discussies.

Dan mijn vrienden uit mijn tijd in Leiden. Allereerst de mannen van A.H.C. Sap, dat de volgende lustrumreis alweer gepland staat zegt genoeg! Binnen deze groep mag Mooieman Jesse niet ongenoemd blijven (Sorry Ties). Kaisers, bedankt! Lennard "El gallo loco" Meulens, dank voor onze goede gesprekken over nieuwe muziek, het leven, of wat dan ook!

Roderick, vanaf de eerste dag van de studie geneeskunde waren wij maatjes en vonden wij overal (samen met ridder Jamie) er het onze van. Je bent iemand met tomeloze energie, daadkracht en klus-drang, zowel bij de orthopedie als in het paleisje waar je met je prachtige gezin woont. Fijn om altijd op je te kunnen rekenen, bijvoorbeeld wanneer ik mij met een kapotte emmer verf in de nesten heb gewerkt..! Fantastisch dat jij als paranimf naast mij staat!

Osses, my twin brother from another mother, altijd goed voor een vrolijke noot, maar je bent vooral een fantastische vriend. Bedankt dat ook jij als paranimf naast mij staat. Ik waardeer je gevoel voor sociale situaties, hartelijkheid en topografisch geheugen ;). Samen met Anoukita en de kids heb je iets prachtigs opgebouwd in Beuningen, maar je bent gelukkig nooit ver weg!

Dan de rest van de familie: Allereerst familie Sharifi, Ali & Mehri, Yassi, Nick & de kinderen. Bedankt dat jullie mij vanaf het eerste moment thuis hebben laten voelen in de familie!

Mijn zus en broertje: Mariette, van jongs af aan tot en met de master Biomedische wetenschappen heb ik jouw pad gevolgd. Je bent een voorbeeld voor hoe je passie in je werk kunt vinden en dit ook nog met ouderschap combineert. Ook dank voor Michiel, Arthur en Evi! Ruben, ik ben trots op de unieke persoon jij bent en de dingen die je doet. Dat zal met Alyssa samen zeker zo blijven!

Lieve pap en mam, bedankt voor de fantastische en liefdevolle basis die ik van jullie heb gekregen. Ik heb alle mogelijkheden van jullie gekregen om mijn pad uit te stippelen, van een jeugd vol tennis tot een studententijd met prachtige reizen.

Als laatste wil ik Sarvi bedanken. Lieffie, je bent de mooiste, meest innemende en (vooruit) grappigste persoon van de wereld en vult mij in alles aan. Ons jaar kon al niet meer stuk met de geboorte van kleine Kasper, op naar een prachtige toekomst met ons gezinnetje, ik hou van jou!

About the author

Lennard Ivo Boon was born on May 24th 1990 in Castricum. After completing secondary school in 2008 at Bonhoeffer college, he started his study Medicine at the Leiden University Medical Center (LUMC) in Leiden. After his bachelor's degree, he combined the master Medicine with the master Health of Biomedical Sciences, because of his special interest in pathophysiological mechanisms (both at the LUMC).

The first scientific internship of his master Biomedical Sciences was about regeneration of peripheral nerve damage at the Netherlands Institute of Neurosciences under supervision of prof. dr. Joost Verhaagen. His clinical internships neurology took place at the Neurology department of the Haga Hospital in the Hague, which triggered his enthusiasm for neurology in general, especially movement disorders.

In 2015, Lennard started his second scientific internship on Parkinson's disease at the department of Neurology and Clinical Neurophysiology of Amsterdam UMC, VU University Medical Center under supervision of prof. dr. Henk Berendse, prof. dr. Kees Stam and dr. Arjan Hillebrand. This internship resulted in his first peer-reviewed publication (chapter 4 of this thesis). After a temporary return to the Haga Hospital to work as a neurology resident (dr. Bas de Bruijn), Lennard began his PhD project in 2016 on the same topic as his internship, in collaboration with Amsterdam UMC, Academic Medical Center (dr. Anne-Fleur van Rootselaar). In July 2020, he started his training to become a neurologist in Amsterdam UMC, VUmc location (prof. dr. Henk Berendse, dr. Bob van Oosten) and hopes to combine his clinical work with his scientific interest in movement disorders.